Title

A systems-level understanding of electron flow in TCE-dechlorinating microbial communities using modeling and molecular biology tools

Author

Mao, Xinwei

Publication Date

2014

Peer reviewed|Thesis/dissertation

A systems-level understanding of electron flow in TCE-dechlorinating microbial communities using modeling and molecular biology tools

By

Xinwei Mao

A dissertation submitted in partial satisfaction of the
Requirements for the degree of
Doctor of Philosophy
in
Engineering-Civil and Environmental Engineering
in the
Graduate Division
of the
University of California, Berkeley

Committee in charge:

Professor Lisa Alvarez-Cohen, Chair
Professor Slav Hermanowicz
Professor John Coates

Spring 2015

Abstract

A systems-level understanding of electron flow in TCE-dechlorinating microbial communities using modeling and molecular biology tools

By

Xinwei Mao

Doctor of Philosophy in Environmental Engineering

University of California Berkeley

Professor Lisa Alvarez-Cohen, Chair

Groundwater and soils have been frequently contaminated by trichloroethene (TCE), perchloroethene (PCE) and other chlorinated compounds in the U.S. and worldwide, in spite of their established toxicity and mutagenicity towards many organisms, including humans. In order to protect public health, bioremediation using *Dehalococcoides*-containing microbial communities is a promising approach to reach ecotoxicological-safety endpoints. The overall goal of this research is to understand electron flows in complex dechlorinating microbial communities, and to develop mathematical models to predict the performance of the microbial communities in different environmental conditions. To accomplish these goals, we first studied the electron flow and material exchange of constructed TCE-dechlorinating consortia. We also applied emerging molecular techniques to study TCE-dechlorinating microbial communities under different remediation conditions. Furthermore, we developed integrated thermodynamic and kinetic models to predict the dechlorination performance and microbial growth of syntrophic consortia under batch and continuous-flow conditions, and the suite of models were further validated using enrichment cultures.

The first objective of this research was to understand the material and energy exchange between *Dehalococcoides* and its supporting syntrophic bacteria. We investigated dechlorination activity, cell growth, cell aggregate formation, and global gene expression of *D. mccartyi* strain 195 (strain 195) grown with *Syntrophomonas wolfei* in co-cultures amended with butyrate and TCE. By applying thermodynamically consistent rate laws to study the electrons flows in the co-culture, we found that the growth rates of the two species were strictly coupled by H_2 transfer, and that the growth yield of syntrophic bacteria and the ratio maintained in the co-cultures were mainly controlled by thermodynamics. We demonstrated, for the first time, that *D. mccartyi* could form cell aggregates with its supporting fermenter *S. wolfei* on butyrate. Furthermore, we found carbon monoxide (CO) may serve as a supplemental energy source for *S. wolfei* during syntrophic fermentation with strain 195, and that the observed increased cell yields of strain 195 is likely due to the continuous removal of CO in the co-culture.

In order to understand the microbial community structure shift from "feast-and-famine" condition (semi-batch) to the continuous feeding of low nutrients condition (completely-mixed flow reactor (CMFR)), molecular techniques based on 16S I-tags and metagenomic sequencing were applied to investigate the dechlorinating community structural shift after transition from semi-batch to a long-term steady-state CMFR condition. A *Dehalococcoides* genus-wide microarray was also applied to study the transcriptional dynamics of *D. mccartyi* strains within the CMFR community that was grown in the continuous-flowing diluted, nutrient poor environment. I-tags and metagenomic sequencing analysis revealed that dominant species in the CMFR shifted significantly from the semi-batch culture condition while the ratio of *D. mccartyi* was maintained at relatively stable levels. Transcriptional analysis identified *tceA* and *vcrA* to be among the most expressed genes in the CMFR, *hup* and *vhu* were more critical hydrogenases utilized by *Dehalococcoides* sp. in the continuous-flowing system. In contrast, corrinoid-related uptake and modification genes were expressed at lower levels in the CMFR than in the semi-batch culture during active dechlorination.

A systems-level approach was applied to determine accurate kinetic parameters involved in reductive dechlorination from simple constructed syntrophic consoria to complex microbial communities. The results demonstrated that the kinetic parameters involved in reductive dechlorination were in similar ranges for simple and complex *Dehalococcoides*-containing cultures. Cell growth calculations showed H_2 was the most sensitive factor limiting the growth of H_2-utilizing microorganisms involved in dechlorinating communities. High concentrations of acetate resulted in slower dechlorination rates by inhibiting the growth of specific fermenting bacteria. High sulfate concentrations also hindered dechlorination performance due to either sulfide inhibition or competition with sulfate reduction. The mechanism for observed slower dechlorination rates with lower bicarbonate concentrations was not clear and further experiments need to be conducted to evaluate the role of bicarbonate in reductive dechlorination communities.

Based on the knowledge obtained in the previous studies, an integrated thermodynamic and kinetic model was developed to predict reductive dechlorination and cell growth under batch growth conditions. The model parameters calculated to fit the experimental data were at the same levels as those determined experimentally. The resultant model accurately captured the dechlorination kinetics in two *Dehalococcoides*-containing syntrphic co-cultures using different fermenting substrates. The model was validated at different donor to acceptor ratios in syntrophic co-cultures and in syntrophic tri-cultures and enrichment cultures performing hydrogenotrophic methanogenesis. The sensitivity of kinetic parameters on model stability was tested. Half velocity constants and inhibition coefficients were found to be the most sensitive factors affecting model predictions.

The significance of this research is to provide a more fundamental understanding of the metabolic exchange and energy transfer among the key players of TCE-dechlorinating communities, as well as the physiology of dechlorinating microbial communities experiencing different environmental stresses. The integrated thermodynamic and kinetic models developed in this study could be used as a platform to incorporate more biological processes under different experimental conditions. The knowledge developed in this research will aid practitioners to

better design, monitor and optimize future *in situ* bioremediation systems.

To my family

Table of content

List of Figures

List of Tables

Acknowledgement

First and foremost, I am grateful to my advisor Lisa Alvarez-Cohen for her mentorship and guidance throughout my graduate study. I am lucky to have the opportunity to work with Dr. Alvarez-Cohen. Her mentorship was paramount in providing a well rounded experience consistent with my long-term career goals. I'd like to thank her for trusting my abilities and offering me the freedom to pursue different research questions.

I sincerely thank the many professors and scientists at the University of California, Berkeley and at the Lawrence Berkeley National Laboratory (LBNL). Slav Hermanowicz, John Coates and David Sedlak were members of my qualifying exam and dissertation committee and special thanks go to them for their insights and interests in my research. The expertise and support of Dr Guangwei Min at Electron Microscope Lab Berkeley, Yvette Piceno and Ping Hu at LBNL have made much of my research possible. Dr. Chen Xu at SLAC has taught me very valuable knowledge on the modeling work. Professor Michael McInerney at University of Oklahoma has been a generous collaborator and insightful mentor. I also want to thank Dr. Nikhil S. Malvankar and Professor Derek Lovley at University of Massachusetts carried out the experiments of conductivity test for the co-cultures.

Special thanks go to all members of the Alvarez-Cohen group for their assistance and comradeship. Dr. Ben Stenuit worked together with me on the microbial structure study, he taught me important aspects of molecular biology, scientific writing and has become a very good friend. Dr. Yujie Men was a fabulous mentor, she taught me every detail of working in the lab at the very beginning of my research, and has been a loyal friend for a long time. Patrick Lee and Kimberlee West were fabulous, generously helping me with the microarray analysis. Especially, Ke Yu, Weiqin Zhuang, Shan Yi and Ariel Grostern were experienced researchers and fantastic collaborators, who offered me experimental discussion and taught me vast fundamental knowledge throughout my Ph.D period. Alexandra Polasko is an excellent senior undergraduate, and also a fantastic collaborator. I was always impressed by her passion in science and have enjoyed the collaboration with her. Other group members including Katie Harding, Peerapong Pornwongthong and Sara Gushgari contributed in a variety of ways. The assistance of previous and current lab managers Tiffany Louie and Charles Lee have made my research in the lab more efficient.

I am blessed to have many trustworthy friends who stood by my side during my Ph.D study. The friendships of Yujie Men, Ben Stenuit, Weiqin Zhuang, Shan Yi, Cherie Tan, Jing Lu, Bo Sun, Guangyan Xiong, Shanshan Yang, Mofei Han, Yin Yu, Haizhou Liu, Bowen Zhou, Andy Cheng Zheng, Ye Liu, Rui Wang and many others have made my stay at Berkeley pleasant and memorable. It was their comfort and encouragements that helped me to overcome every obstacle on my PhD journey.

Finally and most importantly, I thankfully acknowledge my parents Yingjun Mao and Jikao Ding. No word can ever express the gratitude I have towards my parents for their unconditional love, support and faith in me. It was under their watchful eye that I have gained so much drive and an ability to tackle challenges head on. I know Dad and Mom will always be my greatest supporters and I feel fortunate because of them.

1. Introduction and Objectives

1.1 Introduction

The final U.S. Environmental Protection Agency's health risk assessment of TCE recognized this chemical as a potential human health hazard for non-cancer toxicity to the central nervous system, the kidney, the liver, the immune system, the male reproductive system, and developing fetuses (U.S. EPA 2011, a). In spite of their established toxicity and mutagenicity towards many organisms (Bhatt *et al.* 2007; U.S.EPA 2011), thousands of public and private groundwater sites are contaminated by chlorinated solvents in the U.S. (McCarty, 2010).

The development of environmentally friendly, cost-effective, and reliable cleanup options is a priority to tackle the worldwide contamination by TCE. Compared to physical and chemical treatment technologies which were prevalent during 1980s to 1990s (U.S.EPA 2007; Stroo, 2010 a), *in situ* bioremediation is a promising alternative approach to reach the ecotoxicological-safety endpoints by (i) reducing the concentration of TCE below the MCL and (ii) circumventing the accumulation of toxic and carcinogenic TCE metabolites, i.e. dichloroethene isomers (e.g., *cis*-DCE) and vinyl chloride (VC). Indeed, the versatility and ubiquity of microorganisms make them interesting candidates to support *in situ* remediation options (Mackay and Cherry 1989; Amann *et al*., 1995; Isken and de Bont 1998). As of 2009, bioremediation had become the most common technology that is used in remediating polluted groundwater (Pandey *et al*., 2009).

Among the reported dehalorespiring species (Magli *et al*., 1996; Holliger *et al*., 1998; Maymó-Gatell *et al*., 1999; Löffler *et al*., 2000; Suyama *et al*., 2001), *Dehalcoccoides* are the only known microorganisms that can reductively dechlorinate PCE all the way to the benign end product ethene. *D. mccartyi* exhibits specific restrictive metabolic requirements for a variety of exogenous compounds, such as hydrogen, acetate, corrinoids, biotin and thiamine, which can be supplied by other microbial genera through a complex metabolic network (Maymó-Gatell *et al*., 1997; He *et al*., 2007; Zhuang *et al*., 2011; Men *et al*., 2013; Yan *et al*., 2013; Schipp *et al*., 2013). Therefore, the growth of *D. mccartyi* is more robust within functional-diverse microbial communities than in pure cultures (He *et al*., 2007; Ziv-El *et al*., 2011; Schipp *et al*., 2013). In order to better understand and predict the activity of reductive dechlorination in the field sites, the metabolic and electron exchange, as well as the effect of other terminal electron accepting processes (TEAPs) on reductive dechlorination need to be further investigated.

Unusual cell surface features, such as filamentous appendages, have been observed in scanning electron microscopy of *Dehalcoccoides* cells (He *et al*., 2003), however the function of the appendages is unclear. They may play a role in attachment of cells to each other or to surfaces as observed in laboratory and field studies (Lendvay *et al*., 2003; Amos *et al*., 2009). In engineered dechlorinating systems, *D. mccartyi* species have been detected within biofilms and bioflocs of dechlorinating communities (Chung *et al*., 2008; Rowe *et al*., 2008).

There have been a few approaches employed to characterize dechlorinating performance and community structure in continuous-flow systems, such as H_2 membrane-biofilm reactors (Chung *et al*., 2008), flow-through column studies (Azizian *et al*., 2008) and up-flow anaerobic sludge bed reactors (Maphosa *et al*., 2010). There have been a limited number of studies devoted to evaluating biological reductive dechlorination in continuous flow suspended growth systems (Gerritse *et al*., 1997; Carr *et al*., 2000; Drzyzga *et al*., 2001; Zheng *et al*., 2001; Sabalowsky *et*

al., 2010). These studies showed that the hydraulic retention times and hydrogen concentrations in the reactors affected dechlorination activity in complex microbial communities. However, they all lack information of the abundance, distribution and dynamics of key dechlorinating species.

A number of different modeling approaches have been used to describe reductive dechlorination, ranging from simple first-order sequential dechlorination to complex suites of modeling coupled kinetics, thermodynamic, self-inhibition, competitive-inhibition of other TEAPs, as well as bacterial growth. Among the existing models that simulate reductive dechlorination, only a few numerical models have been developed for reductive dechlorination in groundwater plumes that have simultaneously considered multiple parameters like fermentative substrates, electron donor limitation, dechlorination kinetics, non-chlorinated TEAPs competitions, and product self-inhibition (Bagley *et al*., 1998; Fennell and Gossett, 1998; Cupples *et al*., 2004; Lee et al., 2004; Berggren *et al*., 2013).

The suitability and accuracy of developed models depend on adequate estimates of biomass for each specific functional group of microorganisms in the system. However, total biomass concentrations of the microbial community are commonly assessed by volatile suspended solid measurements (mg VSS) or protein masses (mg protein), which don't represent the activity of specific groups of bacteria in the system without significant biases (Bagley *et al*., 1998; Haston *et al*., 1999; Yu *et al*., 2005). Furthermore, reductive dechlorination only accounts for a small portion of the electron flow occurring in the dechlorinating microbial communities that include a variety of non-*D.mccartyi* H_2-utilizing microorganisms (e.g., hydrogenotrophic methanogens and homoacetogens). Other terminal electron accepting processes (TEAPs), such as sulfate reduction, iron reduction, nitrate reduction, and volatile fatty acids formation (e.g., fermentation, acetogenesis), account for a large portion of the electron flow in these systems. In addition, many models previously developed have focused on the bioremediation of DNAPL source zones, whereas there is an ongoing interest in the bioremediation of TCE-contaminated groundwater plumes where contaminant concentrations are generally relatively low under continuous flow conditions (Stroo, 2010).

Future development and application of models that predict electron flow in microbial communities involved in *in situ* bioremediation requires understanding the mechanisms that govern the activity and syntrophy of the dechlorinating systems. Therefore a systems-level understanding of electron flow in dechlorinating microbial communities is needed.

1.2 Research objectives

The overall goal of this research is to understand electron flows in complex dechlorinating microbial communities in order to develop mathematical models to predict the performance of the microbial communities under different environmental conditions. To accomplish this overall goal, the following objectives were proposed and accomplished.

1) Study the efficient metabolic exchange and electron transfer within a syntrophic TCE degrading co-culture of *Dehalococcoides mccartyi* (*D. mccartyi*) strain 195 and *Syntrophomonas wolfei* (*S. wolfei*).

2) Investigate structural changes and transcriptomes of *D. mccartyi* within a TCE-dechlorinating community in a completely mixed flow reactor (CMFR).
3) Use a systems-level approach to evaluate kinetic coefficients and environmental effects on *D. mccartyi*-containing microbial consortia.
4) Develop an integrated thermodynamic and kinetic model to describe reductive dechlorination of chlorinated ethenes in microbial communities.

1.3 Dissertation Overview

This dissertation is organized into seven chapters. The background and introduction leading to the overall research goal and the specific objectives are outlined in **Chapter 1**. Previously published literature that is relevant to the study of reductive dechlorination in *Dehalococcoides* spp. and kinetic modeling development are summarized and presented in **Chapter 2**. Study of the efficient metabolic exchange and electron transfer within a syntrophic TCE degrading co-culture of *D. mccartyi* 195 and *S. wolfei* are presented in **Chapter 3**. Study of structural changes and transcriptomes of *D. mccartyi* within a TCE-dechlorinating community in a CMFR are presented in **Chapter 4**. The systematic determination of kinetic coefficients and the effects of environmental factors on various *D. mccartyi*-containing cultures are presented in **Chapter 5**. The Development of an integrated thermodynamic and kinetic model to describe reductive dechlorination of chlorinated ethenes in microbial communities, model validation in enrichment cultures, as well as sensitivity analysis of kinetic coefficients are presented in **Chapter 6**. In **Chapter 7**, the key findings of this research are summarized and directions for future research are proposed.

2. Literature Review

2.1 Chlorinated solvents and groundwater contamination in the U.S.

Chlorinated solvents, including trichloroethene (TCE), perchloroethene (PCE), 1,1,1-trichloroethane (TCA) and carbon tetrachloride (CT) have been widely used for cleaning and degreasing in the US (U.S.EPA, 2006; McCarty, 2010) and also worldwide (WHO, 2000) (figure 2-1).

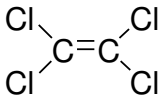

Tetrachloroethene (PCE)

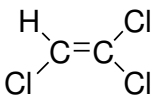

Trichloroethene (TCE)

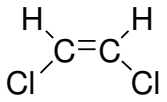

cis-Dichloroethene (*cis*-DCE)

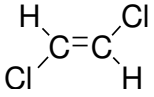

trans-Dichloroethene (trans-DCE)

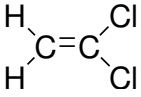

1,1-Dichloroethene (1,1-DCE)

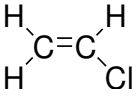

Vinyl Chloride (VC)

Figure 2-1 Chemical structures of some common chlorinated solvents

The final U.S. Environmental Protection Agency's health risk assessment of TCE recognized this chemical as a potential human health hazard for non-cancer toxicity to the central nervous system (CNS), the kidney, the liver, the immune system, the male reproductive system, and developing fetuses (U.S. EPA 2011, a). In spite of their established toxicity and mutagenicity towards many organisms (Bhatt *et al.* 2007; U.S.EPA 2011a), soils and groundwater are still being frequently contaminated by trichloroethene (TCE), perchloroethene (PCE) and other chlorinated solvents mainly because of poor disposal practices and accidental releases from dry cleaning and degreasing of metals (Moran *et al*., 2007).

Thousands of public and private sites with groundwater contaminated by chlorinated solvents have been detected in the U.S. (McCarty, 2010). In addition, the U.S. EPA's National Priorities List counts 171 sites contaminated by TCE that require remediation (U.S.EPA 2011,b). In addition, TCE is listed as number 16, and VC is listed as number 4 on Superfund's priority list of hazardous substances (ATSDR, 2014). Furthermore, TCE is still the most frequently detected organic contaminant at Superfund sites (U.S. EPA, 2011c). The U.S. EPA established national drinking water standards for TCE with a maximum contamination level (MCL) of 5 $\mu g \cdot L^{-1}$. However, at many contaminated sites, TCE is detected at concentrations higher than the MCL because of its persistence in the subsurface (Janssen *et al.,* 2005). The physical and chemical properties of chlorinated solvents (Table 2-1) affect their movement and fate in the environment, as well as the potential technologies for dealing with them.

Table 2-1Physical and chemical properties of chlorinated ethenes and their transformation products at 25 °C (Yaws, 1999; Haynes, 2014)

Chlorinated ethenes	Density ($g\ cm^{-3}$)	Henry's law constant, K_H ($atm\ M^{-1}$)	Water solubility ($mg\ L^{-1}$)	Octanol/Water Partition coefficient ($\log K_{ow}$)	MCL ($mg\ L^{-1}$)[a]
PCE	1.62	27	150	3.4	0.005
TCE	1.46	12	1100	2.42	0.005
cis-DCE	1.28	7.4	3500	1.85	0.07
trans-DCE	1.26	6.7	6300	2.09	0.1
1,1-DCE	1.22	23	3400	2.13	0.007
VC	0.91	22	2700	1.62	0.002

a. data source: USEPA (2013) http://water.epa.gov/drink/contaminants/#Organic

2.2 *In-situ* bioremediation of chlorinated ethenes

2.2.1 *In situ* remediation

There are a large number of remedial approaches that have been developed for chlorinated solvents contamination in groundwater. Initially, pump-and-treat techniques were installed at the majority of remediation sites (Stroo, 2010 a). However, this method requires continued operation and maintenance, often at a considerable cost. *In situ* treatments were applied more to contaminated sites later on, notably for the lower cost and shorter time frame for clean-up compared to pump-and-treat methods (U.S.EPA, 2007). Based on dominant mechanisms responsible for treatment, *in situ* remediation could be classified as the following:

i) Physical treatment: *in situ* air sparging (IAS). Air is injected into the saturated subsurface directly to volatize contaminants, this technique was successfully used for groundwater contaminated with halogenated volatile organics (USEPA, 2007), and it is most applicable to the sites with moderate to high permeabilities (Stroo, 2010 a).

ii) Chemical treatment: a) *in situ* chemical oxidation (ISCO). Strong oxidants (e.g. hydrogen peroxide, permangagate, persulfate, etc.) were injected into the contaminated subsurface, and this method was more commonly used for high concentrations of chlorinated solvents at source zone (Watts and Teel, 2006). b) *in situ* chemical reduction (injection or barrier), occurs by contact with reduced metals, typically zero valent iron (ZVI), or other forms of reduced iron (Gillham and O'Hannesin, 1994; Butler and Hayes, 1999). c) electro-chemical reduction, the reduction of chloroethenes is driven by electricity from a panel of closely spaced electrodes in the subsurface (Sale *et al*., 2005). This technique is still in development phase and the application may be limited to shallow sites and may not be feasible for groundwater with high total dissolved solids (TDS) (Stroo, 2010 a).

iii) Biological treatment: a variety of microbial mechanisms have been employed, including aerobic oxidation, anaerobic reductive dechlorination, cometabolic biodegradation, anaerobic oxidation and phytoremediation strategies. (Stroo, 2010 a).

2.2.2 *In-situ* bioremediation

The development of environmental friendly, cost-effective, and reliable cleanup options is a priority to tackle the worldwide contamination by TCE. Compared to physical and chemical treatment technologies which were prevalent during 1980s to 1990s (U.S.EPA 2007; Stroo, 2010 a), *in situ* bioremediation is a promising alternative approach to reach the ecotoxicological-safety endpoint by (i) reducing the concentration of TCE below the MCL and (ii) circumventing the accumulation of toxic TCE metabolites, i.e. dichloroethene isomers (e.g., *cis*-DCE) and vinyl chloride (VC). Indeed, the versatility and ubiquity of microorganisms make them interesting candidates to support *in situ* remediation options (Mackay and Cherry 1989; Amann *et al*., 1995; Isken and de Bont 1998). As of 2009, bioremediation has become the most common technology used in remediating polluted groundwater (Pandey *et al*., 2009).

2.3 Microorganisms used in reductive dechlorination

Various microorganisms are able to catalyze the degradation of chlorinated compounds. Numerous studies have been carried out to enrich and isolate these organisms and they have been the subjects of several reviews in the literature (e.g. Bhatt *et al*., 2007). Although a few bacteria have been characterized for the ability to use VC and *cis*-DCE as carbon and energy sources (Coleman *et al*., 2002; Mattes *et al*., 2005) under aerobic conditions, no bacterial isolate has been identified so far that metabolically oxidizes TCE or PCE. In addition, several bacteria that are capable of oxidizing toluene, methane, and ammonia can also oxidize TCE, DCE and VC through cometabolic processes. Cometabolism is a fortuitous process in which microorganisms degrade a chemical in the presence of a primary growth substrate by taking advantage of broad-substrate, promiscuous enzymes (e.g. oxygenases) (Alvarez-Cohen *et al*., 1992; Hopkins *et al*., 1993; Krumme *et al*., 1993). However, aerobic co-metabolism has proven to be difficult to implement *in situ* because of (i) the potential toxicity of the byproducts to the microorganisms responsible for biodegradation, (ii) the challenges associated with *in situ* injection of optimal concentrations of oxygen and the cometabolic substrate and (iii) potential clogging problems due to biomass growth (Hopkins and McCarty 1995).

In contrast, under anaerobic conditions, specific microorganisms have been reported to catalyze the reductive dechlorination of PCE and TCE to less chlorinated compounds, such as *Desulfitobacterium* (Magli *et al*., 1996; Suyama *et al*., 2001), *Geobacter* (Sung *et al*., 2006, *Desulfuromonas* (Löffler *et al*., 2000), *Dehalobacter* (Holliger *et al*., 1998), as well as *Dehalococcoides* (Maymó-Gatell *et al*., 1999). Because many contaminated subsurface environments are anoxic or anaerobic, using the degradative potential of anaerobic dechlorinators that grow in the absence of oxygen for *in situ* bioremediation is of high interest. Among these dehalorespiring species, *Dehalcoccoides mccartyi* (*D. mccartyi*) is the only known bacterium that can reductively dechlorinate PCE all the way to the benign end product ethene (Fig. 2-2).

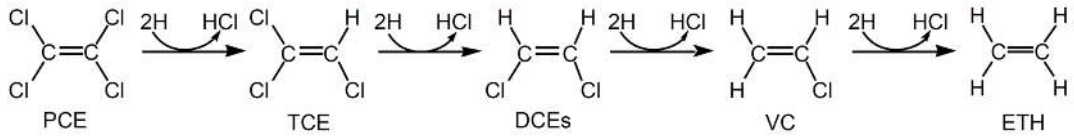

Figure 2-2 Reductive dechlorination pathway of chloroethenes (Maymó-Gatell *et al*., 1997) PCE: perchloroethene; TCE: trichloroethene; DCEs: dichloroethenes; VC: vinyl chloride; ETH: ethene

2.4 Phylogeny, Morphology and Physiology of *Dehalococcoides* species

2.4.1 Phylogeny

The first isolated strain that was able to reductively dechlorinate PCE to VC, ethene and inorganic chloride was originally designated "*Dehalococcoides ethenogenes* 195" (Maymó-Gatell *et al.*, 1997). Subsequently, more "*Dehalococcoides*" strains were isolated from digester sludge, contaminated aquifers, river sediment and even freshwater locations (Löffler *et al.*, 2013). The name "*Dehalococcoides*" has been used extensively in the literature and the genus of "*Dehalococcoides*" was informally introduced to accommodate organohalide-respiring bacteria related to strain 195. In 2013, a formal taxonomic description of the genus *Dehaloccoides* was proposed (Löffler *et al.*, 2013). Based on 16S rRNA phylogeny, the isolated strains were shown to be affiliated with the phylum *Chloroflexi* within the domain *Bacteria*, that included six major lineages: *Anaerolineae*, *Caldilineae*, the marine SAR202 cluster, "traditional" *Chloroflexi*, *Thermomicrobia* with *Dehalococcoides* proposed to be the new genus, and *Dehalococcoides mccartyi* (*D. mccartyi*) as the type species to accommodate the new isolates (Löffler *et al.*, 2013). Table 2-2 summarized the pure *D. mccartyi* cultures that have been sequenced to date and reported in the literature. Three phylogenetic subgroups of *D. mccartyi* were distinguished based on sequencing signatures in the hyper-variable V2 and V6 regions of the 16S rRNA gene (Hendrickson *et al*. 2002). The 'Cornell' subgroup includes strain 195, strain ANAS1, strain ANAS2 and strain MB (Maymó-Gatell *et al*., 1997; Cheng and He, 2009; Lee *et al*., 2011). Subgroup 'Victoria' includes strain VS and subgroup 'Pinellas' includes other *D. mccartyi* strains, such as strain CBDB1 (Adrian *et al*., 2000), strain BAV1 (He *et al.,* 2003), strain GT (Sung *et al.,* 2006) and strain FL2 (He *et al*., 2005).

D. mccartyi strains possess highly similar 16S rRNA gene sequences, sharing greater than 98% sequence identity (Cupples, 2008; Ritalahti *et al.*, 2006). However, strains (within the same subgroup) that share identical 16S rRNA gene sequences can exhibit distinct dechlorination activities. For example, strain MB, strain ANAS1 and strain ANAS2 share identical 16S rRNA gene sequences with strain 195, but MB can only metabolize PCE and TCE to *trans*-DCE (Cheng and He, 2009), while ANAS1 can metabolize TCE to VC, and ANAS2 can metabolize VC to ethene (Lee *et al*., 2011). Another example is strain BAV1 and strain KS-1 that share identical 16S rRNA sequences, but KS-1 can't grow on chlorinated ethenes (Ritalahti and Löffler, 2004). The discrepancy of 16S rRNA gene sequence identity and dechlorination activity indicates that 16S rRNA based analysis is insufficient to infer dechlorination activity, and this fact has triggered the need to search for process-specific biomarkers for reductive dechlorination.

Table 2-2 Typical parameters of pure *D.mccartyi* strains that are able to metabolicly and co-metabolicly reduce chlorinated ethenes

Strain	Metabolized chlorinated ethenes	Major product	Co-metabolized chlorinated ethenes	Known RDase genes involved	Reference
195	PCE, TCE, *cis*-DCE, 1,1-DCE	VC, ETH	*trans*-DCE, VC	*pceA* (PCE→TCE), *tceA* (TCE→VC)	Maymó-Gatell *et al.*, 1997
CBDB1	PCE, TCE	*trans*-DCE (*cis*-DCE)	None	N/A	Adrian *et al.*, 2000
BAV1	*cis*-DCE, *trans*-DCE, 1, 1-DCE, VC	ETH	PCE, TCE	*bvcA* (DCEs, VC → ethene)	He *et al.*, 2003
VS	TCE, *cis*-DCE, 1,1-DCE, VC	ETH	None	*vcrA* (DCEs, VC → ethene)	Müller *et al.*, 2004
FL2	TCE, *cis*-DCE, *trans*-DCE	VC, ETH	PCE, VC	*tceA* (TCE→VC)	He *et al.*, 2005
GT	TCE, *cis*-DCE, 1,1-DCE, VC	ETH	None	*vcrA* (DCEs, VC → ethene)	Sung *et al.*, 2006
MB	PCE, TCE	*Trans*-DCE	None	N/A	Cheng *et al.*, 2009
ANAS1	TCE, *cis*-DCE, 1,1-DCE	VC, ethene	VC	*tceA* (TCE → VC)	Lee *et al.*, 2011
ANAS2	TCE, *cis*-DCE, 1,1-DCE, VC	Ethene	None	*vcrA* (DCEs, VC → ethene)	Lee *et al.*, 2011
BTF08	PCE, TCE,VC	Ethene	None	*pceA* (PCE→TCE), *tceA* (TCE→VC)*vcrA* (DCEs, VC → ethene)	Pöritz *et al.*, 2013

2.4.2 Morphology

D. mccartyi cells are among the smallest described bacteria (Duhamel *et al.*, 2004). Electron microscope analysis revealed a spherical, disc-shaped morphology about 0.5~1 μm in diameter and 0.1~0.2 μm thick with characteristic biconcave indentation on opposite flat sides of the cell (Maymó-Gatell *et al.*, 1997; Adrian *et al.*, 2000; He *et al.*, 2003), with a cell weight of about 4.2×10^{-15} g cell^{-1} (Duhamel *et al.*, 2004). The small size and disc-shape of *D. mccartyi* maximize their surface area-to-volume ratio, which could aid in scavenging scarce metabolites, such as hydrogen, vitamins and chlorinated solvents. The turbidity of *D. mccartyi* pure cultures is very low even at the highest achieved cell concentrations (10^6~10^8 cells per mL). Therefore optical density measurements are not applicable for monitoring the cell growth.

Unusual cell surface features, such as filamentous appendages, were observed by scanning electron microscopy (He *et al.*, 2003), however the function of the appendages is unclear. They may play a role in attachment of cells to each other or to surfaces as observed in laboratory and field studies (Lendvay *et al.*, 2003; Amos *et al.*, 2009). In engineered dechlorinating systems, *D. mccartyi* species have been detected within biofilms and bioflocs of dechlorinating communities (Chung *et al.*, 2008; Rowe *et al.*, 2008). *D. mccartyi* cells are non-motile and non-spore forming, dechlorination or cell growth is not affected by vancomycin or ampicillin addition. Since these antibiotics generally interfere with peptidoglycan biosynthesis, this finding suggested that *D. mccartyi* has an unusual cell-wall structure. Staining of strain 195 confirmed the lack of a peptidoglycan cell wall and transmission electron micrographs revealed the presence of an S-layer protein structure that is commonly found in Archaea. Morris *et al.* proposed a 105-110 kDa Protein (DET1407) to be an S-layer component (Morris *et al.*, 2006).

2.4.3 Physiology

D. mccartyi are strict hydrogenotrophs that require hydrogen as an electron donor and acetate with carbon dioxide as carbon sources for growth (Tang *et al*., 2009). Pure *D. mccartyi* strains grow slowly with a doubling time of 1 to 2 days at an optimum temperature of 35°C (Maymó-Gatell *et al.*, 1997). Various growth factors, such as hydrogen and cobalamin, are essential to its growth and reductive dechlorination performance (Yang *et al*., 1998; Löffler *et al*., 1999; He *et al*., 2007; Tang *et al*., 2009). Cell yields of the isolates range from 6.3×10^7 to 3.1×10^8 cells per µmole of chloride released (Löffler *et al.*, 2013). In addition, studies showed that the growth of *D. mccartyi* can decouple from the dechlorination reaction, suggesting that there might be other factors that limit the growth of this species (Johnson *et al.*, 2008).

Dechlorination and growth occur at pH's between 6 and 8, with highest activity measured between 6.9 and 7.5 (Robinson *et al*., 2009). Oxygen exposure irreversibly inhibits dechlorination, growth and viability (Amos *et al*., 2008). Temperature effects on dechlorination have been investigated in the range of 4~45 °C. Optimum growth occurs at temperatures of 30~34°C, while 45 °C results in complete loss of dechlorination activity (Fletcher *et al*., 2010). However cultures stored at 4°C or room temperature for several months can recover dechlorination activity after a long lag phase (Delgado *et al*., 2014).

2.5 Microbial ecology of *D. mccartyi*-containing microbial communities

D. mccartyi exhibits specific restrictive metabolic requirements for a variety of exogenous compounds, such as hydrogen, acetate, corrinoids, biotin and thiamine, which can be supplied by other microbial genera through a complex metabolic network (Maymó-Gatell *et al*., 1997; He *et al*., 2007; Zhuang *et al*., 2011; Men *et al*., 2013; Yan *et al*., 2013; Schipp *et al*., 2013). Therefore, the growth of *D. mccartyi* is more robust within functionally-diverse microbial communities than in pure cultures (He *et al*., 2007; Ziv-El *et al*., 2011; Schipp *et al*., 2013). Previous studies have shown that *D. mccartyi* efficiently uses hydrogen as the sole electron donor for TCE dechlorination and out-competes other terminal electron-accepting processes such as methanogenesis and acetogenesis at low hydrogen partial pressures (Yang *et al*., 1998, Löffler *et al*., 1999). Laboratory enrichment cultures have been extensively studied for the past decades (Carr *et al*., 2000; Cupples *et al*., 2004; Yu *et al*., 2005; Freeborn *et al*., 2005; Duhamel *et al.*, 2007; Daprato *et al*., 2007; Ziv-El *et al.*, 2011). In order to better understand and predict the activity of reductive dechlorination in both laboratory enrichments and field-site communities, the metabolic and electron exchanges, as well as the effect of other terminal electron accepting processes (TEAPs) on reductive dechlorination need to be further investigated.

2.5.1 Metabolic and electron exchanges between *D. mccartyi* and supporting microorganisms

D. mccartyi strains are frequently detected in chlorinated solvent contaminated sites, and complete PCE/TCE biodegradation has only been observed at sites where *D. mccartyi* were present (Löffler, *et al*., 2010). In anaerobic communities, reducing equivalents can be transferred between microorganisms by shuttle components (e.g. H_2 and/or formate) through an interspecies electron transfer process (Stams and Plugge 2009). Interspecies hydrogen transfer is the process

by which organic compounds are degraded by the sequential interaction of several groups of microorganisms with closely coupled hydrogen production and consumption (Madigan and Martinko 2006). Besides shuttles components, direct interspecies electron transfer (DIET) has also been reported to occur in nature. E.g., *Geobacter* was found to be able to facilitate DIET with its syntrophic partners through conductive pili within cell aggregates (Summers *et al*., 2010; Shrestha *et al*., 2013). Syntrophy is defined as a nutritional situation in which two or more organisms combine their metabolic capabilities to mutual benefit, for example to catabolize a substrate that cannot be catabolized by either one of them alone. Interspecies hydrogen transfer is the canonical example of an essential electron flow between syntrophs and hydrogen utilizing microorganisms in anaerobic systems (Stams and Plugge 2009).

During groundwater bioremediation processes, primary electron donors (e.g., molasses, lactate or glucose) are often injected to the subsurface to stimulate dechlorination (Bhatt *et al*., 2007; Maphosa *et al*., 2010; Aulenta *et al*., 2011). Specific microorganisms (fermenting bacteria) first ferment the primary electron donors to hydrogen, acetate and/or other organic acids. *D. mccartyi* subsequently uses this hydrogen as electron donor and acetate as carbon source to dechlorinate TCE to ethene. Common fermentable organics used for dechlorinating community enrichment include lactate, methanol, propionate, and butyrate. (Duhamel *et al.*, 2004; Gu *et al.*, 2004; Freeborn *et al.*, 2005; Daprato *et al.*, 2007; Rowe *et al.*, 2008). The phylogenetic analyses of dechlorinating microbial communities have revealed organisms that were able to carry out fermentation including species from the genera *Acetobacterium*, *Bacteroidetes*, *Clostridium*, *Desulfovibrio*, *Eubacterium*, *Syntrophus*, *Spirochaetes*, and *Syntrophobacter* (Gu *et al.*, 2004; Duhamel and Edwards, 2006; Daprato *et al.*, 2007; Rowe *et al.*, 2008).

One possible explanation for the robust growth and faster dechlorination of *D. mccartyi* when growing in microbial communities than when grown in isolation is the efficient interspecies hydrogen transfer between *D. mccartyi* and syntrophs. He *et al*. (2007) successfully grew strain 195 with *Desulfovibrio desulfuricans* using lactate as the electron donor and obtained 1.5 times greater cell density of strain 195 in the co-culture than in the isolate. Men *et al*. (2012) showed that strain 195 can grow in a long-term sustainable syntrophic association with *Desulfovibrio vulgaris* Hildenborough (DvH) as a co-culture as well as with hydrogenotrophic methanogen *Methanobacterium congolense* (MC) as a tri-culture. The maximum dechlorination rates and cell yield of strain 195 were enhanced significantly in the defined consortia.

Cobalamin (vitamin B_{12}) is an important co-factor of reductive dehalogenase (RDases), and the other two classes of enzymes: isomerases and methyltransferases (Banerjee and Ragsdale, 2003; Seshadri *et al*., 2005). Only a small portion of prokaryotes (some Bacteria and Archaea) that require corrinoids are capable of corrinoid synthesis *de novo* (Martens *et al.*, 2002; Ryzhkova, 2003). The rest of the corrinoid-dependent microorganisms, like *D.mccartyi*, must rely on either exogenous corrinoids or transfer from corrinoid-synthesizing microorganisms. He *et al*. (2007) found strain 195 growth in defined medium could be optimized by providing high concentrations of vitamin B_{12} and that over the short term, the strain could grow to higher densities in co-cultures/tri-cultures with fermenters *Desulfovibrio desulfuricans* and/or *Acetobacterium woodii* that convert lactate to generate the required hydrogen and acetate. Yi *et al* (2012) found only specific corrinoids containing benzimidazole lower ligands could be used by strain 195. However, strain 195 was capable of remodeling other corrinoids by lower ligand replacement when a functional benzimidazole base was provided. Recent studies demonstrated

interspecies corrinoid transfer between *Geobacter lovleyi* and *D. mccartyi* strain BAV1 or strain FL2 (Yan *et al*., 2012) and interspecies cobamide transfer from a corrinoid-producing methanogen and acetogen to *D. mccartyi* (Yan *et al*., 2013). Men *et al*. (2014 a) discovered p-cresolylcobamide ([p-Cre]Cba) and cobalamin were the most abundant corrinoids in a dechlorinating microbial community, and 5,6-dimethylbenzimidazole (DMB, the lower ligand of cobalamin) played a key role in corrinoid remodeling (Men *et al*., 2014 a; Men *et al*., 2014b).

D. mccartyi genome analysis indicated that although a pathway for CO_2 fixation exists, several key components responsible for reduction of CO_2 to CO were missing (Seshadri *et al*., 2005). However, in microbial communities, CO can serve as an energy source for many anaerobic microorganisms (Oelgeschläger *et al*., 2008). Recently an unexpected syntrophic association has been discovered between carbon monoxide (CO)-producing strain 195 and CO-metabolizing anaerobe *Desulfovibrio vulgaris* Hildenborough (DvH), which enhances growth and dechlorination activity of strain 195 by preventing the accumulation of toxic CO as an obligate by-product from acetyl-CoA cleavage (Zhuang *et al*., 2014).

2.5.2 Competing Terminal Electron Accepting processes

Although interspecies H_2 transfer between syntrophs and *Dehalcoccoides* is the key process that controls the electron flow to drive reductive dechlorination in dechlorinating communities, reductive dechlorination only accounts for a small portion of electron flow during bioremediation (Yu and Semprini 2002; Ma *et al*., 2003; Lee *et al*., 2004). Other terminal electron accepting processes (TEAPs), such as methanogenesis, homoactogenesis, sulfate-reduction, iron-reduction, nitrate-reduction, and volatile fatty acids formation account for a large portion of the electron flow in the system. Since the reduction potentials of PCE (574 mV), TCE (527~550 mV), DCE (397~420 mV), and VC (450 mV) (Figure 2-3) are at similar levels to those occurring in common subsurface reducing environments (sulfate reducing, iron reducing etc.) (Dolfing and van Eekert, 2006), reductive dechlorination could potentially occur in various redox conditions, such as those enabling nitrate reduction, sulfate reduction, iron reduction and methanogenesis (Bradley and Chapelle *et al*., 2010).

Redox potentials are used to indicate the oxidation state of the system (Zehnder and Stumm, 1988). A successful way to classify the redox conditions in subsurface environments is to measure the presence of various compounds that have the potential to serve as electron acceptors, and (ideally) measure their reduced counterparts (Dolfing and van Eekert, 2006). Lovley and Goodwin (1988) proposed to use H_2 as an indicator of the terminal electron accepting reactions in subsurface and sedimentary environments. This approach may be effective for distinguishing between dominant TEAPs, such as methanogensis and sulfate reduction (Cord-Ruwisch *et al*., 1988). However, it is hard to distinguish between TEAPs that occur simultaneously, such as reductive dechlorination and sulfate reduction, since the favorable hydrogen range is similar for these processes (Lovley and Goodwin, 1988; Heimann *et al*., 2007). Although redox potential and Gibbs free energy are correlated by the equation $\Delta G^{0'}=-nF\Delta E^{0'}$ (Madigan *et al*., 2006), this relationship only indicates the potential for a reaction to occur. Physiologically, the minimum free energy threshold for any TEAP respiration is -20 KJ mol^{-1} (Schink *et al*., 1997). Therefore, calculations of Gibbs free energy can be useful for predicting the extent of ongoing biological reactions. Figure 2-4 shows a simplified scheme of the main

electron flows in a complex microbial community, and the trend of Gibbs free energy changes for different redox reactions.

Besides thermodynamics, kinetic constraints are also important factors that control the dechlorination performance, such as enzyme affinity of hydrogen, potential inhibition effects of the reduced products that may affect the activity of reductive dechlorination and the electron flow in a microbial community (Haston *et al*., 1999; Yu and Semprini, 2004; Sabalowsky *et al*., 2010). Contradictory results of sulfate effects on reductive dechlorination have been reported (Aulenta *et al*., 2008; Heimann *et al*., 2005; Azizian *et al*., 2008; Malaguerra *et al*., 2011). Furthermore the effect of iron reduction on dechlorination has not been thoroughly studied (Azizian *et al*., 2010; Wei *et al*., 2011; Malaguerra *et al*., 2011). Because of these complex and competing interactions, incomplete dechlorination, accumulation of chlorinated intermediates, poor correlation between biomarkers (e.g. 16S rRNA, reductive dehalogenases) and dechlorination activity are frequently reported in bioremediation practice (Lu *et al*., 2006).

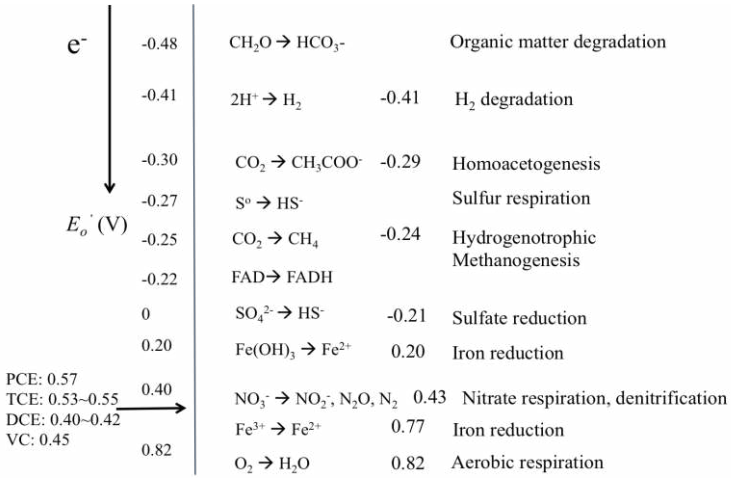

Figure 2-3 Microbiologically important reduction potentials (Madigan *et al*., 2006; Dolfing and van Eekert, 2006)

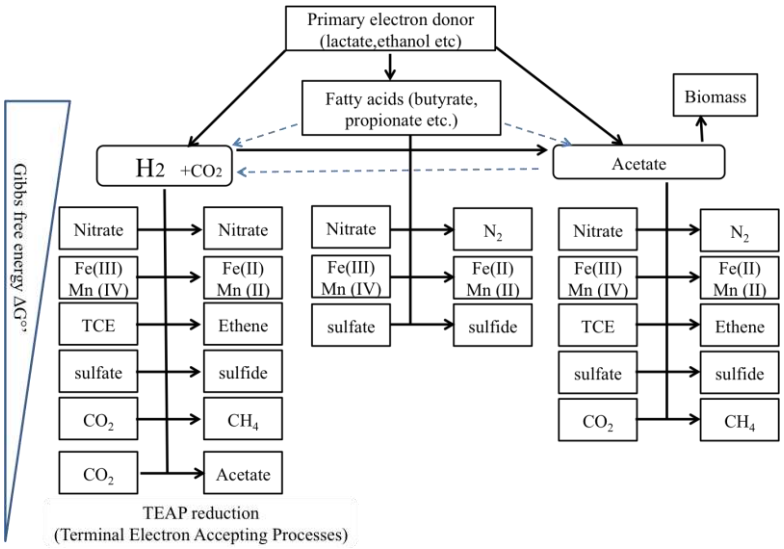

Figure 2-4 A simplified scheme showing the main electron flows in a complex dechlorinating community. The diagram is modified from the figure by Aulenta *et al*. (2006)

2.6 Methods for assessing *D. mccartyi*-containing microbial communities

2.6.1 Experimental systems used in laboratory studies.

In order to understand the community structure and function during reductive dechlorination processes, dechlorinating microbial communities have been enriched from various environments and have been extensively studied for the past decades (Carr *et al*., 2000; Cupples *et al*., 2004; Yu *et al*., 2005; Freeborn *et al*., 2005; Duhamel *et al.*, 2007; Daprato *et al*., 2007; Ziv-El *et al.*, 2011). However, most studies performed on dechlorinating communities have been performed under batch conditions at the lab scale. In contaminated subsurface environments, groundwater plumes are flow systems, where groundwater is continuously moving and the nutrients levels are relatively low compared to the DNAPL source zone (Stroo *et al*., 2010 a). Furthermore, the continuously changing environment (nutrient concentrations, microorganisms at different growth phases) in a batch reactor makes it difficult to interpret the results gained from both "-omics" studies and electron flow studies (Smith and Waltman, 2005).

There were a few approaches to characterize dechlorinating performance and community structure in flow systems, such as H_2 membrane-biofilm reactors (Chung *et al*., 2008), flow-through column studies (Azizian *et al*., 2008) or up-flow anaerobic sludge bed reactor (UASB) studies (Maphosa *et al*., 2010). While there have been a limited number of studies devoted to evaluating biological reductive dechlorination in continuous flow suspended growth systems (Gerritse *et al*., 1997; Carr *et al*., 2000; Drzyzga *et al*., 2001; Zheng *et al*., 2001; Sabalowsky *et al*., 2010). These studies showed that the hydraulic retention times and hydrogen concentrations in the reactor affected dechlorination activity in complex microbial communities. However, they all lack the information on the abundance, distribution or dynamics of key dechlorinating species.

Only a few studies in the literature have achieved successful and sustainable reductive dechlorination in continuous flow systems. Yang (1998) reported a hydrogen concentration range and threshold level that favors dehalogenators in competition with other possible hydrogen-utilizing microorganisms within a methanogenic mixed culture in a CMFR fed with PCE and benzoate (Yang and McCarty, 1998). Berggren *et al*. (2013) studied the effects of sulfate reduction on kinetics and microbial structure of a dechlorinating culture maintained in a chemostat. They found dechlorination efficiency decreased after complete sulfate reduction was achieved, and this phenomenon was associated with shifts in the *D. mccartyi* strain distribution in the microbial community. Delgado *et al*. (2013) reported the successful cultivation of a *D. mccartyi*-containing culture in a CMFR with a short three-day hydraulic retention time (HRT). They suggested that the low bicarbonate concentration (5 mM) in the medium minimized the electron flows to other microorganisms that use bicarbonate as electron acceptor and competition with *D. mccartyi* for H_2 as electron donor.

2.6.2 Molecular approaches (biomarkers, "omics" techniques)

16S rRNA based method

Microbial community structures, which include the identities of the different microorganisms that are present (Prosser *et al*., 2010), and key dehalorespiring microorganisms can be identified by using molecular biology tools, such as 16S rRNA gene clone libraries (Richardson *et al*., 2002; Men *et al.*, 2013), PCR-DGGE (denaturing gradient gel electrophoresis) (Madigan *et al*., 2006), T-RFLP (terminal-restriction fragment length polymorphism) (Richardson *et al*., 2002), high-throughput 16S rRNA-based microarray (He *et al*., 2007 b), high-throughput 16S rRNA sequencing (Ziv-El *et al*., 2011) and qPCR (quantitative PCR) analysis. qPCR provides us with information of abundance of detected species in the community with appropriate specific primers and probes (Cupples, 2008). In addition, fluorescence in situ hybridization (FISH) is a 16S rRNA gene based culture-independent method to study environmental communities without PCR bias (Su *et al.*, 2012). FISH techniques have been used to characterize dechlorinating community structures (Richardson *et al*. 2002) and for quantification of *D. mccartyi* species and Archaeal populations in culture bioflocs (Rowe *et al*., 2008).

Although 16S rRNA-based approaches can provide overall phylogenetic characterization of microorganisms in communities (Amann *et al*., 1995; Lovley *et al*., 2003), given that *D. mccartyi* strains with different dechlorinating capabilities share highly conserved 16S rRNA gene sequences (Ritalahti and Löffler, 2004; Cheng and He, 2009; Lee *et al*., 2011), it isn't possible to use this gene as a biomarker to indicate dechlorination activities. Consequently, the detection of *D. mccartyi* 16S rRNA gene alone does not demonstrate the metabolic capacities of interest (Da Silva *et al*.,2008). Therefore, it is necessary to target genes that are specific to the functions of interest in order to effectively monitor the activities of *D. mccartyi* and other microorganisms in the community.

Functional genes-based method

In order to overcome the limitation of 16S rRNA-based analysis, certain functional genes directly correlated with dechlorination activity were selected as biomarkers. Specifically, the RDase genes (*tce*A, *vcr*A, *pce*A, *bvc*A etc.) (Table 2-2) have typically been used to indicate dechlorination activities (Krajmalnik-Brown *et al*., 2004; Lee *et al*., 2006; Ritalahti *et al*., 2006). In addition, other process-specific functional genes were sought as biomarkers including hydrogenase genes (*hup, hym, hyc, ech and vhu*) (Marshall *et al*., 2012; Berggren *et al*., 2013). Other genes indirectly associated with reductive dechlorination, such as corrinoid related genes may also serve as a proxy for monitoring the actively dechlorinating microbial community (Löffler *et al*., 2013b).

Given that the presence of a gene does not necessarily mean that it is functional active, RNA samples are more often used to investigate the transcriptional level of the functional genes of interest. Whole genome microarrays (Johnson *et al.*, 2008; Lee *et al.*, 2011), as well as functional gene arrays (FGA), have been applied to investigate gene expression at different conditions. Specifically, microarrays targeting the whole genome of strain 195 and microarrays targeting four genomes of *D. mccartyi* strains (i.e. strain 195, CBDB1, BAV1, VS) have been applied to isolates, defined consortia and enrichment cultures, to investigate the effects of growth phase, B_{12} level, the presence of other syntrophic microorganisms on dechlorination and growth of *D.mccartyi* at a molecular level (Johnson *et al.*, 2008; West *et al.*, 2008; Johnson *et al.*, 2009; Hug *et al.*, 2011; Lee *et al.*, 2011; Men *et al*., 2014b).

GeoChip techniques (He *et al.*, 2007b; Tu *et al.,* 2014) have been developed and applied to study functional diversity, metabolic potential/ activities, microbial structure and dynamics of microbial communities from different habitats, such as soils, contaminated sites, extreme environments, and bioreactors (He *et al*., 2007b; He *et al*., 2012). Various GeoChip-based FGA studies have demonstrated that FGAs are a robust, powerful, high-throughput tool to specifically, sensitively and quantitatively profile microbial communities and link their composition and structure with environmental factors and ecosystem functioning (Taroncher-Oldenburg *et al.*, 2003; Miller *et al.*, 2008; Hazen *et al.*, 2010; Lu *et al.*, 2012). The latest version of Geochip 4 includes key genes involved in biogeochemical cycling of carbon, nitrogen, sulfur, phosphorus and metals, antibiotic resistance, organic remediation, stress responses and virulence (Tu *et al.*, 2014). The application of FGA can help to analyze biogeochemical processes and microbial responses to environmental perturbations, in order to comprehensively understand the function of the dechlorinating microbial community in bioremediation process.

Stable isotopes

Microarray technologies mentioned above can only target known genomes or functional gene sequences and can not detect those that do not have corresponding probes on the array. Therefore the identification of all functionally active microorganisms supporting the activity of *D. mccartyi* sp. is not possible using these techniques. Stable isotope probing (SIP) is an emerging technology that can provide the link between community structure and function. SIP uses stable-isotope-labeled carbon (^{13}C) substrates that are assimilated into metabolically active microorganisms followed by isopycnic separation and molecular analysis of labeled nucleic acids (DNA or RNA) to reveal phylogenetic and functional information about active community members (Neufeld *et al*., 2007).

DNA-SIP has been used for studying methanotrophs and methylotrophs, as those microorganisms were known to utilize single-carbon compounds as their sole carbon source (Radajewski *et al.*, 2000; Morris *et al.*, 2002). DNA-SIP has also been applied to determine the primary member of a complex community that is responsible for *in situ* naphthalene catabolism (Jeon *et al.*, 2003). RNA-SIP was used to identify bacteria that degrade phenol in an aerobic industrial bioreactor (Manefield *et al.*, 2002). These studies demonstrate that SIP techniques are powerful tools for identifying microorganisms that are actively involved in specific metabolic processes, such as those functionally active microorganisms involved in reductive dechlorination, under different environmental conditions.

"-omics" techniques by next generation sequencing (NGS) technologies

Metagenomics is a powerful tool for cultivation-independent assessment and exploitation of microbial communities present in complex ecosystems (Simon *et al*., 2011). With the employment of next-generation sequencing (NGS) techniques, large sequence data sets have been derived from various environments, with the majority exploited habitats from temperate environments, extreme environments, as well as contaminated environments (Ferrer *et al*., 2005; Dinsdale *et al*., 2008; Simon *et al*., 2009; Brisson *et al*., 2012). With the huge data sets obtained for metagenomic analysis, enormous taxonomic and functional diversity of environmental microbial communities can be explored. In order to assess the functional dynamics and

interactions of microbial communities, and to further link these physiological characteristics to environmental processes, metatranscriptomics, metaproteomics and metabolomics have also been developed (Leininger *et al*., 2006; Shi *et al*., 2009; Ram *et al*., 2005).

Typical NGS platforms used for metagenomics and metatranscriptomics include PCR-based 454 pyrosequencing, Illumina sequencing, SOLiD, Ion Torrent, as well as single-molecule (non-PCR) sequencing technologies, such as HeliScope and SMRT (Shokralla *et al.*, 2012). A summary of currently available next-generation sequencing (NGS) technologies is listed in table 2-3. Compared to traditional 16S rRNA gene sequencing approaches (i.e. DGGE, T-RFLP, Sanger sequencing etc.), pyrosequencing of 16S rRNA gene amplicons provides unprecedented sampling depth, and the sequencing time is relatively short. However, the intrinsic error rate of pyrosequencing may result in the overestimation of rare phylotypes (Sogin *et al*., 2006). The advantages of Illumina sequencing, such as more reads, higher sequencing output per run, lower cost per megabase sequencing output, accurate sequencing of homopolymer regions, make these "short-read" technologies the most well-suited to deep-coverage sequencing (Desai *et al.*, 2012; Scholz *et al.*, 2012). However, the short reads (36~150 bp) make read based analyses difficult, incomplete, or even impossible especially in situations where no reference sequence is available to align, assign and annotate the short sequences (Shokralla *et al.*, 2012; Scholz *et al.*, 2012).

Table 2-3 Summary of currently available next-generation sequencing (NGS) technologies[a]

NGS technologies	Platform	Read length (bp)	Max. number of reads/run	Sequencing output/run	Run time	Error rate
PCR-based	Roche 454	400-800	$(0.1\text{-}1) \times 10^6$	35-700 Mb	10-23h	1%
	Illumina HiSeq	100-200	$(3\text{-}6) \times 10^9$	≤ 270-600 Gb	8.5-11d	>0.1%
	Illumina MiSeq	100-150	7×10^6	≤ 1-2 Gb	19-27h	>0.1%
	SOLiD	35-75	$2.4\text{-}6 \times 10^9$	100-250 Gb	4-8d	>0.06%
	Ion Torrent	100-200	$1\text{-}11 \times 10^6$	≥ (10-1000) Mb	3.5-5.5h	1%
SMS	HeliScope	30-35	1×10^9	~20-28 Gb	≤ 1d	1%
(non-PCR)	SMRT	≥ 1500	50×10^3	~60-75 Mb	0.5h	15%

a. data are modified from table 1 Shokralla *et al.*, 2012 and table 1 Scholz *et al.*, 2012.

2.7 Methods for predicting the performance of *D. mccartyi*-containing microbial communities

A number of different modeling approaches have been used to describe reductive dechlorination, ranging from simple first-order sequential dechlorination to complex suite of modeling coupled kinetics, thermodynamic, self-inhibition, competitive-inhibition of other TEAPs, as well as bacterial growth. Most of the models developed in previous studies have been validated in lab scale batch studies by specific microbial enrichments, while very few models have been applied to predict the dechlorination performance at field sites (Malaguerra, 2011). The models reported in literature could be classified in two categories i) Modeling of reductive dechlorination; ii) Modeling of reductive dechlorination together with fermentation and other TEAPs.

2.7.1 Modeling of reductive dechlorination

First-order kinetics have often been assumed in field applications of bioremediation (Clement *et al*., 2000; Falta *et al*., 2008). This involves a simplified form of Monod-kinetics (equation 2.1), where C_i is the concentration of a chlorinated ethene in the liquid phase (µM) and k is the first order reaction rate constant (time^{-1})). The applicability of first-order kinetics is limited due to its over-simplification (Corapcioglu *et al*., 2004; Da Silva *et al*., 2008) since it is only valid for substrate concentrations well below the half-velocity constant. In addition, microbial growth and inhibition effects were not considered in this approach. Monod kinetics have most commonly been employed to describe sequential degradation of chlorinated ethenes (equation 2.2) with $K_{s,i}$ as the half-staturation constant (or the half velocity coefficient) of chlorinated ethene i (µM), $k_{max,i}$ as the maximum utilization rates of chlorinated ethene i (µmol cell^{-1} d^{-1}), X as the concentration of the dechlorinating microorganisms in the system (cell L^{-1}) When bacterial growth or decay is negligible, the biomass term is neglected and a form of Michaleis-Menten enzyme kinetics is used to describe microcosm experiments over short time periods (Haston and McCarty *et al*., 1999; Smatlak *et al*., 1996).

$$\frac{dC_i}{dt} = kC_i \tag{2.1}$$

$$\frac{dC_i}{dt} = \frac{k_i C_i X}{K_{S,i} + C_i} \tag{2.2}$$

Two types of inhibitions have been considered in previous studies: i) competitive inhibition (equation 2.3), where C_n is the liquid concentration of a competing chlorinated ethene n that poses a reversible inhibitory effect (µM), $K_{I,n}$ is the competitive inhibition constants for chlorinated ethene n (µM); and ii) self-inhibition (equation 2.4), where $K_{I,i}$ is the self-inhibition constant (µM). The mathematical expression of these inhibition kinetics are generally given as follows:

$$\frac{dC_i}{dt} = \frac{k_i C_i X}{K_{S,i}(1 + \sum\left(\frac{C_n}{K_{I,n}}\right) + C_i} \tag{2.3}$$

$$\frac{dC_i}{dt} = \frac{k_i C_i X}{K_{S,i} + C_i(1 + \frac{C_i}{K_{I,i}})} \tag{2.4}$$

Competitive inhibition occurs between the chlorinated ethenes, and the model is based on the assumption that a common enzyme is responsible for multiple dechlorinating steps. In most of the models reported, higher chlorinated ethenes tend to have inhibitory effects on lower chlorinated ethenes (i.e. PCE inhibits PCE to TCE degradation, TCE inhibits cis-DCE and VC degradation, cis-DCE inhibits VC to ethene degradation), while the other competitive inhibition processes were more scarcely reported in the literature (Clapp *et al*., 2004; Lee *et al*., 2004; Yu and Semprini 2004; Cupples *et al*., 2004; Yu *et al*., 2005; Amos *et al*., 2007; Huang and Becker 2009; Haest *et al*., 2010; Sabalowsky *et al*., 2010; Popat and Deshusses 2011). Self-inhibition and toxicity have been observed at higher chlorinated ethene concentrations, which correspond to the presence of dense non-aqueous phase liquids (DNAPLs) at the contamination source. The most common approach to integrate toxicity into models is based on Haldane inhibition kinetics (Rittmann and McCarty, 2001; Yu and Semprini, 2004). Other toxicity models, such as the log-logistic dose-response model (Hasest *et al*., 2010), and modified Haldane inhibition model considering enhanced biomass decay (Sabalowsky and Semprini, 2010) have also been developed to better fit the experimental data.

The Monod models describe bacterial growth associated with substrate degradation and cell decay according to equation 2.5, where X is the concentration of dechlorinating microorganisms in the system (cells L^{-1}), μ is the maximum growth rate (d^{-1}), and b is the endogenous cell decay coefficient (d^{-1}). Since different bacterial populations carry out different dechlorination steps, several biomass populations with different specific cell yields and decay coefficients have been used (Clapp *et al*., 2004; Lee *et al*., 2004; Christ and Abriola 2007; Haest *et al*., 2010). Donor limitation has rarely been considered except for Cupples *et al*., (2004), since the donor was usually provided in excess (in the form of H_2 or fermentation products). Later on when fermentation was considered together with dechlorination, donor limitation was incorporated in the modeling approaches.

$$\frac{dX}{dt} = \mu \frac{C_i X}{K_{S,i} + C_i} - bX \tag{2.5}$$

2.7.2 Modeling of reductive dechlorination together with fermentation and other TEAPs

Dechlorination often occurs very slowly and under electron donor, redox and nutrient limiting conditions in the subsurface. Meanwhile, other co-occurring reactions and different microbial populations besides dechlorinating bacteria exist in the subsurface, making reductive dechlorination only a part of a complex system of reactions (Figure 2-3). Therefore the dechlorination rates are affected by environmental conditions, such as fermentation of organic substrates, competition for hydrogen by other hydrogen reducers and methanogens, inhibition by geochemical conditions, etc. The influence of these processes on reductive dechlorination has been investigated by lab-scale experiments. Modeling approaches have also been applied to understand, quantify and predict these interactions (Chambon *et al*., 2013).

Fermentation

Various fatty acids, such as lactate, propionate, butyrate, benzoate, formate, ethanol, methanol, glucose and vegetable oils have been reported to sustain dechlorination to ethene (Stroo, 2010). Contradictory results have been reported for acetate as the sole electron donor for dechlorination to ethene (He *et al.*, 2002; Wei *et al.*, 2011) and incomplete dechlorination to cis-DCE (Lee *et al.*, 2007). Organic acids support dechlorination through the production of H_2 and acetate by fermentation. Considering the thermodynamic limitation of fermentation controlled by Gibbs free energy (Schink, 1997), a general modified monod- type equation was developed by Fennell (1998) which includes a thermodynamic control factor of product formation (H_2 and acetate) on the fermentation rate.

$$\frac{dC_{donor}}{dt} = \frac{-k_{donor} X_{donor} (S - S^*)}{K_{s,\,donor} + S}, \; (S\text{-}S^*) = S\,\Phi = S\left(1 - e^{\left(\frac{\Delta G_{rxn} - \Delta G_{critical}}{RT}\right)}\right) \tag{2.6}$$

C_{donor} is the concentration of the fermentable substrate in the system (μM), k_{donor} is the maximum specific rate of fermentable substrate degradation (μmol $cell^{-1}$ d^{-1}), $K_{s,donor}$ is the half velocity coefficient for the fermenting substrate (μM), X_{donor} is the biomass fermenting the substrate in the system (cell L^{-1}), and S is the concentration of fermenting substrate (μM). S^* is the hypothetical concentration of fermenting substrate that would result in ΔG_{rxn} (the free energy available from the fermentation) = $\Delta G_{critical}$ (some marginally negative free energy that the organisms must have available to live and grow), given the concentrations of all the other reactants and products. Φ is

a measure of the distance of the reaction from thermodynamic equilibrium (Fennell and Gossett, 1998). If the electron donor concentration is high relative to the concentration of the products of the reaction, the driving force is high and Φ approaches 1, so the fermentation reaction is limited primarily by intrinsic kinetics. As the reaction approaches equilibrium (i.e., donor concentration has decreased and H_2 and acetate have increased), the driving force is lessened and the value of Φ approaches zero, so the fermentation is limited primarily by thermodynamics.

Competing TEAPs

Competition with methanogenesis has been studied extensively in lab experiments. Studies have shown that methanogenesis accounted for most electron flows in some dechlorination communities (Lee *et al*., 2004; Men *et al*., 2011), but dechlorinators were generally assumed to out-compete methanogens at low H_2 concentration due to their higher affinity for hydrogen (Yang and McCarty 1998; Azizian *et al*., 2010). Therefore slow fermenting electron donors, such as propionate, butyrate or vegetable oils, which result in low hydrogen concentrations, were thought to favor dechlorination over methanogens (Fennell *et al*., 1997; Yang and McCarty 2000).

Other TEAPs, such as iron reduction and sulfate reduction have been less studied. Few studies have been carried out on the effects of iron reduction on dechlorination, and limited studies tested whether concomitant iron reduction and dechlorination can occur (Azizian *et al*., 2008;Wei *et al*., 2011). Model simulations predicted that a large percentage of electrons added to dechlorinating communities would go to iron reduction (Malaguerra *et al*., 2011). The results on the effects of sulfate on reductive dechlorination were inconsistent. Complete dechlorination was observed under sulfate reducing conditions at a slower rate (Aulenta *et al*., 2008; Heimann *et al*., 2005), while other studies showed complete sulfate reduction was necessary before dechlorination of *cis*-DCE could proceed (Azizian *et al*., 2008; Malaguerra *et al*., 2011). A review of sulfate concentration effects on reductive dechlorination showed that sulfate reduction could reduce dechlorination efficiency, leading to a delay of *cis*-DCE and VC dechlorination (Pantazidou *et al*., 2012). Berggren *et al*. (2013) reported that continuously feeding sulfate to a dechlorinating community in a chemostat could significantly change the community structure and adversely affect dechlorination performance. However, another study showed the addition of sulfate statistically enhanced dechlorination (Harkness *et al*., 2012). The toxicity and mechanism of sulfate occurance on dechlorination has not been comprehensively studied. The contradicting results illustrated the complexity of the processes involved in reductive dechlorination and the difficulties in charactering these reactions in models.

In complex models, the competition between electron acceptors has been characterized by using different approaches. Thermodynamic constraints were considered in some studies by introducing the H_2 threshold term to the Monod-type kinetics (Fennell and Gossett, 1998; Kouznetsova *et al*., 2010). Then the order in which different reactions proceed would be controlled by the H_2 threshold value. Another approach has been via a non-competitive inhibition term in redox reactions to characterize the competition. Reductive dechlorination has been reported to proceed at reduced rates under iron and sulfate reducting conditions, but at higher rates with higher H_2 levels (Widdowson *et al*., 2004; Malaguerra *et al*., 2011). .

Geochemical conditions

A pH decrease after biostimulation was frequently observed at field sites (AFCEE, 2004). pH inhibition might be an important process that affects reductive dechlorination in poorly buffered environments. Few studies have focused on the effect of groundwater pH (Robinson *et al*. 2009; Kouznetsova *et al*., 2010; Brovelli *et al*., 2012). In lab studies, well-buffered mineral media is usually used to grow microbial consortia. The effect of alkalinity changes on dechlorination has been sparsely studied and has not been incorporated into the modeling approaches. Delgado *et al*. (2014) reported that low bicarbonate concentrations (5 mM) minimized the electron flows to other microorganisms that use bicarbonate as electron acceptor and competition with *D. mccartyi* for H_2 as electron donor. Other geochemical processes, such as mineral dissolution and precipitation have been little studied, and the inhibitory effects of other existing species or reduction products on dechlorination are inadequately understood (Chambon*et al*., 2013).

2.7.3 Major findings and limitations

Among the existing models that simulate reductive dechlorination in groundwater plumes, only a few numerical models have been developed that simultaneously considered multiple parameters like fermentative substrates, electron donor limitation, dechlorination kinetics, non-chlorinated TEAPs competitions, and product self-inhibition (Bagley *et al*., 1998; Fennell and Gossett, 1998; Cupples *et al*., 2004; Lee *et al*., 2004; Berggren *et al*., 2013). A summary of some typical mathematical models published in the literature is listed in table 2-4.

Table 2-4 Mathematical models published in the literature [a]

Fermentable substrates	Nonchlorinated TEAPs	Reactor systems	Targeted contaminated zones	Biomass quantification (qPCR analysis)	References
Ethanol	Acetogenesis and methanogenesis	Batch reactor	DNAPL source zone and plume	/	Bagley, 1998
Pentanol	Methanogenesis	Packed column	DNAPL source zone	/	Christ, 2007
Butyrate, ethanol, lactate, propionate	Methanogenesis	Batch reactor	/	/	Fennell, 1998
Linoleic acid	Sulfate reduction	Batch reactor	DNAPL source zone	/	Kouznetsova,2010
Glucose	Methanogenesis	Batch reactor	/	/	Lee, 2004
Lactate	Sulfate and iron reduction, methanogenesis	Batch reactor	/	/	Malaguerra, 2011
Lactate, propionate and Newman Zone®[b]	Sulfate and iron reduction, methanogenesis	Batch and Field site	DNAPL source zone	/	Manoli, 2012
Linoleic acid, lactate, glucose, butyrate, methanol, ethanol, formate	Sulfate and iron reduction, methanogenesis	/	DNAPL source zone	/	Robinson, 2009
Yeast extract, butyrate	Acetoclastic and hydrogenotrophic methanogenesis	Fixed-volume, semi-batch fed reactor	DNAPL source zone	Yes	Heavner, 2013
Lactate	Sulfate reduction	Completely-mixed flow reactor	Groundwater plume	Yes	Berggren, 2013

a. Rows in grey highlight more comprehensive models that include environmentally-relevant conditions and/or qPCR-based biomass quantification.
b. Newman Zone emulsified vegetable oil (EVO) (Remediation and Natural Attenuation Services, Inc. (RNAS), Monterey, CA) provides electron donors to enhance *in-situ* bioremediation of chlorinated solvents. Newman Zone® contains both fast- and slow-release electron donors. All Newman Zone® formulations contain 46% soybean oil by weight (including linoleic acid) and 4% sodium lactate.

All of the models listed in Table 2-4 simulate and predict reductive dechlorination performance, and provide a fundamental basis to evaluate *in-situ* bioremediation processes. They describe the fermentation of organic substrates occurring simultaneously with the consumption of fermentation end products by different TEAPs, including reductive dechlorination, and therefore differ from most of the previous biogeochemical models (e.g., BIOCHLOR, BioRedox) (Rifai *et al.,* 2010), in which the contaminant is consumed via a sequence of electron acceptors (redox zonation). However, the intricate syntrophic associations within the dechlorinating microbial communities wherein multiple functional guilds cooperate or compete simultaneously are not well understood or adequately captured by the current models. Current gaps in understanding that impede progress in predictions of reductive dechlorination have been identified and are listed below.

1) ***Sensitive and accurate biomass quantification***.

The suitability and accuracy of developed models depend on the legitimate estimates of biomass for each specific functional group of microorganisms in the system. However, total biomass concentrations of the microbial community are commonly assessed by volatile suspended solid measurements (mg VSS) or protein masses (mg protein), which don't represent the activity of specific groups of bacteria in the system without significant biases (Bagley *et al*., 1998; Haston *et al*., 1999; Yu *et al*., 2005). This may also lead to an underestimation of k_{max} values (maximum specific substrate consumption rates for dechlorination) due to an overestimation of the active concentration of dechlorinating biomass (Bagley *et al*. 1998) (their proportion among the total biomass depending on numerous factors such the level of enrichment of the community or the feed cycle). Furthermore, most models normalize the k_{max} values to the total mixed culture biomass (Yu *et al*., 2005). A few studies calculated cell concentrations by using data previously reported in the literature, such as biomass yield (mg of VSS μmol^{-1} substrate consumed, mg protein μmol^{-1} chloride ions) (Fennell and Gossett, 1998; Bagley *et al*., 1998; Yu *et al*., 2005). While total biomass concentrations can be estimated using this approach, the fractions of biomass and the concentrations of individual populations, i.e., dechlorinators, fermenters, etc., are generally estimated using an analysis of steady-state influent and effluent concentrations of individual substrates and reported biomass yields (Fennell and Gossett, 1998). This makes the accuracies of the estimated distributions of total biomass among various microbial groups unknown. Other models incorporate product formation rates ($\mu mol\ L^{-1}\ d^{-1}$) and the maximum utilization coefficient ($\mu mol\ cell^{-1}\ d^{-1}$) previously determined for a specific dechlorinating bacterial isolate (Cupples *et al*., 2004) or biomass concentrations by calculating the theoretical biomass production based on thermodynamic and bioenergetic principles ($C_5H_7O_2N$ is the empirical formula of microbial dry matter (i.e., VSS)) (Malaguerra *et al*., 2011).

2) ***Discrimination of dechlorinating populations***.

The modeling of PCE/TCE dechlorination kinetics does not discriminate the different dechlorinating microbial populations present in the system whereas different dechlorinators can be responsible for different reductive steps of the process.

3) ***Inhibition constants***.

The inhibition kinetics of chlorinated compounds on reductive dechlorination processes is still not clear and competitive inhibition and/or substrate inhibition (self-inhibition) occurring among TCE and the intermediates needs to be further studied and to be adequately incorporated in models (Malaguerra *et al*., 2011).

4) ***Competitive TEAPs***.

Reductive dechlorination only accounts for a small portion of the electron flow occurring in the dechlorinating microbial communities that include a variety of non-*D.mccartyi* H_2-utilizing microorganisms (e.g., hydrogenotrophic methanogens and homoacetogens). Other terminal electron accepting processes (TEAPs), such as sulfate reduction, iron reduction, nitrate reduction, and volatile fatty acids formation (e.g., fermentation, acetogenesis), account for a large portion of the electron flow in the system. Methanogenesis is often considered to be a

competitive TEAP in the model simulations, while the competition among other non-chlorinated TEAPs such as sulfate reduction, homoacetogenesis, iron reduction or dechlorination by non-*D.mccartyi* dehalorespiring species also need to be incorporated into the predictive model (Lee *et al*., 2004; Duhamel *et al*., 2007; Wei *et al*., 2011). The electron flow of acetate to acetoclastic methanogens has been less well studied, while measurements of methane in some highly methanogenic habitats (e.g., sewage sludge) have shown that about two-thirds of the generated methane originated from acetate (Madigan *et al*., 2009).

5) ***Relevance of culture conditions***.

Although all of the models listed in the Table 2-4 have been applied to dechlorinating microbial communities, the majority of these studies have been carried out under batch conditions which generate a continuously changing environment (nutrient concentrations, microorganisms at different growth phases, etc.) making difficult the interpretability of laboratory measurements and decreasing the relevance of the experimental data to knowledge of microorganisms in flow-through sites. Besides batch studies, a few approaches have been used to characterize the dechlorinating performance and community structure in flow systems, such as H_2 membrane-biofilm reactors (Chung *et al*., 2008) or flow-through column studies (Azizian *et al*., 2008; Azizian *et al*., 2010; Maphosa *et al*., 2010). Only a few studies have been devoted to evaluating biological reductive dechlorination in continuous flow suspended growth systems (Berggren *et al*., 2013; Carr *et al*., 2000; Gerritse *et al*., 1997; Sabalowsky *et al*., 2010; Yang *et al*., 1998; Zheng *et al*., 2001). Although these studies highlight the effects of the hydraulic retention times and hydrogen concentrations in the reactor on dechlorination rates exhibited by complex microbial communities, kinetic studies and mechanistic mathematical modeling of the electron flows in such systems have not been carried out.

6) ***Target contaminated zones***.

Most of models presented in the Table 2-4 target bioremediation of DNAPL source zones whereas there is a renewed focus on bioremediation of TCE-contaminated groundwater plumes where contaminant concentrations are generally relatively low under continuous flow conditions (Stroo, 2010).

2.8 Summary

Although there have been many previous studies of dechlorinating microbial communities (Carr *et al.*, 2000; Cupples *et al.*, 2004; Freeborn *et al*., 2005; Duhamel and Edwards, 2006; Daprato *et al*., 2007; Behrens *et al*., 2008), the specific details of electron flows in these communities, as well as those in bioremediation processes are still unclear and difficult to predict due to the complexity of the involved microbial communities. Compared to the relatively well-characterized anaerobic wastewater treatment process (Rodriguez *et al*., 2009), quantitative electron flows in dechlorinating communities that affect bioremediation efficiency are still ill defined (He *et al*., 2007; Stroo *et al*., 2010).

Improved understanding of complex microbial communities can be achieved using tools from molecular biology, such as metagenomics, transcriptomics, proteomics, or metabolomics. These high-throughput technologies have been applied to many microbial ecology studies

(Stenuit *et al*., 2008; West *et al*., 2008; Wang *et al*., 2009) to obtain a holistic understanding of complex microbial communities that respond to environmental changes/stresses by intricate, multi-level regulation mechanisms (Hoskisson and Hobbs, 2005). With the application of emerging molecular techniques to study TCE-dechlorinating microbial communities under different remediation conditions, the development of mathematical models to predict the microbial growth and metabolism can be envisaged. Particularly, using the physiological characteristics of constructed TCE-dechlorinating consortia and TCE-dechlorinating complex microbial communities, we predict the electron flows among species in the system. Future development and application of models that predict electron flow in microbial communities involved in *in situ* bioremediation requires understanding the mechanisms that govern the activity and syntrophy of the dechlorinating systems. Therefore a systems-level understanding of electron flow in dechlorinating microbial communities is needed.

3 Efficient metabolic exchange and electron transfer within a syntrophic TCE degrading co-culture of *Dehalococcoides mccartyi* 195 and *Syntrophomonas wolfei*

3.1 Introduction

Groundwater contamination by trichloroethene (TCE), a potential human carcinogen, poses a serious threat to human health and can lead to the generation of vinyl chloride (VC), which is a known human carcinogen (Maymó-Gatell *et al*., 1997). Strains of *Dehalococcoides mccartyi* are the only known bacteria that can completely degrade TCE to the benign end product ethene. Biostimulation of indigenous *Dehalococcoides* sp. and bioaugmentation using *Dehalococcoides*-containing cultures are recognized as the most reliable *in situ* bioremediation technologies resulting in complete dechlorination of TCE to ethene (Stroo *et al*., 2010). However, the mechanisms that regulate the activity of *D. mccartyi* within natural ecosystems and shape its functional robustness under disturbed environments are poorly understood due to multi-scale microbial community complexity and heterogeneity of biogeochemical processes involved in the sequential degradation (Lu *et al*., 2006; Lee *et al*., 2011). *D. mccartyi* exhibits specific restrictive metabolic requirements for a variety of exogenous compounds, such as hydrogen, acetate, corrinoids, biotin and thiamine, which can be supplied by other microbial genera through a complex metabolic network (Maymó-Gatell *et al*., 1997; He *et al*., 2007; Men *et al*., 2013; Yan *et al*., 2013; Schipp *et al*., 2013). Therefore, the growth of *D. mccartyi* is more robust within functionally-diverse microbial communities than in pure cultures (He *et al*., 2007; Ziv-El *et al*., 2011; Schipp 2013). Previous studies have shown that *D. mccartyi* efficiently uses hydrogen as its sole electron donor for TCE dechlorination and out-competes other terminal electron-accepting processes such as methanogenesis and acetogenesis at low hydrogen partial pressures (Yang *et al*., 1998, Löffler *et al*., 1999). Interspecies hydrogen transfer between *D. mccartyi* and supportive organisms is a key process of electron flow that drives reductive dechlorination in the environment. Although dechlorinating microbial communities have been extensively studied over the past decades (Yang *et al*., 1998; Duhamel *et al*., 2002; Rowe *et al*., 2008; Lee *et al*., 2011), community assembly processes in the highly specialized ecological niche of *Dehalococcoides* and the network of interactions between *D. mccartyi*, its syntrophic partners and other co-existing community members have yet to be deciphered. The optimization of *D. mccartyi*-based bioremediation systems to treat TCE-contaminated groundwater would be facilitated by a systems-level understanding of interspecies electron, energy and metabolite transfers that shape the structural and functional robustness of TCE-dechlorinating microbial communities.

To date, only a few studies of *D. mccartyi*-containing constructed co-cultures/tri-cultures have been published (He *et al*., 2007; Cheng *et al*., 2010; Men *et al*., 2011; Yan *et al*., 2012; Yan et al., 2013). A study with *D. mccartyi* 195 (strain 195) revealed that its growth in defined medium could be optimized by providing high concentrations of vitamin B_{12} and that over the short term, the strain could be grown to higher densities in co-cultures/tri-cultures with fermenters *Desulfovibrio desulfuricans* and/or *Acetobacterium woodii* that convert lactate to generate the hydrogen and acetate required by *D. mccartyi* (He *et al*., 2007). Recent studies demonstrated interspecies corrinoid transfer between *Geobacter lovleyi* and *D. mccartyi* strains BAV1 and FL2 (Yan *et al*., 2012) and interspecies cobamide transfer from a corrinoid-producing methanogen and acetogen to *D. mccartyi* (Yan *et al*., 2013). Another study showed that strain 195 can grow in a long-term sustainable syntrophic association with *Desulfovibrio vulgaris* Hildenborough (DvH) as a co-culture as well as with hydrogenotrophic methanogen *Methanobacterium congolense* (MC) as a tri-culture (Men *et al*., 2011). The maximum

dechlorination rates and cell yield of strain 195 were enhanced significantly in the defined consortia. Another unexpected syntrophic association has recently been discovered between carbon monoxide (CO)-producing strain 195 and CO-metabolizing anaerobes which enhance the growth and dechlorination activity of strain 195 by preventing the accumulation of toxic CO as an obligate by-product from acetyl-CoA cleavage (Zhuang *et al*., 2014). Although these studies demonstrated the robust growth of *D. mccartyi*-containing co-cultures on PCE/TCE with higher dechlorination activity and cell yields than isolates, a clear and mechanistic understanding of metabolic cross-feeding and electron transfer between *D. mccartyi* and its syntrophic partner(s) is needed to establish predictive models for dechlorination activity.

Butyrate fermentation is an endergonic reaction under standard conditions (Table 3-1) that can only be carried out for energy generation by syntrophic microorganisms growing with H_2 consumers (Jin, 2007; Sieber *et al*., 2010; Stams *et al*., 2012). *Syntrophomonas wolfei* is a model butyrate fermenter that grows syntrophically with hydrogenotrophic methanogens (McInerney *et al*., 1981; Sieber *et al*., 2010). *S. wolfei* can also grow without a syntrophic partner on crotonate as the sole energy source through its disproportionation to acetate and butyrate (Table 3-1) (Beaty *et al*., 1987). In previous studies, *Syntrophomonas spp*. have been detected in butyrate-fed dechlorinating enrichment cultures in significant relative abundance (Freeborn *et al*., 2005; Rowe *et al*., 2008). In this study, a TCE and butyrate-fed syntrophic co-culture of *D. mccartyi* strain 195 (strain 195) with *S. wolfei* was established and maintained to study the physiology and transcriptome of syntrophically growing *D. mccarty*. Spatial architecture and the physical proximity of the cells were also analyzed in the co-culture *S. wolfei*/strain 195 and another syntrophic co-culture DvH/strain 195. The knowledge gained from this study provides us with a more fundamental understanding of the metabolic exchange and energy transfer among the key players of TCE-dechlorinating communities.

Table 3-1 Stoichiometry reactions in the co-culture.

Process	Redox reaction	ΔGo' kJ/mola	No.
Crotonate oxidation and reduction	$2C_4H_5O_2^- + 2H_2O \rightarrow 2C_2H_3O_2^- + C_4H_7O_2^- + H^+$	-350	1
Butyrate fermentation reaction	$C_4H_7O_2^- + 2H_2O \rightarrow 2C_2H_3O_2^- + H^+ + 2H_2$	46.9[a]	2
TCE reduction to *cis*-DCE	$C_2HCl_3 + H_2 \rightarrow C_2H_2Cl_2 + H^+ + Cl^-$	-133	3
cis-DCE reduction to VC	$C_2H_2Cl_2 + H_2 \rightarrow C_2H_3Cl + H^+ + Cl^-$	-144	4
VC reduction to ETH	$C_2H_3Cl + H_2 \rightarrow C_2H_4 + H^+ + Cl^-$	-154	5

a. $\Delta G^{o'}$ was corrected to 307.15K

3.2 Materials and Methods

3.2.1 Chemicals

TCE, *cis*-dichloroethene (*cis*-DCE), and vinyl chloride (VC), were purchased from Sigma-Aldrich-Fluka (St. Louis, MO) or Supelco (Bellefonte, PA). Ethene was obtained from Alltech Associates, Inc. (Deerfield, IL). Vitamin B_{12} was obtained from Sigma-Aldrich-Fluka (St. Louis, MO).

3.2.2 Bacterial co-cultures and growth conditions

Culture set-up and maintenance

Bacterial co-cultures of strain 195 and *S. wolfei* (5% vol/vol inoculation of each bacterium) were initially established in 160 mL serum bottles containing 100 mL defined medium (5) with TCE supplied at a liquid concentration of 0.6 mM (corresponding to 78 µmol TCE per bottle), 10 mM crotonic acid, 100 µg L^{-1} vitamin B_{12} and N_2/CO_2 (90:10 v/v) headspace at 34 °C with no agitation. Cultures were subsequently transferred (5% vol/vol inoculation) for growth on 4 mM butyric acid with 0.6 mM TCE as the electron acceptor. The established syntrophic co-culture was continuously and stably maintained on butyrate in 100 mL defined medium over 45 sub-culturing events before the experiments were performed. The electron donor-limited condition (on a hydrogen production/consumption basis) was achieved by feeding the co-culture 0.25 mM butyrate (25 µmol per bottle that could theoretically generate 50 µmol H_2 based on stoichiometry) and 0.6 mM TCE (78 µmol per bottle that requires 234 µmol H_2 to reductively dechlorinate TCE to ethene). The strain 195 isolate was grown in defined medium with H_2/CO_2 (90:10 v/v) headspace, 0.6 mM TCE as electron acceptor and 2 mM acetate as carbon source. Pure *S. wolfei* was grown on crotonate in 160 mL serum bottles as described previously (Beaty *et al*., 1987). Co-culture DvH and strain 195 were grown in the same medium with the substitutions of 5 mM lactate. Pure culture and co-culture purities were routinely checked by phase-contrast microscopy and DGGE (Denaturing Gradient Gel Electrophoresis).

H_2 threshold determination

The method used to determine H_2 threshold in the co-culture was based on the method described in previous study (Löffler *et al*., 1999). Briefly, triplicate 100-mL co-cultures were inoculated (2%, vol/vol) from active dechlorinating cultures that had completely reduced all of the TCE present to ethene. One set of the triplicate cultures were amended with 7 µL neat TCE (~ 78 µmol), and 25 µL 1M butyrate stock solution (0.25 mM butyrate) while the other set did not receive an electron acceptor. The concentrations of chlorinated compounds were determined weekly, and the H_2 concentration was measured accordingly. Values for H_2 threshold were assessed when the H_2 concentration remained stable.

3.2.3 Analytical methods

Chloroethenes, ethene and methane were measured by FID-gas chromatograph using 100 µL headspace samples as described previously (Freeborn *et al*., 2005; Lee *et al*., 2006). Hydrogen (H_2) and carbon monoxide (CO) were measured on a RGA5 Reduction Gas chromatography (Trace Analytical, Menlo Park, USA) with a 60/80 mesh pre-column with a 60/80 molecular sieve 5A column and a reduction gas detector (RGD) at temperature 264 °C and column temperature 104°C. Ultra-high purity N_2 gas (99.999%) was used as carrier gas at flow rate of about 25 mL/min. The identification of hydrogen and carbon monoxide were based on the reactions:

$$H_2 + HgO \rightarrow H_2O + Hg_{(gas)}$$
$$CO + HgO \rightarrow CO_2 + Hg_{(gas)}$$

Where mercury vapor was generated from a mercuric oxide bed, and the mercury vapor was detected by adsorption in the UV part of the spectrum. 300 µL headspace sample was collected and injected into a 100 µL sample loop. Samples with greater than 100ppmv H_2 were diluted

with H_2-free N_2 before injection. A 17 mL serum tube with black stopper was used for dilution. The tube was first flushed with H_2-free N_2, and the dilutions were done immediately before analysis. Mass of each compound measured by GC was calculated based on gas/liquid equilibrium by using Henry's law constants at 34°C according to: mass (μmol/bottle) = $C_l \times V_l + C_g \times V_g$, $k_H^{cc} = C_l / C_g$. C_l: liquid phase concentration (μM); V_l : volume of liquid phase (L); C_g: gas phase concentration (μM); V_g: volume of gas phase (L); k_H^{cc} : Henry's law constant (unitless). Organic acids, including butyrate and acetate, were analyzed with a high-performance liquid chromatograph as described previously (Freeborn *et al*., 2005).

3.2.4 Scanning electron microscope

The co-cultures (*S.wolfei* and strain 195 grown on butyrate, and DvH and strain 195 on lactate) provided with 0.6 mM TCE were collected when cell growth had ceased and treated by following standard protocols for SEM observation. Briefly, cultures were collected by slowly filtering 1 mL fresh liquid sample through a 0.2μm GTTP (Isopore^{TM} membrane, polycarbonate, hydrophilic, 25mm in diameter from Millipore) filter, followed by chemical fixation, dehydration, critical point drying and conductive coating (Gorby *et al*., 2006). (http://em-lab.berkeley.edu/EML/protocols/psem.php). SEM images were obtained according to standard operation protocols (Dykstra, 1992). The maximum interspecies distances between strain 195 and *S.wolfei* that would enable the observed dechlorination rates for butyrate fermentation were estimated using Fick's diffusion law according to the procedure described by Ishii, *et al*., 2005:

$$J_{H_2} = D_{H_2} \times \frac{C_{H_2-sw} - C_{H_2-195}}{d_{sw-195}}$$

J_{H2} = H_2 flux across the total surface areas ($A_{s,tot}$) of *S. wolfei* (pmol $m^{-2}{}_{cell}$ d^{-1});
A_S = 2.1×10^{-12} m^2 $cell^{-1}$, *S. wolfei* surface area calculated based on the assumption of 0.25 by 2.5 μm cells (based on SEM observation). $A_{s,tot}$ = $A_S \times$ *S.wolfei* cell number
D_{H2} = 6.31×10^{-5} cm^2 s^{-1}, molecular diffusion coefficient in water for hydrogen at 35 °C (Haynes *et al*., 2013);
$C_{H2\text{-}sw}$ = maximum H_2 concentration enabling exergonic fermentation (μM) (the highest H_2 level at which *S. wolfei* can ferment butyrate);
$C_{H2\text{-}195}$ = theoretical minimum H_2 concentration useable by strain 195 for energy generation (μM) (the lowest H_2 level at which strain 195 can dechlorinate TCE);
$d_{sw\text{-}195}$ = allowed interspecies distance for accomplishing syntrophic oxidation at an observed substrate utilization rate (μm).

3.2.5 DNA extraction and cell number quantification

1.5 mL liquid samples were collected for cell density measurements and cells were harvested by centrifugation (21,000 × *g*, 10 min at 4°C). Genomic DNA was extracted from cell pellets using Qiagen DNeasy Blood and Tissue Kit according to the manufacturer's instructions for Gram-positive bacteria. qPCR using SYBR Green-based detection reagents was applied to quantify gene copy numbers of each bacterium with *S.wolfei* 16S rRNA gene primers (forward primer 5'-GTATCGACCCCTTCTGTGCC-3', and reverse primer 5'-CCCCAGGCGGGATACTTATT-3') (Sieber *et al*., 2010), and *D. mccartyi tceA* gene primers

(forward primer 5'-ATCCAGATTATGACCCTGGTGAA-3' and reverse primer 5'-GCGGCATATATTAGGGCATCTT-3'), as previously described (Johnson *et al*., 2005). The electron equivalents (µmol) diverted to biomass were calculated based on biomass formula $C_5H_7O_2N$ (MW=113 g mol^{-1}).

3.2.6 RNA preparation

Cultures were sampled for RNA on day 6 during exponential growth when around 75% of 78 µmol TCE was dechlorinated (~20 µmol TCE remained). In order to collect sufficient material for transcriptomic microarray analysis, 18 bottles of pure strain 195 and 18 bottles of the co-culture were inoculated and grown from triplicate bottles of the isolate and co-culture, respectively. For each biological triplicate, cells from six bottles were collected by vacuum filtration on day 6 during active dechlorination for the co-culture and day 12 for the strain 195 pure culture (200 mL culture per filter, 0.2-µm autoclaved GVWP filter (Durapore membrane, Millipore, Billerica, MA). Each filter was placed in a 2 mL orange-cap micro-centrifuge tube, frozen with liquid nitrogen and stored at -80 °C until further processing.

RNA was extracted using the phenol-chloroform method described previously (Johnson *et al*., 2008) with the following minor modifications. The ratio of phenol (pH 4.0)-chloroform-isoamylalcohol used for extraction was 25:24:1 (vol:vol), and the RNA pellet was re-suspended in 100 µL of nuclease-free water. RNA samples were purified following manufacturer's instructions with the AllPrep DNA/RNA Mini Kit (Qiagen). Additional DNA contamination was removed with Turbo DNA free kit (Ambion, Austin, TX) according to the manufacturer's instructions. The quality of RNA samples was checked by electrophoresis (1.0 µL RNA sample), and the concentrations of RNA samples were quantified using a nano-photometer (IMPLEN, Westlake Village, CA, USA). The ratio of A260/A280 for all samples was between ~1.80-2.0. Purified RNA was stored at -80 °C prior to further use.

3.2.7 Transcriptomic microarray analysis

A complete description of the Affymetrix GeneChip microarray used in this study has been reported elsewhere (Lee *et al*., 2011). Briefly, the chip contains 4744 probe sets that represent more than 98% of the ORFs from four published *Dehalococcoides* genomes (strain 195, VS, BAV1, and CBDB1). cDNA was synthesized from 9 µg RNA**,** then each cDNA sample was fragmented, labeled and hybridized to each array. All procedures were performed with minimal modifications to the protocols in section 3 of the Affymetrix GeneChip Expression Analysis Technical Manual (Affymetrix, Santa Clara, CA http://www.affymetrix.com). Microarray data analysis methods were described previously (Men *et al*., 2012; West *et al*., 2013).

3.3 Results

3.3.1 Physiological characteristics of the syntrophic co-culture

Degradation characteristic and cell growth

TCE did not inhibit growth of the *S. wolfei* isolate at concentrations up to 0.6 mM (Figure 3-1), so co-cultures were maintained with 0.6 mM TCE and 4 mM butyrate. After subculturing

this co-culture 45 times, the maximum dechlorination rate of strain 195 was approximately 2.6 fold (9.9 ± 0.1 μmol d^{-1}) (Figure 3-2 A) greater than the strain 195 isolate (3.8 ± 0.1 μmol d^{-1}) (Men *et al*., 2011). The calculation of strain 195 cell yield was based on the metabolic reductive TCE dechlorination to VC, and the cell yield of strain 195 was 1.6 times greater in the co-culture ($1.1 \pm 0.3 \times 10^8$ cells μmol^{-1} Cl^-) (Figure 3-2 B) compared to the pure culture ($6.8 \pm 0.9 \times 10^7$ cells μmol^{-1} Cl^-) (Men *et al*., 2011), similar to results from a co-culture containing a sulfate-reducing bacterium ($9.0 \pm 0.5 \times 10^7$ cells μmol^{-1} Cl^-) (Men *et al*., 2011) (Table 3-2). The initial concentration of butyrate (from 1 mM to 20 mM) did not affect the dechlorination rate (data not shown), showing that high butyrate concentrations are not inhibitory to dechlorination. Cell numbers of strain 195 ($1.3 \pm 0.2 \times 10^8$ cells mL^{-1}) were consistently about 16 times higher than *S. wolfei* ($7.7 \pm 0.1 \times 10^6$ cells mL^{-1}) in the co-cultures growing on butyrate. In contrast, when maintaining the co-culture on crotonate after 80 transfers (5% vol/vol inoculation) of the original set-up culture, the cell number ratio was about 1.3:1 (Figure 3-3 B). In the syntrophic co-culture with DvH growing on lactate, the cell number ratio of strain 195 to DvH was reported to be about 5:1 (Men *et al*., 2011).

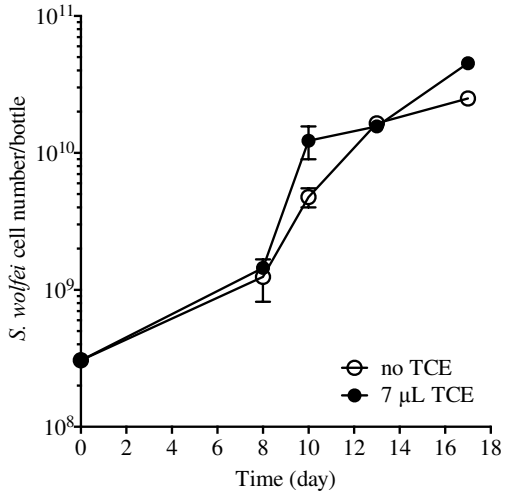

Figure 3-1Increase in the cell numbers of *S. wolfei* growing in pure culture with 10 mM crotonate with or without TCE amendment. Error bars are standard deviations (SD).

Table 3-2 Dechlorination rate and cell yield of *D. mccartyi* strains in various co-culture studies.

Co-cultures[a]	Dechlorination rate (μmol d^{-1})	*D. maccartyi* cell yield (cells μmol^{-1} Cl^- released)	Reference
Strain 195 and *Desulfovibrio desulfuricans*	0.4	2.4×10^8	He, 2007[b]
Strain 195 and *Sedimentibacter* sp.	6.8	4.2×10^8	Cheng, 2010[c]
Strain 195 and DvH	11 ± 0.01	$9.0 \pm 0.5 \times 10^7$	Men, 2011
Strain BAV1 and *Geobacter lovleyi*	6.1	6.7×10^7	Yan, 2012[d]
Strain FL2 and *Geobacter lovleyi*	4.2	3.3×10^7	
Strain BAV1 and *Sporomusa* sp. strain KB1	3.3	$2.1 \pm 0.2 \times 10^8$	Yan, 2013[e]
Strain GT and *Sporomusa* sp. strain KB1	2.1	$2.1 \pm 0.3 \times 10^8$	
Strain FL2 and *Sporomusa* sp. strain KB1	2.5	$9.0 \pm 1.4 \times 10^7$	
Strain 195 and *S. wolfei*	9.9 ± 0.1	$1.1 \pm 0.3 \times 10^8$	This study

a. *Dehalococcoides mccartyi* strain 195 (strain 195), *Dehalococcoides mccartyi* strain BAV1 (strain BAV1), *Dehalococcoides mccartyi* strain GT (strain GT), *Dehalococcoides mccartyi* strain FL2 (strain FL2).
b. Calculated from Fig. 4B and Table 2 therein.
c. Calculated from Fig. 1C and Fig. 3 therein.
d. Calculated from Fig. 2 and Table 1 therein.
e. Calculated from Fig. 6 and Table 1 therein.

Electron balance of the syntrophic co-culture

When the ratio of butyrate to TCE in the co-culture was maintained under electron acceptor limitation with 79 ± 6.7 μmol TCE and 440 ± 29 μmol butyrate (measured by HPLC) as the electron donor, H_2 levels remained steady at ~24-180 nM during active dechlorination (from day 0 to day 7) and increased to 350 ± 20 nM right after TCE and DCE were consumed on day 8 (Figure 3-2 C, Table 3-4). This H_2 concentration was similar to the level (480 nM) that resulted in cessation of *S. wolfei* growth on butyrate in isolation (Wallrabenstein & Schink, 1994). At the end of the experiment (day 18), 88.4% of the amended TCE could be accounted for in dechlorination products VC (7.4± 0.3 % molar equivalents) and ethene (81.0± 0.1% molar equivalents). The missing 11.6% of initial TCE was likely due to the numerous sampling events during the experiment, as confirmed by losses in the abiotic controls (8.7% loss of initial TCE added). In addition, 115 ± 3.0 μmol butyrate was consumed while 234 ± 9 μmol acetate and 3.9 ±1.1 μmol H_2 remained in the bottles (in the abiotic control, the amount of butyrate decreased 26 μmol with no production of acetate or H_2). This indicates that around 88.6% of electrons (0.886, this corresponds to f_e° close to 0.84 from Figure 3-2 D) (in the form of H_2) generated from butyrate fermentation (ca. 230 μmol H_2) supported dechlorination. A calculation based on biomass cell numbers (Assumed 0.5 gram dry weight per gram cell, i.e. water accounts for 50% of the cell weight. The cell formula was $C_5H_7O_2N$, with 20 electron equivalent per mol biomass) indicates that 7.4 % (17 μmol H_2) of the electrons from butyrate fermentation (in the form of H_2) were diverted to biomass production, giving a total electron recovery of about 98 %. This result demonstrates that butyrate was efficiently used as the electron donor in the co-culture with high electron transfer efficiency between the two bacteria.

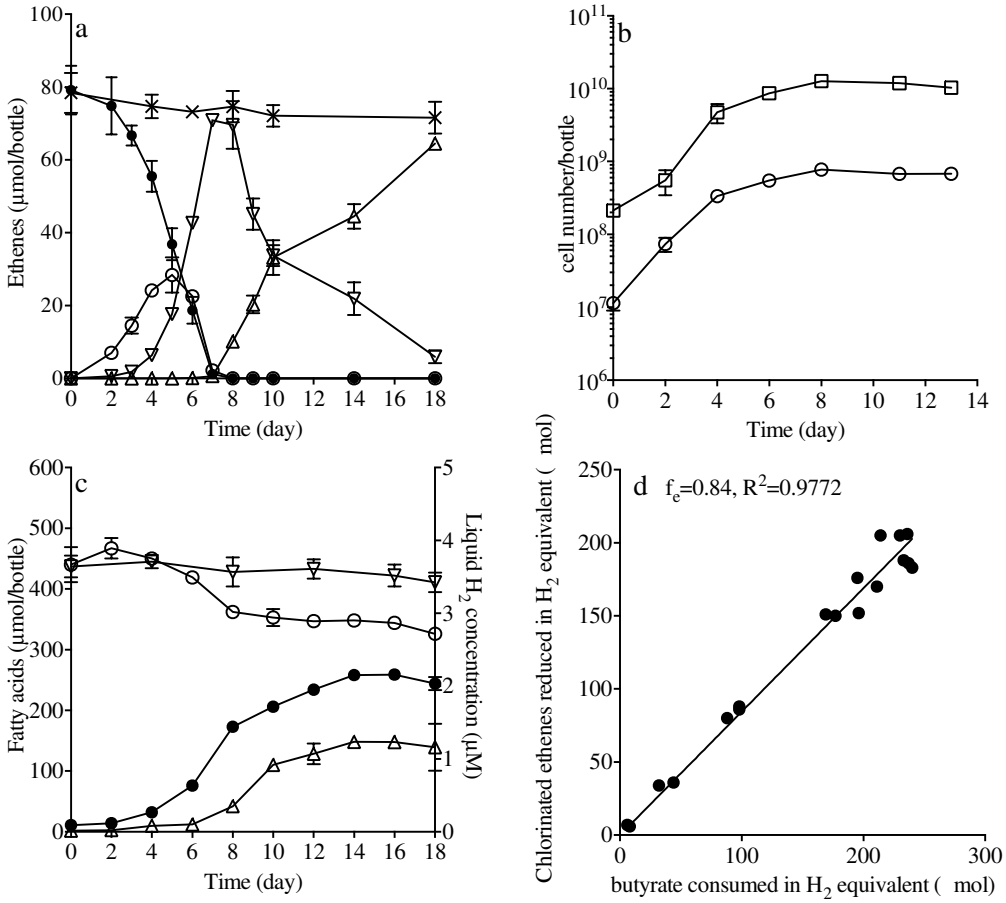

Figure 3-2 Co-culture *S. wolfei* with *D. mccartyi* strain 195 growing with 78 µmol TCE and 4 mM butyrate amendment a) TCE dechlorination profile of co-culture during the feeding cycle (●TCE, ⊖ *cis*-DCE, ▽ VC, △ ETH, ✳control), b) cell numbers of co-culture (⊟ strain 195, ⊖ *S. wolfei*) , c) H_2 level and organic acids formation of co-culture (●acetate, ⊖ butyrate, △ hydrogen, ▽ control butyrate) , d) graphical determination of f_e value for strain 195 in the co-culture, in which the amounts of reducing equivalent H_2 generated during butyrate fermentation were plotted against the amounts of electron acceptor reduced. The f_e is indicated by the slope of the regression line. Values are the averages of biological triplicates, error bars are standard deviations.

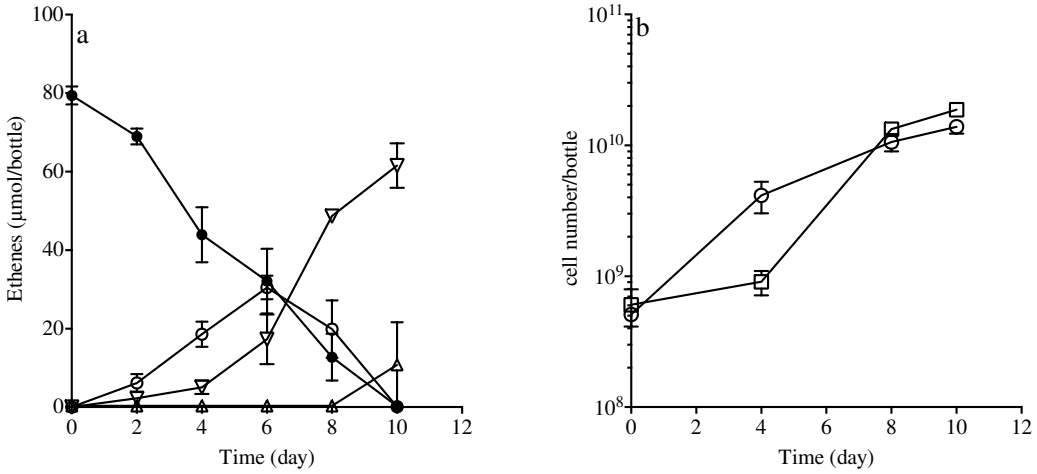

Figure 3-3 a) Time course of TCE removal and production of TCE-reduced metabolites in strain 195 and *S. wolfei* co-culture growing on 5 mM crotonate (●TCE, ⊖ *cis*-DCE, ▽ VC, △ ETH), and b) Cell growth of ⊖ *S. wolfei* and ⊟ strain 195 growing on 5 mM crotonate. The cell numbers were normalized to 16S rRNA gene copy numbers. The symbols indicate the averages based on biological triplicate determinations. The error bars indicate standard deviation.

Thermodynamics of the syntrophic growth

The calculated Gibbs free energy of reaction (butyrate fermentation and associated hydrogen generation by *S.wolfei*) was -21.7 ± 0.3 kJ mol^{-1} on day 6 and decreased to -13.7 ± 0.2 kJ mol^{-1} on day 8 when TCE and *cis*-DCE was depleted. This number was smaller than the hypothetical minimum energy (-20 kJ mol^{-1}) required by a bacterium to exploit the free energy change in a reaction and support growth (Schink, 1997) (detailed calculation is summarized in page 10-13). After TCE and *cis*-DCE depletion, we observed a slight decrease in butyrate (36.0 ± 6.6 µmol) during co-metabolic VC dechlorination (Figure 3-2 C) with H_2 concentrations increasing to a stable level of 1.2 ± 0.3 µM after day 10 while the cell numbers of strain 195 and *S. wolfei* were observed to decrease (Figure 3-2 B and C). The calculated Gibbs free energy of butyrate fermentation during the cometabolic process was less negative and reached -5.7 ± 1.4 kJ mol^{-1} by the end of the experiment (Figure 3-4).

Gibbs free energy calculation in the co-culture

Calculation of (i) standard Gibbs free energy and entropy changes of acetogenic butyrate fermentation catalyzed by *S. wolfei* and (ii) Gibbs free energy of acetogenic fermentative degradation of butyrate in the course of TCE dechlorination by the strain 195 and *S. wolfei* co-culture.

$$C_4H_7O_2^- + 2H_2O \rightarrow 2C_2H_3O_2^- + H^+ + 2H_2$$

$$\Delta G = \Delta G^\circ + RT\,lnK = \Delta G^\circ + RT\,ln\frac{[\text{Acetate}]^2\,[H^+]\,p_{H_2}^2}{[\text{Butyrate}]} = \Delta G^\circ_{pH} + RT\,\ln K'$$

$$= \Delta G^\circ_{pH} + RT\,ln\frac{[\text{Acetate}]^2\,p_{H_2}^2}{[\text{Butyrate}]}$$

$$\Delta G^{\circ}_{\mathrm{pH,298.15K}} = \Delta G^{\circ} + nRT\ ln[\mathrm{H^+}] = \Delta G^{\circ} - 2.3026\, nRT \times \mathrm{pH} = \Delta G^{\circ} - 5.708\, n \times \mathrm{pH}$$

$$R = 0.00831451\ \mathrm{kJ\ mol^{-1}\ K^{-1}} = 0.083451\ \mathrm{L\ bar\ mol^{-1}\ k^{-1}}$$

$n =$ number of protons

ΔG° = Standard Gibbs free energy change of reaction when all reactants and products are present at unit activity at a specified standard state (i.e., 298.15 K, 100 kPa = 1bar).

$p_{\mathrm{H_2}}$ = Hydrogen partial pressure (bar); $[\mathrm{H_{2(aq)}}] = \frac{p_{\mathrm{H_{2(g)}}}}{k_{\mathrm{H}}}$.

$k_{\mathrm{H}}(\mathrm{H_2}, 298.15\ \mathrm{K}) = 1.299038 \times 10^3\ \mathrm{bar\ L\ mol^{-1}}$ (1.236747×10^3 bar L mol^{-1} at 307.15 K) (Sander, 1997)

The pH during syntrophic butyrate fermentation and TCE dechlorination was maintained at 7.3 by dual-buffer system, therefore $[H^+] = 5 \times 10^{-8}$ mol L^{-1}.

The standard Gibbs free energy change of reaction (ΔG_r°) for acetogenic butyrate fermentation $C_4H_7O_2^- + 2H_2O \rightarrow 2C_2H_3O_2^- + H^+ + 2H_2$ is calculated using the Hess's law and the standard molar Gibbs energy of formation (Table 3-3).

Table 3-3 Standard molar Gibbs energy of formation ($\Delta_f G_i^{\circ}$), standard molar enthalpy of formation ($\Delta_f H_i^{\circ}$) and standard molar entropy (S_i°) values (298.15 K) used for the calculation of $\Delta G_r^{\circ}, \Delta H_r^{\circ}$ and ΔS_r° of butyrate fermentation reaction of butyrate fermentation reaction

Reactant/product	$\Delta_f G_i^{\circ}$ (kJ mol^{-1})[a]	$\Delta_f H_i^{\circ}$ (kJ mol^{-1})[a]	S_i° (kJ mol^{-1} K^{-1})[a]
Butyric acid (ionized form), pK_a = 4.821	-352.6[b]	-536[c]	0.1358[d]
Acetic acid (ionized form), pK_a = 4.757	-369.4[b]	-486.0	0.0866
H^+ (pH = 0)	0	0	0
H_2O	-237.17	-285.8	0.070
H_2(g)	0	0	0.1307
H_2(aq)	17.8[e]	-4.16[f]	0.0577[f]

(a) Data obtained from Madigan *et al*., 2006 and CRC Handbook of Chemistry and Physics, 95th; (b) Thermodynamic values for ionized forms of butyric acid and acetic acid are from Hanselmann, 1991, (c) calculated from Conrad and Wetter, 1990, (d) Adams *et al*., 2006, (e) calculated from $\Delta_f G_{i(\mathrm{aq})}^{\circ} = \Delta_f G_{i(\mathrm{g})}^{\circ} + RT\ lnk_{\mathrm{H},i}$ as described in Schwarzenbach *et al*., 2003, (f) Hanselmann, 1991.

$$\Delta G_r^{\circ} = \left(2 \times \Delta_f G^{\circ}_{\mathrm{CH_3COO^-\,(aq)}}\right) + \left(\Delta_f G^{\circ}_{\mathrm{H^+(aq)}}\right) + \left(2 \times \Delta_f G^{\circ}_{\mathrm{H_{2(g)}}}\right) - \left[\left(2 \times \Delta_f G^{\circ}_{\mathrm{H_2O\,(aq)}}\right) + \left(\Delta_f G^{\circ}_{\mathrm{C_4H_7O_2^-\,(aq)}}\right)\right]$$

$$\Delta G_r^{\circ} = [2\times(-369.4\ \mathrm{kJ\ mol^{-1}}) + (0\ \mathrm{kJ\ mol^{-1}}) + 2\times(0\ \mathrm{kJ\ mol^{-1}})] - [2\times(-237.17\ \mathrm{kJ\ mol^{-1}}) + (-352.63\ \mathrm{kJ\ mol^{-1}})] = 88.17\ \mathrm{kJ\ mol^{-1}}$$

For the calculation of the standard Gibbs free energy of reaction using the standard Gibbs free energy of formation of hydrogen in the aqueous phase (i.e., all reactants and products are in dissolved or liquid state, $\Delta G^{\circ}_{r,(aq)}$),

$$\Delta G^{\circ}_{r,(aq)} = [2\times(-369.4\ \text{kJ mol}^{-1}) + (0\ \text{kJ mol}^{-1}) + 2\times(17.8\ \text{kJ mol}^{-1})] - [2\times(-237.17\ \text{kJ mol}^{-1}) + (-352.63\ \text{kJ mol}^{-1})] = 123.7\ \text{kJ mol}^{-1}$$

Because the experiments are carried out at 307.15 K, the standard Gibbs free energy change of reaction is corrected for the incubation temperature using the Gibbs-Helmholtz equation.

$$\left(\frac{\partial(\Delta G/T)}{\partial T}\right)_p = -\frac{\Delta H}{T^2}$$

$$\Delta S^{\circ}_r = [2\times(0.0867\ \text{kJ mol}^{-1}\ \text{K}^{-1}) + (0\ \text{kJ mol}^{-1}\ \text{K}^{-1}) + 2\times(0.1307\ \text{kJ mol}^{-1}\ \text{K}^{-1})] - [2\times(0.07\ \text{kJ mol}^{-1}\ \text{K}^{-1}) + (0.1358\ \text{kJ mol}^{-1}\ \text{K}^{-1})] = 0.159\ \text{kJ mol}^{-1}\ \text{K}^{-1}$$

$$\Delta S^{\circ}_{r(aq)} = [2\times(0.0867\ \text{kJ mol}^{-1}\ \text{K}^{-1}) + (0\ \text{kJ mol}^{-1}\ \text{K}^{-1}) + 2\times(0.0577\ \text{kJ mol}^{-1}\ \text{K}^{-1})] - [2\times(0.07\ \text{kJ mol}^{-1}\ \text{K}^{-1}) + (0.1358\ \text{kJ mol}^{-1}\ \text{K}^{-1})] = 0.013\ \text{kJ mol}^{-1}\ \text{K}^{-1}$$

$$\Delta H^{\circ}_r = [2\times(-486\ \text{kJ mol}^{-1}) + (0\ \text{kJ mol}^{-1}) + 2\times(0\ \text{kJ mol}^{-1})] - [2\times(-285.8\ \text{kJ mol}^{-1}) + (-536\ \text{kJ mol}^{-1})] = 135.6\ \text{kJ mol}^{-1}$$

$$\Delta H^{\circ}_{r(aq)} = [2\times(-486\ \text{kJ mol}^{-1}) + (0\ \text{kJ mol}^{-1}) + 2\times(-4.16\ \text{kJ mol}^{-1})] - [2\times(-285.8\ \text{kJ mol}^{-1}) + (-536\ \text{kJ mol}^{-1})] = 127.28\ \text{kJ mol}^{-1}$$

Using the Gibbs-Helmholtz equation,

$$\Delta G^{\circ}_{307.15} = 307.15\left(\frac{\Delta G^{\circ}_{298.15}}{298.15}\right) + \left(\frac{\Delta H^{\circ}\ (298.15 - 307.15)}{298.15}\right) = 86.74\ \text{kJ mol}^{-1}$$

Using another form of the Gibbs-Helmholtz equation,

$$\Delta G^{\circ}_{307.15} = \Delta G^{\circ}_{298.15} - \Delta S^{\circ}\ (307.15 - 298.15) = 88.17\ \text{kJ mol}^{-1} - [0.159\ \text{kJ mol}^{-1}\ \text{K}^{-1} \times 9\ \text{K}] = 86.74\ \text{kJ mol}^{-1}$$

When all reactants and products are in dissolved or liquid state,

$$\Delta G^{\circ}_{307.15(aq)} = 307.15\left(\frac{\Delta G^{\circ}_{298.15(aq)}}{298.15}\right) + \left(\frac{\Delta H^{\circ}_{(aq)}\ (298.15 - 307.15)}{298.15}\right) = 123.59\ \text{kJ mol}^{-1}$$

As reported by Schink, 1997, a minimum of about -20 kJ per mol is required by a bacterium to exploit the free energy change in a reaction and support growth. Therefore, each data point of Gibbs free energy change of reaction was calculated based on the measurement of each compound concentration at specific time (Rittmann and McCarty, 2001). Table 3-4 presents an example of calculation of Gibbs free energy available for *S. wolfei* during syntrophic growth with strain 195 in the presence of butyrate as the sole electron donor.

Table 3-4 Sample calculation for free Gibbs energy available for *S. wolfei* [a]

Time (day)	H_2 partial pressure ($\times 10^{-5}$ bar)	$H_{2\,(aq)}$ (nM)[b]	Acetate concentration (M)	H^+ (M)	Butyrate Concentration (M)	$\Delta G^{\circ}_{307.15K}$ (kJ mol^{-1})	Final delta G (kJ mol^{-1})
0	2.7	21.8	9.0×10^{-5}	5×10^{-8}	4.3×10^{-3}	86.7	-43.6 [(c)]
2	5.9	47.5	1.5×10^{-4}	5×10^{-8}	4.6×10^{-3}	86.7	-37.1
4	15.3	123.8	3.1×10^{-4}	5×10^{-8}	4.5×10^{-3}	86.7	-28.5
6	21.9	177.0	7.5×10^{-4}	5×10^{-8}	4.2×10^{-3}	86.7	-22.0
8	42.9	347.0	1.7×10^{-3}	5×10^{-8}	3.7×10^{-3}	86.7	-13.9
10	126.6	1023.7	2.0×10^{-3}	5×10^{-8}	3.4×10^{-3}	86.7	-7.5
12	118.2	955.5	2.3×10^{-3}	5×10^{-8}	3.5×10^{-3}	86.7	-7.2
14	152.4	1232.4	2.54×10^{-3}	5×10^{-8}	3.5×10^{-3}	86.7	-5.4
16	160.8	1300.1	2.61×10^{-3}	5×10^{-8}	3.5×10^{-3}	86.7	-5.0
18	192.4	1555.5	2.32×10^{-3}	5×10^{-8}	3.2×10^{-3}	86.7	-4.5

[a] The calculation summarized in the table is for one biological replicate in the feeding cycle,
[b] Henry's law constant at 307.15 K = 1.236747×10^3 bar L mol^{-1},
[c] If we use aqueous concentration of H_2,

$$\Delta G = \Delta G^{\circ}_{(aq)} + RT\, ln \frac{[\text{Acetate}]^2\,[H^+]\,[H_2]^2}{[\text{Butyrate}]}$$
$$= 123.59\ \text{kJ mol}^{-1} + (0.00831451\ \text{kJ mol}^{-1}\ \text{K}^{-1} \times 307.15\ \text{K})\, ln \frac{((9\times10^{-5}\ \text{M})^2\,(5\times10^{-8}\ \text{M})\,(21.8\times10^{-9}\ \text{M})^2)}{(4.3\times10^{-3}\ \text{M})}$$

= -43.1 kJ mol^{-1}.

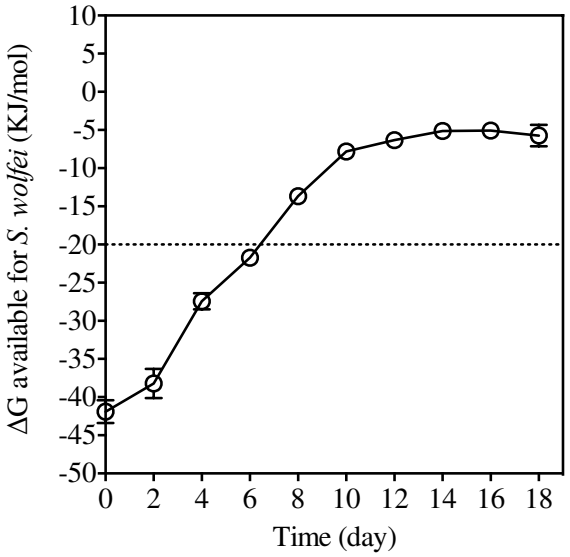

Figure 3-4 Gibbs free energy available for *S. wolfei* during syntrophic fermentation of butyrate with strain 195

Hydrogen threshold

In order to determine the H_2 threshold of strain 195 in the co-culture, it was grown under electron donor-limited conditions (TCE fed in excess). H_2 concentrations dropped to thresholds of 0.6 ± 0.1 nM at which point TCE was not further degraded by strain 195 and butyrate depletion ceased (Figure 3-5). In order to validate our method for quantifying the minimum H_2-threshold concentration, we measured the hydrogen threshold of the sulfate reducing microorganism *Desulfovibrio vulgaris* Hildenborough (DvH), and obtained 15.2 ± 1.4 nM which is in agreement with literature results (14.8 nM) for this bacterium (Cord-Ruwisch *et al*., 1988).

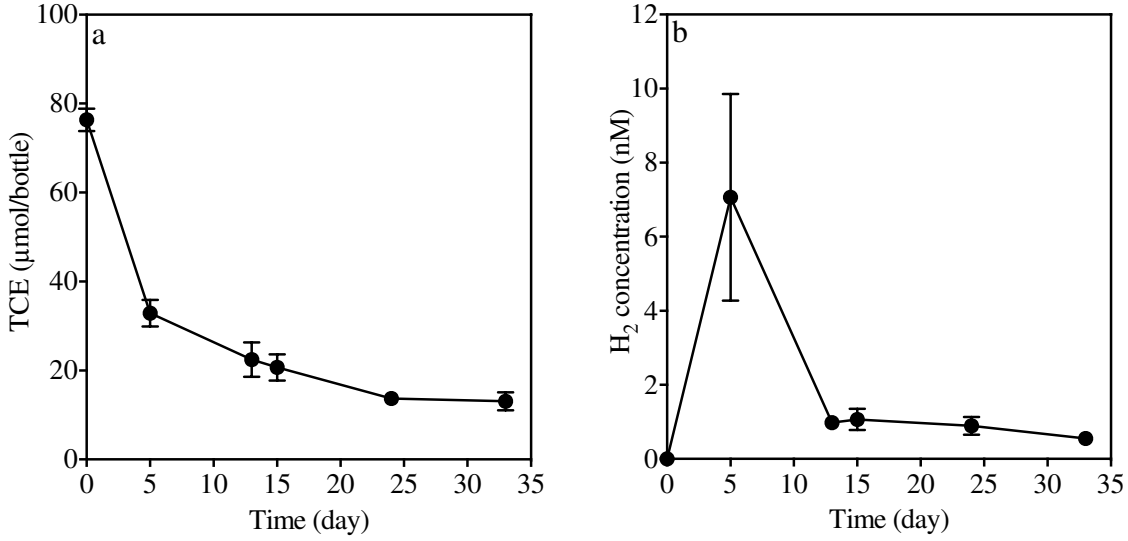

Figure 3-5 a) Time course of TCE removal and b) aqueous H_2 concentration in the bottle while co-culture Dhc195 and *S. wolfei* was fed with 0.25 mM butyrate and 78 µmol TCE. 5µL butyrate (0.05 mM) was re-spiked to the bottle (on day 15) when TCE removal significantly decreased (no peak of H_2 was observed because of the long delay of sampling). The measured values correspond to the averages based on biological triplicate determinations. The error bars are SD.

Carbon monoxide (CO) in the syntrophic co-culture

We tested the inhibitory effect of CO on *S. wolfei* by exposing cells to 0.6 to 8 µmol CO per bottle and observed no significant effect on cell growth (Figure 3-6 A). CO accumulation for the *S. wolfei* isolate growing on crotonate was 0.02 µmol / bottle throughout the experiment (Figure 3-6 B), which was at the same level as the abiotic control (data not shown). In the co-culture growing on butyrate, CO was measured at ~0.06 µmol per bottle. This was lower than that detected for the strain 195 isolate (0.5 ± 0.1 µmol per bottle after one dose of TCE (77 µmol) was depleted) (Zhuang *et al*., 2014). Furthermore, we found that pure *S. wolfei* could consume CO from 14.5 ± 1.5 µmol to 0.4 ± 0.1 µmol in 42 days (Figure 3-6 C) when growing on crotonate.

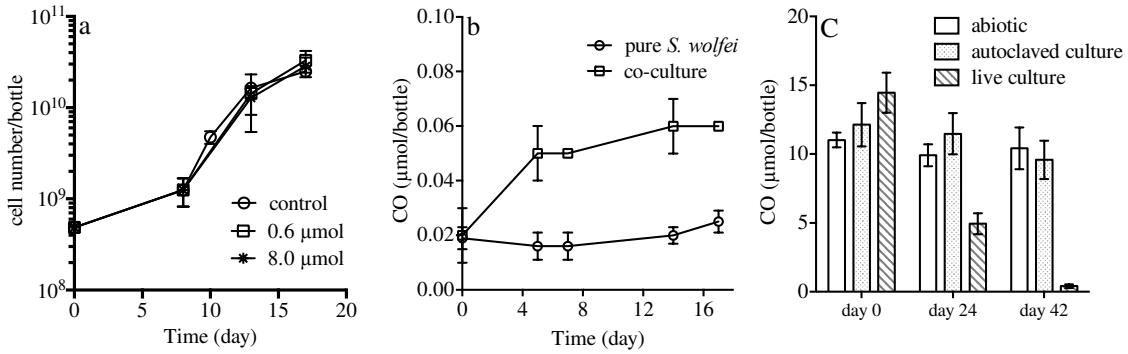

Figure 3-6 a) Inhibitory effect of different CO concentrations on *S. wolfei* cell growth, b) CO accumulation for the *S. wolfei* isolate and in co-culture with strain 195 on butyrate and; c) CO consumption by the *S. wolfei* isolate. Values are the averages of biological triplicates, error bars are standard deviations.

3.3.2 Cell aggregates formation during syntrophic growth

Strain 195 and *S. wolfei* isolates as well as the co-cultures of *S. wolfei* and strain 195 maintained on butyrate were grown to stationary phase before samples were analyzed by scanning electron microscopy (SEM). Figures 3-7 A and B show specific cell morphology of the isolates with strain 195 growing in individual coccus-shapes with diameters of about ~0.5-1 µm while most *S. wolfei* cells grew individually or in pairs as 0.25 - 0.5 by 2.5 - 5 µm rods as observed in previous studies (MaymóGatell *et al*., 1997; McInerney *et al*., 1981). When butyrate was amended to the co-culture as electron donor with TCE as electron acceptor, the cells form cell aggregates with size ranges from 2 µm to 10 µm (Figure 3-7 C-E). In relatively small aggregates, cells were found connected with flagellum-like filaments (Figure. 3-7 C, D). In large aggregates, EPS-like structures were observed (Figure 3-7 D, E). Cell aggregates were also observed during exponential growth phase. However, when strain 195 was grown as a co-culture with DvH on lactate, the two strains grew together but did not form obvious cell aggregates (Figure 3-7 F).

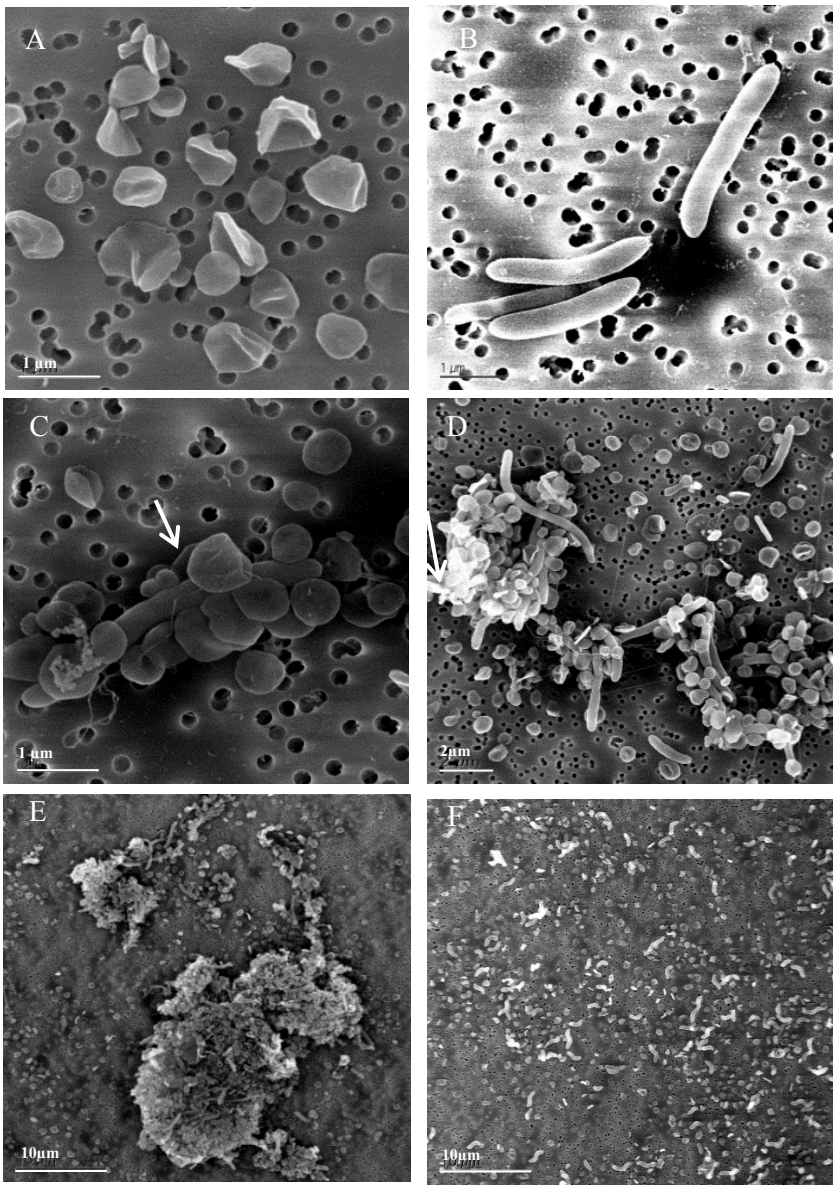

Figure 3-7 A) monoculture of pure strain 195 growing on pure H_2 gas plus acetate and TCE, B) monoculture of *S. wolfei* growing on crotonate, C to E) co-culture of *S. wolfei* and strain 195 growing on butyrate plus TCE, F) co-culture DVH and strain 195 growing on lactate plus TCE. Arrows show flagellum-like filaments of *S. wolfei*.

In order to determine whether the co-cultures may be capable of sharing electrons via direct interspecies electron transfer (DIET), the crotonate and butyrate co-cultures were sent to Professor Lovley's laboratory for conductivity testing (Shrestha *et al*., 2013). The co-cultures exhibited three orders of magnitude lower conductivity than *Geobacter*, indicating that H_2 rather than DIET is the transfer mechanism. In addition, since *S. wolfei* could potentially use both hydrogen and formate as electron carriers for interspecies electron transfer (Sieber *et al*., 2014), we tested the expression levels of several formate dehydrogenase genes (*fdhA*: Swol_0786, Swol_0800, Swol_1825) in co-cultures grown on crotonate or butyrate and *S. wolfei* grown in isolation. The relative expression of *fdhA* subunits to *gyrB* gene was generally in the range of

0.6-1.2 units for all three conditions (Bryan, 2014), confirming that hydrogen rather than formate was the exclusive electron shuttle between these two bacteria.

The theoretical maximum interspecies distance for an observed rate of molecular transfer between two microorganisms can be calculated using Fick's diffusion law (Stams *et al*., 2012). Here, this distance was calculated for co-culture growth on butyrate (Table 3-5, detailed calculation is summarized in page 18-20) by defining J_{H2} as the hydrogen flux between *S. wolfei* and strain 195. J_{H2} was calculated from the total surface areas of *S. wolfei* and substrate oxidation rate (hydrogen production rate = 2 × butyrate oxidation rate) measured in the co-culture experiment using equation 2 in Table 3-1. $C_{H2\text{-}sw}$ (0.35 ± 0.02 μM, Figure 3-2 C) is the maximum H_2 concentration immediately outside of an *S. wolfei* cell when *S. wolfei* is grown in isolation on butyrate and $C_{H2\text{-}195}$ is the theoretical minimum H_2 concentration above which strain 195 can gain energy, estimated in this study as 0.6 ± 0.1 nM. $d_{syn\text{-}195}$ is then the calculated maximum interspecies distance for accomplishing syntrophic oxidation at the observed substrate oxidation rate.

The theoretical mean cell-cell distance of randomly dispersed cells is calculated based on the total cell numbers (quantified using qPCR) suspended in the unstirred liquid culture. In this study, cell settling was not observed for the strain 195 isolate or co-cultures growing on butyrate (strain 195 and *S. wolfei*) or lactate (strain 195 and DvH). Considering that the cell number ratio of strain 195 to *S. wolfei* was about 20:1 on day 4 (Figure. 3-2 C), strain 195 cells account for the majority of all cells in the bottle, therefore the average cell-cell distance between suspended strain 195 and *S. wolfei* cells (i.e., >> 27.1 μm, Table 3-5) would be larger than the calculated theoretical maximum cell-cell distance for achieving butyrate fermentation. In order to accomplish syntrophic butyrate oxidation at the rate observed, the average interspecies distance must be much less than the distance between randomly dispersed cells (Table 3-5), necessitating the formation of aggregates. In addition, according to the thermodynamically consistent rate law, the calculated free energy available for *S. wolfei* growth on day 4 was -27.4 ± 1.1 kJ mol^{-1} which is small (Figure 3-4), indicating that close physical contact between the two species is particularly important for efficient syntrophic butyrate fermentation. In contrast, when strain 195 was grown with DvH as a co-culture, the maximum calculated interspecies distance was large enough (755 μm) to enable interspecies hydrogen transfer between the two bacteria (Table 3-6) and aggregates were not formed.

Table 3-5 Calculation of cell-cell distance of co-culture *S. wolfei* and strain 195[a].

	Total cell number (strain 195 + *S. wolfei*)	Mean cell-cell distance[b](μm)	Allowable average interspecies distance for H_2 transfer (*S. wolfei* to strain 195) at the observed substrate oxidation rate[c] (μm)
day2	6.2×10^6 cells mL^{-1}	55.3	13.8
day4	5.0×10^7 cells mL^{-1}	27.1	6.3
day6	9.2×10^7 cells mL^{-1}	22.2	2.7
day8	13.7×10^7 cells mL^{-1}	19.6	1.9

a.The cell-cell distance calculated in the table was based on one biological replicate.
b.Calculated by using the cell number quantified from quantitative PCR analysis.
c.Calculated by using Fick's Diffusion Law

Calculation of allowed interspecies distance for butyrate fermentation in strain 195 and *S. wolfei* co-culture by using Fick's diffusion law

$$J_{H_2} = D_{H_2} \times \frac{\Delta C_{H_2}}{d_{sw-195}}$$

$$d_{sw-195} = D_{H_2} \times \frac{\Delta C_{H_2}}{J_{H_2}}$$

J_{H2} = H_2 flux (pmol μm^{-2}_{cell} d^{-1}) across the total surface area ($A_{S,tot}$) of H_2-producing *S. wolfei*. The H_2 flux J_{H2} in the co-culture experiment was calculated on the basis of the oxidation rate of butyrate by *S. wolfei* at a specific interval time and the hydrogen consumption rate of strain 195.

$A_{S,tot}$: total surface area over which hydrogen diffuses (total surface area of H_2-producing *S. wolfei*) (μm^2).

Surface area of *S. wolfei*: assume diameter= 0.25µm, length= 2.5 µm

$$A_S = \pi dl + \frac{1}{2}\pi d^2 = 2.1\ \mu m^2\ cell^{-1}$$

$$A_{S,tot} = A_S \times \text{cell number}$$

D_{H2}= molecular diffusion coefficient in water for hydrogen at 35 °C, 6.31×10^{-5} cm^2 s^{-1} = 6.31×10^{-9} m^2 s^{-1} (Haynes, 2013).

ΔC_{H2} is the maximum difference of hydrogen concentration at the outside cell surface between the H_2-producing *S. wolfei* and H_2-consuming strain 195, taking into account the highest H_2 level at which *S. wolfei* can ferment butyrate and the lowest H_2 level at which strain 195 can dechlorinate TCE (H_2 threshold for strain 195).

ΔC_{H2}= $C_{H2\text{-}sw}$-$C_{H2\text{-}195}$=3.494×10^{-1}µM

$C_{H2\text{-}sw}$ =0.35±0.1µM

$C_{H2\text{-}195}$=0.6×10^{-3}µM

Calculated from Figure 3-2 B-C.

* Incubation period: $t_{day2\text{-}day4}$ = 2 days

* H_2 produced in the defined time interval by *S. wolfei* (day4-day2) was 3.4×10^7 pmol. The number was calculated from theoretical hydrogen production by butyrate fermentation using Equation 2 in Table 3-1 of the manuscript. Because hydrogen production (from butyrate fermentation) is directly linked to generation of energy in *S. wolfei* cells, hydrogen will be formed during bacterial growth. The theoretical yield of hydrogen from biomass $Y_{H2/X}$ can be calculated from the measured amount of hydrogen produced during the incubation time Δt per unit of biomass formed.

Biomass formation during incubation period (day2 and day4) = 2.7×10^8 cells.

Cell number of *S.wolfei* on day 2 = 7.4×10^7 cells.

Cell number of *S.wolfei* on day 4 = 3.4×10^8 cells.

$$Y_{H_2/X} = \frac{3.4 \times 10^7\ \text{pmol}}{2.7 \times 10^8\ \text{cells}} = 0.1259\ \text{pmol cell}^{-1}$$

* H_2 consumed in the defined time interval by strain 195 (day 4-day 2) was 2.8×10^7 pmol. Hydrogen consumption during the targeted incubation time is mainly due to TCE dechlorination activity of strain 195.The number was calculated from the Cl^- production rate based on direct GC measurements using Equations 3-5 in Table 3-1. This number is slightly lower than the H_2 produced, due to part of the electrons went to biosynthesis.

The hydrogen flux is calculated using the following equation:

$$J_{H_2} = \frac{H_2 \text{produced (pmol) in the defined time interval } \Delta t \text{ by } S.wolfei}{\text{total surface area of growing } S.wolfei \text{ in } \Delta t \times \Delta t}$$

$$J_{H_2} = \frac{3.4 \times 10^7 \text{ pmol}}{2.7 \times 10^8 \text{ cell} \times 2.1 \times 10^{-12} \frac{m^2}{\text{cell}} \times 1.728 \times 10^5 \text{ s}} = 3.47 \times 10^5 \text{ pmol m}^{-2} \text{ s}^{-1}$$

$$d_{sw-\text{strain 195}} = D_{H_2} \times \frac{C_{H_2-sw} - C_{H_2-\text{strain 195}}}{J_{H_2}}$$

$$d_{sw-\text{strain 195}} = \frac{6.31 \times 10^{-9} \frac{m^2}{s} \times \frac{3.494 \times 10^5 \text{ pmol}}{10^{-3} m^3}}{3.47 \times 10^5 \frac{\text{pmol}}{m^2 \times s}} = 6.3 \text{ μm}$$

On day 4, *S.wolfei* cell number was 3.4×10^8 per bottle and strain195 cell number was 4.7×10^9 per bottle (i.e. 5.04×10^9 total cells / bottle containing 100-mL culture medium). In a previous study, people calculated *S. wolfei* (H_2 producer) could only exert an influence on local H_2 concentrations within 10μm of its surface (Boone *et al*., 1989).

There are two scenarios of cell distribution in the bottle:

Scenario 1: Cell aggregation between strain 195 and S. wolfei
Cell-cell distances in cell aggregates <1 μm. Previous studies calculated the cell-cell distance of aggregated cells to be 0.08~2 μm in propionate degrading co-cultures (De Bok *et al*., 2004; Ishii *et al*., 2005).

Scenario 2: Equal distribution of cells growing in planktonic state:
Assuming the cells were evenly dispersed in the bottle, the average cell-cell distance will be 27.1 μm.

$$d_{cell-cell} = \frac{1cm}{\sqrt[3]{5.04 \times 10^7}} \times \frac{10^4 \mu m}{1cm} = 27.1 \text{ μm}$$

This distance is larger than the predicted distance (6.3 μm) that can support interspecies hydrogen transfer at the measured butyrate oxidation rate (calculated above). Therefore, in order to accomplish syntrophic butyrate oxidation at the rate observed, the average interspecies distance should be much less than the distance between randomly dispersed cells.

We also calculated the allowed interpecies distance in another syntrophic co-culture *Desulfovibiro vulgaris* Hildenborough (DvH) with strain195 growing on lactate. A comparison of the allowed interspecies distances is summarized below:

Table 3-6 Parameters in Fick's equation and allowed interspecies distance calculation[(a)]

	S. wolfei with strain 195 on butyrate	DvH with strain 195 on lactate
As (μm^2)	2.1	1.3[(b)]
$\Delta Cell_{syn}$ (day4-day2)[(c)]	2.7×10^8	1.1×10^9
$C_{H2\text{-}syn}$ μM	0.35±0.1	38.9[(d)]
J_{H2} (pmol m^{-2} s^{-1})	3.5×10^5	3.2×10^5
$d_{syn\text{-}strain195}$ (μm)	6.3	755

[(a)] The values were calculated in a time interval from day 2 to day 4, at 307.15 K, [(b)] Surface area of DvH: assume diameter= 0.25 μm, length= 1.5 μm, [(c)] Syntroph cell number increase from day

2 to day4. DvH cell number increase was calculated from unpublished data, [(d)] The highest H_2 level at which DvH can ferment lactate was calculated from Figure 3a. (Men *et al*., 2011).

3.3.3 Strain 195 transcriptome analysis during syntrophic growth with *S. wolfei*

Transcriptomic microarray analysis comparing the co-culture growing on butyrate and strain 195 growing in isolation identified 214 genes that were differentially transcribed (Figure 3-8). Among these differentially expressed genes, 18 were up-regulated and 196 were down-regulated in the syntrophic co-culture compared to the strain 195 isolate. Among the up-regulated genes, most significantly expressed genes (signal level 5000~20,000) belonged to transport and metabolism functions including several types of ABC (ATP binding cassette) transporters. Genes located within an operon of a Fec-type ABC transporter (from DET1173 to DET1176) which are involved in periplasmic iron-binding were up-regulated 2.7 to 4.2 times, respectively; genes (DET1491, DET1493) from a cluster encoding a peptide ABC transporter responsible for ATP binding were up-regulated 2.1 and 2.3 times, respectively; genes (DET0140-0141) encoding a phosphate ABC transporter and ATP-binding protein were up-regulated 2.0 to 2.6 times, respectively. There were also a few genes with unknown functions up-regulated at high signal levels compared to the isolate. DET1008, with highest homology to a gene encoding a cell-division initiation protein (Ueda *et al*., 2004) was up-regulated 3.2 times and acetyl-CoA synthase (DET1209) was up-regulated 2.4 times at a high signal level (~20,000).

Genes associated with membrane-bound oxidoreductase complexes, which are related to energy metabolism, such as RDases, hydrogenases, molybdopterin oxidoreductases, putative formate dehydrogenases, as well as NADH-oxidoreductases, showed no significant differential expression patterns between the co-culture and pure culture throughout the experiment. Among the 196 down-regulated genes in the co-culture compared to the isolate, 75 were genes with signal levels lower than 1000 in both treatments (suggesting low expression level), and most of them encode for hypothetical proteins. Many of the down-regulated genes were not related to energy metabolism, such as those encoding a phage domain protein (DET0354); mercuric reductase (DET0732); Mg chelatase-like protein (DET0986) and virulence-associated proteinE (DET1098).

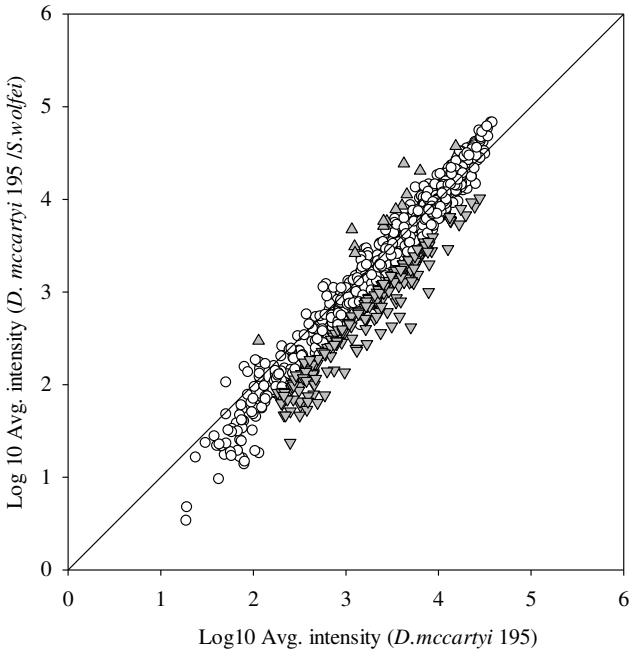

Figure 3-8 Microarray signal intensities of transcripts from strain 195 grown alone versus grown in co-culture with *S. wolfei* (grey colored points represent statistically significant differential transcription, average intensity> 20, p<0.05, more than two-fold difference, genes significantly up-regulated (▲) or down-regulated (▼) in co-culture versus strain 195 monoculture). All measurements are averages from three biological replicates.

3.4 Discussion

In the strain 195 and *S. wolfei* syntrophic co-culture studied here, strain 195 grew exponentially at the rate of 0.69 d^{-1} with a doubling time of 1.0 day, calculated from cell numbers (*tceA* copies) during exponential growth on day 2 and day 6. This doubling time is shorter than previously reported for the isolates of *D. mccartyi sp.* (He *et al*., 2005; Sung *et al*., 2006; Johnson *et al*., 2008; Löffler *et al*., 2013). The dechlorination rate was 9.9 ± 0.1 µmol d^{-1} which is similar to the value observed with strain 195 and DVH co-cultures (11.0 ± 0.01 µmol d^{-1}, Men *et al*., 2011) and higher than the dechlorination rates observed with other *D. mccartyi* containing co-cultures ~4.2-6.8 µmol d^{-1} (He *et al*., 2007; Cheng *et al*., 2010; Yan *et al*., 2012; Yan *et al*., 2013). The cell yield of strain 195 in this co-culture (1.1 ± 0.3 × 10^8 cells μmol^{-1} Cl^- released) was similar to that observed in other *D. mccartyi* co-culture studies, e.g., 9.0 ± 0.5 ×10^7 cells μmol^{-1} (Men *et al*., 2011) and 9.0 ± 1.4 ×10^7 cells μmol^{-1} Cl^- (Yan *et al*., 2013). Given that the minimum free energy change required for ATP synthesis is in the range of 15-25 kJ mol^{-1} reaction for most syntrophic fermentations under *in situ* conditions (Stams *et al*., 2009), only a small amount of energy saved as ATP is expected to be available during *S. wolfei* syntrophic butyrate fermentation (Sieber *et al*., 2010). Indeed, *S. wolfei* in the co-culture was growing very near the thermodynamic threshold (delta G from -41.9 to -5.7 kJ mol^{-1}), and consequently the cell numbers remained at low levels (1:16 ratio with strain 195 cells) when growing on butyrate compared to growth on crotonate. The ratio of calculated free energy available for strain 195 to reduce TCE to VC (-272.0 kJ mol^{-1}) and *S. wolfei* (-43.6 kJ mol^{-1}, Table 3-4) growing on

butyrate was about 6.2:1 at the beginning of the experiment. Considering that the cell size of *S. wolfei* is about 2.5 times larger than strain 195, the theoretical cell production ratio (based on free energy) of strain 195 to *S. wolfei* (15.6:1) is similar to our observation (16:1). While growing on crotonate, the ratio of available energy for strain 195 (-295.3kJ mol^{-1}) and *S. wolfei* (-465.2 kJ mol^{-1}) was 0.6, and the theoretical cell production ratio of 1.2:1 is similar to our observation of 1.3:1. Roden and Jin (2011) found a linear correlation between microbial growth yields (Y_{XS}, g cell mol^{-1} substrate) and estimated catabolic ΔG_r for metabolism of short-chain fatty acids and H_2 coupled metabolic pathways. Table 3-7 compares the growth yields calculated using the Roden and Jin (2011) method ($Y_{XS,cal}$) with observed growth yields ($Y_{XS,obs}$) of syntrophs growing in a variety of co-cultures. Our results confirmed that it is possible to estimate syntrophic cell yields by percentage error of less than 100% by applying an empirical equation for the listed syntrophic co-culture studies (Roden and Jin, 2011), suggesting that the growth yield of syntrophic bacteria and the ratio maintained in the co-cultures were mainly controlled by thermodynamics. Furthermore, we found H_2 concentrations to be the key factor affecting the ΔG_r in the co-cultures, which in turn affects predictions of microbial growth yields

Table 3-7 Estimation of syntrophic bacterial growth yields based on Gibbs free energy calculations

e-donor	Organism	ΔG'[a] KJ/mol donor	$Y_{XS,cal}$[b] (g cells/mol)	$Y_{XS,obs}$[c] (g cells/mol) (percent error)	Reference
Lactate	DVH/ *M. bakeri* co-culture	-61.4	3.4	6.7 (97%)[d]	Traore, 1983
Lactate	DVH/ strain 195 co-culture	-61.4	3.4	3.3 (3%)	Men, 2011
Lactate	DVH/strain 195/*Methanobacterium conglense* tri-culture	-61.4	3.4	5.3 (56%)	Men, 2011
Butyrate	*S. wolfei/ M. hungatei* co-culture	-9.1	2.3	1.36 (41%)	Beaty, 1989
Butyrate	*S. wolfei/ Desulfovibrio G11* co-culture	-9.1	2.3	0.55 (76%)	Beaty, 1989
Butyrate	*S. wolfei/M. hungatei/M.barkeri* tri-culture	-9.1	2.3	1.08 (53%)	Beaty, 1989
Butyrate	*S. wolfei*/strain 195 co-culture	-9.1	2.3	2.7 (17%)	This study

a. ΔG' (Gibbs free energy change) was calculated for H_2 in the gaseous state at 1.3 Pa (~10 nM in the aqueous phase). All other compounds are calculated at 10 mM.
b. Calculated cell yields (Y_{cal}) were based on the equation of Y= 2.08+ 0.0211× (-ΔG') (Roden *et al*., 2011).
c. Observed cell yields (Y_{obs}) were based on directly measured cell masses (Traore *et al*., 1983) or masses converted from protein concentrations by assuming 2 g cells/ g protein (Beaty *et al*., 1989), or converted from cell numbers based on the assumption of 6×10^{-13} g per syntrophic cell (Beaty *et al*., 1989; Men *et al*., 2011) (Roden *et al*., 2011).
d. Absolute error E = 3.3 g cells mol^{-1}; Relative error = 0.97; Percent error = 97%

When TCE was supplied in excess to the co-culture (on a H_2 production/consumption basis), the H_2 level dropped to the threshold concentration of 0.6 ± 0.1 nM and dechlorination ceased. Although the calculated ΔG_r available for dechlorination by strain 195 was still negative (-145.5 kJ mol^{-1}) at this concentration (Table 3-8), it did not support growth. Thermodynamic calculations indicate that hydrogen concentrations would have to reach liquid concentrations of 10^{-27} nM to drive the ΔG_r for strain 195 positive, a value that is unrealistic in the environment (Heimann *et al*., 2006). Therefore, the minimum H_2 threshold for strain 195 cells is likely not based on thermodynamics, but is rather based upon other factors such as enzyme binding affinity and specificity (Dolfing *et al*., 2003). This finding is consistent with previously published H_2 thresholds for dechlorination by *Dehalcoccoides*-containing communities (Yang *et al*., 1998; Löffler *et al*., 2013), and falls in the same range as thresholds for sulfate reduction (Luijten *et al*., 2004). Other dechlorinating isolates have been reported to have minimum H_2 thresholds around ~0.04-0.3 nM (Löffler *et al*., 1999, 2006; Luijten *et al*., 2004; Lu *et al*., 2001). In previous studies of *S. wolfei* growing with H_2-oxidizing hydrogenotrophic methanogens, sulfate reducers, and nitrate reducers, the estimated energy available for *S. wolfei* ranged from 0.9 to 15.0 kJ mol^{-1} (Jin, 2007), when butyrate fermentation ceased and the ratio of acetate to butyrate was around 900. While in this study we observed estimated energy available for *S. wolfei* was -13.7 ± 0.2 kJ mol^{-1} with the acetate to butyrate ratio of 0.4:1. Previous studies have shown calculated ΔG_r value fell in the range (-10 to -15 kJ mol^{-1}) observed in H_2-dependent terminal electron accepting processes under starvation conditions in sulfate reducing bacteria and methanogenic archaea (Hoehler *et al*., 2001, 2004; Heimann *et al*., 2010). Furthermore, the value obtained in this study was close to the average threshold value of butyrate metabolism (-13.8 ± 1.2 kJ mol^{-1}) reported in co-culture *S. aciditrophicus* and *Desulfovibrio* strain G11 at different acetate to butyrate ratios by Jackson and McInerney (2002).

Table 3-8 Calculation of Gibbs free energy of reductive dechlorination of TCE to *cis*-DCE in the presence of H_2[a].

H_2 ($\times 10^{-5}$ bar)	$H_{2(aq)}$[b] (M)	Cl^- (M)	H^+ (M)	TCE (M)	*cis*-DCE (M)	$\Delta G^{\circ}_{r,TCE-cDCE}$ (kJ mol^{-1})	ΔG (kJ mol^{-1})
7.4×10^{-2}	6.0×10^{-10}	0.025	5×10^{-8}	9.6×10^{-5}	4.3×10^{-4}	-133.0	-145.5
7.4×10^{-10}	6.0×10^{-18}	0.025	5×10^{-8}	9.6×10^{-5}	4.3×10^{-4}	-133.0	-98.4
7.4×10^{-18}	6.0×10^{-26}	0.025	5×10^{-8}	9.6×10^{-5}	4.3×10^{-4}	-133.0	-51.4
7.4×10^{-24}	6.0×10^{-32}	0.025	5×10^{-8}	9.6×10^{-5}	4.3×10^{-4}	-133.0	-16.1
7.4×10^{-28}	6.0×10^{-36}	0.025	5×10^{-8}	9.6×10^{-5}	4.3×10^{-4}	-133.0	7.4

a. TCE and *cis*-DCE concentrations were measured on day 33 under electron donor-limited condition (Figure 3-5). Gas-liquid equilibrium was assumed for calculation. H_2 concentration on day 33 was 0.6 nM (Figure 3-5). Henry's law constants used for calculation at 307.15 K are 15.309744 bar L mol^{-1} (dimensionless value: 0.591) and 7.65337 bar L mol^{-1} (dimensionless value: 0.216) for TCE and *cis*-DCE, respectively (Gossett, 1987).

b. Henry's law constant of H_2 at 307.15 K = 1.236747×10^3 bar L mol^{-1}.

It is interesting that the amount of butyrate in the bottles continued to decrease slightly (36 μmol) after TCE was depleted and ethene was being produced from VC (from day 8 to day 18). According to thermodynamics, microbial metabolism ceases when the ΔG_r available from a reaction becomes positive. At the beginning of the experiment, the ΔG_r available for *S. wolfei* butyrate fermentation was negative (-41.9 ± 1.5 KJ mol^{-1}), and on day 6, this number increased to -21.7 ± 0.3 kJ mol^{-1}, then on day 8, it increased further to -13.7 ± 0.2 kJ mol^{-1} (Figure 3-4), which is less than the minimum energy (-20 kJ mol^{-1}) required by a bacterium to synthesize ATP (34). During this time, the cell numbers decreased indicating cell death and lysis. It has been reported that butyrate fermentation by *S. wolfei* stops when aqueous H_2 concentrations reach 480 nM (Wallrabenstein & Schink, 1994). In this work, the H_2 concentration was 350 ± 20 nM in the co-culture on day 7 when all TCE was reduced to VC. However, the concentration of H_2 steadily increased to 1,200 ± 300 nM by the end of the experiment on day 18, indicating that additional butyrate fermentation occurred although cell growth had ceased, suggesting that regulation of the fermentation enzymes may not be stringent. During active dechlorination, H_2 concentrations remained at levels below 200 nM (Figure 3-2 B) indicating that the H_2 generation rate was at about the same level as the consumption rate (Figure 3-2 D) and that the growth rate of the two species was strictly coupled by hydrogen transfer.

In strain 195, acetyl-CoA is cleaved in an incomplete Wood-Ljungdahl pathway to provide the methyl group for methionine biosynthesis, whereby carbon monoxide (CO) is produced as a byproduct that accumulates and eventually inhibits *D. mccartyi* growth and dechlorination (Tang *et al*., 2009; Zhuang *et al*., 2014). However, in microbial communities, CO can serve as an energy source for many anaerobic microorganisms (Oelgeschläger and Rother, 2008). A previous study showed a high CO concentration (15%) to have an inhibitory effect on *S. wolfei* (Sieber *et al*., 2014). Here we found that not only did low levels of CO not exhibit inhibitory effects on *S. wolfei* cell growth, but *S. wolfei* could consume CO (μmol per bottle) while growing on crotonate. CO levels in the co-culture growing on butyrate were maintained at low levels during the feeding cycle rather than accumulating as it does with the 195 isolate. Therefore it is possible that CO serves as a supplemental energy source for *S. wolfei* during syntrophic fermentation with strain 195. This finding is interesting since there were no anaerobic carbon monoxide dehydrogenase genes annotated in the *S. wolfei* genome (Sieber *et al*., 2010). However Swol_1136 and Swol_1818, which were originally annotated as iron-sulfur cluster binding domain-containing protein and 2Fe-2S binding protein in *S. wolfei*, were more recently annotated in the KEGG database (Kanehisa *et al*., 2014) as carbon-monoxide dehydrogenase small sub-units for CO conversion to CO_2, suggesting the genomic potential for CO metabolic ability in *S. wolfei*.

Formation of cell aggregates has been shown to be a distinctive feature of obligate syntrophic communities containing acetogenic bacteria and methanogenic archaea (Stams *et al*., 2012). Clustering of cells with decreasing inter-microbial distances leads to increased fluxes and increased specific growth rates (Schink and Thauer, 1988). Previous studies reported that the syntrophic co-culture of a propionate degrader and a hydrogenotrophic methanogen could form cell aggregates while growing on propionate for optimal hydrogen transfer (Ishii *et al*., 2005, 2006). A similar phenomenon was also observed in mixed cultures containing propionate degraders and methanogens enriched from an anaerobic bio-waste digester where flocs formed showing that reducing the interspecies distances by aggregation was advantageous in complex

ecosystems (Felchner-Zwirello *et al*., 2012). In engineered dechlorinating systems, *D. mccartyi* species have been observed in biofilms within a membrane bioreactor (Chung *et al*., 2008) and in bioflocs maintained in a continuous flow bio-reactor fed with butyrate (Rowe *et al*., 2008). Based on morphological observation in this study, strain 195 cells grown in isolation are more likely to grow in planktonic form and when grown with DvH as a syntrophic co-culture on lactate, no significant aggregates were observed. However when grown with *S. wolfei* on butyrate, the co-cultures formed aggregates during syntrophic growth. Thermodynamic calculations show that syntrophic butyrate oxidation is endergonic unless the circumstantial H_2 partial pressure is maintained very low (Table 3-1 Table 3-4). Furthermore *fdh* dehydrogenase expression in *S. wolfei* under different growth conditions confirmed that these genes were not up-regulated in in the co-culture grown on butyrate compared to growth on crotonate, or in isolation (Crable, 2013). This is the first study to report *D. mccartyi* forming cell aggregates with a syntrophic partner. In addition, because the average inter-microbial distances are smaller for syntrophic aggregates, the H_2 and metabolite flux between cells would be expected to increase, leading to higher material transfer efficiencies, which could partly explain the observed increased cell yields of strain 195. Another reason for the observed increased cell yields of strain 195 is likely due to the continuous removal of CO, which was shown to exert an inhibitory effect on *D.mccartyi* growth (Zhuang *et al*., 2014).

In a previous study of *Methanococcus maripaludis* growing in syntrophic association with *Desulfovibrio vulgaris* under hydrogen limitation in chemostats (Walker *et al*., 2012), *M. maripaludis* was growing close to the thermodynamic threshold for growth and the acetyl-CoA synthase transcripts levels of *M. maripaludis* in the co-culturedecreased compared to the isolate. While in our study, the acetyl-CoA synthase transcripts levels of strain 195 in the co-culture increased compared to the isolate. A recent study (Pande *et al*., 2014) showed a division of metabolic labor and mutualistic interactions were the reason for increased rates of growth in a vast majority of cross-feeding strains. The benefit of cross-feeding was larger than the cost (Pande *et al*., 2014; Mee *et al*., 2014).

3.5 Summary

The syntrophic association between *S. wolfei* and strain 195 would facilitate efficient material exchange and electron transfer, which in turn would increase the specific growth rate with decreasing inter-microbial distances. Here we represent a study shows strain 195 growth and dechlorination limitation in a syntrophic relationship with specific quantification of electron flow using thermodynamic consistent rate laws. The transcriptomic microarray results demonstrated that specific ABC transporter genes were up-regulated compared to the isolate and expression were at a certain high level. The unique feature of this co-culture makes it a good model to study the co-evolution of *D. mccartyi* species with its syntrophic partner.

Acknowledgements
We Acknowledge Professor Michael McInerney at University of Oklahoma kindly provided us the pure strain *Syntrophomonas wolfei* for this study. We also thank Dr. Nikhil S. Malvankar and Professor Derek Lovley at University of Massachusetts carried out the experiments of conductivity test for the co-cultures. This work was funded through research grants from NIEHS (P42-ES04705-14)

4. Structural and Transcriptomic Study of *Dehalococcoides mccartyi* within a TCE-dechlorinating Community in a Completely Mixed Flow Reactor

4.1. Introduction

Completely mixed flow reactors (CMFR, also known as chemostats) were widely used to study fundamental problems in biochemistry, ecology, genetics and physiology in the 1970s-1980s, but the explosion of molecular biology techniques resulted in a decline in their use as a fundamental tool in microbiology starting in 1990s (Smith and Waltman, 2005). However, post-genomic assessments of microbial processes have led to a resurgence in the use of chemostat cultures to study growth, nutrient limitation and stress responses at the whole-organism level (Elias *et al*., 2006; Zengler, 2008; Douma *et al*., 2011).

Most studies performed on dechlorinating communities have occurred under batch conditions at the lab scale. However, groundwater contamination plumes are generally systems with continuous fluid flow, and contaminant and nutrient levels in the subsurface environment tend to be consistent over time and relatively low compared to laboratory batch systems (Stroo *et al*., 2010). Furthermore, the continuously changing environment (nutrient concentrations, microorganisms at different growth phases) in a batch reactor makes it difficult to interpret the results gained from both "-omics" studies and electron flow studies (Smith and Waltman, 2005; Ferenci, 2008). In order to better understand electron flows in a complex microbial system and to improve predictions of dechlorinating performance, we need a better understanding of the microbial abundance, distribution, dynamics, and functions in a continuous flow system that is more representative of contaminated plumes.

There have been a few approaches to characterize the dechlorinating performance and community structure in flow systems, such as H_2 membrane-biofilm reactors (Chung *et al*., 2008), flow-through column studies (Azizian *et al*., 2008) and up-flow anaerobic sludge bed reactor (UASB) studies (Maphosa *et al*., 2010). While there have been a limited number of studies devoted to evaluating biological reductive dechlorination in continuous flow suspended growth systems (Gerritse *et al*., 1997; Carr *et al*., 2000; Drzyzga *et al*., 2001; Zheng *et al*., 2001; Sabalowsky *et al*., 2010). These studies showed that the hydraulic retention times and hydrogen concentrations in the reactor affect dechlorination activity in complex microbial communities but they all lack information on the abundance, distribution and dynamics of key dechlorinating species. There have only been three studies that reported successful and sustainable PCE/TCE dechlorination to ethene in a CMFR. Yang reported a hydrogen concentration range and threshold level that favors dehalogenators in competition with other possible hydrogen-utilizing microorganisms within a methanogenic mixed culture. A CMFR fed with PCE and benzoate was used to confirm the findings that were observed in batch studies (Yang and McCarty, 1998). Berggren *et al*. studied the effect of sulfate reduction on kinetics and microbial structure of a dechlorinating culture PM maintaining in a CMFR. They found dechlorination efficiency decreased after complete sulfate reduction was achieved, and this phenomenon was associated with the shift of *D. mccartyi* strains in the microbial community (Berggren *et al*., 2013). Delgado reported the successful cultivation of a *D. mccartyi*-containing culture in a CMFR with a short three-day hydraulic retention time (HRT). They suggested that low bicarbonate concentrations (5 mM) in the medium minimized the electron flows to other microorganisms that use bicarbonate as electron acceptor and competition with *D. mccartyi* for H_2 as electron donor (Delgado *et al*., 2013).

The CMFR developed in this study as a controllable engineered system provides several advantages over batch systems, such as (i) continuous and consistent cultivation of cultures, (ii) highly reproducible platforms for dynamic perturbation studies and (iii) growth under "steady-state" conditions that provide more reproducible, controlled and interpretable data for "-omics" studies. In this study, the CMFR was inoculated from the long-term dechlorinating enrichment culture ANAS which has been maintained under semi-batch conditions for over 15 years. (Richardson *et al*., 2002; Lee, *et al*., 2006). The community structure, specific *D. mccartyi* strains, and response to different environmental stresses have been extensively studied (Freeborn *et al*., 2005; Lee *et al*., 2011; West *et al*., 2013). In the continuous flow culture inoculated with ANAS(CANAS), sustained selective pressure (i.e., constant supply of chlorinated ethenes) was applied to the microbial community in the presence of low concentrations of electron donor and corrinoids, as frequently observed in contaminated oligotrophic groundwater plumes (Stroo *et al*., 2010). In order to understand the microbial community structure shift from "feast-and-famine" conditions (ANAS) to the continuous feeding of low nutrients condition (CANAS), 16S I-tags and metagenomic analysis were applied to investigate the shift in community structure from semi-batch to stable dechlorination. A *D. mccartyi* genus-wide microarray was also applied to study the transcriptional dynamics of *D.mccartyi* species within CANAS.

4.2 Materials and Methods

4.2.1 Inoculum culture

A 3.0 liter completely mixed flow reactor (CMFR) was inoculated at 5% dilution with dechlorinating enrichment culture ANAS. ANAS was originally enriched from contaminated soil obtained from Alameda Naval Air Station, and has been functionally stable for over 15 years in a continuously stirred semi-batch fed reactor. 25 mM lactate was supplied as both electron donor and carbon source and 0.1 mM TCE was supplied as the terminal electron acceptor. The growth and maintenance procedures of ANAS have been previously described (Lee *et al*., 2006). Two distinct *D. mccartyi* strains in ANAS were identified as ANAS1 which contains known TCE reductive dehalogenase gene *tceA*, and ANAS2 which contains known VC reductive dehalogenase gene *vcrA* (Lee *et al*., 2011). The community of ANAS contains over 1000 Bacterial and Archaeal taxa (Brisson *et al*., 2012), and has been extensively studied (Richardson *et al*.; Lee *et al*., 2006 West *et al*., 2008). The culture maintained in this CMFR is referred as CANAS.

4.2.2 CMFR reactor set-up and maintenance

The CMFR was constructed by using a 3.0 L fermenter (New Brunswick, New Jersey), fitted with Teflon caps and viton tubing (Masterflex®, Co-Parmer Instrument co.) enabling anoxic operation (Figure 4-1). Pure TCE is stored in a 1.0 mL gas tight syringe (Hamilton), and is fed to the reactor by a syringe pump (NE-300 programmable syringe pump, New Era Pump Systems). Lactate is fed to the reactor from a separate influent bottle at 10 mM, which is in stoichiometric excess to TCE (1.7 mM) based on electron equivalents enabling dechlorination of TCE to ethene. The feeding rates resulted in a both hydraulic and solids retention times (HRT and SRT) of 40 days (during steady-state) to avoid washout of the slow-growing microorganisms.

The composition of the influent was modified from previously described defined medium for growing the *D.mccartyi* 195 isolate (Johnson, *et al*., 2008) with the following modification: the reducing agent cysteine-sulfide concentration was doubled from 0.2 mM to 0.4 mM in order to ensure the anoxic condition through the tubing as well as within the reactor. pH of the influent was maintained between 7.0 to 7.3 by 30 mM sodium bicarbonate and 10mM TES buffer. pH in the reactor was maintained at be 7.2 ± 0.1 using a pH monitor (Hanna Instruments). The CMFR was continuously stirred with a magnetic stir bar (~10 rpm) at room temperature (23±2°C) to ensure rapid equilibrium dissolution of TCE and to minimize mass-transfer limitations (detailed information of maintaining parameters of CANAS and ANAS culture was summarized in table 4-1).

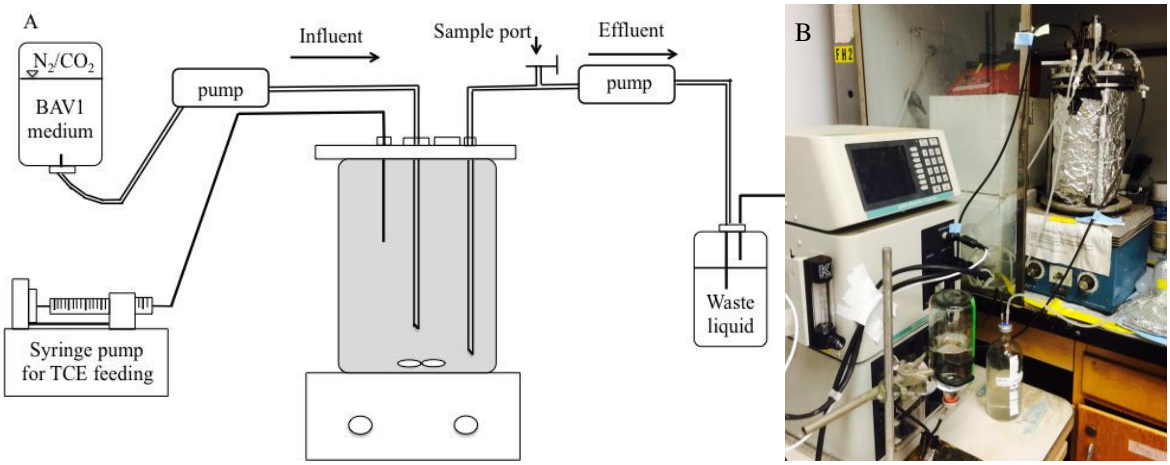

Figure 4-1 A) Schemetic and B) photograph of the experimental apparatus used in this study. A slight positive pressure was applied to the influent BAV1 medium bottle in order to avoid oxygen intrusion to the influent bottle.

Table 4-1 Key components and maintaining parameters of ANAS and CANAS.

Parameters	ANAS	CANAS
Running mode	Semi-batch "feast-and-famine"	Continuous flow "steady-state" condition
Average SRT (days)	93	40
Medium	Defined medium for ANAS[a]	Defined medium for strain 195[b]
Working volume (mL)	400	2900~3000
Vitamin B_{12} (mg/L)	0.001	0.1 (in influent)
Buffer	41.7mM HCO_3^-	10mM TES and 30mM HCO_3^-
Electron donor/acceptor ratio (based on e^--equiv)[c]	180	11.8

a. West *et al*., 2008.
b. Johnson *et al*., 2008.
c. 10 mmol lactate and 10µL TCE were amended to ANAS every14 days; 10mM Lactate and 1.7 mM TCE were supplied independently in influent to CANAS.

Routine sample collection steps are as following: For GC analysis, 2mL liquid sample is routinely collected from the sample port and immediately transferred to a 10mL sample vial

sealed with blue stopper. The liquid samples are vortexed for 20 seconds and then rested for 1 minute before GC measurement. Mass of each compound was calculated based on gas/liquid equilibrium by using Henry's law constants at 25 °C. Mass (μmol/bottle) = $C_l \times V_l + C_g \times V_g$, $k_H^{cc} = C_l / C_g$. For organic acid and cell analysis, 1.5 mL liquid samples are taken from the effluent tube and centrifuged at 14,000g, 10 °C. The supernatant was used for organic acids quantification and the cell pellet was stored at -20 for DNA extraction.

After the CMFR reached "steady state" for five SRTs (all measured metabolites: chlorinated solvents, ethene, methane, H_2, organic acids, and specific biomarker concentrations were at stable levels), duplicate cell samples were collected during one SRT for DNA/RNA extraction. Briefly, 100 mL aqueous samples were collected at the sample port and filtered on a 0.2 μm filter. Each filter was then placed in a 2 mL orange-cap micro-centrifuge tube, frozen with liquid nitrogen and stored at -80 °C until further process. This sample collection procedure was repeated in three consecutive SRTs to generate biological triplicates.

4.2.3 Chemical and molecular methods

Chloroethenes, ethene and methane were measured by injecting 100 μL headspace of the sample vial to an FID-gas chromatograph, and 300 μL headspace sample of hydrogen was measured by RGD-gas chromatography as described previously (Freeborn *et al*., 2005; Lee *et al*., 2006). Organic acids, including lactate, acetate and propionate were analyzed with a high-performance liquid chromatograph as described previously (Freeborn *et al*., 2005).

Gene quantification in CANAS was performed using real-time quantitative PCR (qPCR), including the number of *tceA* and *vcrA* genes, total numbers of Bacteria, Archaea and *D.mccartyi* targeting the 16S rRNA genes, as reported previously (West *et al*., 2013). The primers used in this study are summarized in table 4-2.

Table 4-2 Primer sets used in qPCR analysis

Target	Primer	Reference
Total bacteria16S rRNA	Forward 5'-TCCTACGGGAGGCAGCAG-3' Reverse 5'-GTTTAVDGCRTRGACTACCA-3'	West, 2013
Archaea 16S rRNA	Forward 5'-ATTAGATACCCSGBTAGTCC-3' Reverse 5'-GCCATGCACCWCCTCT-3'	West, 2013
*tce*A (AF228507)	Forward 5'- ATCCAGATTATGACCCTGGTGAA-3' Reverse 5'- GCGGCATATATTAGGGCATCTT -3'	Johnson, 2005
*vcr*A (AY322364)	Forward 5'-CTCGGCTACCGAACGGATT -3' Reverse 5'-GGGCAGGAGGATTGACACAT-3'	Holmes, 2006
D.mccartyi 16S rRNA	Forward 5'GGTAATACGTAGGAAGCAAGC-3' Reverse 5'-CCGGTTAAGCCGGAAATT-3'	West, 2013

DNA/RNA were extracted using the phenol-chloroform method described previously (West *et al*., 2008). Briefly, DNA and RNA were separated by using AllPrep DNA/RNA Mini Kit (Qiagen) according to the manual instruction. RNA pellet was re-suspended in 100 μL of nuclease-free water and were further purified by using Turbo DNA free kit (Ambion, Austin, TX) to remove additional DNA contamination according to the manufacturer's instructions. The

quality of RNA samples was checked by electrophoresis, and the concentrations of RNA samples were quantified by using a nano-photometer (IMPLEN, Westlake Village, CA, USA). The ratio of A260/A280 for all samples was between ~1.80-2.0. Purified RNA was stored at -80 °C prior to further use.

4.2.4 Genus-wide microarray analysis of the microbial community

Microarray sample preparation and application procedures were described previously (Johnson *et al*., 2008; Lee *et al*., 2011; West *et al*., 2013). Briefly, 1 µg of community gDNA was applied for DNA analysis and 10 µg of community total RNA was used as starting material for RNA analysis as previously described (West *et al*., 2008).

All probe sets that were detected as "present" by DNA microarray analysis were considered in the RNA analysis. DNA for any particular ORF was deemed "present" if each replicate probe set for that ORF had signal intensity greater than 140 and a P value less than 0.05 in the DNA chips. RNA for any particular ORF was considered "present" if the average signal intensity of the probe sets for that ORF was greater than 120. The criteria applied in this study are the same as previously described for the ANAS transcriptomic study (West *et al*., 2013).

4.2.5 Metagenomic analysis of community structure

DNA samples for metagenome sequencing were prepared using Nextera XT DNA Sample Preparation Kit (Illumina, CA, USA) according to the manual instruction. The prepared DNA libraries were sent to the California Institute for Quantitative Biosciences (QB3 facility, Vincent J. Coates Genomics Sequencing Laboratory, University of California, Berkeley) for short-gun sequencing on the illumina® HiSeq 2000 platform according to the manufacturer's instructions. A binning process developed by Albertsen *et al*. (2013) was modified and applied to recover the genomes from metagenomic datasets. The trimmed paired-end reads from the metagenomes were first assembled by CLC's *de novo* assembly algorithm, using a k-mer of 63 and a minimum contig length of 1k bp. Reads from each metagenome were then individually mapped to scaffolds using CLC with a minimum similarity of 95% over 100% of the read length. The relative metagenome abundance of each genome bin was determined as a percentage of metagenome reads mapped to a specific bin in the total metagenome reads (Albertsen *et al*., 2013).

Assembled contigs grouped to different bin-genomes were further BLASTx against NCBI-nr database for taxonomic classification. If more than 50% of the genes within a contig were attributed to the same family, the contigs were assigned to that family (Ishii *et al*., 2013). Contigs were aligned with Silva SSUref database (115) with a cutoff of 1e-20 to identify 16S rRNA gene and based on 16S raRNA information, further taxonomic assignment was carried out.

Contigs produced by *de novo* assembly were submitted to Metagenmark server (Zhu *et al*., 2010) for ORF calling. The ORFs as well as contigs belonging to particular bin-genomes were further identified and annotated using the RAST server (Aziz *et al*., 2008) and were manually annotated with KEGG database. Simultaneously, functional prediction of novel

sequences was performed by Pfam (Punta *et al*., 2012). The potential TCE degrading genes involved were investigated subsequently for understanding of functional sequences diversity and relationship of degrading microorganisms.

4.2.6 16S-"itag" analysis of community structure

PCR amplification was carried out for each sample in triplicate, on ice, in 50-μL reaction mixtures containing 0.025 U μL^{-1} Herculase® II Fusion (Agilent Technologies, Santa Clara, CA) (1.25 U/reaction for target amplicons of <1 kb; 2.5 U/reaction for target amplicons of 1-10 kb), 1× Herculase® Buffer, 250 μM dNTPs, 0.2 μM of each primer and genomic DNA (input DNA of 10-50 ng unless otherwise indicated). PCR amplification was performed with a Mastercycler Gradient (Eppendorf, Hauppauge, NY) under the following conditions: thermocycler set at 98 °C before insertion of PCR tubes (simplified hot start method); an initial denaturation step at 98 °C for 2 min; 35 cycles of 95 °C for 20 s, 50 °C for 30 s, 72 °C for 30 s (30 s for target amplicons of <1 kb or 30 s kb^{-1} for target amplicons of ≥1 kb); a final extension at 72 °C for 3 min.

PCR reactions for each sample were combined, size-selected and purified by electrophoresis on a 2% agarose gel. Target amplicons were recovered using the Ultra-Clean® GelSpin® DNA Extraction Kit (Mo Bio Laboratories, Inc., Carlsbad, CA) in 50 μL Tris buffer (10 mM). For each individual sample, triplicate PCR products with unique barcodes were mixed in equimolar ratios and quantified on a Nanophotometer P-300 (Implem, Westlake Village, CA) and by Picogreen-based fluorimetry using a Nanodrop ND-3300 (Thermo Scientific, Inc., Waltham, MA). The pooled sample with a Bioanalyzer trace (Agilent DNA 1000 Kit), along with three sequencing primers, was sent to the California Institute for Quantitative Biosciences (QB3 facility, Vincent J. Coates Genomics Sequencing Laboratory, University of California, Berkeley) for 150-nucleotide paired-end multiplex sequencing on the illumina® HiSeq 2000 platform according to the manufacturer's instructions. Quality control using Qubit® 2.0 Fluorometer (Life Technologies, Grand Island, NY) and qPCR was carried by QB3 facility. To offset the limited sequence diversity among the 16S rRNA or ITS amplicons (low-diversity libraries), balanced base genomic libraries were set as a control lane.

Sequence Assembly and Annotation. Paired-end illumina reads were assembled using Fast Length Adjustment of SHort reads (FLASH, version1.2.6) (Magoc & Salzberg, 2011). The assembled sequences were then demultiplexed in the open source software package Quantitative Insights Into Microbial Ecology (QIIME, version1.7.0) (Caporaso *et al.*, 2010), using maximum consecutive low-quality bases of 5, minimum consecutive high-quality bases of 60% of the original reads, maximum N's of 25 and the default Phred quality threshold of 3. Taxonomic assignment was performed in QIIME, a threshold of 97% pairwise identity was applied for 16S rRNA analysis.

4.3 Results

4.3.1 Reactor development and performance

The CMFR was initially inoculated with 5% (vol/vol) of the ANAS semi-batch culture. 300 mmol (i.e. ~10 mM) lactate and 10 μL TCE was fed (i.e. ~40 μM in liquid) to the reactor to

initiate growth. After 15 days incubation under batch condition at room temperature, methane (MTH) and *cis*-DCE were simultaneously produced while vinyl chloride (VC) and ethene (ETH) production were observed on day 20. After several doses of TCE were consecutively reduced to VC and ETH (Figure 4-2 A), the reactor was switched to intermittent flow mode (Stage II). The liquid flow rate was gradually increased from 20 mL day^{-1} to 40 mL day^{-1} with MTH as the main detected product (Figure 4-2 B). At this stage, the chlorinated solvent mass balances were poor, so on day 55, the whole system was flushed with ultra pure nitrogen (Praxair) and ~200 mL fresh medium was pumped into the reactor in order to eliminate the headspace. During stage III, the flow rate was steadily increased from 40 mL day^{-1} to 75 mL day^{-1} and better mass balances were achieved. However as the flow rate increased, incomplete TCE dechlorination (main product VC) was observed (Figure 4-2 C). The system was flushed again with ultra pure nitrogen, and the silicone connection tubings were replaced by viton tubing (Masterflex®, Co-Parmer Instrument co.) in order to avoid any oxygen intrusion during liquid delivery. Furthermore a syringe pump was applied to continuously pump TCE to the system at a rate of 133 μmol day^{-1}, resulting in an influent concentration of 1.7 mM. After 10 days, ethene became the main dechlorination product and methane concentration was stably maintained at 450 μM (Figure 4-2 D).

Table 4-3 CMFR maintenance strategies at different stages

Stage	Flow pattern	Flow rate (mL/day)	Headspace (mL)	Main product	Feeding	Comment
I	Batch	-	300	MTH,VC	TCE and lactate were injected to the reactor subsequentially	System set-up Poor mass balance
II	Intermittent	20~40	300	MTH	TCE and lactate were injected to the reactor subsequentially	System unstable Poor mass balance
III	Intermittent	40-75	0	MTH, VC	TCE and lactate were injected to the reactor subsequentially	incomplete reduction but better mass balance
IV	Continuous	75	0	MTH, ETH	TCE was injected through syringe pump	complete reduction and better mass balance

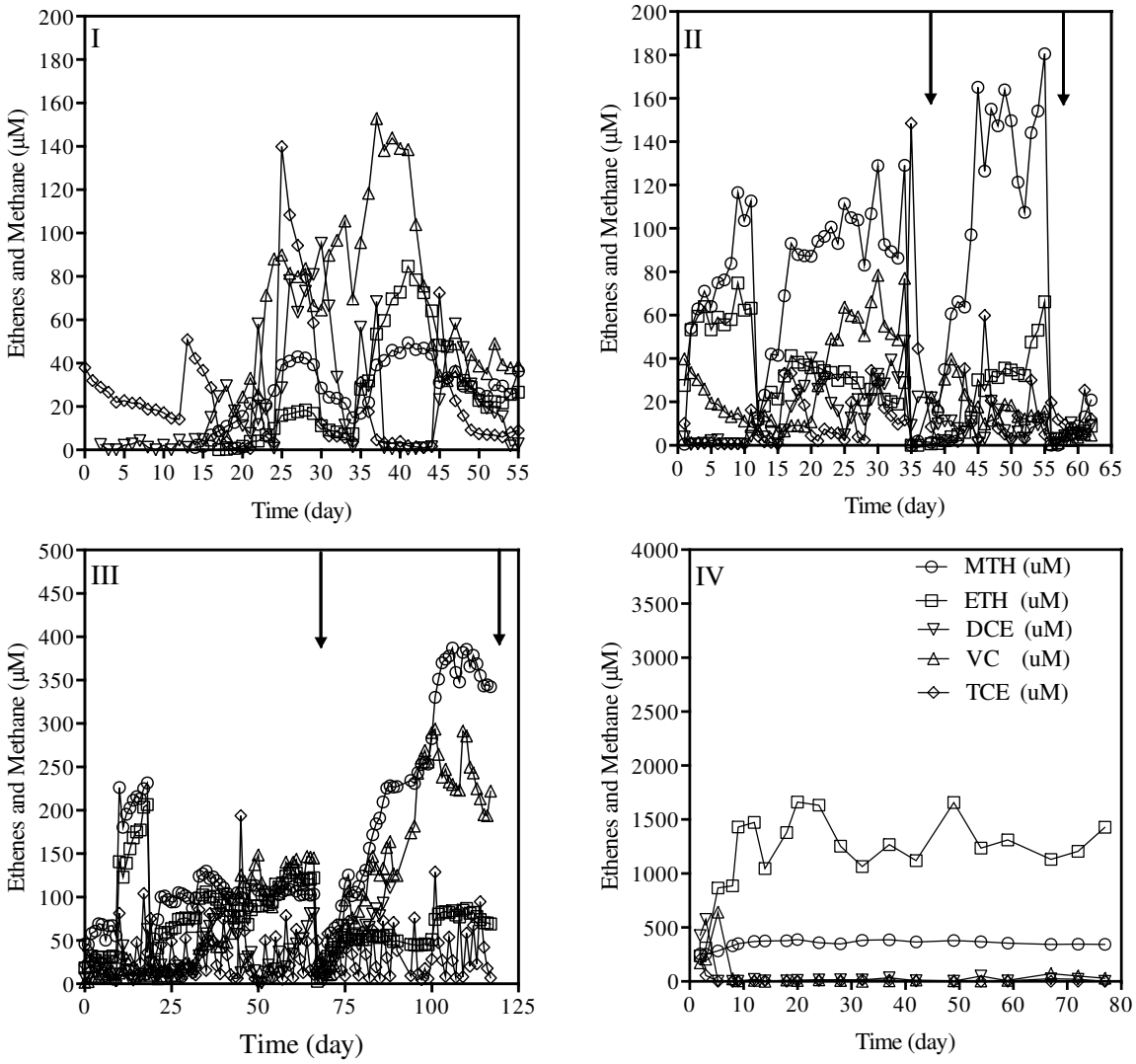

Figure 4-2 Reductive dechlorination performance of the microbial community in the CMFR during the four stages listed in Table 4-3. Arrows indicate when system was flushed by N_2 gas.

4.3.2 Steady-state performace of the microbial community

Two main criteria were applied to choose the 40-day SRT for this study. First, the SRT needed to be long enough to maintain the slow growing microorganisms in the system in order to avoid washout. Second, the SRT needed to be short enough that sufficient biomass was generated for the molecular analyses. The basic operating parameters for CANAS are compared with previous CMFR studies that generated ethene as the main end product are summarized in table 4-4. Separating TCE (1.7mM) and lactate (10 mM) feeding enabled the control of electron donor and acceptor concentrations independently. After the CMFR reached steady state for five SRTs (Figure 4.3), samples were collected for both microbial community structure and transcriptomis analysis.

Around 88% of TCE in the influent was converted to ethene 1.50± 0.10 mM, vinyl chloride (VC) 0.09± 0.06 mM and *cis*-DCE 0.03 ± 0.01 mM (Fig 4-3 A). The chlorinated solvent recovery rate was 83~108% during the experimental period (200 days). The dechlorination rate of the reactor was 118 μmol Cl^- L^{-1} day^{-1}. Methane production was maintained at a low level of 0.56 ± 0.10 mM. Two *D. mccartyi* strains, ANAS1 and ANAS2, that were present in the ANAS inoculum, were stably maintained in CANAS with copy numbers of *tceA* and *vcrA* at 6.2 ± 2.8 $\times 10^8$ copies/mL and 5.8 $\pm 1.2 \times 10^8$ copies/mL, indicating that the ratio of ANAS1 to ANAS2 in CANAS was approximately 1:1, while the ratio in ANAS was around 10:1(Lee, *et al*., 2011).

Electron balance in the system was calculated throughout the experimental period. As a result of fermentation of 10 mM lactate in the influent, propionate and acetate concentrations in the reactor effluent were 3.1 ± 0.4 mM and 6.7 ± 0.7 mM, respectively throughout the experimental period. H_2 concentrations were maintained at around 0.2 μM (data not shown in the graph), which was well in excess of the reported minimum H_2 threshold (2 nM) for dechlorination reactions to occur. Recovery of electrons (calculated based on electron equivalents) was observed to be 95-108% throughout the experiment. A typical electron balance measured over a 2-day period resulted in 104 % of electron recovery (Table 4-5), a result simlary to overrecoveries reported in previous bioreactor studies (Drzyzga *et al*., 2001). Only 8 % of the electrons consumed went to dechlorination while 77 % were stored in propionate and acetate, and 2 % went to methane production and trace H_2. Biomass production accounts for a large portion (12%) of electron flow in this reactor, compared to previous bioreactor studies with 7.5 ~ 9.2% (Azizian *et al*., 2010; Berggren *et al*., 2013). Biomass calculations assumed a cell formula of $C_5H_7O_2N$, an average dry cell weight of 4.2×10^{-15} g $cell^{-1}$ (Duhamel *et al*., 2007) and total cell numbers of Bacteria ($2.3 \pm 0.8 \times 10^{10}$ mL^{-1}) and Archaea ($1.1 \pm 0.4 \times 10^7$ mL^{-1}) taken as the average values quantified throughout the experiment (Figure 4-3 A). With the relative longer SRTs, it may be that neglecting cell decay could affect both calculated dechlorination rates and the net cell production rates. Further, decaying cells could serve as an electron donor source (Yang *et al*., 2000; Sleep *et al*., 2005), contributing to the observed overrecovery of electrons. Another possible explanation for overrecoveries could be that we used 16S rRNA copy numbers to represent cell numbers, making it possible to overestimate cell numbers for the bacteria that carry multiple 16S rRNA gene copies.

Table 4-4 Comparison of key parameters of the current study with previous CMFR studies with ethene as the main dechlorination end product.

	CANAS	PM[a]	CSTR-R^2[b]
Culture source	Methanogenic TCE enrichment culture	Non methanogenic PCE enrichment culture	Methanogenic TCE enrichment culture
SRT (days)	40	55.5	3
Working volume (mL)	3000	5000	500
Headspace (mL)	0	0	150
Vitamin B_{12} (µg/L)	100	50	500
pH buffer	30mM HCO_3^- plus 10mM TES	35mM Na_2CO_3 plus 6mM K_2HPO_4	15mM HEPES plus 5mM HCO_3^-
Electron donor	10mM Lactate	4.3mM lactate	7.5mM Lactate + 15mM methanol
Electron acceptor	1.7mM TCE	1.12mM PCE	1~2mM TCE
Cell yield ($\times 10^8$ cells/ µmol Cl^- released)	2.9±0.7[c]	N.A.	4.3~5.3 [d]
D.mccartyi production rate (cell L^{-1} d^{-1})	3×10^{10}	N.A.	3.3×10^{11}

a. Values were from Berggren *et al*. 2013
b. Values were from Delgado *et al*. 2013
c. Value was the average of cell yield based on *D. mccartyi* cell concentrations (sum of strain ANAS1 and ANAS2) and Cl^- released at each data point throughout the experiment.
d. Values were calculated from *D. mccartyi* cell number 1.3×10^{12} cell L^{-1} at1mM TCE influent, and 1.6×10^{12} cell L^{-1} at 2mM TCE influent, all TCE was reduced to ethene.

Table 4-5 Mass balance of CANAS over a typical 2-Day period

Parameter	e^--equiv factor	Mass changed (µmol)	e^--equiv formed (µ e^--equiv)	e^--equiv consumed (µ e^--equiv)
Lactate	12	-750		9000
H_2	2	0.02	0.04	
cis-DCE	4	1.6	6.4	
VC	2	4.5	9	
Ethene	8	95	760	
Methane	8	28	227	
Acetate	8	502	4020	
Propionate	14	233	3260	
Biomass	20	55	1110	
Total			9392 (104 %)	9000

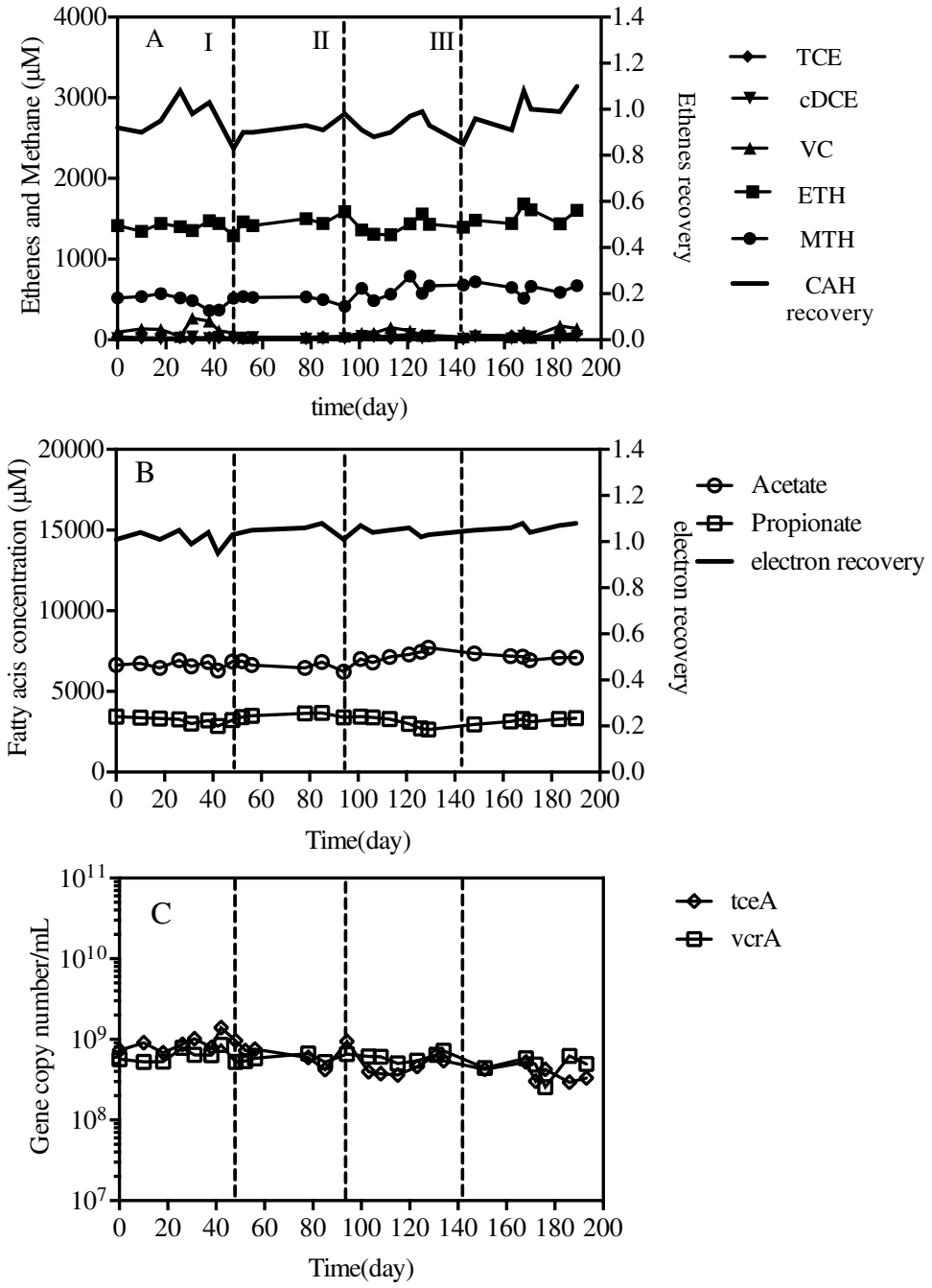

Figure 4-3 A) Reductive dechlorination performance and chlroinated solvents recovery; B) fatty acids formation and electron recovery; and C) reductive dehalogenase gene copy numbers in the CMFR at steady state during the experimental period. Strains ANAS 1 and ANAS2 contain the *tceA* and *vcrA* genes, respectively. DNA/RNA samples were collected in three consecutive SRTs (I, II and III indicated in A) for microbial structure and functional analysis.

4.3.3 Microbial community structure analysis

Quantification of total D. mccartyi, Bacteria and Archaea

Cell numbers of total Bacteria, Archaea and *D. mccartyi* were monitored through the experimental period by qPCR of 16S rRNA copy numbers (Figure 4-4). Total Bacteria, Archaea and *D. mccartyi* at four continuous SRTs to be $2.3 \pm 0.8 \times 10^{10}$ mL^{-1}, $1.1 \pm 0.4 \times 10^{7}$ mL^{-1} and $1.4 \pm 0.3 \times 10^{9}$ mL^{-1}, respectively. The ratios of *D.mccartyi* 16S rRNA copy number to the total 16S rRNA copy numbers were 4.2%, 5.8%, and 5.3% for CANAS at stage I, II, III and 4.1% and 4.7% for ANAS during active dechlorination (i.e. 20 hours after TCE amendment, all declorination metabolites were present) and inactive dechlorination (13 days after TCE amendment, only ethene and methane present).

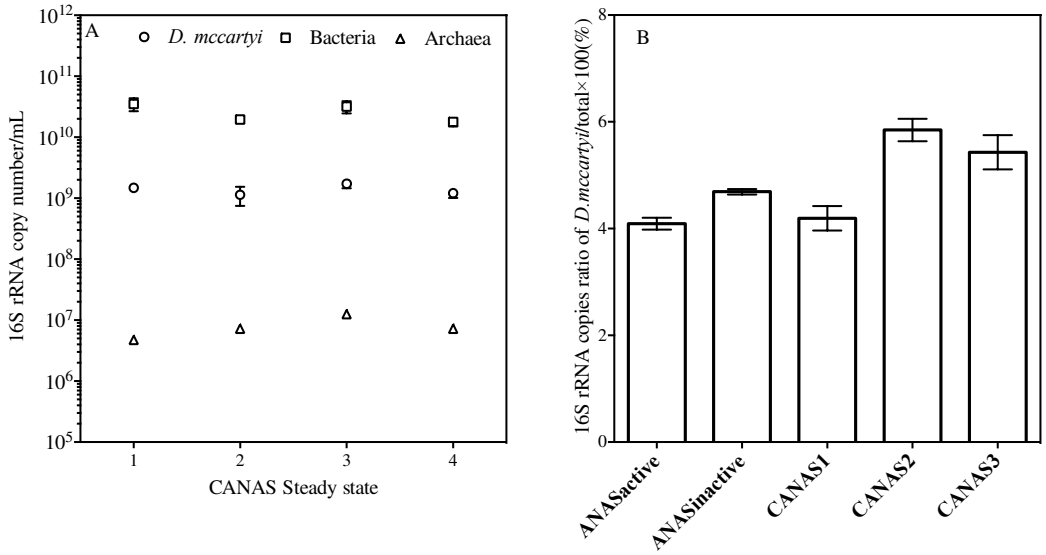

Figure 4-4 A) Cell densities of total Bacteria, Archaea and *D.mccartyi*, during four stages of the experiment (days X, Y, Z and W). Values are the average of twelve biological replicates collected independently during each stage. Error bars indicate SD. B) ratio of 16S rRNA copy numbers of *D.mccartyi* to total Bacterial and Archaea. , The ratios for ANAS were reported previously (West *et al*., 2013).

16S rRNA analysis (iTag)

16S rRNA sequencing results (iTag) revealed 10 dominant microbial families in CANAS. The composition and abundance of each group of microorganisms demonstrated that the community structure has been significantly changed and become much simpler than the ANAS inoculum (Figure 4-5). In ANAS, a comparison between the active dechlorination stage (20 hours, i.e. ANAS20hr) and inactive dechlorination stage (14 days, i.e. ANAS14days) revealed minimal differences (data not shown). Among the microorganisms present in both CANAS and ANAS, *D. mccartyi* was relatively stable (0.34~0.78%) in CANAS at three sampling time, while in ANAS, the percent was 0.74-0.78 %. In all conditions, the percentage of *D. mccartyi* species detected by 16S rRNA sequencing was lower than that detected by using qPCR analysis (4-6%). *Desulfovibrionaceae* was quite stable in CANAS at 1.3~2.1%, which was much lower than that maintained in ANAS 42-52%. *Methanobacteriaceae* was stable at 0.16~0.46% in CANAS, while in ANAS, this number was 5.4~6.3%. The decrease of methanogens in the community structure

was consistent with the decrease in methane production in CANAS compared with ANAS (Figure 4-3 A, West *et al*., 2013). The number of *Clostridiaceae* increased from 6.4 to 15% in CANAS from stage I to III with a decrease of the *Peudomonadaceae* from 81% to 60%, while in ANAS, *Clostridiaceae* represented about 7.8~9.9% of the sequences. There were a few other groups of microorganisms that were detected in CANAS but were not detected by sequencing in ANAS, such as *Comamonadaceae* (0.16~11%), *Xanthomonadaceae* (0.06~15%), *Spirochaetaceae* (1.8~3.5%) and *Peptococcaceae* (1.4~2.3%).

A surprise finding in the community structure analysis was that CANAS community sequences were dominated by *Pseudomonas* (47~81%), which are mostly asscoated with aerobic and facultative anaerobic bacteria. In addition, there were also a few groups of microorgnisms that were only detected in ANAS, such as *Porphyromonadadaceae* (6.4-12%), which is composed of two genera of environmental bacteria, *Porphyromonas* (anaerobe) and *Dysgonomonas* (facultative anaerobe) (Boone *et al*., 2012); *Thermovirgaceae* (6.4%-8.6%); BacteroidalesOR (0.84%-2.4%); *Sphaerochaetaceae* (5.9~6.2%); *Anaerolinaceae* (2.4~3.2%); *Dethiosulfovibrionaceae* (1.7% -2.5%) and *Thermotogaceae* (2.1-2.3%).

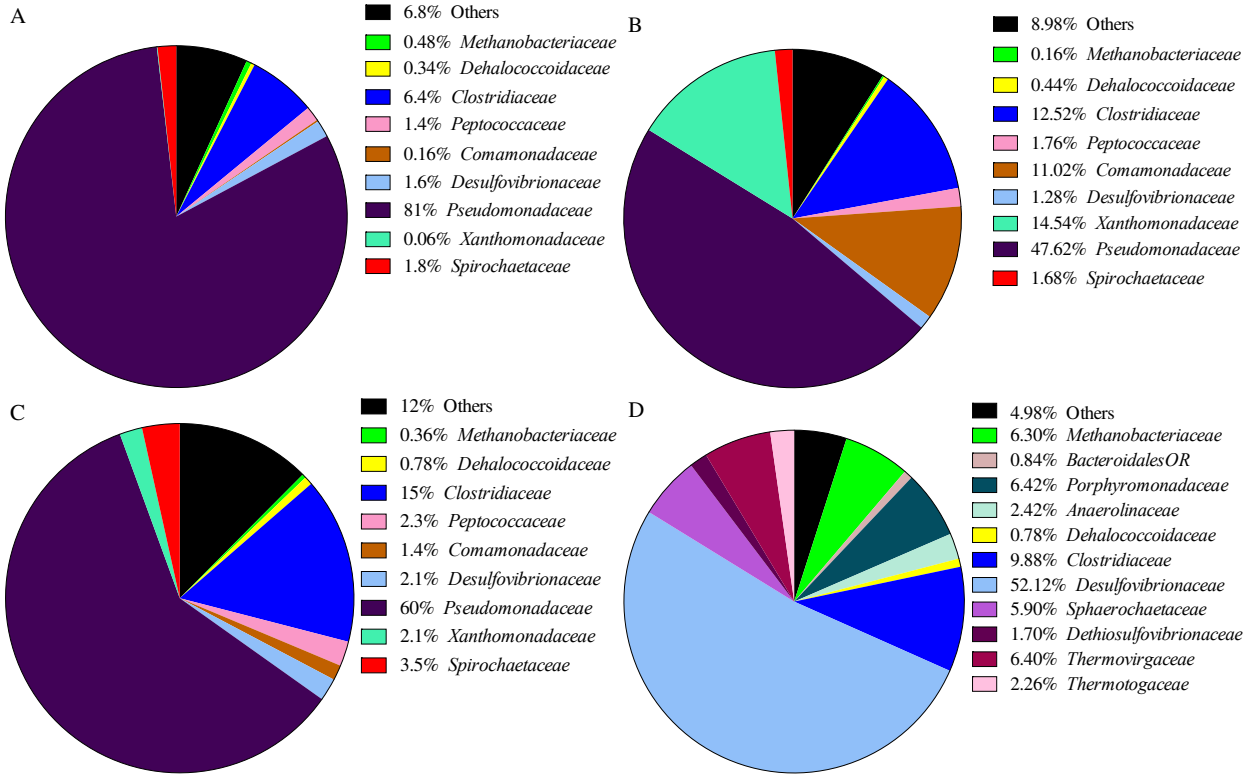

Figure 4-5 A-C) Community structure composition based on iTag sequencing of 16 S rRNA genes of CANAS during three consecutive stages (I, II and III) and D) ANAS during active dechlorination (20 hours after TCE feeding, all dechlorination metabolites were present).

Metagenomic analysis

The coverage of bin-genomes recovered from metagenome sequencing of ANAS during active dechlorination (20 hours) and and from CANAS suring stage III were compared and

presented in Figure 4-6. Analysis revealed 18 dominant bin genomes in CANAS that shifted significantly from the original ANAS inoculum. Different colored islands with specific numbers indicate distinct bin-genomes recovered from metagenomic datasets of ANAS and CANAS at the phylum level. Although coverage of the majority of microbial groups shifted significantly between the two reactor conditions, the coverage of *D. mccartyi* species (ANAS1 and ANAS2, denoted 1a and 1b in Figure 4-6) were maintained at relatively stable levels and were the dominant sequences recoverd in both growth conditions. Comparison of coverage for metagenomic from active and starved ANAS data showed little discrepancy (data not shown), consistent with the 16S rRNA analysis.

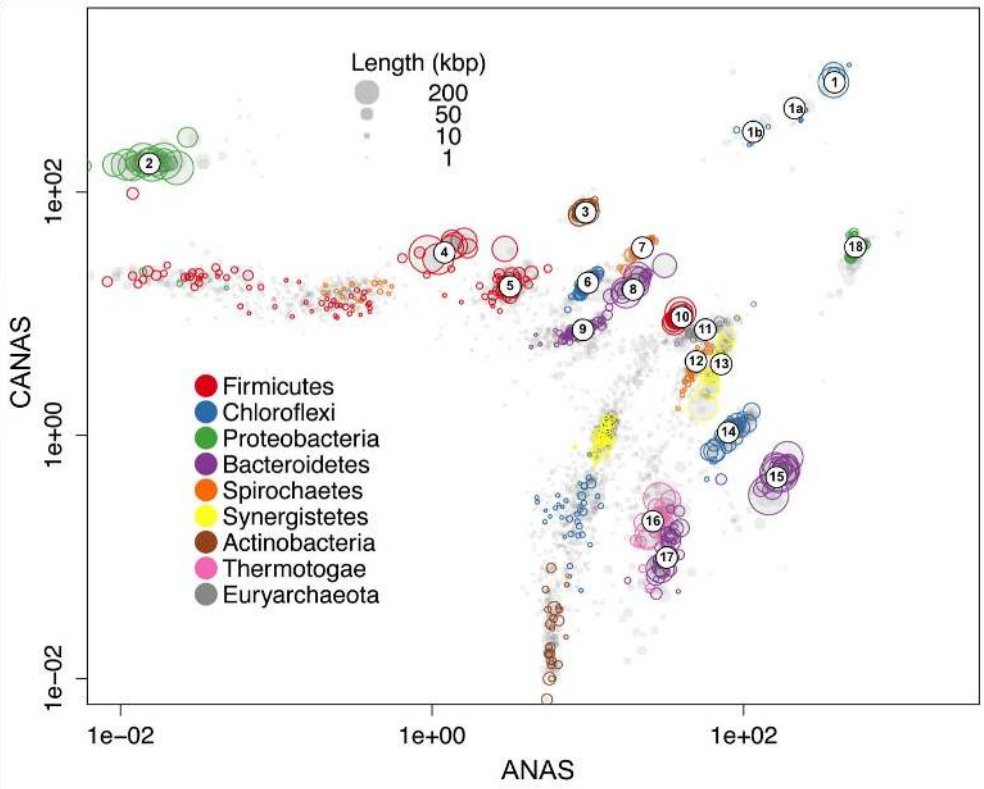

Figure 4-6 Bin-genomes recovered from metagenomic datasets. The x-axis is the coverage in ANAS at 20 hours while the y-axis is the coverage in CANAS at stage III.

The bin-genomes coverage of each microbial group labeled in Figure 4-6 under both conditions are summarized in Table 4-6. Similar to the results obtained from the 16S rRNA analysis, the CANAS population had higher coverage of *Pseudomonas* (Genome ID: 2) and *Clostridium* (Genome ID: 4, 5, 10) than ANAS. In order determine whether these organisms participate directly in dechlorination within CANAS, we searched their bin-genomes for reductive dechlorinases and found none suggesting that they perform other functions within the community. The coverage of *Desulfovibrio* (Genome ID: 18) and *Euryarchaeota* (Genome ID: 11) decreased significantly from ANAS to CANAS, also consistent with the 16S rRNA analysis. Furthermore, metagenome analysis identified two distinct bin-genomes *Chloroflexi*1 (Genome ID: 6) and *Chloroflexi*2 (Genome ID: 14), and revealed that the coverage of these two species differed significantly between the two reactor conditions.

Table 4-6 Coverage of bin-genomes recovered in ANAS20H and CANAS

Genome ID	Bin-genomes	Average coverage of contigs		Ratio
		CANAS	ANAS20hr	
1a	*D. mccartyi* ANAS1 partial contigs	440	170	2.7
1b	*D. mccartyi* ANAS2 partial contigs	300.1	79	3.8
2	*Pseudomonas*	190	0.020	7900
3	*Actinobacter*	72	8.4	8.5
4	*Firmicutes* 1	17	1.7	10
5	*Firmicutes*2	34	12	2.8
6	*Chloroflexi*1	18	6.0	3.0
7	*Spirochaetes*	35	14	2.5
8	*Bacteriodetes*1	17	5.2	3.3
9	*Bacteriodetes*2	7.0	0.71	9.8
10	*Firmicutes*	9.5	19	0.51
11	*Euryarchaeota*	7.5	36	0.21
12	*Spirochaetes*	3.8	14	0.27
13	*Synergistetes*	4.6	35	0.13
14	*Chloroflexi*2	1.1	56	1.9×10^{-2}
15	*Bacteroidetes*3	0.45	76	5.9×10^{-3}
16	*Thermotogae*	0.19	19	9.9×10^{-3}
17	*Bacteroidetes*4	0.12	16	7.5×10^{-3}
18	*Desulfovibrio*	34	629	5.4×10^{-2}

4.3.4 Transcriptomic analysis of *Dehalococcoides* in CANAS

The goal of the transcriptomic study was to examine and compare the gene expression of *D. mccartyi* within a long-term dynamic microbial community sustained under different environmental conditions (ANAS in semi-batch and CANAS in CMFR). All expression levels were normalized to spike-in samples for both ANAS and CANAS, since *Dehalococcoides* species were present as similar percents of the whole community in both (Figure 4-7 B). Most highly expressed genes in CANAS through out the experimental period were genes encoding for ribosomal RNA (5s, 16s and 23s rRNA) and reductive dehalogenases *tceA* and *vcrA*.

The expression levels (fluorescence signals) of *tceA* (DET0079) and DET0078 (the anchor protein of *tceA*), and *vcrA* (DET0079) in CANAS were about the same as in actively dechlorinating ANAS, as were other RDase genes, DET0173 and DET 1545 (Figure 4-8 A). In contrast, the expression of several putative hydrogenase (*hyc*, *ech*, *hup*, *hym*, *vhu*) and several oxidoreductase genes (*fdh*, *mod*, *nuo*, *pfoF*, *por*) were moderate compared to active ANAS, but were higher than inactive ANAS (Figure 4-7 B). Specifically, the most highly expressed hydrogenases were *hup* and *vhu*, which were expressed similarly to active ANAS, but were twice as high as starving ANAS. Other oxidoreductases followed the same trend as the hydrogenases expression. For a putative formate dehydrogenase (*fdh*), the signal intensity was about 20% of ANAS active dechlorination, but well above ANAS inactive dechlorination. Previous studies have shown that *D.mccartyi* must rely on exogenous corrinoids for RDase activity (Men *et al*., 2014; West *et al*., 2013; Johnson *et al*., 2009; Yan *et al*., 2013). Genes associated with corrinoid salvaging and transport were most highly expressed in the active ANAS culture with lower

expression levels of both corrinoid transport and synthesis genes throughout the stages of CANAS (Figure 4-7 C).

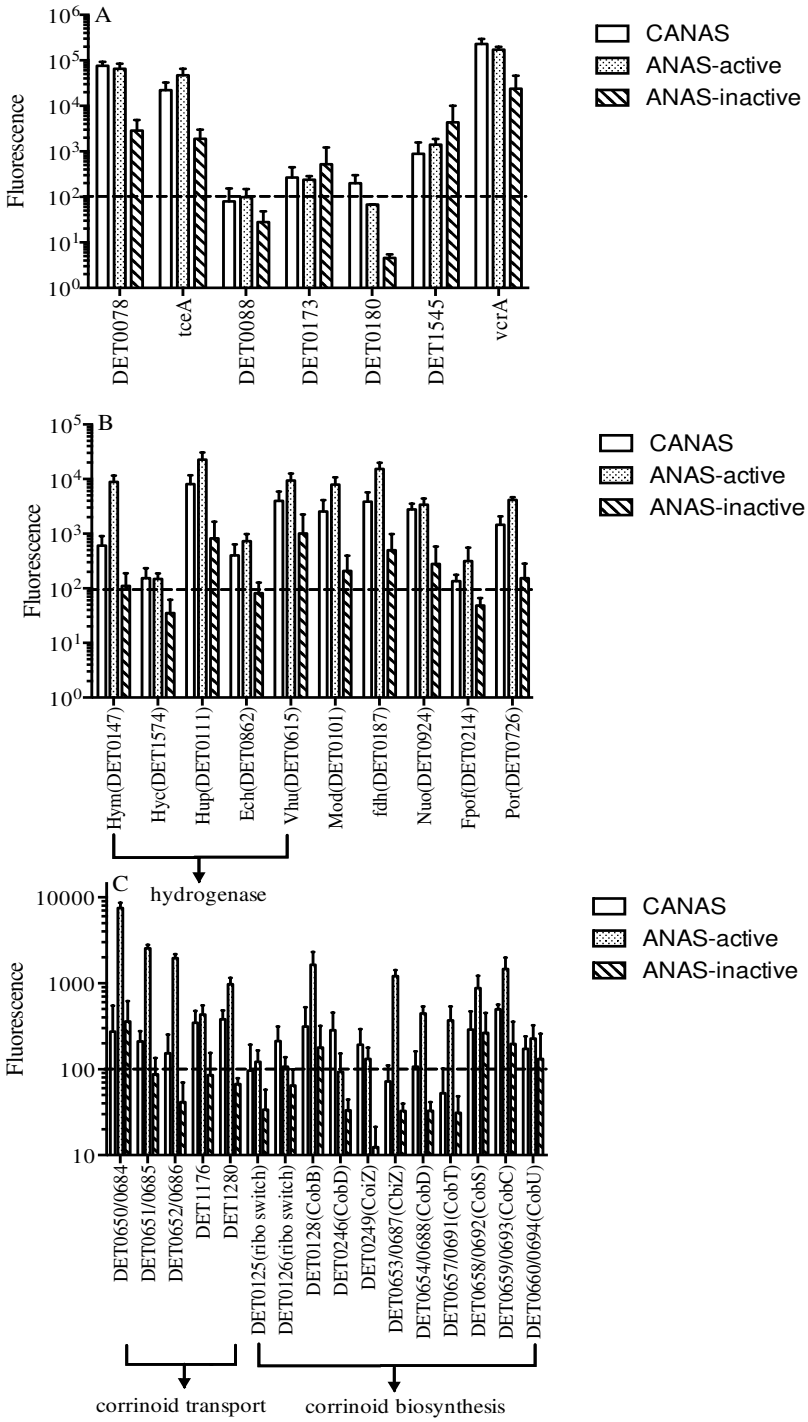

Figure 4-7 Functional gene expression profiles of A) reductive dehalogenases genes, B) oxidoreductase genes and C) corrinoid transport/biosynthesis genes in CANAS and ANAS during active dechlorination (20 hours after feeding substrate) and starvation (13 days after fed substrate). Dashed lines in all figures indicates significant fluorescence level (fluorescence signal>100)

4.4 Discussion

The donor to acceptor ratio fed to CANAS was about 12:1 (based on electron equivalents), ensuring TCE to be the limiting reactant for dechlorination with the electron donor and corrinoid concentrations in excess. There has only been one other study that reported cell densities and production rates of *D. mccartyi* in a CMFR with sustainable dechlorination to ethene (Delgado *et al*., 2013). Here, the TCE concentration in the influent was maintained at 1.7 mM, and the cell yield of *D. mccartyi was* $2.9 \pm 0.7 \times 10^8$ cells per µmol Cl^- released (Table 4-4), a value in the range of reported cell yields of *D. mccartyi* isolates (Cupples *et al*., 2003; Sung *et al*., 2006;) but lower than the previous study with a three day SRT and 2 mM influent TCE yielding 5.3×10^8 cells per µmol Cl^- released (Delgado *et al*., 2013). This lower cell yield is possibly due to enhanced cell decay within the CANAS with its significantly longer SRT, especially given the ability of *D. mccartyi* to decouple dechlorination from growth. In the inoculum semi-batch culture ANAS, *D. mccartyi* strain ANAS1 grows much faster than ANAS2, maintaining a stable ratio of 10:1 (Lee *et al*., 2011). However in CANAS with a 40-day SRT, the ANAS1: ANAS2 ratio was 1.1:1, demonstrating that the exposure to low consistent TCE levels within the reactor differentially selects for *D. mccartyi* strains. The high *D. mccartyi* cell density ($\times 10^9$ copies mL^{-1}) observed in CANAS is comparable to the previously report maximum *D. mccartyi* densities obtained in lab scale studies (Vainberg *et al*., 2009; Delgado *et al*., 2013).

The dechlorination rate in CANAS was 118 µmol Cl^- released L^{-1} day^{-1} which was similar to a previous CMFR study with a 55-day SRT of 80 µmol Cl^- released L^{-1} day^{-1} (Berggren *et al*. 2013), but much lower than the 3-day SRT study of 130 µmol Cl^- released L^{-1} hr^{-1} (Delgado *et al*., 2013). The *D. mccartyi* production rate in CANAS was 3×10^{10} cells L^{-1} day^{-1}, which was about 10% of the number reported in the 3-day SRT study (Table 4-4), likely due to the much longer SRT.

In this study, we found when the microbial community was adapting to the new environment (from "feast/famine" to "continuously exposing to low nutrients levels"), the microbial structure shifted significantly and the composition became much simpler at the family OTU level. Although the community structure changed significantly over the 3 stages of the reactor operation, the microbial community was functionally stable (metabolite measurements were constant) while not structurally stable (composition of the community). Further, although there were large numbers of facultative microorganisms present in CANAS, the dechlorination function was stably maintained, suggesting that the dechlorinators represented a significant portion of the community. It is possible that PCR bias associated with the iTag technique or microorganism carrying more than one copy of 16S rRNA gene resulted in over-prediction of certain populations. For example, in qPCR measurement, *D.mccartyi* accounted for 4-6% of the total community in both ANAS and CANAS, similar to measurements in previous studies (Behrens *et al*., 2008; Azizian *et al*., 2008), however in the iTage analysis, the detection was below 1% for all conditions. Metagenome analysis for the same microbial community provided similar overall community structures, however, it was shown to be more sensitive in identifying both high and low abundance species within the community (Figure 4-6). Another benefit of using the metagenomic approach is that we recovered all genome information from the community, and the specific genes with certain functions could be further analyzed.

In this study, H_2 levels were maintained at about 0.2 μM, which was higher than the methanogenenic threshold. However methane production was only about 30% compared to ethene production based on electron equivalents (Table 4-5), compared to ANAS where methane production was about 500% of ethene production (West *et al*., 2013). The cell numbers of methanogens in CANAS are about 10% of those in ANAS measured by qPCR (West *et al*., 2013). Since methanogenesis requires more strict redox conditions than fermentation (E_h<-200 mV) (Le Mer *et al*., 2001), methane production has been limited by the decrease of the redox potential (Mayer *et al*., 1990; Le Mer *et al*., 2001).

It makes sense that the transcriptome level of *D. mccartyi* remained relatively constant in the three consecutive stages while the community structure changed significantly during the experimental period. Since CANAS culture was continuously exposed to low substrates levels, which would largely affect the gene regulation pattern. Another interesting finding is the expression pattern of putative formate dehydrogenase (*fdh*) in CANAS. Previous studies have shown that the expression level of *fdh* in dechlorinating microbial communities was higher than those of the hydrogenases in batch growth conditions (Morris *et al*., 2007). However in a CMFR, the expression level is lower than hydrogenases *hup*, *hym*, and *vhu.* The differential expression pattern of corrinoid-related genes was largely due to the medium composition and the growth condition. In ANAS, vitamin B_{12} was supplied at trivial concentration (1μg/L, Table 4-1) that led it to be one limiting factor for the community growth. However in CANAS, vitamin B_{12} was supplied in excess at 100 μg/L. This down-regulation pattern with excess vitamin B_{12} supply is consistent with a previous study of *Dehalococcoides mccartyi* 195 grown with excess or limiting vitamin B_{12} (Johnson *et al*., 2009). The different B_{12} expression patterns compared to genes for RDases indicate the expression of corrinoid-related genes may not be good biomarkers to indicate dechlorination activity.

This is the first study to examine global gene expression of *Dehalococcoides* species under continuous flow conditions, and suggests that we need to be careful when selecting biomarkers to indicate reductive dechlorination actitivty. Previous studies have proposed hydrogenase genes (*hupL*) as biomarkers to indicate the activity of reductive dechlorination (Morris *et al*., 2007; Rowe *et al*., 2008; Berggren *et al*., 2013). In this study, we found similar positive correlation between *hupL* and *tceA* gene expression. Previous modeling studies have indicated that transcripts instead of DNA/proteins/VSS may serve as better biomarkers to predict reductive dechloriantion performance (Bælum *et al.*, 2013; Heavner *et al*., 2013), however, the consistent high levels of expression demonstrated for active and starving conditions of ANAS suggest that this approach would be problemattic.

4.5 Summary

In this study, we investigated the community structural changes and transcript expression of *Dehalocccoides* within a CMFR with explicit calculation of electron balances. This is the first study to analyze the metagenome and transcriptome of a *Dehalococcoides*-containing microbial community growing under completely mixed flow conditions. We found the community structure shifted significantly while the dechlorination performance was stably maintained. The findings in this study will improve our understanding of transcriptional dynamics of reductive dechlorinating functional cells under different environmental conditions. The CMFR system

used in this study could be further used to validate kinetic reductive dechlorination modeling under electron donor- /acceptor-limiting conditions, in order to properly predict the bioremediation performance of contaminated groundwater plumes characterized by concentrations below those of the source zone.

Acknowledgement

Dr. Stenuit provided tremendous help on the experiment design and experiment of metagenome and 16S rRAN “i-tag” study. Dr. Yu provided helped a lot on the metagenome data interpretation and analysis. Dr. Hu from LNBL lab provided the plasmids standards for DNA microarray study. Dr. Men and Ms West have helped on experimental design and data analysis on the microarray study.

5 A system level understanding of the kinetics and Environmental factors effects on *Dehalococcoides*-containing microbial consortia

5.1 Introduction

Reductive dechlorination is the most important biotransformation pathway of chlorinated ethenes in anaerobic environments (Maymó-Gatell *et al*., 1997). In order to effectively predict this process, it is crucial to improve our understanding of reductive dechlorination kinetics as well as the interactions of dechlorinating process with fermentation and other terminal electron accepting processes (TEAPs). Furthermore, the characterization and prediction of reductive dechlorinating performance by model simulations would provide us with a fundamental basis to evaluate remedial strategies. Most studies have employed Monod kinetics as the mathematical approach to predict reductive dechlorination, with simplifications (e.g. first order kinetics) or introduction of inhibition terms (e.g. competitive inhibition or self-inhibition) (Yu and McCarty 2005; Popat and Deshusses, 2011). Monod kinetics has also been adopted to describe organic acid fermentations and other terminal electron accepting processes (Lee *et al*., 2004; Azizian *et al*., 2008; Malaguerra *et al*., 2011).

The kinetic parameters involved in the reactive kinetic models could be classified into the following groups: i) kinetic parameters for reductive dechlorination, including the specific maximum dechlorination rate for each chlorinated ethene ($k_{max,acceptor}$, μmol substrate·cell^{-1}·d^{-1}); half velocity for each chlorinated ethene ($K_{S,acceptor}$, μM); inhibition coefficient K_I (μM); ii) kinetic parameters for fermentation: specific maximum fermentation rates ($k_{max,donor}$, μmol substrate·cell^{-1}·d^{-1}), half velocity of substrate utilization ($K_{S,donor}$, μM); iii) kinetic parameters for other TEAPs, such as hydrogenotrophic methanogenesis, sulfate reduction, iron reduction, etc (Malaguerra *et al*., 2011); iv) kinetic parameters for biomass production and decay, which include the cell yield Y (cells per μmol substrate consumed) and specific decay coefficient k_b (day^{-1}); and v) other kinetic parameters derived based on different geochemical conditions (Kouznetsova *et al*., 2010).

The kinetic parameters were generally determined experimentally, e.g. in batch microcosms. The experimental data that have been used to determine kinetic parameters during reductive dechlorination could be classified into three categories based on the length of the experimental period:

i) Short duration (a few hours): k_{max}, K_S, K_I and μ_{max} are determined over a few hours and biomass growth was assumed to be negligible given the short experiment period (Yu *et al*., 2005; Popat and Deshusses, 2011). Specific yields Y can't be determined since growth is neglected. Competitive inhibition between chlorinated ethenes can be determined by introducing different concentrations of a competitive compound (Yu *et al*., 2005; Popat and Deshusses, 2011). In addition, the accuracy of the maximum substrate utilization rates (k_{max}) and maximum growth rates (μ_{max}) depend on the accuracy of biomass concentrations (Yu and Semprini, 2004; Huang and Becker, 2009).

ii) Medium duration (several days to a few weeks): biomass production can be measured at the beginning and the end of the experiment so specific cell yields Y can be determined, but biomass decay is neglected. In addition, model predictions of cell growth can be compared with lab observations where transient microbial data are available, increasing model reliability (Schaefer *et al*., 2009; Haest *et al*., 2010).

iii)Long duration (a few weeks): biomass decay coefficients k_b (day^{-1}) and hydrogen thresholds for dechlorinaiton (nM) can be determined (Cupples *et al*., 2004; Löffler *et al.*, 1999).

A summary of kinetic parameters reported in the literature is listed in table 5-1. In general, the kinetic parameters listed in the table (maximum growth rate, specific growth yield, half-velocity constant, and decay rate) represent a very wide range of values. Partly this is the result of the inaccurate methods used for quantification in the experiments. For example, the experimental microbial data were limited and model simulations were typically fitted to chemical data only in one study (Liu and Zachara, 2001) while biomass was represented by total volatile suspended solid (VSS) with an assumed percentage to be responsible for certain reactions in another (Fennell *et al*., 1998). Other researchers used protein concentrations (Yu *et al*., 2005) but did not distinguish between different functional groups.

Table 5-1Range of kinetic parameters estimated for reductive dechlorination communities.

Parameter	Time period	Value range	Unit	Reference
$k_{max\ acceptor}$	hours	10^{-13}~10^{-8}	μmol substrate·cell^{-1}·d^{-1}	Haston and McCarty 1999 Clapp, 2004; Popat, 2011 Lee, 2004;
$K_{s,acceptor}$[a]	hours	0.08~602	μM	Cupples, 2004;Yu, 2004; Malaguerra, 2011
$k_{max,donor}$	hours	10^{-10}~10^{-9}	μmol substrate·cell^{-1}·d^{-1}	Fennell, 1998; Kouznetsova, 2010
$K_{s,donor}$	hours	0.007~240	μM	Cupples, 2003; Maillacheruvu and Parkin, 1996;
Y	days	10^{6}~10^{9}	Cells per μmol substrate consumed	Cupples, 2004; Yu, 2004 Becker, 2009; Malaguerra, 2011
k_b	weeks	0.003~0.09	day^{-1}	Cupples, 2003; Yu, 2004 Haest, 2010; Karadali, 2005
μ[b]	days	0.08~0.49 (*Dehalococcoides*)	day^{-1}	Clapp, 2004; Cupples, 2004 Malaguerra, 2011
H_2 threshold	weeks	0.3~4.5(*Dehalococcoides*) 11~318(*Methanogens*) 2 (sulfate reducers)	nM	Yang, 1998; Löffler, 1999; Clapp, 2004; Cord-Ruwisch, 1988; Conrad & Wetter, 1990Kouznetsova, 2010

a. Half-velocity constant was determined by using non-linear least square fitting of $k_{max.}$

b. There is limited reference available for the maximum growth rate of dehalorespring bacteria. For rest of the parameters μ is calculated based on $\mu=Y\times k_{max.}$

Very few studies have evaluated the effects of important environmental factors on reductive dechlorination, such as alkalinity changes, sulfate reduction, and elevated organic anions. Acetate is an important intermediate during the anaerobic decomposition of organic

matter (McInerney and Bryant, 1981) and could accumulate to high levels in the absence of acetoclastic methanogens. Relatively high acetate concentrations have been found in the semi-batch anaerobic dechlorinating bioreactor ANAS (~43 mM, unpublished data). Higher (5 mM) initial acetate concentrations have been reported to inhibit methane productions in peatlands (Williams and Crawford, 1984; Horn *et al*., 2003). However, there has been little research on the effect of high organic acid anions on dechlorinating communities and on key microorganisms which play a role in electron flows, such as fermenters and methanogens. Typical bicarbonate concentrations in groundwater are between 0.7 to 10 mM (Wilkin *et al*. 2010), which is lower than in typical laboratory culture conditions. Besides the role of a buffering reagent, bicarbonate also serves as the electron acceptor in hydrogenotrophic methanogensis and homoacetogenesis. As a result, these two processes could increase pH due to the consumption of protons. Few studies have analyzed the effects of different bicarbonate concentration on reductive dechlorination.

Chlorinated ethene dechlorination under sulfate-reducing conditions is complicated and less studied. A review of published field data from TCE-contaminated sites with sulfate concentrations ranging from 39 mg L^{-1} to 4,800 mg $L^{-}1$ reported the overall trend that as sulfate concentrations increased, dechlorination reactions became incomplete or delayed (Pantazidou *et al*., 2011). There are a limited number of laboratory studies with detailed information on the effects of sulfate on dechlorination. In addition, a variety of results, ranging from enhanced dechlorination (Hoelen *et al*., 2004; Heimann *et al*., 2005; Aulenta *et al*., 2008) to inhibited dechlorination (Hoelen *et al*., 2004; Panagiotakis *et al*., 2014), and incomplete dechlorination (El Mamouni *et al*., 2002) due to sulfate presence have been reported over the past decade. Furthermore, among these previous studies, there has only been one that used a microbial community with the confirmed presence of *D. mccartyi*. Finally, none of these studies have used modern molecular techniques for specific detection and quantification of the number of relevant populations.

In order to get a better understanding of the kinetic paramters that affect the accuracy of models used to predict reductive dechlorination, we carried out a systematic investigation of the controlling parameters of *D. mccartyi* –containing syntrophic cultures as well as *D. mccartyi* –containing microbial communities. In addition, we evaluated potential environmental factors (such as bicarbonate and sulfate) that may affect the dechlorination performance. Furthermore, we validated whether the kinetic parameter tested in pure culture/ syntrophic cultures could be applied to more complicated systems. With the knowledge gained from this study, we will improve dechlorination model predictions by simplifying the less relevant processes and better characterizing interfering side reactions.

5.2 Materials and Method

5.2.1 Microbial cultures and growth conditions

D. mccartyi strain 195 was grown in defined medium with H_2/CO_2 headspace, 0.6 mM TCE as electron acceptor and 2 mM acetate as carbon source. Bacterial co-cultures of strain 195 and *S. wolfei* (5% vol/vol inoculation) were maintained on 5 mM butyric acid (5% vol/vol inoculation) with 0.6 mM TCE as described in Chapter 3. Bacterial co-cultures of strain 195 and Desulfovibrio vulgaris Hildenborough (DvH) (5% vol/vol inoculation) were maintained on 5

mM lactic acid (5% vol/vol inoculation) with 0.6 mM TCE as described described previously (Men *et al*., 2012).

In order to study the competition between reductive dechlorination and methanogenesis, we introduced a hydrogenotrophic methanogen strain *Methanobacterium conglense* (MC) to the constructed co-cultures DvH and strain 195 (DvH/strain 195). The culture construction process and dechlorination performance have been described previously (Men *et al*., 2012). Tri-cultures of DvH/195/MC were maintained on 5 mM lactic acid (5% vol/vol inoculation) with 0.2 mM TCE as electron acceptor. Similarly, another tri-culture *S.wolfei*/195/MC was constructed by adding 10 mL of *S.wolfei*/MC and 10 mL *S. wolfei*/strain 195 to 80 mL butyrate medium in triplicate bottles. 5 mM butyric acid and 0.2 mM TCE were added as electron donor and acceptor, respectively. Both of the tri-cultures were maintained in the same medium as the co-cultures above, with the exception that TCE was added in ~ 30 μmol per dose to avoid inhibition effect on methanogenesis. A new tri-culture of *S. wolfei*/195/DvH was constructed by adding 10 mL of *S.wolfei*/strain 195 and 10 mL of DvH/strain 195 to 80 mL butyrate medium in triplicate bottles. The tri-culture was maintained in the same medium as the co-cultures with the exception that sulfate (2 mM) was also added at the beginning of the subculture. The tri-culture was sub-cultured three times before the experiment was carried out.

The methanogenic dechlorinating community (LoTCEB12) was enriched from groundwater at a TCE-contaminated site in New Jersey. The culture was sustainably maintained in the laboratory for over three years before the experiments were conducted. The community structure and dechlorination performance was monitored and characterized previously (Men *et al*., 2013). Briefly, for each subculture event, 5% of the culture was inoculated into 95 mL fresh basal medium. In order to avoid inhibition effects of TCE on the methanogen, 0.9 mmol lactate with 22 μmol TCE were fed as electron donor and electron acceptor, respectively. Three doses of lactate (0.4 mmol per dose) and TCE (55 μmol per dose) were consecutively fed to the culture prior to subculturing. The microbial consortia used in the kinetic study are summarized in table 5-2.

Table 5-2. *Dehalococcoides*-containing microbial consortia used for kinetic studies under batch conditions

Consortia	Primary electron donor	Kinetic parameters determined in this study	Environmental factors tested
strain195[a]	H_2	k_d	HCO_3^-/acetate/ SO_4^{2-} /HS^-
S. wolfei/195[b]	Butyrate	Y_{Dhc}, $k_{max,TCE}$ $k_{max,DCE}$ $K_{S,TCE}$ $K_{S,DCE}$ b_{Dhc}, Y_{Dhc}, Y_{SW}	HCO_3^-/acetate
S.wolfei/195/MC[c]	Butyrate	$k_{max,TCE}$ $k_{max,DCE}$ $K_{S,TCE}$ $K_{S,DCE,}$ b_{Dhc}, Y_{Dhc}, Y_{DvH}	HCO_3^-/acetate
S.wolfei/195/DvH	Butyrate	-	SO_4^{2-}
DvH/strain195[d]	Lactate	$k_{max,TCE}$ $k_{max,DCE}$ $K_{S,TCE}$ $K_{S,DCE}$ Y_{Dhc}, Y_{DvH}	SO_4^{2-}/HS^-/ HCO_3^-
DvH/195/MC	Lactate	$k_{max,TCE}$ $k_{max,DCE}$ $K_{S,TCE}$ $K_{S,DCE}$ b_{Dhc} Y_{Dhc}, Y_{DvH}	SO_4^{2-}/ HCO_3^- /acetate
LoTCEB12	Lactate	k_d, Y, $k_{max,TCE}$ $k_{max,DCE}$ $K_{S,TCE}$ $K_{S,DCE}$ b_{Dhc} Y_{Dhc},	SO_4^{2-}/ HCO_3^-/acetate

[a]. *Dehalococcoides mccartyi* 195; [b]. *Syntrophomonas wolfei*; [c]. *Methanobacterium congolense*, [d]: *Desulfovibrio vulgaris Hildenborough*

5.2.2 Analytical and molecular methods

Chloroethenes and ethene were measured by FID-gas chromatograph using 100 µL headspace samples, and hydrogen and carbon monoxide was measured by RGD-gas chromatography using 300 µL headspace sample as described previously (Freeborn *et al*., 2005; Lee *et al*., 2006). Mass of each compound was calculated based on gas/liquid equilibrium by using Henry's law constants at 34°C according to: mass (µmol/bottle) = $C_l \times V_l + C_g \times V_g$, $k_H^{cc} = C_l / C_g$. Organic acids were analyzed with a high-performance liquid chromatograph as described previously (Freeborn *et al*., 2005).

Sulfate concentration was measured by iron-chromatography (Dionex-120 chromatograph w/ auto-sampler) using 650 µL liquid cell sample. Ultra high purity helium was used as carrier gas. Ultra high purity nitrogen was used as sparing gas. The anion eluent contained 0.424 g/L Na_2CO_3 and 0.21 g/L $NaHCO_3$. Flow rate was maintained at 1 mL/min with Anion column (Dionex IonPac AG14 4x50mm) pressure at about 21 Mpa.

1.5 mL liquid samples were collected for cell density measurements and cells were harvested by centrifugation (21,000 × *g*, 10 min at 4°C). Genomic DNA was extracted from cell pellets using Qiagen DNeasy Blood and Tissue Kit according to the manufacturer's instructions for Gram-positive bacteria. qPCR using SYBR Green-based detection reagents was applied to quantify gene copy numbers of each bacterium. Primers used for quantification of different microorganisms are summarized in table 5-3.

Table 5-3 Primers used for q-PCR analysis of different microorganisms

Gene (Locus tag)	Predicted function	Primer Sequences (5'-3', forward and reverse)
DET0079	Reductive dehalogenase *tce*A	GTGAACTGGGCTATGGCGAC
		TGGCGGCATATATTAGGGCA
Dhc16S	16S ribosomal RNA of *Dehalococcoides*	CTTCGATCGGTAGCTGGTCTG
		TCTCAGTCCCAGTGTGGCTG
SW16S	16S ribosomal RNA of *S. wolfei*	GTATCGACCCCTTCTGTGCC
		CCCCAGGCGGGATACTTATT
DvH16S	16S ribosomal RNA of DvH	AATCGGAATCACTGGGCGTA
		CCCTGACTTACCAAGCAGCC
MC16S	16S ribosomal RNA of *Methanobacterium*	GGGTTGTGAGAGCAAGAGCC
		GCCTGGAACCTTGTCTCAGG

5.2.3 Kinetic study for determination of k_{max} and K_S

Batch dechlorination rate tests were conducted under non-limiting hydrogen conditions (chlorinated solvent is the limiting substrate) to determine specific maximum dechlorination rates ($k_{max,TCE}$ and $k_{max,DCE}$) of each microbial consortium. The experimental period was limited to 10 hours in order to minimize the effects of microbial growth given that doubling times for *D.*

mccaryi are approximately 2 days (He *et al*., 2003; Cupples *et al*., 2003). The kinetic batch experiments were conducted in duplicate as modified from a previous study (Yu *et al*., 2005) summarized below.

Microbial consortia were first inoculated (5%, vol/vol) in 100 mL BAV1 medium in duplicate 160mL serum bottles. 0.7 mM TCE was added as electron acceptor and excess electron donor was added according to the culture type. When TCE was 90% gone and cells were at exponential growth phase (*D. mccartyi* cell number was at ~10^8 cell/mL) the bottles were flushed with ultra pure N_2 gas in the fume hood for 20 minutes to remove the solvents, then with anaerobic mixed gas (H_2/N_2) for 5 minutes to provide excess electron donor H_2 for dechlorination. The bottles were then amended with a low concentration of either TCE or cis-DCE saturated in anaerobic BAV1 medium. The bottles were shaken at 150rpm at 34°and the rates of parent compound disappearance and daughter product production were measured over a period of less than 1.5h (duplicate bottles). The bottles were then purged with mixed gas (H_2/N_2) for 10 min to remove the solvents, and introduce H_2. The bottles were then re-fed with a higher concentration of the chlorinated solvent, and the process repeated (Figure 5-1). At the end of the kinetic experiment, 1.5 mL liquid was collected from each bottle and cells collected by centrifugation (21,000 × *g*, 10 min at 4°C). Genomic DNA was extracted and qPCR was performed to quantify cells and k_{max} and K_S were estimated based on nonlinear least-square regression fitting to the data (Prism 6, GraphPad).

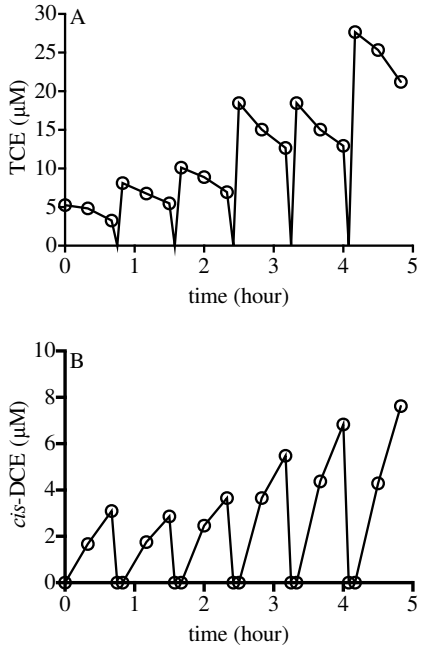

Figure 5-1 Measurement of TCE transformation (A), and *cis*-DCE production (B) by co-culture strain 195/DvH using the multiple equilibrium method.

5.2.4 Cell growth and decay kinetics

Cell growth calculations

In general, theoretical cell growth yield can be calculated based on biomass synthesis and electron donor/acceptor reactions (equation 5.1 to equation 5.4, Rittmann and McCarty, 2001). Relative half reactions used in this study are summarized in table 5-4.

$$R = f_e R_a + f_s R_C - R_d \tag{5.1}$$

$$f_s + f_e = 1 \tag{5.2}$$

$$f_s = \frac{1}{1+A} \tag{5.3}$$

$$A = \frac{-\frac{\Delta G_p}{\epsilon^n} + -\Delta G_{pc}/\epsilon}{\epsilon \Delta G_r} \tag{5.4}$$

ε: electron transfer efficiency (assume ε=0.6).
ΔG_P: free energy in kJ/ e^--eq required to convert the cells carbon source to pyruvate, a common intermediate in cell synthesis.
ΔG_{PC}: free energy in kJ/ e^--eq required to convert pyruvate and a nitrogen source into biomass. ΔG_{PC} =18.8 kJ/ e^--eq when NH_4^+ is the nitrogen source.
ΔG_r: is the free energy infor the overall energy generating reaction (electron donor/acceptor couple) ΔG_r<0.

Table 5-4 Half reactions and their Gibb's standard free energy per electron equivalent at standard conditions, pH=7

Reaction number	Half reaction	e^--eq mole^{-1} product	ΔG' kJ/ e^--eq	Reference
Cell synthesis	$\frac{1}{5}CO_2 + \frac{1}{20}HCO_3^- + \frac{1}{20}NH_4^+ + H^+ + e^- = \frac{1}{20}C_5H_7O_2N + \frac{9}{20}H_2O$	20	N.A	Rittmann, 2001
Pyruvate	$\frac{1}{5}CO_2 + \frac{1}{10}HCO_3^- + H^+ + e^- = \frac{1}{10}CH_3COCOO^- + \frac{2}{5}H_2O$	10	35.09	Rittmann, 2001
Acetate	$\frac{1}{8}CO_2 + \frac{1}{8}HCO_3^- + H^+ + e^- = \frac{1}{8}CH_3COO^- + \frac{3}{8}H_2O$	8	27.40	Rittmann, 2001
electron –acceptor equations (R_a)				
TCE-*cis*DCE	$\frac{1}{2}C_2HCl_3 + \frac{1}{2}H^+ + e^- = \frac{1}{2}C_2H_2Cl_2 + \frac{1}{2}Cl^-$	2	-44.8	Duhamel, 2007
*cis*DCE-VC	$\frac{1}{2}C_2H_2Cl_2 + \frac{1}{2}H^+ + e^- = \frac{1}{2}C_2H_3Cl + \frac{1}{2}Cl^-$	2	-30.1	Duhamel, 2007
VC-ETH	$\frac{1}{2}C_2H_3Cl + \frac{1}{2}H^+ + e^- = \frac{1}{2}C_2H_4 + \frac{1}{2}Cl^-$	2	-35.1	Duhamel, 2007
sulfate-sulfide	$\frac{1}{8}SO_4^{2-} + \frac{19}{16}H^+ + e^- = \frac{1}{16}H_2S + \frac{1}{16}HS^- + \frac{1}{2}H_2O$	8	20.9	Rittmann, 2001
CO_2-CH_4	$\frac{1}{8}CO_2 + H^+ + e^- = \frac{1}{8}CH_4 + \frac{1}{4}H_2O$	8	23.5	Rittmann, 2001
electron -donor equations (R_d)				
Lactate	$\frac{1}{6}CO_2 + \frac{1}{12}HCO_3^- + H^+ + e^- = \frac{1}{12}C_3H_5O_3^- + \frac{1}{3}H_2O$	12	32.3	This study
butyrate	$\frac{3}{20}CO_2 + \frac{1}{20}HCO_3^- + H^+ + e^- = \frac{1}{20}C_4H_7O_2^- + \frac{7}{20}H_2O$	20	27.7	This study

Cell decay estimations

Direct measurements of decay coefficients were carried out using a method modified from a previous study *Dehlococcoides* strain VS (Cupples *et al*., 2003). In brief, 12 replicate bottles were filled with 100 mL of pre-grown culture on TCE with electron donor in excess with headspace of either H_2/CO_2 for pure culture or N_2/CO_2 for consortia. Four abiotic controls consisted 100 ml of medium with no inocula. The experiment started (day 0) when all TCE was depleted in the bottle. At day 0, day 8, day 14 and day 21, triplicate culture bottles and one control bottle were filled with 44~78 μmol TCE as electron acceptor. Chlorinated solvents and ethene were monitored within 28 hours (0hour, 4h, 8h, 22hr, 24hr, 26hr, 28hr). Electron donor was maintained in excess and $[TCE] >> K_S$ throughout the 28 hour experimental period. 1.5 mL liquid samples were collected for cell analysis at the end of the experiment (~28 hr). The following equations were used to determine the values for maximum utilization rate (k_{max}) and decay coefficient (k_b). qPCR was performed on day 0 and the end of the experiment. Non-linear least-squares estimates of the decay coefficient k_b (day^{-1}) was carried out by using the "One phase exponential decay" function to fit the experimental data (Prism 9.0, Graphpad)

$$-\frac{dC}{dt} = \frac{k_{max} X C}{K + C} \tag{5.5}$$

$$-\frac{dX}{dt} = \frac{k_{max} Y \cdot X \cdot C}{K + C} - bX \tag{5.6}$$

5.2.5 Effect of other environmental factors

In order to test the effect of bicarbonate concentrations on dechlorination performance, during medium preparation, N_2 was the only gas used for headspace and the reducing agents were 0.2 mM L-cysteine and 0.2 mM $Na_2S \times 9H_2O$. 10 mM TES or 10 mM HEPES buffer were added as pH buffers before autoclaving. For bottling, 160 mL serum bottles were used with 95 mL liquid and 65 mL N_2 headspace sealed with blue butyl rubber stoppers and aluminum crimps. The initial pH was adjusted to 7.3±0.1 using 4 M NaOH. After autoclaving, vitamin solutions (Wolin *et al*., 1963) and electron donors (10 mL pure H_2 for strain 195; 5 mM butyrate for co-culture *S. wolfei*/strain 195 and tri-culture *S. wolfei*/strain 195/MC; 5 mM lactate for co-culture DvH/strain 195 and tri-culture DvH/strain 195/MC; 20 mM lactate for enrichment LoTCEB12) were added to each bottle. 0.5 mM TCE was added as the electron acceptor. 1mM or 30 mM $NaHCO_3$ was added to experiment bottle from 1M sterile anaerobic $NaHCO_3$ stock solution.

In order to test the effects of organic acid anions on the growth and dechlorination performance of the *D.mccartyi*-containing cultures, different concentrations of sodium acetate (5 mM, 10 mM, 25 mM, 40 mM) were amended to the mineral salt medium before autoclaving. Appropriate amounts of NaCl were added to the medium so that the ionic strength of each medium bottle was equal to that of the medium with the highest amount of sodium acetate.

In order to test the inhibitory effects of sulfate and its reduction product sulfide on dechlorination, fermention and methanogenesis processes, 1M anaerobic sodium sulfate (Sigma-Aldrich) stock solution and 100 mM anaerobic sodium sulfide (Sigma-Aldrich) stock solution were prepared. For *D. mccartyi* strain 195, sulfate (1 mM and 2.5 mM) and sulfide (1mM, 2mM

and 5 mM) inhibitory effects were investigated. Similarly, sulfate and sulfide inhibition on the growth of *S. wolfei*, *Methanobacterium conglense*, and *Desulfovibrio vulgaris* Hildenborough were tested. In order to study the H_2 competition between dechlorination and sulfate reduction, co-culture DvH/strain195, tri-culture *S.wolfei*/strain195/DvH, and enrichment culture LoTCEB12 culture were tested.

5.3 Results

5.3.1 Determination of kinetic parameters during reductive dechlorination

The Monod curves for TCE and *cis*-DCE transformation by *Dehalococcoides* isolate 195 and in different constructed consortia were determined using the multi-equilibration kinetic method shown in Figure 5-2. The duplicate (or triplicate) determinations using non-linear least squares fits generated statistically reproducible results for all the cultures tested (all data fell within 95% confidence intervals). The standard deviations of k_{max} and K_S values based on duplicate or triplicate determinations were 3% to 15% of the parameter values, using single equilibrations in multiple reactors. Table 5-5 presents k_{max} and K_S values obtained for *D.mccartyi*-containing microbial consortia for each step of the dechlorination processes.

For all cultures tested in this study, k_{max} values for both TCE and *cis*-DCE were within the range of 1.5 to 4.1 $\times 10^{-9}$ substrate$\cdot$cell$^{-1}\cdot$d^{-1}, well within the range previously reported in the literature (10^{-12} to 10^{-8} substrate$\cdot$cell$^{-1}\cdot$d^{-1}) (Haston and McCarty, 1999; Lee *et al*., 2004; Amos *et al*., 2007). For the co-cultures with different hydrogen stress conditions, the highest $k_{max,TCE}$ was in consortium DvH/strain 195 ($4.1\pm0.2 \times 10^{-9}$ substrate$\cdot$cell$^{-1}\cdot$d^{-1}) with relatively high hydrogen concentrations, which is about 1.5 times higher than that in the low hydrogen *S.wolfei*/strain 195 consortium ($2.7\pm0.1 \times 10^{-9}$ substrate$\cdot$cell$^{-1}\cdot$d^{-1}). However, $k_{max,DCE}$ values of these two co-cultures were the same ($3.2\pm 0.1\times 10^{-9}$ substrate$\cdot$cell$^{-1}\cdot$d^{-1}). In tri-cultures with hydrogenotrophic methonogenesis, $k_{max,TCE}$ and $k_{max,DCE}$ in *S. wolfei*/195/MC and DvH/195/MC were slightly lower (41% to 78%) than those observed in the co-cultures. For the enrichment culture LoTCEB12, which contains one *D. mccartyi* species that carries the *tceA* gene (Men *et al*., 2013), no significant difference of k_{max} ($1.8\pm 0.1\times 10^{-9}$ substrate$\cdot$cell$^{-1}\cdot$d^{-1} for TCE and $2.7\pm 0.1\times 10^{-9}$ substrate$\cdot$cell$^{-1}\cdot$d^{-1}for *cis*-DCE) or K_S (7.4 ± 0.7 μM for TCE and 6.9 ± 0.7 μM for *cis*-DCE) was observed compared to the constructed syntrophic co-cultures and tri-cultures. $K_{S,TCE}$ values are in the range of 6.2~14.5 μM in all cultures tested, values that fall within the range of previously published values 0.08~23.4 μM (Yu *et al*., 2005; Amos *et al*., 2007; Malaguerra *et al*., 2011). $K_{S,DCE}$ values obtained were in the range of 2.6 to 10.0 μM, which is also similar to previously published data 0.5~6.9 μM (Fennell *et al*., 1998; Yu *et al*., 2005; Popat and Deshusses, 2011). $K_{S,TCE}$ and $K_{S,DCE}$ of tri-cultures are slightly smaller than those observed in co-cultures, following the same trend as the k_{max} values. The kinetic parameters obtained in the experiments were applied for model prediction and validation described in Chapter 6.

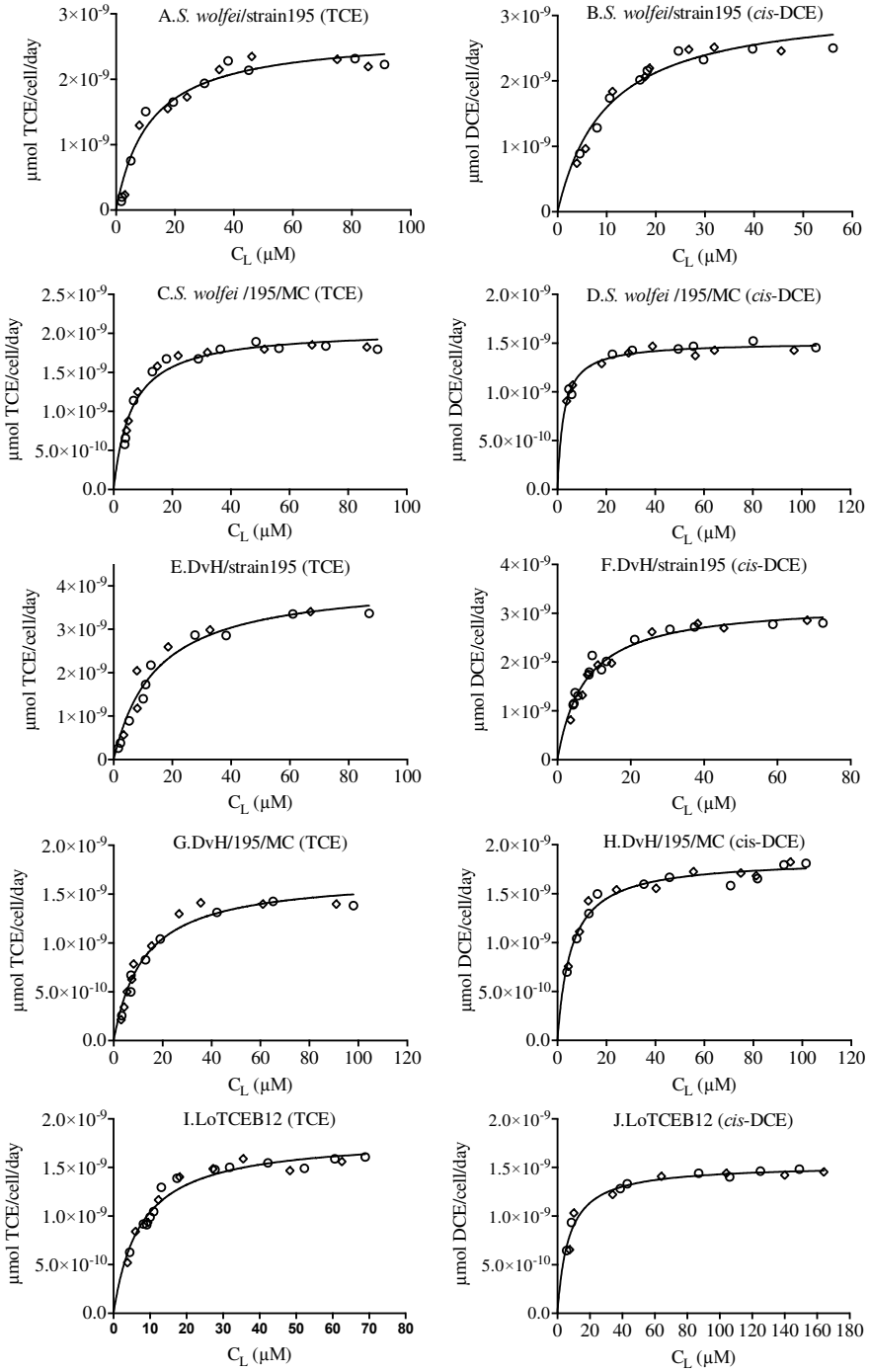

Figure 5-2 Specific reductive dechlorination rates of TCE by (A) co-culture *S. wolfei*/strain 195; (C) tri-culture *S. wolfei*/ 195/ MC; (E) co-culture DvH/strain 195; (G) tri-culture DvH/195/MC; (I) groundwater enrichment LoTCEB12. Specific reductive dechlorination rates of *cis*-DCE by (B) co-culture *S. wolfei*/strain 195; (D) tri-culture *S. wolfei*/195/ MC; (F) co-culture DvH/strain 195; (H) tri-culture DvH/195/MC; (J) groundwater enrichment LoTCEB12. The multi equilibration method was used to determine k_{max} and K_S at each condition. The results of replicate experiments are represented by different symbols. All data falls in 95% confidence range.

Table 5-5 Kinetic parameters of reductive dechlorination obtained from the experiments

	D.mccartyi concentration[a]	TCE		*cis*-DCE	
		k_{max}[b]	K_S[c]	k_{max}	K_S
S. wolfei/strain195	$1.3\pm0.2\times10^{8}$	$2.7\pm 0.1\times10^{-9}$	11.5±1.9	$3.2\pm 0.1\times10^{-9}$	10.0±1.3
S. wolfei/195/MC	$1.1\pm0.1\times10^{8}$	$2.1\pm 0.1\times10^{-9}$	6.2±0.6	$1.5\pm 0.1\times10^{-9}$	2.6±1.2
DvH/strain195	$1.1\pm0.1\times10^{8}$	$4.1\pm 0.2\times10^{-9}$	14.5±2.3	$3.2\pm 0.1\times10^{-9}$	7.6±0.6
DvH/195/MC	$1.0\pm0.1\times10^{8}$	$1.7\pm 0.1\times10^{-9}$	12.4±1.5	$1.9\pm 0.1\times10^{-9}$	5.6±0.5
LoTCEB12[d]	$3.0\pm0.2\times10^{8}$	$1.8\pm 0.1\times10^{-9}$	7.4±0.7	$2.7\pm 0.1\times10^{-9}$	6.9±0.7

[a.] *D. mccartyi* cell number was obtained by quantifying 16S rRNA copy numbers using qPCR at the end of the experiment. Unit: cell number mL^{-1}. The standard deviation represents biological triplicate samples.
[b.] Maximum specific dechlorination rate is in the unit of μmol substrate·$cell^{-1}$·d^{-1}.
[c.] Half velocity is in the unit of μM.
[d.] For enrichment culture LoTCEB12, a total of 185 μmol TCE was added, while 78 μmol TCE was added to co-cultures and 33 μmol TCE was added to tri-cultures.

5.3.2 Kinetic parameters determination of cell growth

The cell growth of each microorganism was measured by qPCR targeting 16S rRNA or functional genes with specific targeting regions (primers are summarized in table 5-3). Theoretical growth yields were calculated using thermodynamic laws with corrections for environmental conditions. Example 5.1 describes how the theoretical cell yield of *D. mccartyi* was calculated, and Example 5.2 describes the calculation for correction to free energy values that more accurately reflect environmental conditions.

Example 5.1 TCE dechlorination to VC by *Dehalococcoides* strain 195, under standard conditions (pH=7.0, 25 °C)

Electron accepting reaction: TCE➔VC
Electron donor: H_2
Carbon source: CH_3COO^-
Balanced half reaction (for $1e^-$ transfer)

R_a: $\frac{1}{4}C_2HCl_3 + \frac{1}{2}H^+ + e^- = \frac{1}{4}C_2H_3Cl + \frac{1}{2}Cl^-$

$$\Delta G^{0\prime}_{accepter} = \left(\frac{1}{4}\Delta_f G^{\circ\prime}_{VC}\right) + \left(\frac{1}{2}\Delta_f G^{\circ}_{Cl^-}\right) - \left(\frac{1}{4}\Delta_f G^{\circ\prime}_{TCE} + \frac{1}{2}\Delta_f G^{\circ}_{H^+}\right)$$

$$\Delta G^{0\prime}_{accepter} = \frac{1}{4}\times(59.65\ \text{kJ mol}^{-1}) + \frac{1}{2}\times(-131.85\text{kJ mol}^{-1}) - \frac{1}{4}\times(25.41\ \text{kJ mol}^{-1})$$

$$-\frac{1}{2}\times(-39.87\text{kJ mol}^{-1}) = -37.43\ \text{kJ eeq}^{-1}$$

R_d: $H^+ + e^- = \frac{1}{2}H_2$

$$\Delta G^{0\prime}_{donor} = -\left(\Delta_f G^{\circ}_{H^+}\right) = 39.87\ \text{kJ eeq}^{-1}$$

$$A = -\frac{\frac{\Delta G_{carbonsource\ to\ pyruvate}}{0.6^n} + \Delta G_{PC}/0.6}{0.6 \times \Delta G_r}$$

$$\Delta G_r = \Delta G_{TCE-VC} - \Delta G_{H_2}$$

$$\left(\Delta G_{pyruvate} - \Delta G_{acetate}\right) > 0, n = 1$$

$$A = -\frac{(35.09 - 27.40 + 18.80)}{0.36 \times (-37.43 - 39.87)} = 0.952 \frac{e^- eq\ used\ for\ energy}{e^- eq\ used\ for\ cell\ synthesis}$$

$$f_s = \frac{1}{1+A} = \frac{1}{1+0.952} = 0.512; \quad f_e = 1 - f_s = 0.488$$

$$R_{total} = f_e \times R_a + f_s \times R_{cells} - R_d$$

Half reactions used for total reaction are listed in table 5-4.

Total Reaction stoichiometry:

$$0.5H_2 + 0.122C_2HCl_3 + 0.756H^+ + 0.1024CO_2 + 0.0256HCO_3^- + 0.0256NH_4^+ =$$
$$0.122C_2H_3Cl + 0.244Cl^- + 0.0256C_5H_7O_2N + 0.2304H_2O + 0.244H^+$$

The above balanced chemical reaction is based on one electron transfer. From the equation, we could calculate the cell yield, substrate consumption and nitrogen requirement for cell growth. A conversion of 113/20=5.65g biomass/e^-eq used is assumed in the calculation (Rittman, 2001). Therefore, the theoretical yield of *D. mccartyi* 195 under standard conditions is

$$\frac{f_s}{f_e} \times 5.65 \frac{g\ biomass}{e^- eq\ used} = 5.93 \frac{g\ cells}{e^- eq\ acceptor}$$

Example 5.2 TCE dechlorination to VC by *Dehalococcoides* strain 195 under time-course experimental conditions, pH 7.0. Concentrations of metabolites are listed as follows:

$[C_2HCl_3]$= 0.60 mM
$[C_2H_3Cl]$= 0.10 mM
$[C_2H_3O_2^-]$= 2.0 mM
$[HCO_3^-]$= 30 mM
$[Cl^-]$= 27 mM (calculated from medium composition)
$[H_2\ (aq)]$= 20 nM (measured at the beginning of the experiment)
Headspace composition: N_2:CO_2 (90:10 vol/vol)

$$\Delta G' = \Delta G^{0'} + RTLn \frac{[products]}{[reactants]}$$

$$\Delta G_{acceptor} = \Delta G^{0'}_{accepter} + \frac{8.314J}{K \cdot e^- eq} \times 307K \times ln \frac{[VC]^{\frac{1}{4}}[Cl^-]^{\frac{1}{2}}}{[TCE]^{\frac{1}{4}}}$$

$$\Delta G_{acceptor} = -43.19\ kJ\ eeq^{-1}$$

This value represents a small, but real change from $\Delta G^{0'}_{accepter} - 37.43\ kJ\ eeq^{-1}$
Similarly, for acetate at a concentration of 2.0 mM,

$$\Delta G_{acetate} = 27.04\text{kJ eeq}^{-1} + \frac{8.314J}{K \cdot e^{-}eq} \times 307K \times ln \frac{[C_2H_3O_2^-]^{\frac{1}{8}}}{(P_{CO_2})^{\frac{1}{8}}[HCO_3^-]^{\frac{1}{8}}} = 26.91\text{kJ eeq}^{-1}$$

For autotrophic microorganisms that use CO_2 as the carbon source, $\Delta G_P = 35.09\text{kJ eeq}^{-1} - (-78.82\text{kJ eeq}^{-1}) = 113.8\text{kJ eeq}^{-1}$. In *Dehalococcoides* central metabolism, one pyruvate molecule was assimilated from one CO_2 and one molecule of acetate (Tang *et al*., 2009), therefore we calculated the energy required to convert carbon source to pyruvate as:

$$\Delta G_{carbonsource\ to\ pyruvate} = \frac{1}{2}(35.09 - 26.91) + \frac{1}{2}(35.09 - (-78.82)) = 60.99kJ\ eeq^{-1}$$

H_2 was measured at around 20 nM (i.e. ~10^{-5} atm) at the beginning of the experiment for co-culture *S. wolfei* and strain 195, 20 nM was used in the calculation below:

$$H^+ + e^- = \frac{1}{2}H_2$$

$$\Delta G^{0'}_{donor} = 39.87\text{ kJ eeq}^{-1} + \frac{8.314J}{K \cdot e^{-}eq} \times 307K \times ln\left(P_{H_2}\right)^{\frac{1}{2}} = 39.87 - 14.69 = 25.18\text{kJ eeq}^{-1}$$

$$A = -\frac{(60.99 + 18.80)}{0.36 \times (-43.19 - 25.18)} = 3.24 \frac{e^{-}eq\ used\ for\ energy}{e^{-}eq\ used\ for\ cell\ synthesis}$$

$$f_s = \frac{1}{1 + A} = \frac{1}{1 + 3.24} = 0.236; \qquad f_e = 1 - f_s = 0.764$$

$$\frac{f_s}{f_e} \times 5.65 \frac{g\ biomass}{e^{-}eq\ used} = 1.75 \frac{g\ cells}{e^{-}eq\ acceptor}$$

For other redox reactions that have been considered in this study, the theoretical cell yields and environmental-corrected cell yield calculations were performed following the same protocols. The results are summarized in table 5-6 and table 5-7.

Table 5-6 Theoretical cell yield of each key microbial processes calculated under standard conditions, pH 7, 25°C

e-donor	e-acceptor	Carbon source	Organism	ΔG_r[a] (kJ/e^-eq)	ΔG_P (kJ/eeq)	ΔG_{PC} (kJ/eeq)	A[b] e^-eq acceptor/eeq cells	f_S=1/(1+A) e^-eq cells/eeq donor	Theoretical yield (g cells/eeq acceptor)
H_2	TCE to VC	acetate	*D.mccartyi*	-77.3	7.69	18.8	0.952	0.512	5.94
H_2	SO_4^{2-}	actate	DvH	-5.00	2.79	18.8	12.0	0.077	0.47
lactate	SO_4^{2-}	lactate	DvH	-11.4	2.79	18.8	5.26	0.160	1.07
butyrate	butyrate	butyrate	*S.wolfei*	-5.00	7.89	18.8	14.8	0.063	0.38
H_2	CO_2 to CH_4	CO_2	*Methanogens*	-16.4	114	18.8	22.5	0.043	0.25
H_2	CO_2 to acetate	CO_2	*Homoacetogens*	-12.5	114	18.8	29.6	0.033	0.19

a. Fermentation reactions listed in the table are endergonic at standard condition, therefore ΔG_r[a] for fermentation reactions listed were assumed to be -5 kJ/ e^-eq, due to the minimum energy required for microorganism is -20 kJ/mol (Schink, 1997), and 4 electrons were transferred to generate hydrogen gas in the fermentation reaction.

Table 5-7 cell yields of key microbial processes determined from free energy values corrected for experimental concentrations[a]

e^--donor	e^--acceptor	Carbon source	Organism	ΔG_r (kJ/eeq)	ΔG_P (kJ/eeq)	ΔG_{PC} (kJ/eeq)	A eeq acceptor/eeq cells	f_S=1/(1+A) eeq cells/eeq donor	Predicted yield (g cells/eeq acceptor)
H_2	TCE to VC	Acetate and CO_2	*D.mccartyi*	-60.9	61.0	18.8	3.24	0.236	1.75
H_2	SO_4^{2-}	acetate	DvH	-5.00	2.15	18.8	11.6	0.079	0.485
lactate	SO_4^{2-}	lactate	DvH	-14.6	2.15	18.8	3.97	0.201	1.422
butyrate	butyrate	butyrate	*S.wolfei*	-5.00	6.7	18.8	14.2	0.066	0.399
H_2	CO_2 to CH_4	CO_2	*Methanogens*	-4.62	114	18.8	79.9	0.012	0.071
H_2	CO_2 to acetate	CO_2	*Homoacetogen*	-0.85	114	18.8	436	0.002	0.013

a. Experimental concentration were: temperature 307.15K, [lactate]=5 mM, [butyrate]=5 mM, [acetate]=2mM, [C_2HCl_3]= 0.60 mM, [C_2H_3Cl]= 0.10 mM, [$C_2H_3O_2^-$]= 2.0 mM, [HCO_3^-]= 30 mM, [Cl^-]= 27 mM, [SO_4^{2-}]= 2 mM, [HS^-]= 1mM, H_2S partial pressure was assumed to be 10^{-6} atm. hydrogen partial pressure for dechlorination and methanogenesis was assumed to be ~10^{-5} atm. For homoacetogenesis, hydrogen partial pressure was assumed to be 10^{-4}atm, CH_4 partial pressure was assumed to be 10^{-5} atm. Headspace composition: N_2:CO_2 (90:10 vol/vol)

Cell decay

The rate of endogenous decay of *D. mccartyi* strain 195 was investigated in this study. The electron acceptor concentration fed to the culture (~ 0.2 mM, around 20x K_s) was maintained at a level below which inhibitory effects have been reported. Therefore we did not take inhibition effects into account during this experiment and used the endogenous-decay approach exclusively (Rittmann, 2001). In order to determine the relationship between dechlorination activity and the cell numbers and to investigate the decay coefficient more directly, maximum dechlorination activity was monitored in cultures for different periods of time in electron acceptor limiting conditions. We observed significant decreases in dechlorination activity over three weeks (Figure 5-3) while no significant change in cell number (quantified by qPCR using functional gene *tceA*) was observed (data not shown). The decoupling between cell number and dechlorination activity observed in this study is consistent with previous studies of *D. mccartyi* VS and 195 (Cupples *et al*., 2004; Johnson et al., 2008).

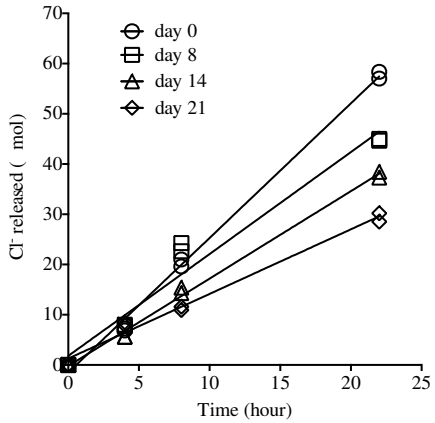

Figure 5-3 Cell decay rate measurement of *D. mccartyi* strain 195 during different time periods. Chloride released following TCE addition to duplicate cultures lacking an electron acceptor for 0, 8, 14 and 21 days. Points are measured values, lines are those predicted by a non-linear least-squares fit to the model to determine the decay rate.

Equations 5.5 and 5.6 were fit to data in Figure 5-3 by non-linear least-square analysis, generating a decay coefficient of 0.0017 hr^{-1} (i.e. 0.04 day^{-1}) for strain 195. The cell numbers quantified by qPCR was not used in the curve fitting since the cell numbers at different times were similar during the experiment ($1.3\pm0.1\times10^{10}$ per bottle at day 0, $1.2\pm0.2\times10^{10}$ per bottle at day 8, $1.4\pm0.2\times10^{10}$ per bottle at day 14, and $0.9\pm0.1\times10^{10}$ per bottle at day 21).

5.3.3 Effect of other environmental factors

Effect of organic acid anions on dechlorination

To determine the effects of elevated acetate concentrations on dechlorination performance and cell growth of *D.mccartyi* species, the co-culture *S. wolfei*/strain 195 was grown with butyrate (2 mM) and TCE (0.6 mM) in medium with different initial concentrations of sodium acetate from 5 mM to 40 mM (Figure 5-4). In the un-supplemented medium, strain 195 grew at a dechlorination rate of 6.0± 0.4 μmol per day with a specific growth yield of

$8.1\pm0.3\times10^7$ cells per Cl^- released. With addition of 5 mM acetate to the medium the dechlorination rate of the co-culture slightly decreased (4.2 ± 0.4μ mol per day) with a lower specific growth yield of 4.5 ± 0.4×10^7 cells per Cl^- released. At higher initial acetate concentrations, the total amount of strain 195 and *S. wolfei* growth attained by the co-culture decreased by at least 74 % and 95 %, respectively when the co-culture was grown in medium with an initial acetate concentration of 10 mM or higher. When a very high initial acetate concentration (40 mM) was used, little or no growth of *S. wolfei* was observed, and the yield of strain 195 decreased by 75%. The growth yield and growth rate of the co-culture under each condition are summarized in table 5-8. Axenic cultures of strain 195 grown in the same medium with H_2/CO_2 (90:10 vol/vol) as the electron donor were stimulated by the addition of up to 20 mM acetate to the medium (data not shown), indicating that the growth and metabolism of *S. wolfei* and not strain 195 was inhibited by acetate in the co-culture.

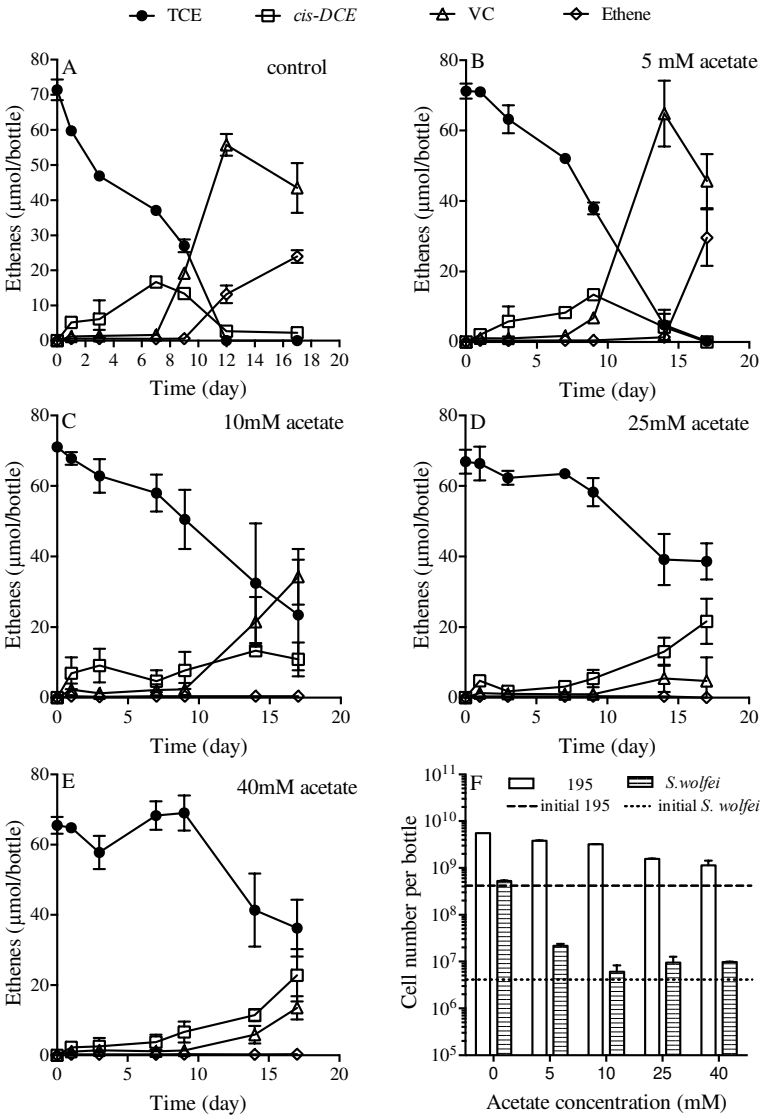

Figure 5-4 TCE dechlorination activity in co-culture *S. wolfei*/ strain 195 (n=3) growing with 2mM butyrate as electron donor with different initial acetate concentrations (A-E), and the respective proxies for the cell number (F) on day 17 of the experiment.

Table 5-8 Effect of acetate on the growth of syntrophic co-culture *D.mccartyi* 195 and *S. wolfei*

Acetate	Percentage of TCE degradation	Specific cell yield of strain 195 ($\times 10^7$ per Cl^- released)	195 cells ($\times 10^9$ per bottle)	*S.wolfei* cells ($\times 10^7$ per bottle)
0 mM	100%	8.1±0.3	11±0.4	57±0.3
5mM	100%	4.5±0.4	6.4±0.5	17.2±0.4
10mM	67%	3.3±0.3	2.9±0.3	2.6±0.8
25mM	42.2%	7.8±0.1	2.4±0.3	2.3 ±0.3
40mM	44.7%	5.5±0.6	2.7±0.3	1.6 ±0.5

In order to investigate the effect of acetate on other *D.mccartyi*-containing dechlorinating communities, the growth and metabolism of tri-culture *S. wolfei*/195/MC was studied with 20 mM acetate addition. Similar results were obtained compared to the co-culture. Only a portion of the TCE (44 %) was degraded, with a dechlorination rate of 1.9 μmol per day and a specific growth yield of 9.4 ±0.7 $\times 10^7$ cells per Cl^- released. No methane production was observed during the experimental period, and *S. wolfei* cell number was about 19% of that in control bottles (Figure 5-5 B).

When a high acetate concentration (20 mM) was added to tri-culture DvH/195/MC and enrichment culture LoTCEB12, the dechlorination rates and H_2 levels were not affected (Figure 5-5 D and table 5-9). However methane production decreased by 93%, and 58% compared to the control groups, and methanogen cell numbers decreased by 85% and 69%. In terms of fermenting bacteria growth, the cell yields of DvH decreased by 35%, while in the enrichment culture, cell numbers of *Desulfovibrio* was 76% of the control (table 5-9). Tests of various initial acetate concentrations (5 mM, 10 mM, 20 mM and 40 mM) on the hydrogenotrophic methanogen *Methanobacterium conglense* demonstrated that methane production was unaffected by these acetate levels.

Table 5-9 Cell yield and methane production in acetate amended cultures [a]

Culture	TCE degradation [b] (μmol)	Methane production (μmol/bottle)	Methanogens ($\times 10^8$ per bottle)	*D.mccartyi* ($\times 10^9$ per bottle)	Fermenter[c] ($\times 10^8$ per bottle)
S. wolfei/195/MC	10.9 (44.2%)	0.9±0.2 (10.2%)	2.5±1.2 (78.1%)	2.2±0.5 (19.1%)	1.9±0.6 (19.4%)
DvH/195/MC	22.7 (91.8%)	12.0±6.5 (7.5%)	9.0±1.5 (15.5%)	7.9±0.5 (79.0%)	19.3±0.5 (35%)
LoTCEB12	172.4 (100%)	14.9±1.8 (42.1%)	20±3 (30.8%)	2.6±0.3 (86.7%)	0.3±0.04 (76%)

a. Values in parentheses are the ratios of the numbers obtained from acetate-amended cultures to the control experiment.

b. Percent degradation was calculated at the end of the experiment (day 6) for tri-cultures and (day 11) for enrichment culture, 100% degradation of TCE was observed in all control bottles.

c. *S. wolfei* cell numbers were measured in *S. wolfei*/195/MC to represent the fermenting microorganisms, DvH cell numbers were measured in DvH/195/MC to represent the fermenting bacteria. In the LoTCEB12 enrichment, we measured *Desulfovibrio* cell numbers, which were only a portion of the fermenting microorganisms.

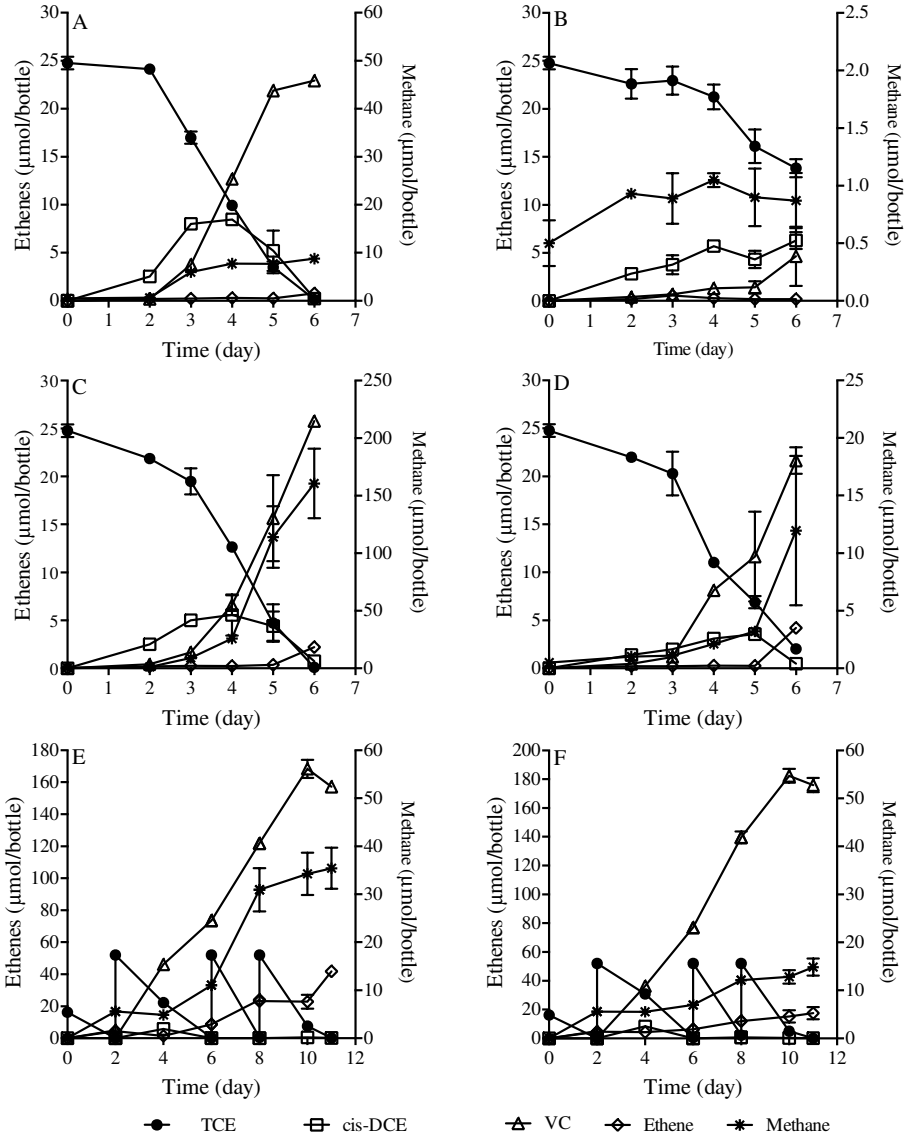

Figure 5-5 TCE dechlorination activity and methane production in controls (A) *S.wolfei*/195/MC, (C) DvH/195/MC, (E) enrichment culture LoTCEB12, and with 20 mM acetate amendment in (B) *S.wolfei*/195/MC, (D) DvH/195/MC, (F) LoTCEB12.

Effect of Bicarbonate on dechlorination

D. mccartyi strain 195 was inoculated 5% (vol/vol) into bicarbonate-free medium with 0.5 mM TCE as electron acceptor and 5 mL filtered ultra-pure H_2 gas as the sole electron donor. Different initial bicarbonate concentrations (from 1 mM to 30 mM) were achieved by adding different volumes of sodium bicarbonate stock solutions (1.0 M). pH was maintained between 7.0 to 7.3 throughout the experiment (data not shown) by adding Good's buffers (TES or HEPES) (He *et al*., 2007; Delgado *et al*., 2012). The dechlorination rates of strain 195 within all buffering system were similar at low (1mM) and high (30 mM) bicarbonate concentrations (Figure 5-6). As bicarbonate concentrations decreased, the dechlorination rate decreased as well.

When reducing bicarbonate concentration from 30 mM (normally used in the lab for culture maintenance) to 1 mM, the dechlorination rate of strain 195 decreased about 30~ 40% (from 8.4± 0.6 μmol per day to 4.9± 0.1 μmol per day in TES buffer, and from 5.8± 0.2 μmol per day to 4.2± 0.2 μmol per day in HEPES buffer) in both systems.

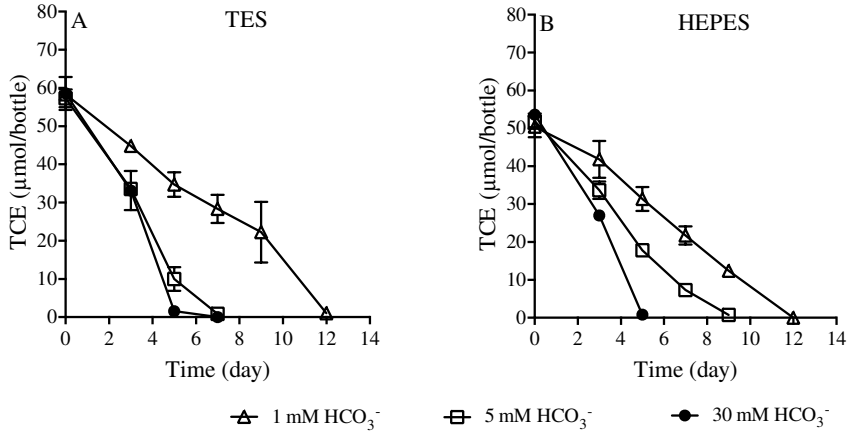

Figure 5-6 TCE degradation activities of strain 195 with (A) TES buffer and (B) HEPES with different initial bicarbonate concentrations (1 mM to 30 mM).

Similar slow dechlorination activity was observed in tri-cultures *S. wolfei*/195/MC and DvH/195/MC when bicarbonate concentrations were decreased from 30 mM to 1 mM (Figure 5-7). In tri-culture *S. wolfei*/195/MC, about half of 25 μmol TCE was dechlorinated by the end of the experiment. The growth yield of strain 195 decreased by 75% compared to the control group. While the specific growth yield ($8.8\pm0.8\times10^7$ per Cl^- released) was similar to that in the co-culture. *S. wolfei* cell yield decreased by 32% ($3.1\pm0.5\times10^8$ per bottle) at low bicarbonate concentration. Methane production was not significantly observed in either control (30 mM bicarbonate) or low bicarbonate (1 mM) bottles. Accordingly little cell yields of methanogens were observed at either condition.

In tri-culture DvH/195/MC, the low bicarbonate concentration decreased dechlorination activity and exerted a negative effect on the growth of DvH (cell yield was 51% of that in the control), while H_2 maintained in the system was sufficiently above the threshold for methanogenesis (data not shown). Methane production was not significantly affected (88% of that in control) and the cell yield of methanogens increased (157% of that in control). In enrichment culture LoTCEB12, low bicarbonate did not affect either dechlorination activity or the cell yield of *D. mccartyi* (table 5-10). Interestingly, a decrease in *Desulfovibrio* cell number ($6.3 \pm 1.5 \times10^6$ per bottle) was observed. Furthermore, methane production increased at the lower bicarbonate concentration, which was about 1.5 times of that in the control group.

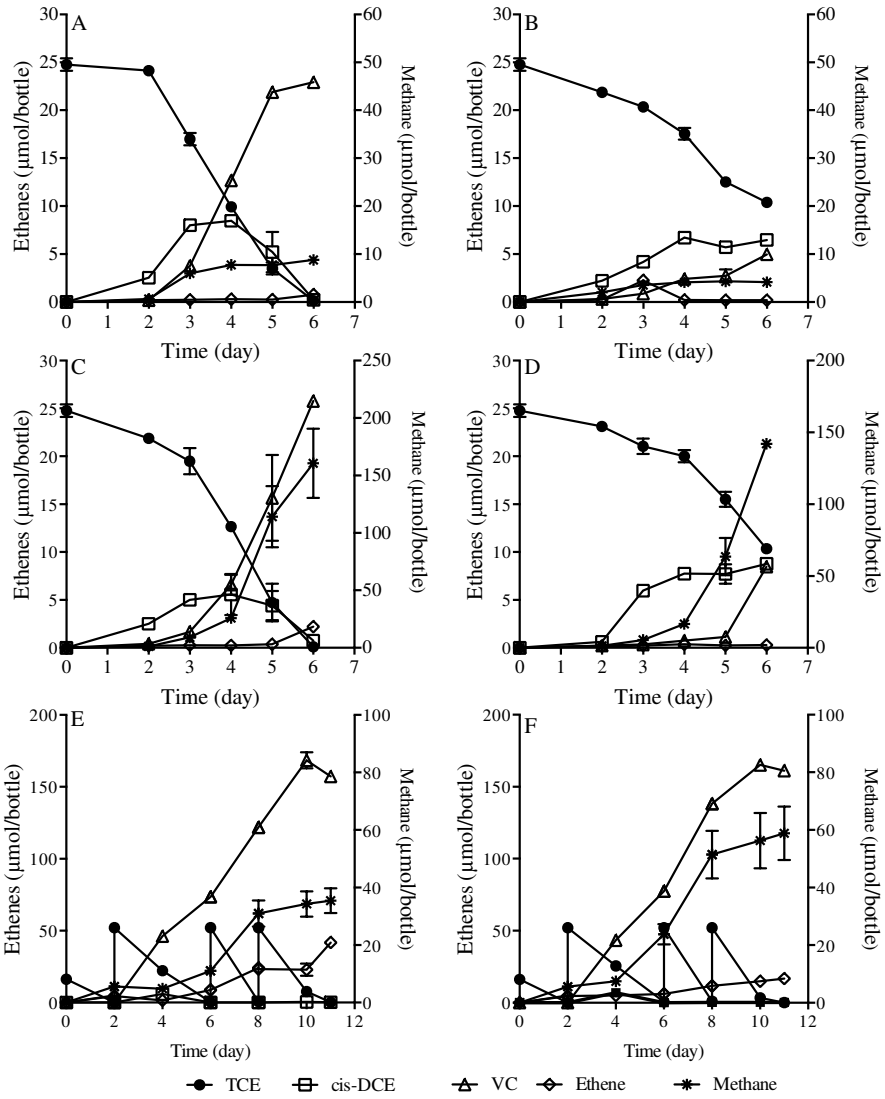

Figure 5-7 Reductive dechlorination profile of *S. wolfei*/195/MC with A) 30 mM bicarbonate B) 1mM bicarbonate; DvH/195/MC with C) 30 mM bicarbonate and D) 1mM bicarbonate; LoTCEB12 enrichment with E) 30 mM bicarbonate and F) 1 mM bicarbonate. Error bars are SD.

Table 5-10 Cell yield and methane production in bicarbonate amended cultures [a]

Culture	TCE degradation [b] (µmol)	Methane production (µmol/bottle)	Methanogen ($\times 10^8$ per bottle)	*D.mccartyi* ($\times 10^9$ per bottle)	Fermenter[c] ($\times 10^8$ per bottle)
S. wolfei/195/MC	14.4 (58%)	4.2±0.2 (48%)	0.6±0.1 (184%)[d]	2.7±0.4 (29%)	3.1±0.5 (32%)
DvH/195/MC	14.4 (58%)	142±2.7 (88%)	9.1±0.2 (157%)	1.9±0.4 (19%)	1.3±0.2 (19%)
LoTCEB12	172.4 (100%)	58.9±9.3 (166%)	7.2±0.4 (111%)	2.9±0.6 (97%)	0.06±0.02 (18%)

a. Values in parentheses are the ratios of the number obtained from 1mM bicarbonate feeding cultures to the control experiment (30 mM bicarbonate).
b. Percentage of degradation was calculated at the end of the experiment (day 6) for tri-cultures and (day 11) for enrichment culture, 100% degradation of TCE was observed in all control bottles.

c. *S. wolfei* cell number was measured in *S. wolfei*/195/MC, DvH cell number was measured in DvH/195/MC and LoTCEB12 enrichment.
d. Cell number of *S. wolfei* was very low, comparable to the value of starting point of the experiment (2.9×10^8 per bottle).

Sulfate and sulfide effect

Excess sulfate addition (2.5 mM) to strain 195 did not affect cell growth or dechlorination rates (data not shown). This result agrees with a previous study showing that sulfate did not exert inhibition on strain *D.mccartyi* FL2 at high concentrations (10 mM) (He *et al*., 2005). Similarly, sulfate amendment (2.5 mM) to *S. wolfei* did not exhibit inhibition on cell growth. In order to determine the effect of sulfide (the reduction product of sulfate) on cell growth of the isolates, we tested dechlorination rate and cell yield with different sulfide concentrations (2mM to 5mM). With 5% inoculation of active strain 195, took 6 days, 10 days and 14 days to dechlorinate 75 µmol TCE while 0mM, 2mM and 5mM sulfide were fed to the culture, respectively. Cells were collected right after TCE was dechlorinated in all conditions and the cell number was quantified using qPCR of the *tceA* gene. The cell yield of strain 195 decreased about 65% as sulfide concentrations increased from 0 to 5 mM (table 5-11). For *S. wolfei*, cells were collected and were quantified from different sulfide amended cultures after 10 days incubation with 10 mM crotonate and the cell yield at 5 mM sulfide decreased by 40% compared to the control group (table 5-11).

Table 5-11 Sulfide effect on growth of strain 195 and *S. wolfei* isolates

Sulfide concenctration	Dechlorination rate (µmol TCE per day)	strain 195 (cell per mL)	strain *S. wolfei* (cell per mL)
0mM	12.5±2.5	$9.1\pm0.4\times10^7$	$4.9\pm0.2\times10^6$
2mM	7.5±1.4	$5.6\pm0.6\times10^7$	$3.2\pm0.5\times10^6$
5mM	5.4±0.9	$3.2\pm0.7\times10^7$	$3.0\pm0.04\times10^6$

In syntrophic co-culture DvH/strain 195, DvH ferments lactate to acetate and H_2, and strain 195 consumes H_2 for reductive dechlorination of TCE. In our study, 5 mM lactate was amended as electron donor, 5mM sulfate and 0.55 mM TCE were amended to the culture at the beginning of the experiment. Based on stoichiometry (equations in Table 5-4), 11.7 mM lactate was required to reduce all the electron acceptors: sulfate (5 mM) to sulfide and TCE (0.55 mM) to ethene. H_2 concentrations increased to 1.4 ± 0.6 µM on day 2 and this concentration was about 10% of that in the control group (Men *et al*., 2012). H_2 detected in the co-culture dropped dramatically to 30 nM on day 4. Another 5mM lactate was amended to the culture on day 4 to avoid electron donor limiting conditions. H_2 increased back to above 1.0 µM after the lactate amendment. However, the TCE dechlorination rate decreased from day 4 to day 9. On day 9, another 2mM lactate was added to the co-culture and H_2 slightly increased to 2.0 µM. However the dechlorination of TCE stalled from day 9 to day 16. At the end of the experiment, we flushed the experimental bottles for 30 minutes with pure nitrogen gas and reamended with 78 µmol TCE. Complete TCE dechlorination was observed after five days (data not shown). Cell numbers of strain 195 did not further increase after day 4 (Figure 5-8 B). At the end of the experiment, the cell number ratio of strain 195 to DvH was about 1:6. In contrast, in the control group where no sulfate was amended, the cell number ratio of strain 195 ($9.8\pm0.8\times10^7$ cells mL^-

^{1}) to DvH (2.4 ±0.1×10^{7} cells mL^{-1}) at the end of the experiment was 4:1. This was similar to the previously reported result of this co-culture (5:1 Men *et al*., 2012).

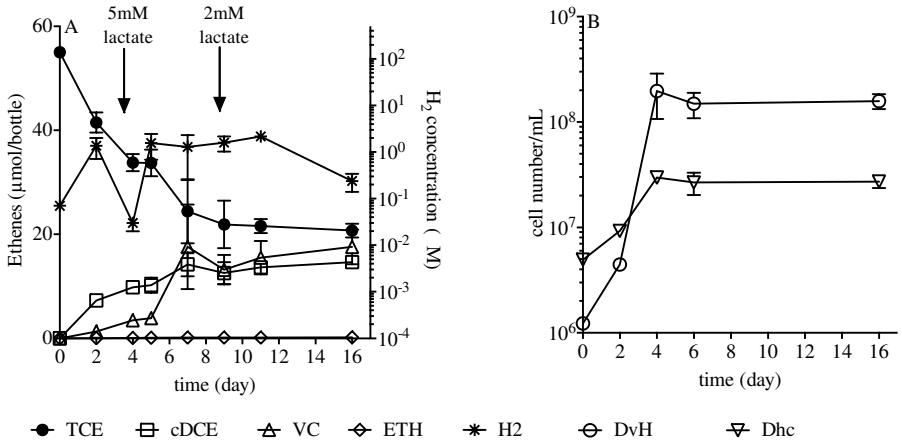

Figure 5-8 TCE dechlorination activity and H_2 production in co-culture strain 195/DvH with 5mM sulfate amendment (A), and the respective proxies for the cell number (B) during the experiment. Error bars showed standard deviation of biological triplicates.

In order to study the competition for H_2 of dechlorination and sulfate reduction, we monitored dechlorination performance as well as cell growth yield in tri-culture *S. wolfei*/195/DvH. In this tri-culture, 0.7 mM TCE and 2 mM sulfate were fed as electron acceptors to eliminate the effect of sulfide inhibition on dechlorination. Based on stoichiometry (equations in Table 5-4), 6.1 mM butyrate was required to reduce each of the electron acceptors: sulfate (2 mM) to sulfide and TCE (0.7 mM) to ethene. Considering part of the electrons would contribute to biomass production, 5 mM butyrate was fed to the culture to generate electron donor limiting conditions. The experiment was conducted after 3 continuous sub-culture events of the culture construction. The dechlorination profile and cell numbers quantification within one subculture is summarized in Figure 5-9. During the experiment period, H_2 remained between 0.03 to 0.6 µM, which was well above the threshold for either dechlorination or sulfate reduction and was comparable to that maintained in the control group (without sulfate addition). The TCE dechlorination rate was not affected by the sulfate addition (2 mM) (data not shown). On day 8, another 0.5 mM TCE was added to the tri-culture. The dechlorination rate for the second dose of TCE (8.4 ± 0.3 µmol day^{-1}) was slower compared to the control group (13.7±0.5 µmol day^{-1}). In addition, ethene production stalled after day 8. Based on cell number production (Figure 5-9 B), strain 195 increased to 1.9± 0.2 ×10^{8} mL^{-1} by the end of the experiment, which was similar to the control group 1.8 ± 0.2 ×10^{8} mL^{-1}. *S. wolfei* cell number (1.2± 0.3 ×10^{7} mL^{-1}) was higher than the control (0.8± 0.1 ×10^{7} mL^{-1}) while DvH increased to 1.4± 0.2 ×10^{7} mL^{-} on day 10, then decreased to 0.8± 0.1 ×10^{7} mL^{-1} by the end of the experiment.

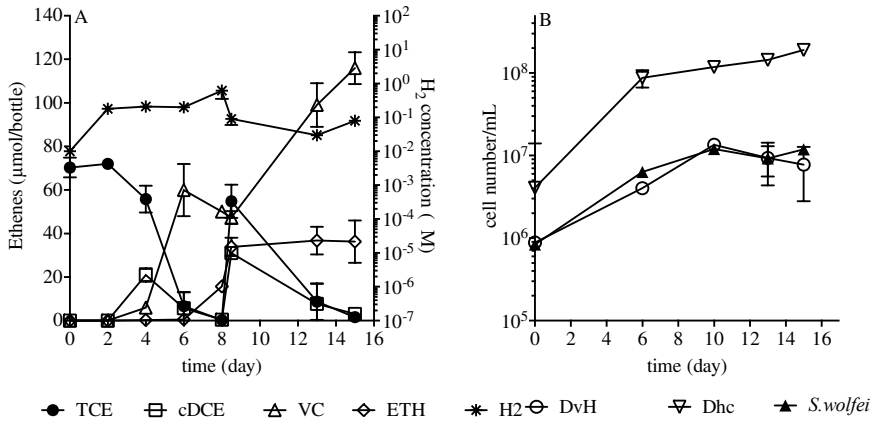

Figure 5-9 TCE dechlorination activity and H_2 production in tri-culture strain 195/DvH/*S.wolfei* with 2mM sulfate amendment (A), and cell numbers (B) during the experiment. Error bars showed standard deviation of biological triplicates.

A methanogenic enrichment culture LoTCEB12 was grown on 20 mM lactate, and the culture was fed with 20 µmol TCE and 2 mM sulfate at the beginning of the experiment. TCE was dechlorinated within two days, with H_2 above 1.0 µM. After a second dose of TCE addition (50 µmol), H_2 dropped to a low level (< 2 nM) on day 4, and dechlorination was stalled after day 6. *D. mccartyi* cell numbers did not further increase after day 4. During the experimental period, methane production was not observed in the enrichment (data not shown in figure 5-10). The addition of sulfate (2 mM) to the enrichment promoted the growth of sulfate reducers (6.0 ± 0.5 $\times 10^5$ cell mL^{-1}) compared to the control group (3.4 ± 0.4 $\times 10^5$ cell mL^{-1}).

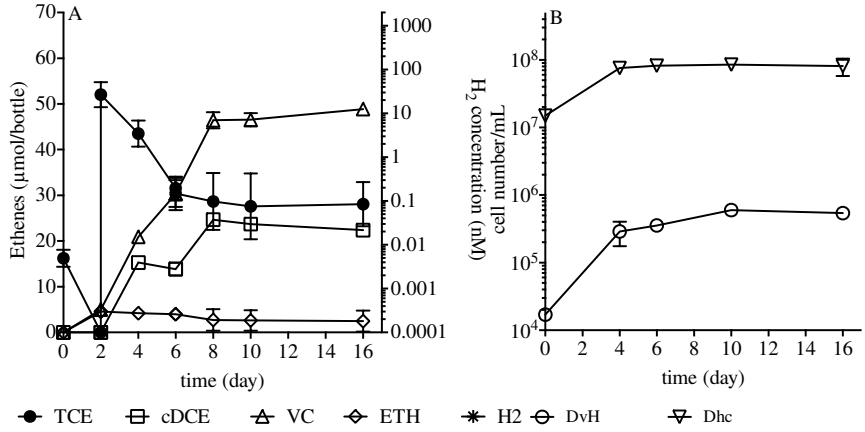

Figure 5-10 TCE dechlorination activity and H_2 production in enrichment culture LoTCEB12 with 2mM sulfate amendment (A), and the respective proxies for the cell numbers (B) during the experiment. Error bars showed standard deviation of biological triplicates.

5.4 Discussion

Table 5.12 summarizes experimentally determined kinetic parameters of TCE/*cis*-DCE dechlorination in the literature. Among published kinetic parameters, only a few were determined by experimental methods (Fennell *et al*., 1998; Yu *et al*., 2004; Lee *et al*., 2004;

Amos *et al*., 2007; Schaefer *et al*., 2009; Popat and Deshusses, 2011), other published parameters were adapted from assumed values or from model fitting values. Specifically, there was a wide range of reported specific maximum dechlorination rates, $k_{max,\ ethenes}$ (0.02~81.3 μmol substrate·mgVSS^{1}·hr^{-1}, table 5-12). In this study, we carried out a systematic investigation to determine the kinetic parameters of *D. mccartyi* from strain 195 isolate to constructed syntrophic co/tri-cultures, and an enrichment dechlorinating community. More accurate values of each specific parameter were obtained by using modern molecular techniques (qPCR quantification). From our investigation, k_{max} for TCE and *cis*-DCE did not change significantly under different growth conditions from pure culture to consortia, all measured values were converted to the unit of μmol substrate·mgVSS^{1}·hr^{-1} by assuming the cell weight of *D.mccartyi* to be 4.2×10^{-15} g per cell (Duhamel *et al*., 2004), and the obtained values were comparable to previous studies with *Desulfomonas michiganensis* BB1 and *Sulfurosprillum multivorans* (Amos *et al*., 2007), as well as and enrichment culture study of PM and EV (Yu *et al*., 2004). However, the values obtained from this study were much higher than those from a bio-trickling filter study (Popat and Deshusses, 2011) and a CMFR study (Haston and McCarty, 1999). The likely reason for the much lower k_{max} values in the previous studies was the use of measured VSS to quantify the dechlorination biomass, a method that would underestimate the k_{max} value for dehalorespiring populations.

In most modeling approaches, half-velocity coefficients for dechlorination were assumed to be the same as measured inhibition constants (Clapp *et al*., 2004; Yu *et al*., 2004; Amos *et al*., 2007; Huang *et al*., 2009; Papat *et al*., 2011) Therefore it is crucial to better characterize the half-velocity coefficients. The K_S values for TCE and *cis*-DCE obtained from the constructed consortia (co-cultures and tri-cultures) were similar to previously determined reports of *Desulfomonas michiganensis* BB1 and *Sulfurosprillum multivorans* (Amos *et al*., 2007), but these values were 1~2 orders of magnitude higher than other enrichment culture studies of 0.05~ 0.54 μM (Haston and McCarty, 1999; Lee *et al*., 2004). In this study, the half velocity coefficients determined from the enrichment culture LoTCEB12 was lower than the constructed cultures, and the values were at the same level as other enrichment cultures (Yu *et al*., 2004; Schaefer *et al*., 2009; Popat and Deshusses, 2011). Higher half velocity coefficients represent lower enzyme affinities. The K_S value for TCE and *cis*-DCE were significantly above the maximum contaminant levels (MCLs) for these compounds (0.04 μM and 0.72 μM, respectively), therefore when the chlorinated ethene concentrations drop to the range of the MCLs, the dechlorination rates could be expected to decrease significantly from the maximum values.

Table 5-12 A comparison of the kinetic parameters determined by kinetic experiments

		Biomass calculation[a]	TCE		*cis*-DCE		Reference
			k_{max}[a]	K_S[b]	k_{max}	K_S	
Isolates	*Desulfomonas michiganensis* BB1	VSS	14.0±1.5	15.1±5.4	N.A.	N.A.	Amos *et al*., 2007
	Sulfurospirillum multivorans	VSS	10.8±1.0	23.4±5.2	N.A.	N.A.	Amos *et al*., 2007
	Strain 195	Estimated	3	0.54	3	0.54	Fennell *et al*., 1998
Constructed consortia	195/ *S. wolfei*	Cell number	26.8±1.2	11.5±1.9	31.7±0.1	10.0±1.3	This study
	195/DvH	Cell number	40.7±2.4	14.5±2.3	31.7±0.8	7.6±0.6	This study
	195/ *S. wolfei*/MC	Cell number	20.8±0.5	6.2±0.6	14.9±0.6	2.6±1.2	This study
	195/DvH/MC	Cell number	16.9±0.7	12.4±1.5	18.8±0.8	5.6±0.5	This study
Enrichment culture	Enrichment	VSS	3	0.54	3	0.54	Fennell *et al*., 1998
	Enrichment	VSS	0.07±0.01	1.4±0.9	0.02	3.3±2.2	Haston and McCarty, 1999
	Enrichment	VSS	15.3	0.05	2.0	3.3	Lee *et al*., 2004
	PM enrichment	Protein	10.3±1.4	2.8±0.3	1.8±0.2	1.8±0.4	Yu *et al*., 2004
	EV enrichment	Protein	10.4±1.2	1.9±0.5	1.2±0.1	1.8±0.3	Yu *et al*., 2004
	Enrichment in biofilm reactor	VSS	0.04	5.3	0.005	6.9	Popat *et al*., 2011
	Enrichment	VSS	81.3±9.4	3.2	32.5±0.9	2	Schaefer *et al*., 2009
	LowTCEB12	Cell number	17.9±0.5	7.4	14.9±0.3	7.4	This study

a. k_{max} values were calculated according to Duhamel 2004, that assuming cell weight of *D. mccartyi* is 4.2×10^{-15} g ·cell^{-1}, all k_{max} values were normalized to the unit of μmol substrate·mgVSS^{1}·hr^{-1}.

b. K_S values were in the unit of μM.

Biomass production and endogenous decay

Theoretical cell yield calculations under standard conditions (table 5-6), not surprisingly showed yields of heterotrophic microorganisms increase as Gibbs free energy of the redox reaction (ΔG_r) becomes more negative. For example, syntrophic bacteria that carry out endergonic fermentation reactions, and autotrophic microorganisms (e.g. methanogens and homoacetogens), that use CO_2 as carbon source, have correspondingly smaller cell yields. When considering environmental relevant concentrations (table 5-7), H_2 was the key factor affecting ΔG and predicted cell yields. This observation is consistent with previous studies on the correlation of cell yields and free energy availability in anaerobic microorganisms (Roden *et al*., 2011). At low H_2 concentrations, the predicted cell yields of *D. mccartyi*, methanogens and homoacetogens decreased significantly. Specifically, when H_2 partial pressures dropped to 10^{-4} atm, little energy (-0.85 kJ/eeq) was produced by homoacetogens, indicating that it would not be an energy-generating process at that level.

In calculating *D. mccartyi* cell yields, we considered both acetate and carbon dioxide as carbon sources (at a ratio of 1:1), since in the central metabolism pathway of *D. mccartyi*, one acetate and one carbon dioxide are required to synthesize one pyruvate (Tang *et al*., 2009). In this way, a much higher thermodynamic penalty for incorporation of carbon was accounted. Roden *et al*. (2011) found a linear correlation between microbial yields (Y_{XS}, g cell mol^{-1} substrate) and estimated catabolic Gibbs free energy for metabolism of short-chain fatty acids and H_2 coupled metabolic pathways. In this study, we calculated the catabolic Gibbs free energy ΔG available for fermenting bacteria and H_2 coupled metabolic pathways, and predicted cell yield Y_{cal} ratios for constructed consortia. Furthermore, we compared the predicted yield ratios to measured values (Table 5-13). In the syntrophic co-cultures, theoretical cell production of strain 195 to *S. wolfei* (14:1) and strain 195 to DvH (7:1) were similar to our observations 16:1 and 5:1, respectively. While, in tri-culture *S. wolfei*/195/MC, the observed MC cell yield was lower than the predicted value. This could be due to dechlorination out-competing methanogenesis under low H_2 concentrations, when both kinetics and thermodynamics control cell growth yields. In tri-culture DvH/195/MC, the observed cell yields of DvH and MC were higher than predicted. This demonstrates that under higher H_2 concentrations, both dechlorination and methanogenesis happen simultaneously, without significant competition and kinetics rather than thermodynamics control the cell yield of methanogens. In enrichment culture LoTCEB12, excess lactate (20mM) was added at the beginning of the experiment and H_2 concentrations in the system were maintained at high levels (> 1μM) throughout the experiment. However, since we used 16S rRNA of *Desulfovibrio* species to quantify the fermenters in the system, it is likely that the fermenting population was largely under-estimated in the calculated ratio.

Table 5-13 Theoretical biomass production and measured biomass in constructed consortia and enrichment culture[a]

	Reductive dechlorination rate (μmol d^{-1})	*D. mccartyi*		*Fermenting bacteria*		*Methanogens*		Cell yield ratio	
		ΔG[b] (kJ/mol)	Y_{obs}	ΔG (kJ/mol)	Y_{obs}	ΔG (kJ/mol)	Y_{obs}[c]	Y_{cal}[c]	Y_{obs}[d]
S. wolfei/195	12.8±1.2	-295.3	1.1×10^{10}	-41.9	7.7×10^{8}	N.A	N.A	14:1	16:1
S. wolfei /195/MC	7.9±0.2	-295.3	1.05×10^{10}	-50.5	9.8×10^{8}	-43.5	3.2×10^{8}	12:1:1	11:1:0.3
DvH/195[e]	19.5±1.7	-246.3	9.9×10^{9}	-72.3	2.1×10^{9}	N.A	N.A	7:1	5:1
DvH/195 /MC	9.4±0.2	-246.3	1.01×10^{10}	-82.3	5.5×10^{9}	-43.5	5.8×10^{9}	6:1:0.5	2:1:1
LoTCEB12	40.0±0.8	-246.3	3.03×10^{10}	-78.2	2.0×10^{9}	-43.5	6.5×10^{9}	3.5:1:0.6	15:1:5

a. Theoretical biomass production was based on thermodynamic calculation of Gibbs free energy for each microorganism at experimental conditions.
b. ΔG was calculated at the beginning of the experiment at certain experimental conditions.
c. The ratio of Ycal is based on ΔG ratios, assume the cell size of *fermenters and methanogen* was about two times bigger than *D.mccartyi*.
d. The cell number ratio Yobs was measured and calculated based on qPCR result.
e. Data was taken and recalculated from Men *et al*. 2012

Endogenous decay

For slowly growing microorganisms, the active biomass requires energy for cell maintenance and cell functions, such as motility, repair, osmotic regulation, transport, and heat loss etc. Endogenous decay is used to represent the flow of the energy and electrons required for cell maintenance (Rittmann, 2001). Due to the nature of endogenous decay, the faster a microorganism grows, the higher the decay rate should be, and slow growing bacteria have relatively small decay rates. Decay of cells could be an important factor in a continuous flow reactor (i.e. nutrient-poor environment) since the growth rate is low (Yang *et al*., 1998; Zheng *et al.*, 2001; Berggren *et al*., 2013). There has only been one study in the literature that used experimental methods to determine the decay coefficient of a *D. mccartyi* strain (Cupples *et al*., 2003). The other studies that have reported decay coefficients for *D. mccartyi* have assumed reasonable values or estimated them by model fitting (Fennell *et al*., 1998; Yu *et al*., 2004; Clapp *et al*., 2004; Haest *et al*., 2010). Cupples et al. (2003) calculated the decay coefficient during no-growth conditions to be 0.09 day $^{-1}$, and during active growth to be 0.05 day^{-1}. Cell concentrations of strain VS determined by competitive PCR were not used in the model due to the problem of measuring inactive cells during the experimental period. Li and Drake (2001) hypothesized that DNA from dead cells could account for higher-than-predicted bacterial numbers. In our study, we encountered the same problem of over estimating active cells using qPCR targeting 16S rRNA of *D. mccartyi*. Therefore, cell numbers were not used in the curve fitting, resulting in a decay coefficient for strain 195 of 0.04 d^{-1}, a value within the range of published decay coefficients for dechlorinating bacteria (0.003~0.09 d^{-1}). The reported decay coefficients for methanogens and sulfate reducers were 0.007~0.085 day^{-1} and 0.06 day^{-1}, respectively. From the results above, we estimated strain-specific decay coefficients that all fell within published ranges. The effect of model prediction by varying decay coefficient values is discussed in Chapter 6.

Effect of organic acid anions

Although high initial acetate concentrations (>10 mM) inhibited the cell growth of *S. wolfei* in the syntrophic co-culture, the growth rate of strain 195 was less affected. And the co-culture was metabolically active as determined by intermediate chlorinated compound production. The specific growth yield of strain 195 under each condition falls in the range of previously reported growth yields for *D. mccartyi* (He *et al*., 2007; Cheng *et al*., 2010; Men *et al*., 2011; Yan *et al*., 2012; Yan *et al*., 2013). The specific cell growth yields indicate that strain 195 coupled growth with dechlorination under all tested conditions. The results demonstrated that dechlorination activity was governed by the butyrate fermentation rate of *S. wolfei* that governs the hydrogen flux to strain 195. In a previous co-culture study of *S. wolfei* with a hydrogenotrophic methanogen *Methanospirillum hungatei* (Beaty and McInerny1989), butyrate degradation rates and cell yields of *S. wolfei* decreased at higher initial acetate concentration (>15 mM), and the inhibition was not due to the counter ion or the effect of acetate on the methanogen. However, the inclusion of an acetate-using methanogen *Methanosarcina barkeri* increased both the cell yield of *S. wolfei* and the efficacy of butyrate degradation. In Beaty's study, lactate was found to be another effective inhibitor of *S. wolfei* cultures at concentrations greater than 10 mM. Similar inhibitory effects on dechlorination were also observed in tri-culture *S.wolfei*/195/MC amended with 20 mM sodium acetate and little methane production was observed. A decrease of methane production as well as methanogen cell numbers were observed in tri-culture DvH/195/MC and the enrichment culture LoTCEB12, indicating that methanogenesis was inhibited by elevated acetate concentrations. Since H_2 levels in these two cultures were comparable to the control group, the inhibition effect was not likely due to H_2 limitation. Previous studies have shown that acetate has inhibitory effects on methanogenesis in microbial communities by altering carbon flow (Williams and Crawford, 1984, Horn *et al*., 2003). In contrast, when *M. conglense* (5% vol/vol inoculation) was amended with high acetate in this study (20 mM sodium acetate), methane production reached the same level as the control within 48 hours, suggesting that it is unlikely that acetate inhibition is the sole reason for methanogenic inhibition in tri-culture 195/DvH/MC and the enrichment culture LoTCEB12.

Bicarbonate

In this study, the medium was well buffered by TES or HEPES, and the pH was maintained at neutral levels (7.0~7.3) during the experiment, and the typical bicarbonate concentration in the medium was reduced from 30 mM to 5 mM or 1 mM. The results demonstrated that the low bicarbonate concentration (1 mM) resulted in decreased dechlorination rates and cell yields of strain 195 both in isolation and constructed tri-cultures. However, in enrichment culture LoTCEB12, the dechlorination profile was unchanged and *D. mccartyi* cell numbers were not affected. In the literature, few studies have been performed to evaluate the effects of bicarbonate on dechlorination. One study reported slower PCB dechlorination rates when bicarbonate concentrations were increased from 1.6 mM to 16 mM (Yan *et al*., 2006). There was only one study that investigated the role of bicarbonate as an electron acceptor in a TCE reductively dechlorinating enrichment (DehaloR^2) (Delgado *et al*., 2012). In Delgado's work, H_2 was used as direct electron donor and the effect of bicarbonate on fermenting bacteria was not considered. When HEPES was used as an additional pH buffer to culture DehaloR^2, varying sodium bicarbonate concentrations (from 2.5 mM to 30 mM) did not show a clear effect

on dechlorination rates. Interestingly, in our study, methane production and the cell yield of methanogens in the tri-cultures were not much affected by varying bicarbonate concentrations. However, in enrichment culture LoTCEB12, methane production in the low bicarbonate (1 mM) condition increased by about 50% compared to the control group (30 mM bicarbonate). This result is consistent with Delgado's work showing low bicarbonate concentrations stimulating methanogenesis. One possible reason for this phenomenon is that methanogens out-compete homoacetogens in the culture at low bicarbonate concentrations (Delgado *et al*., 2012; Men *et al*., 2013).

Sulfate/sulfide effect

This study demonstrates that sulfide rather than sulfate, poses inhibitory effects on dechlorination and the cell growth of *D. mccartyi*. The cell yield of strain 195 decreased significantly at high sulfide concentrations (5 mM) while TCE was degraded over a longer time period, indicating that *D. mccartyi* decoupled growth from dechlorination when sulfide was introduced into the system at moderate to high concentrations.

Results from the DvH/strain 195 co-culture showed that 5mM sulfate addition can inhibit both dechlorination and growth of strain 195, presumably due to reduction to sulfide. In these co-culture experiments, H_2 concentrations remained well above the hydrogen threshold for dechlorination (2nM, Yang and McCarty, 1998) and at the end of the experiment, sulfate was no longer detected. A previous study showed that 5 mM sulfide could inhibit dechlorination performance in an enrichment culture (Hoelen *et al*., 2004). Although Reis *et al*., 1992 reported the growth of a sulfate-reducing bacterium was inhibited at hydrogen sulfide concentrations of 16.1 mM, in this study with strain DvH, we did not observed cell growth inhibition at 2mM to 5mM sulfide concentrations (data not shown).

The competition for H_2 between *D.mccartyi* and a sulfate reducer under electron donor limitation was investigated in tri-culture *S.wolfei*/195/DvH. We found that when H_2 was steadily provided at levels two orders of magnitude higher than the threshold of dechlorination and sulfate reduction, the dechlorination rate and cell yield of strain 195 was little affected under low sulfate/sulfide concentration (2 mM). The rate of dechlorination was mainly driven by the microbial competition between *D. mccartyi* and DvH for the available H_2 and not by the potential sulfide toxic effects on *D. mccartyi*. When the initial *D. mccartyi* cell numbers were higher than DvH (ratio 5:1 in our study), *D. mccartyi* out-competes for available H_2 even in sulfate-rich environments, and DvH was not able to dominate under limiting-electron donor conditions. This finding is consistent with Panagiotakis study on a butyrate-fed dechlorinating microbial community (Panagiotakis *et al*., 2014). However, various initial biomass ratios should be tested in the future, since in sulfate-rich environments, sulfate reducers may be the dominant species compared to *D. mccartyi*, and capable of outcompeting for H_2.

Different concentrations for sulfate inhibition of dechlorination have been reported in the literature. El Mamouni (2002) reported that 10 mM sulfate addition to soil had no significant effect on TCE reducing activity by indigenous microorganisms while higher sulfate concentrations (15 and 20 mM) yielded slower dechlorination. Heimann (2005) showed 2.5 mM sulfate could limit microbial dechlorination by a mixed anaerobic culture by reducing the hydrogen supply (a few nM H_2). Conversely, sulfate did not affect dechlorination when rapid

fermentation of lactate resulted in accumulation up of hydrogen to levels >100 nM level. Aulenta *et al*., (2008) showed 3.7 mM sulfate addition to an enriched dechlorinating community had detrimental effects on the rate of reductive dechlorination. Our results agree with the above studies and indicate that when sulfate reduction takes place simultaneously with dechlorination, sulfide inhibition occurs.

5.5 Summary

We applied a system-level approach to determine the kinetic parameters involved in reductive dechlorination within constructed syntrophic cultures and a complex enrichment community. The experimental results demonstrated that the kinetic parameters involved in reductive dechlorination are at the same level among different *Dehalococcoides*-containing cultures, and cell growth calculations showed that H_2 was the most sensitive factor to limit the growth of H_2-utilizing microorganisms involved in dechlorinating communities. High concentrations of acetate or decreased concentrations of bicarbonate slow dechlorination performance while high sulfate concentrations in consortia can inhibit dechlorination performance either due to sulfide inhibition or competition for hydrogen.

6 Reactive Kinetic Models Describing Reductive Dechlorination of chlorinated ethenes in microbial communities

6.1 Introduction

Analytical and numerical modeling has long been a valuable tool for planning and designing groundwater remediation systems (Rifai *et al*., 2010). Based on the purpose and environmental settings of dechlorination models, they can be classified into three categories: 1) understanding the fundamental processes that control chlorinated solvent fate and transport; 2) setting up methods to integrate information of site hydrology, geology, contaminant distribution, transport and fate; 3) applying aspects of plume management and remediation system design. Many modeling approaches have applied over the past decades to understand the fundamental processes that control the dechlorination of solvents in the subsurface, (Chambon *et al*., 2013). However, the models developed up to date are insufficient to simulate the complexity of the dechlorination processes under field conditions (Rifai *et al*., 2010). Dechlorination may be limited or constrained by a number of factors, including environmental or biological conditions in subsurface, as discussed in Chapter 2. Therefore, there are a number of challenges associated with applying models for dechlorination: 1) modeling the complex biological reactions involved in microbial dechlorination of chlorinated solvents; 2) understanding and modeling the processes that control remediation of chlorinated solvents; and 3) balancing the complexity of the dechlorination models with the available data to support model development and application (Rifai *et al*., 2010).

It has generally been accepted that reductive dechlorination can be performed as an energy generating process (Rifai *et al*., 2010; Chambon *et al*., 2013). Therefore "Monod" kinetics has been the major form of the mathematical models developed to-date to predict dechlorination (Chambon *et al*., 2013). The major differences in the previous models were formulations used to describe competitive inhibition and self-inhibition Several modeling platforms have been used in previous studies, including STELLA Research (High Performance Systems) and Matlab (Matlab, Inc) (Fennell *et al*., 1998; Yu *et al*., 2005; Becker *et al*., 2006; Haest *et al*., 2010). A summary of the modeling tools, calculation methods, simulation times and time steps applied in the literature has been summarized in Table 6-1.

The primary objective of this study is to understand, model and predict the fundamental processes that control microbial dechlorination of chlorinated solvents. Quantitative models based on Monod kinetics were selected as the basis for the overall model used in this study. There are two broad categories of the model parameters in this study: physicochemical properties of the compounds and system specific kinetic constants. We applied a systematic approach to calculate the Monod kinetic constants by fitting the experimental results of constructed cultures with kinetic expressions (Chapter 5). The kinetic model was then validated using more complicated microbial consortia. Potential inhibitors and competing biological processes that affect dechlorination were introduced and validated in the kinetic models. The obtained set of differential equations was solved in Matlab using a variable order solver based on numerical differentiation formulas. The biological processes that have been considered in the modeling approach are summarized in Figure 6-1. Several assumptions have been made in the modeling process: 1) the self-inhibition of chlorinated solvents in DNAPL zones were not considered in the modeling process; 2) higher chlorinated compounds exert competitive inhibition on lower chlorinated compounds, while lower chlorinated compounds do not inhibit higher chlorinated compounds; 3) competition for H_2 is between *D.mccartyi* strain and the H_2-utilizing sulfate

reducers and/or methanogens; 4) electron donor fermentation, reductive dechlorination, hydrogenotrophic methanogenesis and sulfate reduction can also be described using Monod kinetic models; 5) cell growth can be described by Monod kinetics; 6) the study system is completely mixed and no biofilm is formed; 7) interspecies H_2 transfer is the primary mechanism for electron exchange in the system (formate to H_2 transformation or direct electron transport were not considered in the model); .8) reactants and products are all in equilibrium between gas and liquid phase. Key biological processes are considered and will be expressed in mathematical forms.

Table 6-1 Modeling platforms used for kinetic reductive dechlorination studies

Modeling platform	Calculation method	Time-step	Simulation length	Reference	Study objects
STELLA 4.0	Runge-Kutta 4	0.0005hr	48 hours	Fennell, 1998	Enrichment
N.A.	N.A.	N.A.	25 days	Cupples, 2004	Enrichment
Matlab 5.3	Initial value problem solver	Adjusted[a]	140 days	Lee, 2004	Enrichment
STELLA 5.0	Runge-Kutta 4	N.A.	3-5 days	Yu, 2005	Enrichment
STELLA 8.0	Runge-Kutta 4	0.125 hr	150 days	Becker, 2006	Conceptual co-cultures
MISER	N.A.	N.A.	1500 days	Christ, 2007	Field sites
Matlab	Runge-Kutta 4	N.A.	18 days	Amos, 2007	DNAPL zone
STELLA 8.0	Runge-Kutta 4	0.125 hr	80 hours	Huang, 2009	Pure culture
STELLA 9.0	Runge-Kutta 4	N.A.	75 days	Sabalowsky, 2010	Enrichment
Matlab	AMALGAM	N.A.	160days	Haest, 2010	Enrichment
PHREEQC	CVODE	N.A.	300 days	Kouznetsova, 2010	Simulation only
PHREEQC	SCEM algorithm	N.A.	350 days	Malaguerra, 2011	Groundwater Field sites
N.A.	N.A	N.A	4 hours	Popat, 2011	Biofilm
Matlab	COMSOL	N.A	N.A	Manoli, 2012	Clay
N.A.	N.A	N.A	8 days	Berggren, 2013	CMFR reactor
STELLA	Runge-Kutta 4	N.A	8 days	Heavner, 2013	Reactor

a. Adjusted: the time step for calculation was adjusted to yield the relative tolerance smaller than 10^{-5}.

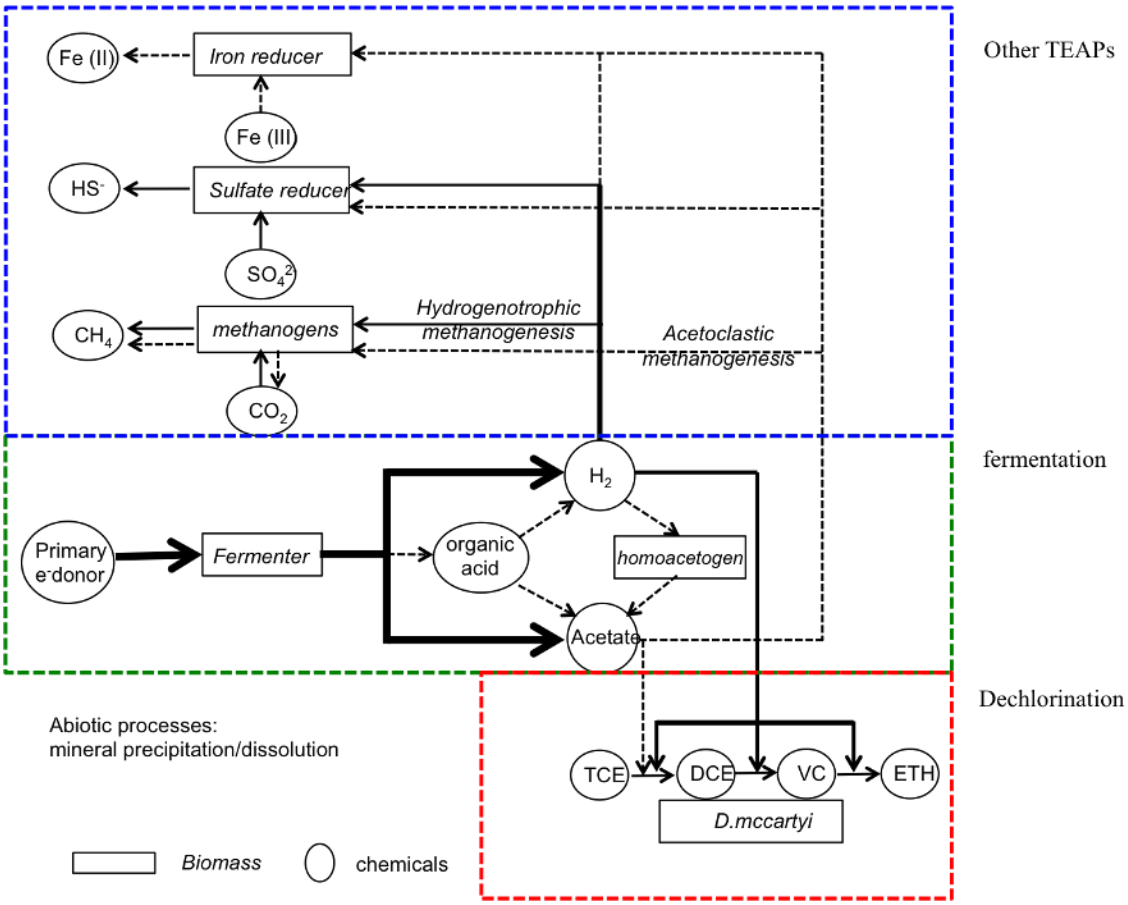

Figure 6-1 Relevant complementary reactions for reductive dechlorination in subsurface. Arrows denoted the reaction directions. Solid black lines indicated the processes that were considered in the kinetic modeling in this study. Dashed black lines indicated other potential redox reactions that have been reported in literature.

6.2 Materials and Methods

6.2.1 Data-set description

The data set was obtained from the laboratory batch studies obtained in Chapter 3, Chapter 4 and Chapter 5. All experiments were conducted in triplicate microcosms as biological replicates.

6.2.2 Modeling approach

A model SRDS (systematic-reductive-dechlorination of solvents), version 1.0 was developed using Matlab Version 2014b (Matlab, Inc) running in a Macintosh environment. The workflow is summarized below in Figure 6-2. Data collected during simulations were transferred to a worksheet in Microsoft Excel 2010 using Publish and Subscribe. After further manipulation of Excel files, graphs were generated including simulation results and experimental data. The backbone of the kinetic model and the separate sectors of the models are summarized in Figure 6-2.

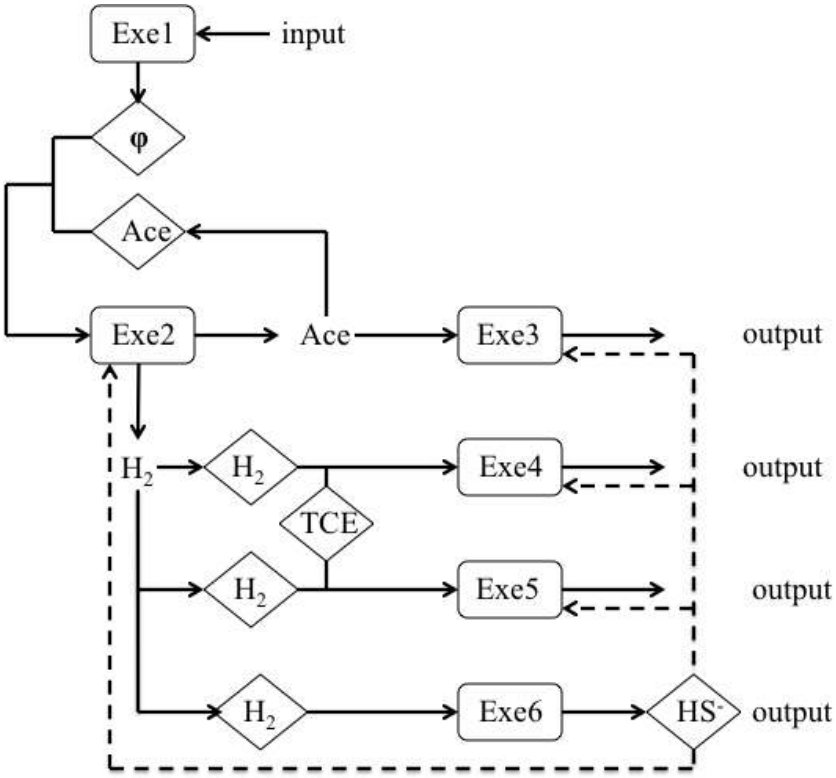

Figure 6-2. Backbone of the kinetic model implemented in Matlab 2014.
(Exe1:Thermodynamic control;Exe2. Fermentation; Exe3. Acetoclastic methanogenesis; Exe4. Hydrogenotrophic methanogenesis; Exe5. Reductive dechlorination. Exe6. Sulfate reduction.)

6.2.3 Model structure and parameters selection

Key biological processes (described in Figure 6-2) are integrated with the following mathematical expressions. (A summary of parameters in the literature and the script of the program are listed in the appendix)

1. *Fermentation*.

H_2 levels during fermentation may differ by orders of magnitude, depending on both the kinetics and thermodynamics of the particular fermentation reactions of each primary electron donor (Schink, 1997). Table 6-2 summarizes frequently used electron donors in previous studies and their standard Gibb's free energy.

Table 6-2 Frequently used electron donors and their standard Gibb's free energy

Type of electron donor	H_2 levels (nM)	$\Delta G^{0'}$ (J/mol)	Reference
Glucose	-	-22,080	Lee *et al*., 2004
Lactate	5-2000	-1,430	Fennell *et al*.,1998; Heimann *et al*., 2007; Malaguerra *et al*., 2011
formate	20-400	13,600	Azizian *et al*., 2010; Lee *et al*., 2007; McCarty, 2007
methanol	-	18,160	Aulenta *et al*., 2005
ethanol	4-1000	10,810	Fennell, 1997
propionate	2-20	76,100	Azizian, 2010; Fennell, 1997; Heimann, 2007
Butyrate	8-60	48,300	Aulenta, 2008; Fennell, 1997
benzoate	2-5	70,600	Yang, 1998
Vegetable oil	-	-	
Acetate	-	94,780	He *et al*., 2005
Biomass	-	-	Yang, 2000; Adamson and Newell, 2009

Butyrate, a slowly fermented electron donor, and lactate, a rapidly fermented electron donor, were both used in this study. A general modified equation developed by Fennell (1998) which includes thermodynamic control of product formation (H_2 and acetate) on fermentation rates, were used to describe the primary donor fermentation process (equation 6.1).

$$\frac{dC_{donor}}{dt} = \frac{-k_{donor} X_{donor} (S - S^*)}{K_{s,\,donor} + S}, \quad (S\text{-}S^*) = S\,\Phi = S\left(1 - e^{\left(\frac{\Delta G_{rxn} - \Delta G_{critical}}{RT}\right)}\right) \tag{6.1}$$

C_{donor} is the concentration of the fermentable substrate in the system (μM), k_{donor} is the maximum specific rate of fermentable substrate degradation (μmol cell^{-1} d^{-1}), $K_{s,donor}$ is the half velocity coefficient for the fermenting substrate (μM), X_{donor} is the biomass fermenting the substrate in the system (cell L^{-1}), S is the concentration of fermenting substrate (μM), S* is the hypothetical concentration of fermenting substrate that, under the instantaneous culture conditions, would result in ΔG_{rxn} (the free energy available from the fermentation) = $\Delta G_{critical}$ (some marginally negative free energy that the organisms must have available to live and grow), given the concentrations of all the other reactants and products at that instant, Φ (phi) is a measure of the distance of the reaction from thermodynamic equilibrium (Fennell *et al*., 1998). If the electron donor concentration is high relative to the concentration of the products of the reaction, the driving force is high, Φ approaches 1 and the fermentation reaction is limited primarily by its intrinsic kinetics. As the reaction approaches equilibrium (i.e., the donor concentration has decreased and H_2 and acetate have increased), the driving force is lessened, the value of Φ approaches zero, and the fermentation is limited primarily by thermodynamics. The thermodynamic factor Φ defined by Fennell and Gossett (Fennell *et al*., 1998) describing how the thermodynamic driving force controls the fermentation rate have been assessed and compared with other energy-based metabolic models for syntrophic cultures (Kleerebezem *et al*., 2000; Jin, 2007; Rodríguez *et al*., 2008; 2009).

2. *Dechlorination kinetics*.

For the constructed syntrophic consortia studied in this research, *D.mccartyi* strain 195 (strain 195) is the only microorganism that carries out all steps of reductive dechlorination from TCE to VC and co-metabolic VC to ETH. A dual-substrate model for dechlorination kinetics (Fennell *et al*., 1998) was adapted and the competitive inhibition of chlorinated compounds was considered in the model (equations 6.2-6.4).

$$-\frac{dC_{L,TCE}}{dt}=\left[\left(\frac{k_{max,TCE}\,X\,C_{TCE}}{K_{s,TCE}+C_{L,TCE}}\right)\right]\left[\frac{(H-H^*)}{(H-H^*)+K_H}\right] \quad (6.2)$$

$$-\frac{dC_{L,cDCE}}{dt}=\left[\left(\frac{k_{max,cDCE}\,X\,C_{L,cDCE}}{K_{s,cDCE}\left(1+\frac{C_{L,TCE}}{K_{i,TCE}}\right)+C_{L,cDCE}}\right)-\left(\frac{k_{max,TCE}\,X\,C_{L,TCE}}{K_{s,TCE}+C_{L,TCE}}\right)\right]\left[\frac{(H-H^*)}{(H-H^*)+K_H}\right] \quad (6.3)$$

$$-\frac{dC_{L,VC}}{dt}=\left[\left(\frac{k_{max,VC}\,X\,C_{L,VC}}{K_{s,VC}\left(1+\frac{C_{L,TCE}}{K_{i,TCE}}+\frac{C_{L,cDCE}}{K_{i,cDCE}}\right)+C_{L,VC}}\right)-\left(\frac{k_{max,cDCE}\,X\,C_{L,cDCE}}{K_{s,cDCE}\left(1+\frac{C_{L,TCE}}{K_{i,TCE}}\right)+C_{L,cDCE}}\right)\right]\left[\frac{(H-H^*)}{(H-H^*)+K_H}\right] \quad (6.4)$$

X is the concentration of strain 195 in the system (cells L^{-1}) and the other parameters have been described above. H^* is the threshold value for H_2 used by strain 195 (experimentally determined in Chapter 3 and compared to reported data (Fennell *et al*., 1998; Yang and McCarty, 1998; Cupples *et al*., 2004)). Other kinetic coefficients were determined in Chapter 5 by modifying protocols from previous studies (Yu *et al*., 2005; Duhamel *et al*., 2007; Sabalowsky *et al*., 2010). For the co-culture DVH/strain 195, the term accounting for the dependence of H_2 concentration in the dual-substrate model should be close to 1 since reductive dechlorination reactions occur under unlimited electron donor concentration while it should be much lower for the *S. wolfei* /strain 195 culture that is expected to be electron donor limited.

3. <u>*Competition for hydrogen in non-chlorinated TEAPs*</u>.

Two non-chlorinated TEAPs that may compete for H_2 were considered in this version of the model, i.e., methanogenesis and sulfate reduction in the tri-cultures and sulfate reduction in the co-culture DVH/strain 195 (equations 6.5-6.6).

$$\left(\frac{dC_{CH_4 from\ H_2}}{dt}\right)_{production}=\frac{1}{4}k_{(H_2)meth}\,X_{hydrogenotroph}\left[\frac{(H-H^*_{meth})}{K_{H,meth}+(H-H^*_{meth})}\right] \quad (6.5)$$

$$\left(\frac{dC_{H_2S from\ H_2}}{dt}\right)_{production}=\frac{1}{4}k_{(H_2)H_2S}\,X_{sulfate\text{-}reducing}\left[\frac{(H-H^*_{sulf})}{K_{H,sulf}+(H-H^*_{sulf})}\right] \quad (6.6)$$

$C_{CH4fromH2}$ is the concentration of CH_4 produced by hydrogenotrophic methanogens (μM); $k_{(H2)meth}$ is the maximum rate of H_2 utilization by methanogens (μmol $cell^{-1}\cdot d^{-1}$), $X_{hydrogenotroph}$ is the biomass concentration of hydrogenotrophic methanogens (cell L^{-1}), $K_{H,meth}$ is the half-velocity coefficient for H_2 use by hydrogenotrophic methanogens (μM); and H^*_{meth} is the threshold value for H_2 use by hydrogenotrophic methanogens (μM). Similar parameters in equation (6.6) are for the sulfate-reducing process. $C_{H2SfromH2}$ is the concentration of H_2S produced by sulfate-reducing bacteria (μM). Each model equation written above was used to characterize the specific biological process in the system and to demonstrate the full complexity of the system. The sensitivity of parameters (kinetic coefficients) will be qualitatively checked before carrying out kinetic studies as described by Malaguerra *et al* (2011).

4. *Biomass production (growth and decay).*

Strain 195 gains energy from reductive dechlorination of TCE to cDCE and cDCE to VC whereas the reduction of VC to ethene is cometabolic (equation 6.7) (Cupples *et al*., 2004).

$$\frac{dX}{dt}=\mu X\left(\frac{C_{L,TCE}}{K_{s,TCE}+C_{L,TCE}}+\frac{C_{L,cDCE}}{K_{s,cDCE}\left(1+\frac{C_{L,TCE}}{K_{i,TCE}}\right)+C_{L,cDCE}}\right)\left[\frac{(H-H^*)}{(H-H^*)+K_H}\right]-bX \quad (6.7)$$

X is the concentration of Dhc 195 in the system (cells L^{-1}), μ is the maximum growth rate (d^{-1}), and b is the endogenous cell decay coefficient (d^{-1}). Cell concentrations of Dhc 195 are determined using qPCR targeting the reductive dehalogenase gene *tceA*. Reported b values for anaerobic cultures have ranged from 0.024 to 0.05 d^{-1} for active cells, and 0.09 d^{-1} during non-growth conditions (Sabalowsky *et al*., 2010).

5. *Temperature correction*

The temperature range of the model calibration is from 283K~308K (10°C~35°C), which is in the range of naturally occurring environmental and laboratory incubation temperatures. Therefore, there is a need to correct Henry's Law constants for chlorinated solvents and relevant gases in the system. Equation 6.8 was used for correction of Henry's Law constants for chlorinated solvents (Gossett 1987)

$$H_{cc}=\frac{12.2}{T}\times exp\left(A-\frac{B}{T}\right) \quad (6.8)$$

Table 6-3 Temperature Regressions for Henry's Law Constants of Chlorinated Solvents

	A	B
TCE	11.37	4780
DCE	8.479	4192
VC	7.385	3286

- Values are obtained from Gossett, 1987.

According to R. Sander (1999), Henry's law constant unit conversion equations

$$H=\frac{1}{k_H} \quad (6.9)$$

$$T\times k_H=12.2\times k_H^{cc} \quad (6.10)$$

$$k_H^{cc}=\frac{1}{H_{cc}} \quad (6.11)$$

6. *Ionic strength effect*

Ionic strength was calculated based on the medium composition (BAV1 medium was used in this study). The activity coefficient f was calculated by using the equation of Debye and Hückel (1923). The activity coefficient (for charged species) was calculated using equation 6.12. The ionic strength was calculated based on the medium composition (Table 6-4) f=0.786.

Table 6-4. Composition of the medium used in this study

Compound	Concentration (M)	Zi	Ci×Zi ^{2}
Na^+	4.75×10^{-2}	1	4.75×10^{-2}
NH_4^+	5.61×10^{-3}	1	5.61×10^{-3}
K^+	5.49×10^{-3}	1	5.49×10^{-3}
Mg^{2+}	2.46×10^{-3}	2	9.84×10^{-3}
Ca^{2+}	1.02×10^{-4}	2	4.08×10^{-4}
Cl^-	3.19×10^{-2}	1	3.19×10^{-2}
$H_2PO_4^-$	1.47×10^{-3}	1	1.47×10^{-3}
S^{2-}	2.00×10^{-4}	2	8.00×10^{-4}
HCO3-	3.00×10^{-2}	1	3.00×10^{-2}
	Ionic strength	I	6.65×10^{-2}

$$logf_z = \frac{-0.51z^2\sqrt{I}}{1+\sqrt{I}} \tag{6.12}$$

For non-charged species H_2, activity coefficient f' is calculated according to equation 6.13 (Gossett, 1987) with the salting out coefficient b=0.102. The activity coefficient f' (γ_0) in equation 6.13) for H_2 was 1.02.

$$log_{10}(\gamma_0) = bI \tag{6.13}$$

Modeling description and calibration contains a listing of equations implemented in Matlab. The equations implemented to the model are summarized in the Appendix.

6.2 Results

6.3.1 Model simulation for syntrophic co-cultures with slow/fast fermenting substrates

The model simulation of the syntrophic co-culture *S.wolfei*/strain 195 is summarized in Figure 6-3. Kinetic parameters for dechlorination and electron donor kinetics were fitted to the experimental data. In general, the simulation was able to capture the overall dynamic behavior of the co-culture very well. Reductive dechlorination of TCE and slower formation of VC and ethene were accurately simulated compared with the observed values (Figure 6-3 C). From the model simulation, it was clear that TCE dechlorination (from day 0 to day 8) was governed by both kinetics and thermodynamics since the thermodynamic factor phi dropped below 1 after day 4 and reached zero on day 6.7. The simulation result was similar to the value calculated based on thermodynamics in Chapter 3 (Figure 6-3 A). The phi value increased slightly and dropped back to zero between day 8 and 12. This was due to the assumption in the simulation that cell decay would contribute to H_2 generation in the form of a slow fermenting substrate. In addition, the model simulation fit the data of electron donor degradation and acetate formation reasonably well. The simulation result for strain 195 growth fell in the same order of magnitude as the experimental observation. The kinetic parameters obtained for the simulation are summarized in table 6-5.

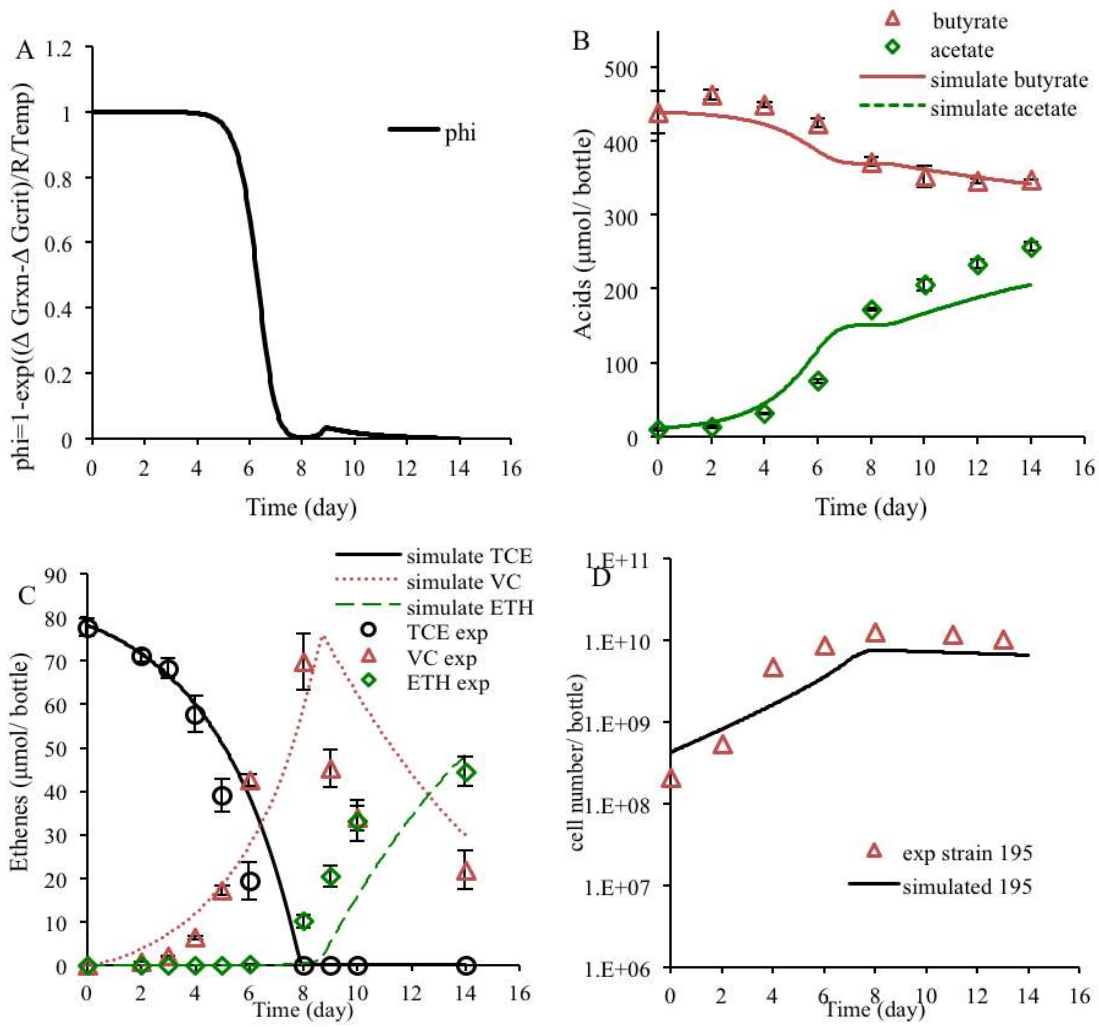

Figure 6-3 comparison of experimental observation (data points) of co-culture *S.wolfei*/strain 195 with model simulation. (solid/dash lines) A) thermodynamic factor phi; B) volatile fatty acids; C) dechlorination; D) cell growth of strain 195. Experimental data are from Chapter 3.

In order to validate the kinetic parameters calculated for co-culture *S.wolfei*/strain 195, we applied the same parameters to fit experimental data for the co-culture at various donor/acceptor ratios. In experimental bottles, 2 mM butyrate was fed as electron donor, and different TCE concentrations were added. The simulation of reductive dechlorination and organic acid changes are summarized in Figure 6-4. The simulation fit reasonably well for TCE dechlorination (Figure 6-4 A) and ethene production (Figure 6-4D) at different TCE concentrations. The simulation of *cis*-DCE production and consumption was slower than experimental observation under all conditions (Figure 6-4D), while the simulation of VC production and consumption fit the experimental data well at low TCE and medium TCE condition (Figure 6-4 C), but VC was predicted to disappear more rapidly than was actually observed at high TCE condition. By applying the same kinetic parameters for electron donor, we found the prediction of donor consumption and acetate formation fit the experimental data well under the medium TCE condition. However, faster dechlorination with low TCE and slower dechlorination with high TCE were predicted compared to experimental results (Figure 6-4 E, F).

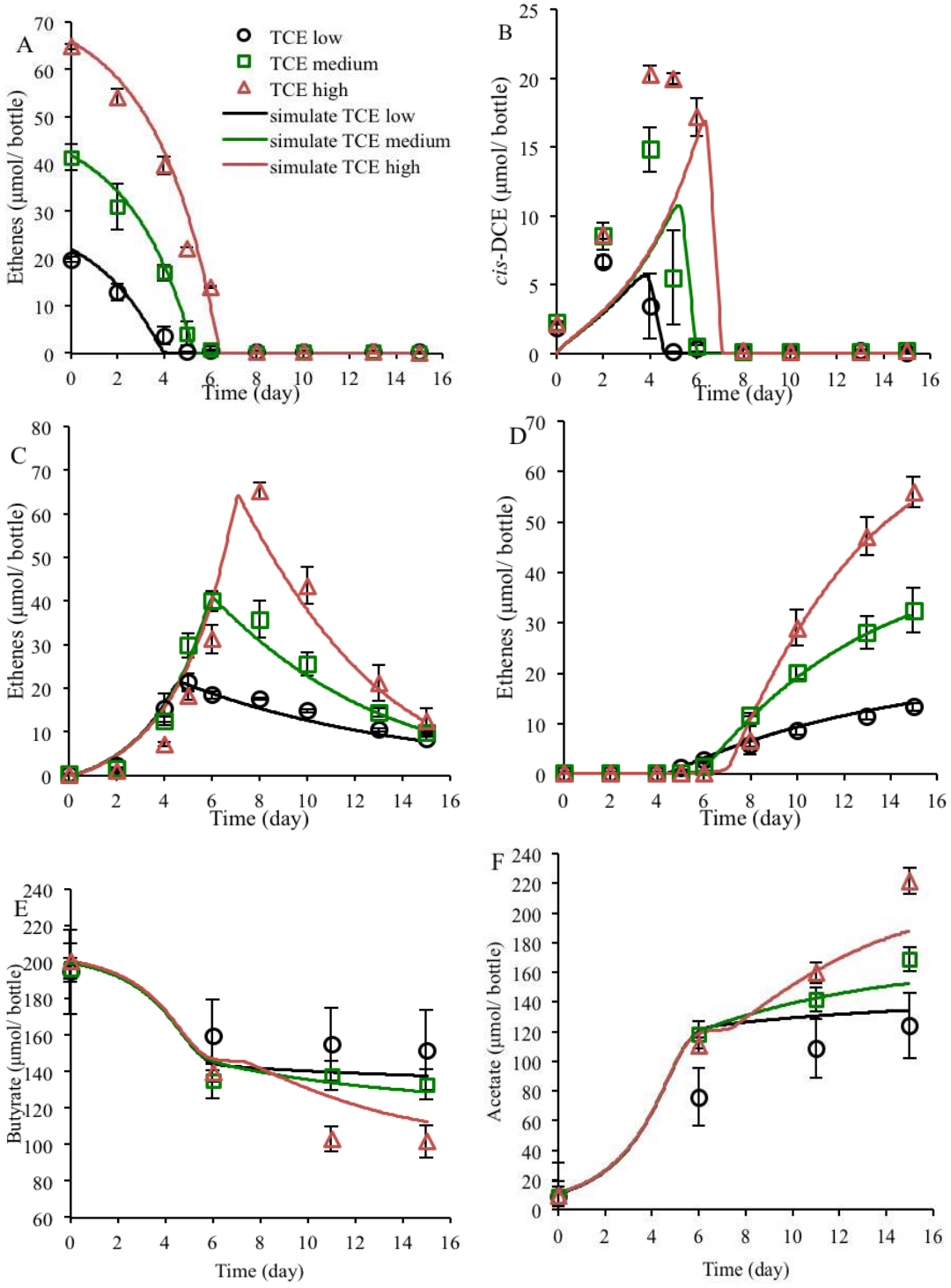

Figure 6-4 Comparison of experimental observations of co-culture *S.wolfei*/strain 195 with model simulations under different donor to accepter ratios. A) TCE; B) *cis*-DCE; C) VC; D) ethene; E) butyrate; F) acetate.

The developed model was further used to simulate the dechlorination performance of syntrophic co-culture DvH/strain 195 growing on lactate. The same kinetic parameters for dechlorination were adopted and the electron donor kinetics was re-calculated by changing the

structure of EXE1 and EXE2 due to the different substrate fermentation pathway. The simulation result is summarized in Figure 6-5. The kinetic parameters obtained for the simulation are summarized in table 6-5.

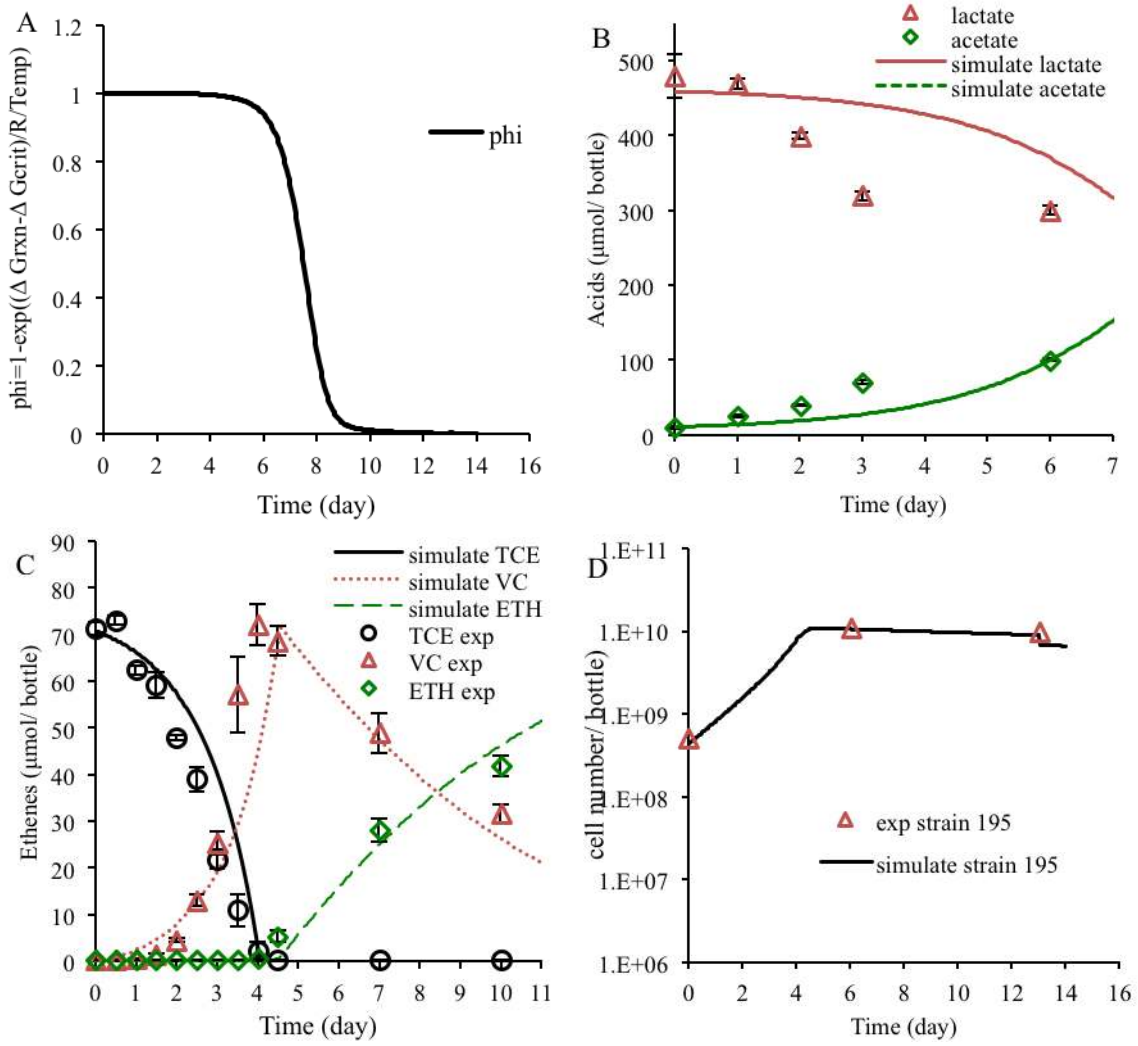

Figure 6-5 Comparison of experimental observations of co-culture DvH/strain 195 with model simulations: A) thermodynamic factor phi; B) volatile fatty acids; C) dechlorination; D) cell growth of strain 195.

In general, the simulation captured the overall dynamic behavior of the co-culture very well. Reductive TCE dechlorination and ethene production were accurately predicted according to observations (Figure 6-5 C). Since the thermodynamic factor phi was maintained between 0.99 and 1 for the co-culture DvH/strain 195 between day 0 and day 5, it was clear that TCE dechlorination during that time was governed solely by kinetics rather than thermodynamics (Figure 6-5 A). In addition, the model prediction fit the trend of acetate formation reasonably well, while the predicted donor degradation rate was slower than experimentally observed (Figure 6-5 B). The prediction of strain 195 growth over time agreed very well with the experimental observations (Figure 6-5 D).

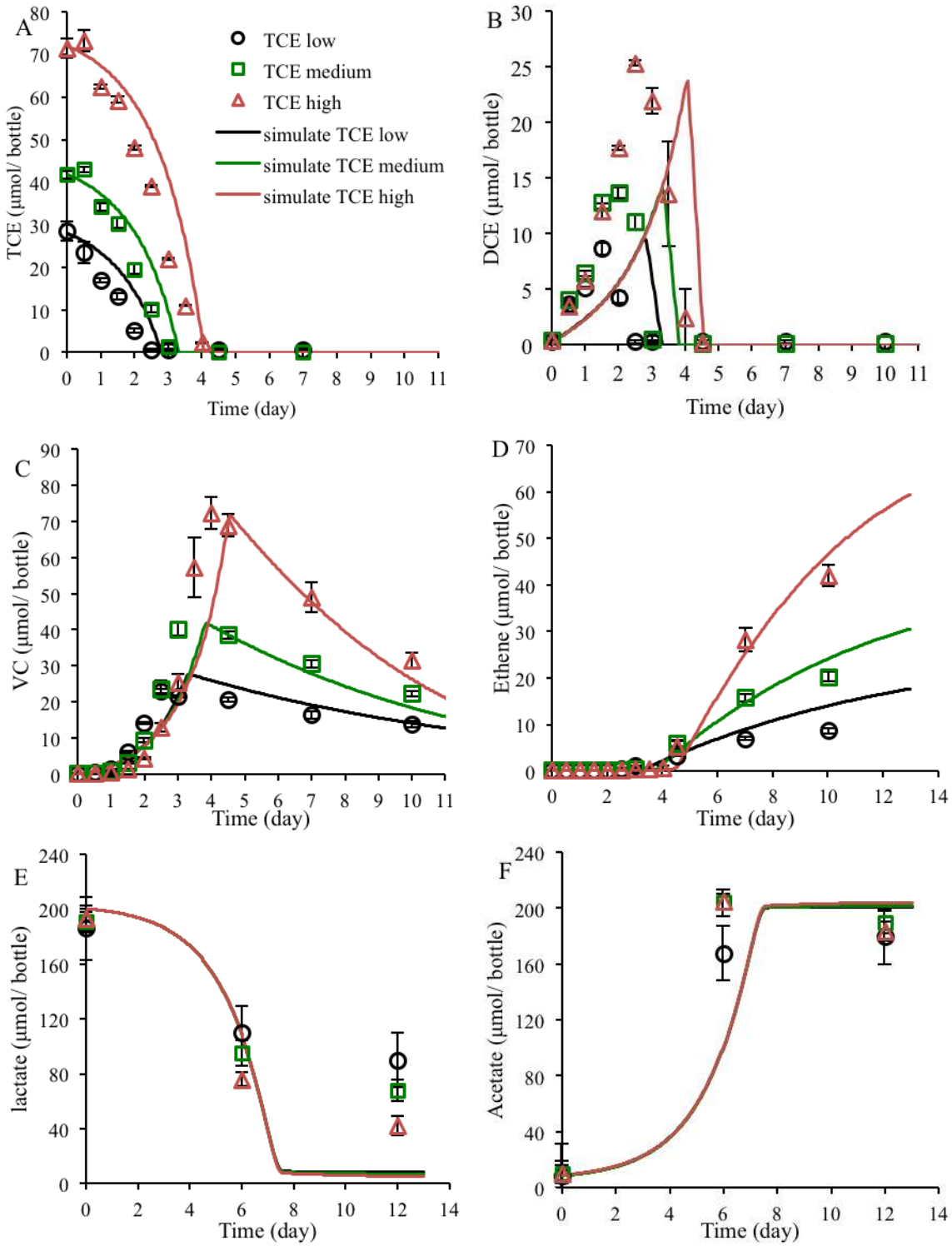

Figure 6-6 Comparison of experimental observation of co-culture DvH/strain 195 with model simulation at different donor to accepter ratios: A) TCE; B) *cis*-DCE; C) VC; D) ethene; E) lactate; F) acetate.

In order to validate the calculated co-culture model parameters, we applied them at different donor/acceptor ratios. The result is summarized in Figure 6-6. In experimental bottles, 2

mM lacate was fed as electron donor with different TCE concentrations (Figure 6-6). Model predictions for TCE dechlorination, *cis*-DCE production and consumption, VC production and consumption were slower than experimentally observed at all conditions (Figure 6.6 A-C), while the prediction of ethene production followed the experimental observation under all conditions very well (Figure 6-6 D). By applying the kinetic parameters of lactate as electron donor, the prediction of donor consumption and acetate formation was similar at all TCE concentrations with slight differences at the end of the simulation. Predicted acetate formation matched experimental values reasonably well, while the predictions of donor degradations were greater than those observed in the experiments (Figure 6-6 E, F).

6.3.2 Model simulations considering competitive TEAPs

When considering other TEAPs that use H_2 as electron donor, it is difficult to distinguish the input H_2 value among different reactions, since they all occur simultaneously. Therefore we modified the model to introduce the term deltat' instead of the old term deltat. Basically, in the simulation process, we divided each deltat (0.04 day, i.e. 1 hour) to even smaller step (100 steps), for this new denoted deltat' (~6 mins), we assumed each TEAP uses the same amount of H_2 as the input, after model calculation for each deltat', the output H_2 became the input for the next deltat'.

We first applied the modified model to predict the dechlorination performance and methane production in two constructed syntrophic tri-cultures: *S.wolfei*/195/MC and DvH/ 195/MC (Figure 6-7 and table 6-5). The kinetic paramters determined in the co-culture study were applied in the tri-culture predictions. The model simulation fit the experimental observation of reductive dechlorination very well in both tri-cultures (Figure 6-7 A. B). For tri-culture *S.wolfei*/195/MC, the prediction of VC production and methane production were slightly slower than the experimental observations, while TCE dechlorination, butyrate fermentation and acetate formation matched the experimental observations (Figure 6-7 A and C). In tri-culture DvH/195/MC, the prediction of reductive dechlorination and methanogenesis fit the experimental observations well while the lactate fermentation was slower than predicted by the simulation (Figure 6-7 D).

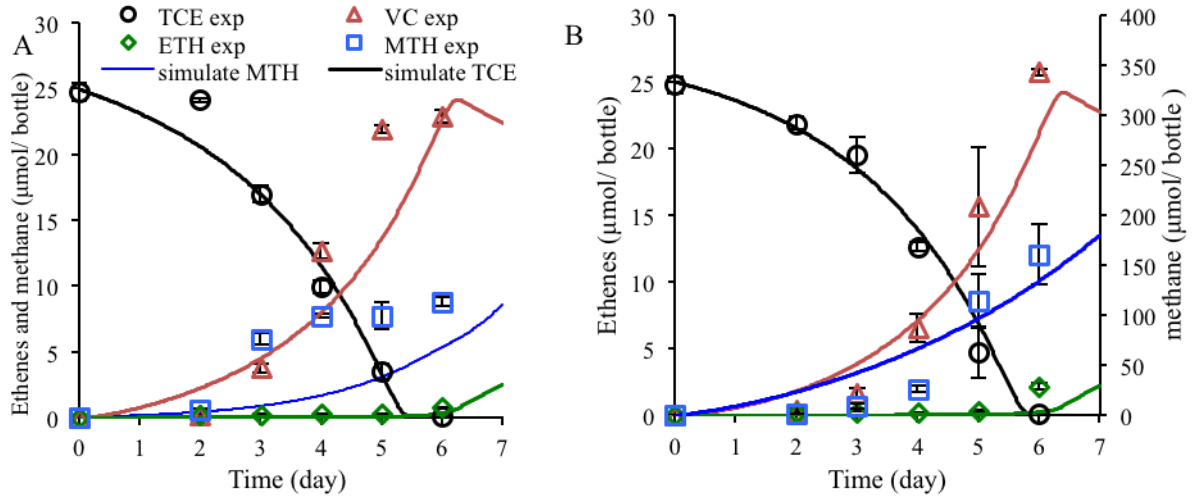

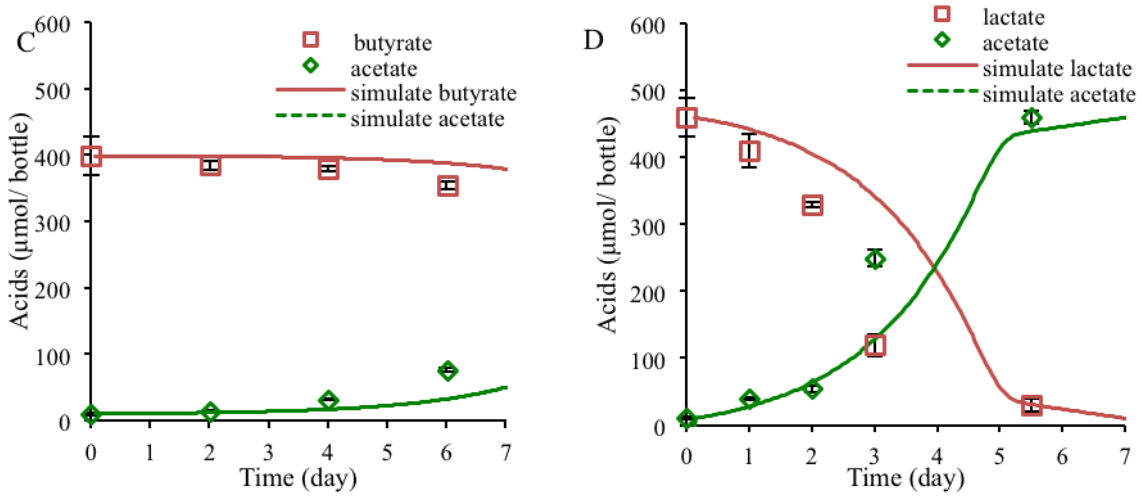

Figure 6-7 Comparison of experimental observations with model simulations of tri-culture *S.wolfei*/195/MC A) dechlorination, C) organic acids formation, and tri-culture DvH/195/MC, B) dechlorination and D) organic acids formation.

The kinetic model was further validated with multiple additions of electron donor/acceptor using enrichment community LoTCEB12. It is more challenging to simulate enrichment cultures due to the complex community structure, especially with other H_2 consuming groups present in the community. The abundance and specific substrate utilization rates are difficult to determine. Here we made an assumption that H_2 was present in sufficient quantities (>50 nM) that it was not a limiting factor for reductive dechlorination and methanogenesis. However, thermodynamic controls should still be applicable for the microbial community. Kinetic parameters were calculated to fit the experimental data, and the simulation results are summarized in Figure 6-8 and Table 6-5. Overall, the model simulation captured the overall dynamic behavior of the enrichment culture very well except, with the exception of the prediction for slower ethene production. It is possibly due to an assumption that the VC to ETH step was cometabolic.

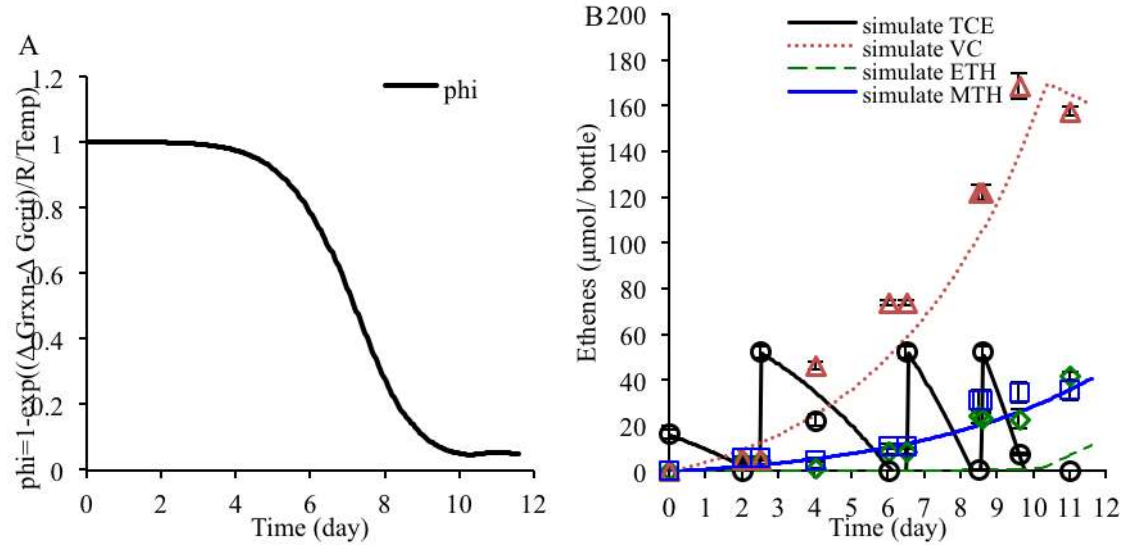

Figure 6-8 Comparison of experimental observation of enrichment culture LoTCEB12 with model simulation. A) thermodynamic factor; B) dechlorination. Experimental data are derived from Chapter 5.

Table 6-5 A summary of kinetic parameters applied in the simulations[a]

	S. wolfei/ strain 195	*S.wolfei*/195/MC	DvH/strain 195	DvH/195/MC	LoTCEB12 enrichment
k_{donor}[b]	1×10^{-8}	2×10^{-8}	4×10^{-8}	8×10^{-8}	8×10^{-8}
k_{TCE}	6×10^{-9}	6×10^{-9}	6×10^{-9}	6×10^{-9}	5×10^{-9}
k_{DCE}	9×10^{-9}	9×10^{-9}	9×10^{-9}	9×10^{-9}	9×10^{-9}
k_{VC}	3×10^{-9}	3×10^{-9}	3×10^{-9}	3×10^{-9}	1×10^{-9}
k_{hmth}	-	3.3×10^{-7}	-	2.5×10^{-7}	4×10^{-8}
K_{donor}[c]	30	30	30	30	30
K_{TCE}	6	6	6	6	6
K_{DCE}	6	6	6	6	6
K_{VC}	290	290	290	290	290
K_{hmth}	0.5	0.5	-	0.5	0.5
μ_{ferm}[d]	0.62	0.62	0.62	0.62	0.3
μ_{dhc}	0.4	0.4	0.4	0.4	0.4
μ_{hmeth}	-	0.8	-	0.8	0.9

a. Endogenous decay factors (k_d) were assumed to be the values as indicated in the materials and methods part.
b. unit: μmol cell^{-1} day^{-1}
c. unit: μM
d. unit: day^{-1}

6.3.3 Sensitivity check of environmental parameters

Bicarbonate

For *D. mccartyi* strain 195 (strain 195), decreasing the bicarbonate concentrations adversely affected dechlorination performance with a significant decrease of k_{TCE} (Figure 6-9 A). When the bicarbonate concentration in the medium was decreased from 30 mM to 5 mM and 1mM, the k_{TCE} value decreased from 6×10^{-9} μmol cell^{-1} day^{-1} to 2.5×10^{-9} μmol cell^{-1} day^{-1} and 1×10^{-9} μmol cell^{-1} day^{-1}, respectively. While methanogentic tri-cultures and an enrichment community were tested, the effect of decreased bicarbonate concentration (1 mM) was not as significant as with the isolate. In tri-culture *S.wolfei*/195/MC, k_{TCE} decreased to 1×10^{-9} μmol cell^{-1} day^{-1}, which was the same as that in strain 195 (6.9 B), k_{DCE} also decreased from 9×10^{-9} μmol cell^{-1} day^{-1} to 8.2×10^{-10} μmol cell^{-1} day^{-1}. Low bicarbonate decreased the methane production, and the calculated k_{hmth} decreased from 3.3×10^{-7} μmol cell^{-1} day^{-1} to 2.0×10^{-8} μmol cell^{-1} day^{-1}. In tri-culture DvH/195/MC, k_{TCE} decreased to 3×10^{-9} μmol cell^{-1} day^{-1}, which was higher than that in strain 195 (Figure 6-9 D), k_{DCE} decreased from 9×10^{-9} μmol cell^{-1} day^{-1} to 3×10^{-9} μmol cell^{-1} day^{-1} and methane production was unaffected.

Bicarbonate concentrations played no role in the calculation of thermodynamic factor phi in tri-culture *S.wolfei*/195/MC when butyrate was used as the electron donor. However in lactate-

fed tri-culture DvH/195/MC, bicarbonate was involved in the phi calculation. If we fixed other kinetic parameters and initial inputs to be constant, the slope of simulated phi changed when lowering bicarbonate concentration from 30 mM to 1mM (Figure 6-9 C), indicating that as bicarbonate concentrations decrease the thermodynamics of the fermentation process remain positive for slightly longer compared to the higher bicarbonate concentrations.

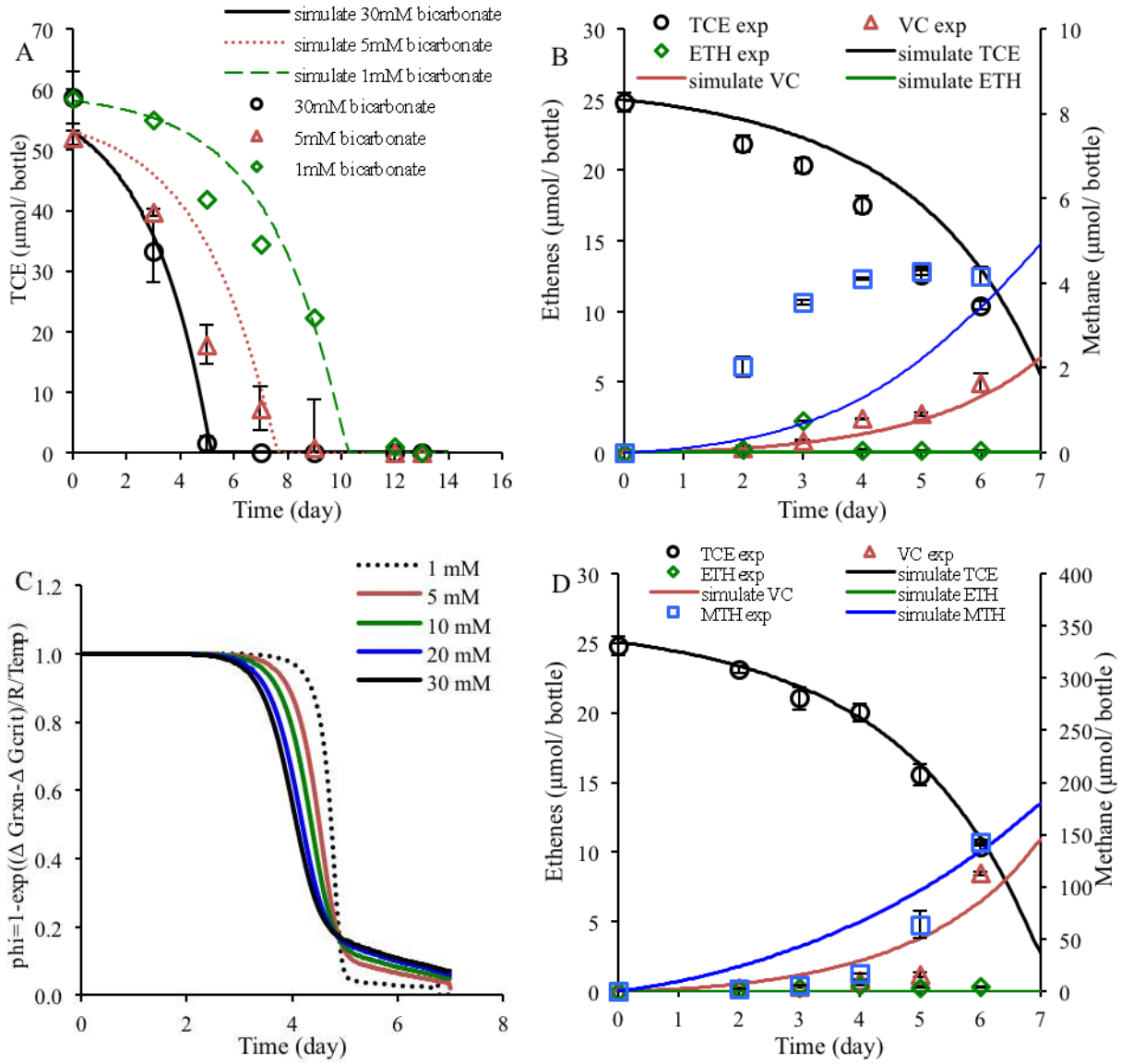

Figure 6-9 Comparison of experimental observations with model simulations of bicarbonate effect on cultures A) pure strain 195; B) *S.wolfei*/195/MC; D) DvH/195/MC; C) thermodynamic control factor changes in DvH/195/MC at different bicarbonate concentrations.

Acetate

The model was used to simulate reductive dechlorination in co-culture *S.wolfei*/strain 195 with various acetate amendments (Figure 6-10 A). The simulation results fit the experimental

observations reasonably well with decreased kinetic parameters of k_{donor}. The calculated k_{donor} values decreased from 2×10^{-8} μmol cell^{-1} day^{-1} (control) to 1×10^{-9} μmol cell^{-1} day^{-1} (5 mM), 5×10^{-10} μmol cell^{-1} day^{-1} (10 mM), and 3×10^{-10} μmol cell^{-1} day^{-1} (25 mM). Unsurprisingly, μ_{ferm} decreased correspondingly with k_{donor} since cell growth is a function of substrate utilization rate ($\mu=k\times Y$, Rittman *et al.*, 2001). In co-culture *S.wolfei*/strain 195, thermodynamic factor phi remained above 0 throughout the experiment (data not shown), indicating thermodynamic control was not the reason that reductive dechlorination ceased. The biomass production for strain 195 was similar to experimental observations (table 6-7) and the cell growth was proportional to TCE degradation. The results for 20 mM and 40 mM acetate amendments were similar. We then applied the k_{donor} value (3×10^{-10} μmol cell^{-1} day^{-1}) at 25 mM acetate to tri-culture *S.wolfei*/strain 195/MC while keeping the other kinetic parameters constant. The model prediction fit the experimental results very well (Figure 6-10 B).

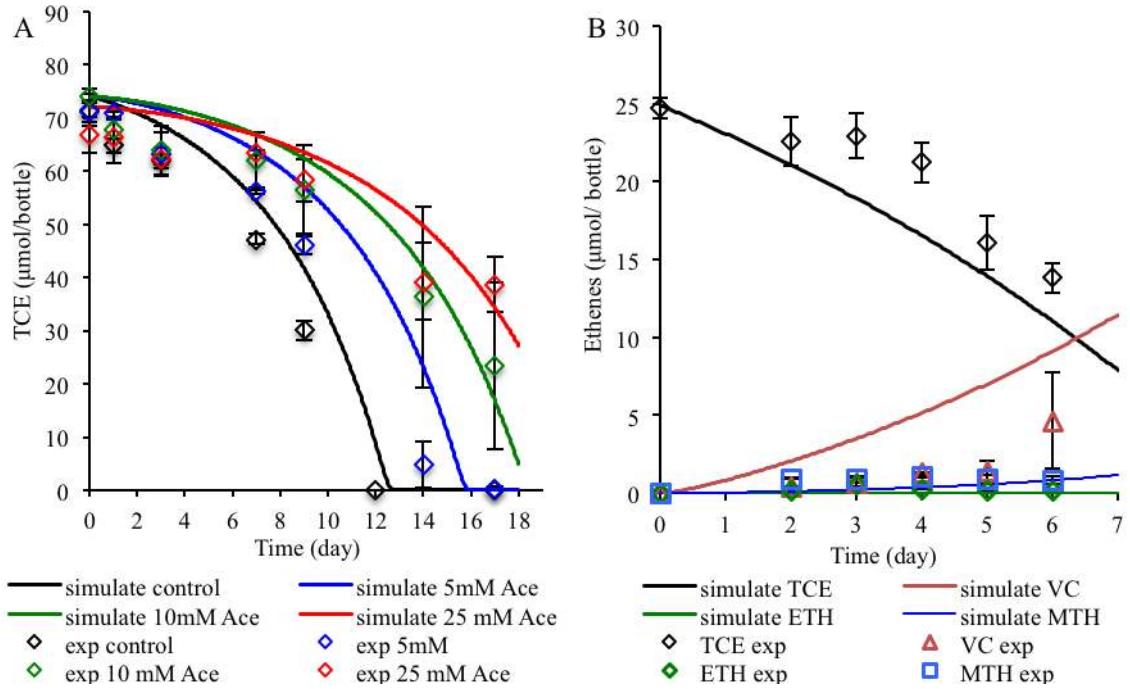

Figure 6-10 Comparison of experimental observations with model simulations of acetate effect on A) co-culture *S. wolfei*/strain 195 on various acetate concentrations, B*)* tri-culture *S. wolfei*/195/MC growing on butyrate with 20 mM acetate amendment.

Ionic strength

Enzyme reactions are known to be a function of temperature and substrate concentration, and can also be affected by pH. In this study, experiments were performed using a bicarbonate-TES dual buffer solution to stabilize the pH. In the derived model, ionic strength factors (f and f') were applied in the calculation of themodynamic factor phi (equation 6-14 and 6-15). We evaluated the ionic strength change effect on the themodynamic factor calculation and compared the results with different microbial media (lab/ nature) (Table 6-6). The model predicted minimal affects due to the small changes in ΔG_{rxn}.

$$\Phi = S\left(1 - e^{\left(\frac{\Delta G_{rxn} - \Delta G_{critical}}{RT}\right)}\right) \quad (6\text{-}14)$$

$$\Delta G_{rxn} = \Delta G_{pH} + R\times T\times Log\frac{(C_{ace}\times f)^2\times(P_{H_2}\times f')^2}{[H_2O](C_{buty}\times f)} \quad (6\text{-}15)$$

$$= \Delta G_{pH} + R\times T\times Log\frac{{C_{ace}}^2\times {P_{H_2}}^2}{[H_2O]C_{buty}} + R\times T\times Log(f\times f'^2)$$

Table 6-6 Effect of ionic strength on themodynamic factor calculation

Medium	I	f	f'	$R\times T\times Log(f\times f'^2)$ [a]	Reference
BAV1	0.067	0.786	1.02	-0.23	He *et al*., 2003
"Bomb"	0.076	0.78	1.02	-0.24	Richardson *et al*., 2002
Groundwater	0.01	0.90	1.00	-0.11	Saleh *et al*., 2008
Seawater	0.72	0.58	1.18	-0.22	Haynes, 2014

a. unit: kJ mol^{-1}

Decay coefficient

We also used the model to evaluate the effects of different endogenous decay coefficients ($k_{d,Dhc}$) on reductive dechlorination and *D. mccartyi* cell growth. The range of $k_{d,Dhc}$ reported in the literature is 0.003~0.09 day^{-1} (Cupples *et al*., 2003; Yu *et al*., 2004; Haest *et al*., 2010). Therefore, we predicted the reductive dechlorination performance and strain 195 growth at the highest and lowest reported decay rate 0.003 day^{-1} and 0.09 day^{-1}, respectively. The simulation results were compared to the original simulation ($k_{d,Dhc}$ =0.024 day^{-1}) and the experimental results. An example of the comparison in co-culture *S.wolfei*/strain 195 is summarized in Figure 6-11.

The TCE dechlorination rate and cell growth were minimally affected by changes (up to 30x) in $k_{d,Dhc}$ values (Figure 6-11 A). However the VC and ethene formation predictions fit the experimental data best when $k_{d,Dhc}$ = 0.09 day^{-1} (Figure 6-11 B, C), and the cell production prediction fit the experimental data best when $k_{d,Dhc}$ =0.003 day^{-1} (Figure 6-11 D).

We also varied the decay coefficient for methanogens ($k_{d,meth}$) from 0.007 day^{-1} to 0.085 day^{-1} (Clapp *et al*., 2004; Karadagli and Rittman, 2005). The model prediction did not show much difference in the methane production when butyrate was used as the electron donor in tri-culture *S.wolfei*/strain 195/MC (Figure 6-11 E). When lactate was used as the electron donor in tri-culture DvH/strain 195/MC, when $k_{d,meth}$ increased three times to 0.085 day^{-1}, the methane production reduced by 22% at the end compared to the result when $k_{d,meth}$ =0.024 day^{-1}.

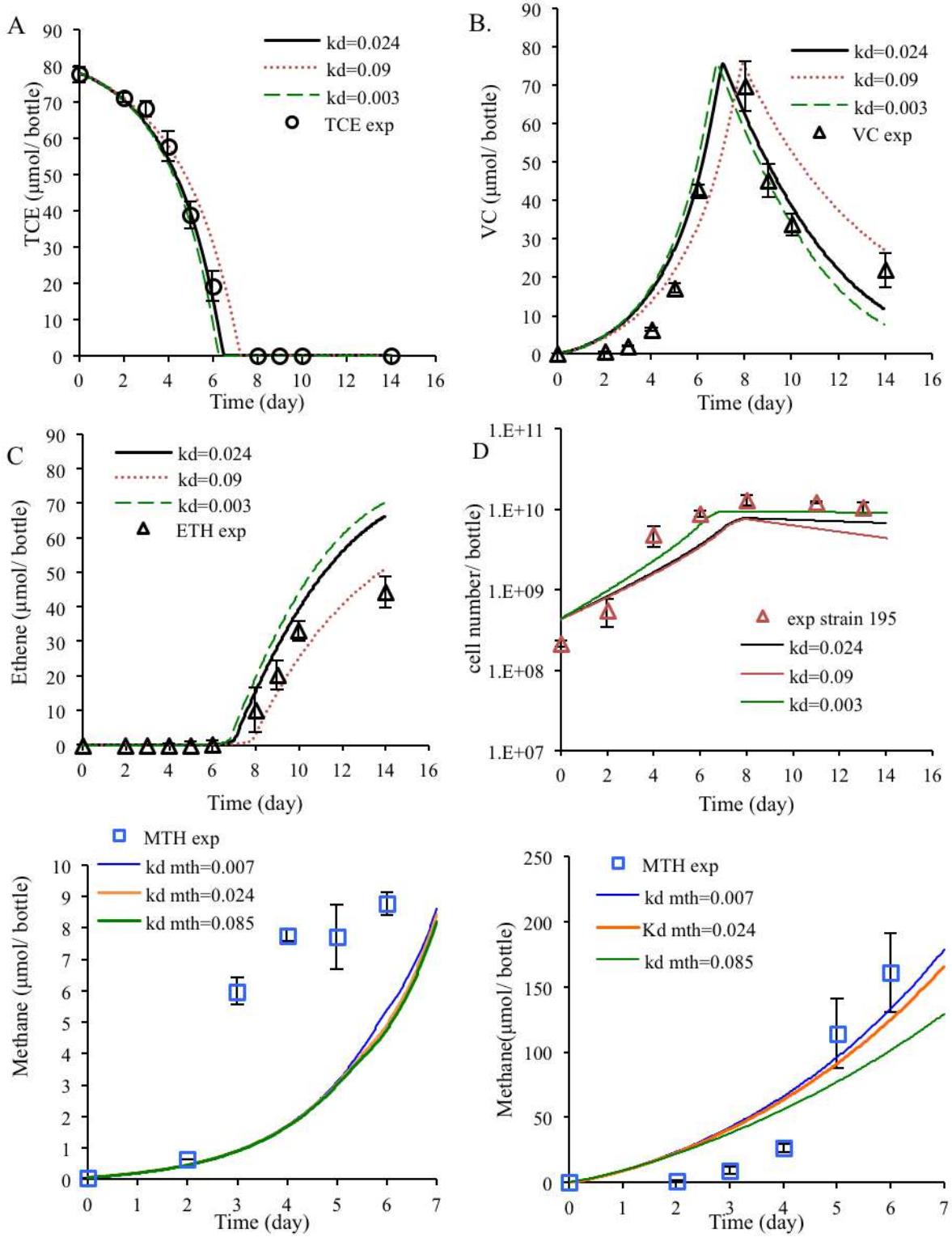

Figure 6-11 Comparison of experimental observations with model simulations of various endogenous decay coefficients effect on A) TCE degradation; B) VC formation; C) ethene formation; D) strain 195 cell number in co-culture *S.wolfei*/strain 195. E) methane production in *S.wolfei*/195/MC; F) methane production in DvH/195/MC.

Half velocity constant

Based on the model, the change of $K_{S,VC}$ should only affect the extent of ethene production while the change of $K_{S,TCE}$ and $K_{S,DCE}$ should affect the formation rate of all daughter products. In the literature, $K_{S,TCE}$ and $K_{S,DCE}$ values are in the range of 0.08~23.4 μM and 0.54 ~ 6.9 μM, respectively (Amos *et al*., 2007; Malaguerra *et al*., 2011). While in our experimentals, $K_{S,TCE}$ and $K_{S,DCE}$ values were determined to be in the range of 6.2~14.5 μM and 2.6~10.0 μM (Chapter 5), respectively. In the model, we applied the highest and lowest reported half velocities to predict reductive dechlorination, and the results were compared to the simulations using experimental determined half velocities (Figure 6-12).

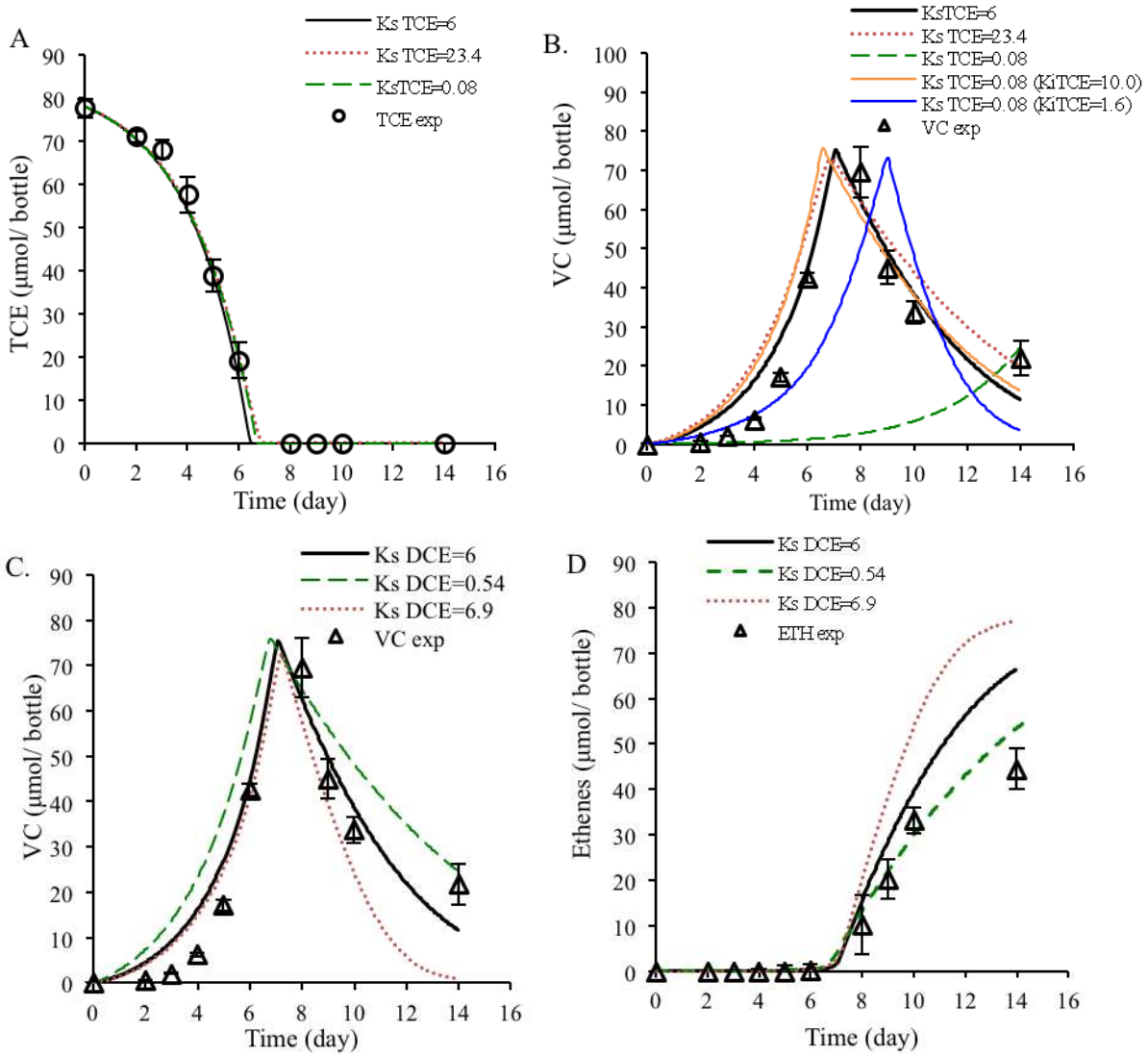

Figure 6-12 Comparison of experimental observations with model simulations of changing $K_{S,TCE}$ ($K_{S,DCE}$ =6 μM, fixed) on A) TCE degradation; B) VC formation, and $K_{S,DCE}$ ($K_{S,TCE}$ =6 μM, fixed) on C) VC formation; D) ethene production in co-culture *S.wolfei*/strain 195.

When $K_{S,TCE}$ changed from 0.08 to 23.4 μM (other parameters were kept constant), no difference was observed in TCE degradation (Figure 6-12 A). Inhibition from lower chlorinated solvents on TCE degradation wasn't considered, thus the K_i term was not involved in the

equation and the TCE concentrations were much higher than the reported K_S values. When $K_{S,TCE}$ increased to 23.4 μM, the prediction of VC formation was similar to that when K_{STCE} =6 μM. However when $K_{S,TCE}$ decreased to 0.08 μM, the predicted curve was far from the experimental observation. The model assumes that higher chlorinated solvents exert inhibition effects on the daughter products and we assumed the inhibition coefficient K_i equals the K_S of each specific compound (Yu *et al*., 2005). After we manually adjusted $K_{i\,TCE}$ to the value in the range of published data 1.6~10.0 μM (Cupples *et al*., 2004; Koznetsova *et al*., 2010), then the data fit the experimental data much better (Figure 6-12 B).

When $K_{S,DCE}$ changed from 0.54 to 6.9 μM. The model prediction of VC and ethene formation fit the experimental result reasonably well at both high and low $K_{S,DCE}$ values (Figure 6-12 C D), the reported $K_{i\,DCE}$ in the literature is within the range of 2.2~3.6 μM (Cupples *et al*., 2004; Christ *et al*., 2007; Koznetsova *et al*. 2010) , which is similar to what we used in the model simulation.

6.4 Discussion

The kinetic model developed and validated in this study was able to fit the experimental data well in syntrophic co-cultures *S.wolfei*/strain 195 growing on butyrate and DvH/strain 195 growing on lactate. The model accurately captured donor fermentation kinetics, dechlorination kinetics, as well as biomass growth of *Dehalococcoides* 195. The model also correctly predicted when dechlorination performance was governed by thermodynamics or kinetics (or both) by means of the thermodynamic factor phi. The calculated kinetic parameters were validated at different donor to acceptor ratios in both co-cultures. The model predictions fit the experimental results well indicating the consistency of the parameters in further application. The kinetic parameters calculated for reductive dechlorination in all simulations were higher by percentage error of less than 100% compared to the values obtained from kinetic experiments. The reason for the discrepancy between the calculated parameters and the experimental observations could be that not all cells were active when we conducted kinetic studies in the late exponential phase. Therefore, we may have underestimate the maximum dechlorination rate in the test cucltures. Another possible reason could be due to the error introduced by biomass measurement process (qPCR analysis of 16S rRNA). Nevertheless, all kinetic parameters calculated in the model fall in the range of those reported in literature.

We demonstrated that the kinetic parameters derived from constructed syntrophic co-cultures could be further applied to predict the performance in syntrophic tri-cultures with some modifications of increased donor kinetics. This is due to increased H_2 utilization by both dechlorination and methanogenesis. We found in both tri-cultures *S.wolfei*/195/MC and DvH/195/MC that phi dropped about half after all TCE was degraded, indicating that the competition between reductive dechlorination and methanogenesis in the tri-cultures was controlled by both kinetics and thermodynamics. Specifically, in the tri-culture fed with butyrate, H_2 was slowly released while in the tri-culture growing on lactate, H_2 was produced at a higher rate resulting in a faster methane production rate. In prediction of the performance of the enrichment culture, we simplified the system by only considering dechlorination and methanogenesis as the H_2-utilizing processes. In this scenario, the model captured dechlorination kinetics and methanogenesis very well, however the H_2 production was higher than the

experimental observations. With information of community structure, we identified the functional microbial groups and used the kinetic model to capture other associated TEAPs.

The effect of bicarbonate and acetate concentrations has not been investigated in previous modeling approaches. From model simulations and experimental results, we found high acetate concentrations inhibit certain fermentation reactions. The inhibition effects were observed only in co-culture *S. wolfei*/strain 195 and tri-culture *S.wolfei*/195/MC growing on slow fermenting substrate butyrate. The model simulation could fit the experimental data well with lower dechlorination kinetics. However, the model predicted poorly on the cultures growing on lactate with excess acetate, in which less inhibition effect of acetate was observed in experiments. It is not the case that bicarbonate concentration changes affected pH or ionic strength in this study, since the medium was well buffered and the ionic strength was supplemented with adding appropriate amount of sodium chloride at low bicarbonate concentrations. In tri-cultures, reducing bicarbonate concentration did not affect dechlorination significantly, while the extent of organic acids consumption was affected. Low bicarbonate concentration did not pose much effect on reductive dechlorination of the enrichment culture. The dechlorination rate predicted by the model was slower than experimental observations. Since the effect of low bicarbonate was not consistent from simplified constructed consortia to complicated microbial community, it would be hard to include the factor of bicarbonate in the modeling approach at this time point. Further experiments need to be conducted to illustrate the role of bicarbonate in reductive dechlorination process.

pH effect on reductive dechlorination was not evaluated in the model, since the experimental system was well buffered to a stable pH. We observed little effect of ionic strength change on model prediction, due to the little change of thermodynamic factor calculation in the model structure. Therefore ionic strength is not a sensitive factor in the model prediction. A few studies have been carried out evaluating the effect of ionic strength and composition effects on Nonoscale zero-valent iron (NZVI) mobility in groundwater (Saleh *et al*., 2008), and enhanced bacterial transport for bioaugmentation by using low ionic strength solutions (Li and Logan, 1999). However, few studies have been conducted on the effect of ionic strength (may caused by higher salinity) on reductive dechlorination bioremediation processes. Further experiments are needed to investigate the effect of higher ionic strength (introduce higher salinity) and lower ionic strength (close to real groundwater environment) to further validate the model prediction.

There is a wide range of decay coefficients for dehalorespring microorganisms (0.003~0.09 day^{-1}) and methanogens (0.007~0.085 day^{-1}) in the literature. The integration of decay coefficients to kinetic models has been proved to fit experimental data better when considering TCE toxicity at high concentrations (Sabalowsky and Semprini, 2010). In this study, we tested the sensitivity of decay coefficients in the model by fitting experimental data with the highest and lowest reported decay coefficient values. For the culture we tested, we found decay coefficients are not a sensitive factor in predicting dechlorination performance, but are sensitive for methane production. Also decay coefficients are sensitive for accurate cell number predictions. In our simulation, the predictions for *Dehalococcoides* cell numbers decreased by half when high decay coefficients were adopted.

Previous studies have showed that dechlorination curves can vary significantly depending on the inhibition processes considered in the model (Chu *et al*., 2004; Chambon *et al*., 2013). In most competitive inhibition studies of reductive dechlorination, it is assumed that the inhibition constant K_i is equal to the half-velocity constant K_S (Lee *et al*., 2004; Clapp *et al*., 2004; Christ *et al*., 2007; Haest *et al*., 2010). Here we applied the same approach, and found that the simulation results fit the experimental data very well. The sensitivity of each parameter tested in the model simulation for different cultures is summarized in Table 6-7.

Table 6-7 A summary of the effect of environmental parameters changes on simulation result[a]

	S. wolfei/ strain 195	*S.wolfei*/195/MC	DvH/ strain 195	DvH/195/MC	LoTCEB12 enrichment
bicarbonate	+	+	+	+	-
acetate	++	++	+	-	-
Ionic strength	-	-	-	-	-
k_d	+	++	+	++	+
K_S	+	+	+	+	+
Ki	++	++	++	++	++

a. keep all other parameters constant while change one parameters. "++" means significant effect; "+" means slight effect; "-" means little effect.

6.5 Summary

In this study, we developed an integrated thermodynamic and kinetic model to predict reductive dechlorination and cell growth in batch growth conditions. The model parameters calculated to fit the experimental data were at the same levels as we experimentally determined in Chapter 5. The model could accurately capture dechlorination kinetics in two *Dehalococcoides*-containing syntrphic co-cultures that use fast or slow fermenting substrate and was further validated to predict the dechlorination performance in syntrophic tri-cultures and enrichment cultures involving hydrogenotrophic methanogenesis. The sensitivity of kinetic parameters for endogenous decay, half velocity and inhibition coefficients were were tested on model stability and found to be the most sensitive factors to affect the model predictions.

7 Conclusions and Future Work

7.1 Summary and conclusions

The overall goal of this research has been to understand electron flows in complex dechlorinating microbial communities, and to develop mathematical models to predict the performance of microbial communities under different environmental conditions. To accomplish these goals, we first studied the electron flow and material exchange of constructed TCE-dechlorinating consortia. We also applied emerging molecular techniques to study TCE-dechlorinating microbial communities under different remediation conditions. Furthermore, we developed integrated thermodynamic and kinetic models to predict dechlorination performance and microbial growth of syntrophic consortia under batch conditions, and the suite of models were validated using enrichment cultures.

The first objective of this research was to understand the material and energy exchange between *D. mccartyi* and its supporting syntroph bacteria in dechlorinating communities. This study investigated dechlorination activity, cell growth, cell aggregate formation, and global gene expression of *D. mccartyi* strain 195 (strain 195) grown with *Syntrophomonas wolfei* in co-cultures amended with butyrate or crotanate and TCE. By applying thermodynamically consistent rate laws to study the electrons flows in the co-culture, we found that the growth rates of the two species were strictly coupled by hydrogen transfer, and that the growth yield of syntrophic bacteria and the ratio maintained in the co-cultures were mainly controlled by thermodynamics. Spatial architecture and the physical proximity of the cells were analyzed by scanning electron microscopy and Fick's diffusion law estimations. We demonstrated, for the first time, that *D. mccartyi* could form cell aggregates when grown with its supporting fermenter *S. wolfei* on butyrate. Furthermore, we showed that carbon monoxide (CO) was maintained at low levels by the syntroph in the co-culture growing on butyrate rather than accumulating as it does with the strain 195 isolate. It is possible that CO serves as a supplemental energy source for *S. wolfei* during syntrophic fermentation with strain 195, and the observed increased cell yields of strain 195 is likely due to the continuous removal of CO in the co-culture. This study provides us with a more fundamental understanding of the metabolic exchange and energy transfer among the key players of TCE-dechlorinating communities. It also provides novel insights to the syntrophic relationships between *D. mccartyi* and the fermenting microorganisms during the *in situ* bioremediation applications.

In order to understand the microbial community structure shift from "feast-and-famine" condition (semi-batch) to the continuous feeding of low nutrients conditions, a completely mixed flow reactor (CMFR) inoculated from the semi-batch reactor (CANAS) was established and steady-state was achieved during the experimental period (200 days). Two distinct *D. mccartyi* strains *(*ANAS1 and ANAS2) were stably maintained within the CMFR. Electron balance analysis showed 104.4% electron recovery, in which 8.4 % of the electrons consumed went to dechlorination while 77.4% were stored in propionate and acetate and a large portion (11.8%) went to biomass production while 2.4% went to methane production and trace H_2 production. 16S "I-tags" technique and metagenome sequencing were applied to investigate the shift in community structure for the CMFR. A *Dehalococcoides* genus-wide microarray was also applied to study the transcriptional dynamics of *D.mccartyi* species within CANAS growing in a diluted, nutrient poor environment. 16S rRNA sequencing analysis and metagenome analysis revealed that the dominant species in CANAS shifted significantly from the original culture while the ratio of *D. mccartyi* was relatively stable. The transcription analysis identified *tceA* and *vcrA* to

be among the most expressed genes in CANAS, while hydrogenases *hup* and *vhu* were the critical electron donor enzymes utilized by *Dehalococcoides* sp. in enrichment cultures, while corrinoid-related genes were expressed at a lower level compared to the original culture (ANAS) during active dechlorination.

A systems-level approach was conducted to determine accurate kinetic parameters involved in reductive dechlorination from simplified constructed syntrophic cultures to complex microbial communities. This is the first study to use qPCR methods to quantify accurate biomass responsible for reductive dechlorination in a series of *Dehalococcoides*-containing cultures. The results showed that the kinetic parameters involved in reductive dechlorination are similar among different *Dehalococcoides*-containing cultures, and that cell growth calculations can be used to demonstrate that H_2 is the most sensitive factor limiting the growth of H_2-utilizing microorganisms involved in dechlorination. High initial acetate concentrations (>10 mM) inhibited the cell growth of *S. wolfei* in the syntrophic co-culture, while the growth rate of strain 195 was less affected. And the co-culture was metabolically active as determined by intermediate chlorinated compound production indicating the growth of *S. wolfei* and not strain 195 was inhibited by acetate in the co-culture. Experimental results demonstrated that decreased bicarbonate concentrations (1 mM) deminished dechlorination rates and cell yields of strain 195 in isolation and constructed tri-cultures. However, in enrichment culture LoTCEB12, dechlorination and methane production rates were not affected by low bicarbonate concentrations. The mechanism of deminshed dechlorination at lower bicarbonate concentrations was not clear and further experiments need to be conducted to illustrate the role of bicarbonate in reductive dechlorination process. High sulfate concentrations inhibited dechlorination performance due to either sulfide inhibition or competition from sulfate reduction.

An integrated thermodynamic and kinetic model was developed to predict reductive dechlorination and cell growth under batch growth conditions. The model parameters calculated to fit the experimental data were at the same levels as experimentally determined. The model accurately captured donor fermentation kinetics, dechlorination kinetics, as well as biomass growth of *Dehalococcoides* 195 in two *Dehalococcoides*-containing syntrphic co-cultures using different fermenting substrates. The calculated kinetic parameters were validated at different donor to acceptor ratios in both co-cultures. The model predictions fit the experimental results well indicating the consistency of the parameters in extended applications. We demonstrated that the kinetic parameters derived from constructed syntrophic co-cultures could be applied to predict the performance in syntrophic tri-cultures with some modifications of increased donor kinetics. The developed model captured dechlorination kinetics and methanogenesis well in tri-cultures and enrichment culture LoTCEB12. The sensitivity of kinetic parameters showed that decay coefficients (k_d), ionic strength and bicarbonate concentrations did not strongly affect the model predictions, while half velocity (K_S) and inhibition coefficients (Ki) were the most sensitive factors to affect the model outcomes.

7.2 Suggestions for future research

Metagenomic and 16S rRNA analyses in this study provided us with information on the dechlorinating microbial community structure growing under continuous flow conditions. The microarray results focused on the transcriptomic level of the key *Dehalococcoides* strains.

However, it would be extremely interesting to determine the function of other supporting/competing microorganisms within the dechlorinating community. The application of more high throughput microarray and proteomic techniques to study the metatranscriptomes and metabolomes of the microbial community in CMFR reactors could be interesting.

In this study, the mechanism of decreased dechlorination rates at lower bicarbonate concentrations was not clear and further experiments need to be conducted to illustrate the role of bicarbonate in reductive dechlorination. Further, the changing environmental conditions, such as a decrease in pH, sulfate/iron rich subsurface arsenic co-contamination etc. that are prevalent in groundwater contamination sites, may potentially have inhibitory/promotional effects on the dechlorinating microbial communities. Therefore, understanding the geochemical effects on dechlorinating microbial communities is important to control and reduce the uncertainty associated with *in situ* bioremediation process. The geochemical effects on the metabolic interactions among microorganisms in dechlorinating microbial communities should be further studied.

The CMFR has been shown to be a good platform to study dechlorination at statey state and to generate biomass at a stable rate. In order to further validate the kinetic models developed in this study, parallel CMFR could be constructed, with varied flow rates, substrate concentrations, and perturbation of environmental conditions. In addition, other potential biomarkers (such as vitamin B12-related genes and hydrogenases) could be tested as model inputs to improve the model stability.

References

Aburto A, Fahy A, Coulon F, Lethbridge G, Timmis KN, Ball AS, McGenity TJ. 2009. Mixed aerobic and anaerobic communities in benzene-contaminated groundwater. *J Appl Microbiol* 106 (1): 317-328 (standard,

Adams CJ, Redmond MC, Valentine DL. 2006. Pure-Culture Growth of Fermentative Bacteria, Facilitated by H_2 Removal: Bioenergetics and H_2 production. *Appl Environ Microbiol* 72 (2): 1079-1085

Adrian L, Szewzyk U, Wecke J, Görisch H. 2000. Bacterial dehalorespiration with chlorinated benzens. Nature 408: 580-583

AFCEE. 2004. Principles and practices of enhanced anaerobic bioremediation of chlorinated solvents. Air Force Center for Environmental Excellence, Naval Facilities Engineering. Service center, and environmental security technology certification program. Washington, DC.

Anderson JK, Smith TG, Hoover TR. 2010. Sense and sensibility: flagellum-mediated gene regulation. *Trends Microbiol* 18:30-37

Albertsen, M., Hugenholtz, P., Skarshewski, A., Nielsen, K.L., Tyson, G.W. and Nielsen, P.H. 2013. Genome sequences of rare, uncultured bacteria obtained by differential coverage binning of multiple metagenomes. *Nature Biotechnology* 31, 5.

Alvarez-Cohen L, McCarty PL, Boulygina E, Hanson RS, Brusseau GA, Tsien HC. 1992. Characterization of a Methane-utilizing bacterium from a bacterial consortium that rapidly degrades trichloroethylene and chloroform. *Appl Environ Microbiol* 58(6): 1886-1893.

Amann RI, Ludwig W, Schleifer KH. 1995. Phylogenetic identification and *in situ* detection of individual microbial cells without cultivation. *Microbiological Reviews* 59(1): 143-169.

Amos BK, Christ JA, Abriola LM, Pennell K, Löffler, FE. 2007. Experimental evaluation and mathematical modeling of microbially enhanced tetrachloroethene (PCE) dissolution. *Environ Sci Technol* 41, 965-970

Amos BK, Ritalahti KM, Cruz-Garcia C, Padilla-Crespo, Löffler FE. 2008. Oxygen effect on *Dehalococcoides* viability and biomarker quantification. *Environ Sci Technol* 42, 5718-5726

Amos BK, Suchomel EJ, Pennell KD, Löffler FE. 2009. Spatial and temporal distributions of *Geobacter lovleyi* and *Dehalococcoides* spp. during bioenhanced PCE-NAPL dissolution. *Environ Sci Technol* 43: 1977-1985

Anderson JK, Smith TG, Hoover TR. 2010. Sense and sensibility: flagellum-mediated gene regulation. *Trends Microbiol* 18:30-37.

ATSDR (Agency for toxic substances and disease registry) The Priority List of Hazardous Substances that will be the subject of toxicological profiles. http://www.atsdr.cdc.gov/spl/

Aulenta F, Majone M, Tandoi V.2006. Enhanced anaerobic bioremediation of chlorinated solvents: environmental factors influencing microbial activity and their relevance under field conditions. *J. Chem. Technol. Biotechnol* 81(9): 1463-1474.

Aulenta F, Beccari M, Majone M, Papini MP, Tandoi V. 2008. Competition for H_2 between sulfate reduction and dechlorination in butyrate-fed anaerobic cultures. Process Biochemistry. 43, 161-168

Aulenta F, Majone M, Papini MP, Rossetti S, Tandoi V. 2011. Reductive Dechlorination of Chloroethenes: From the Laboratory to Field-scale Investigations.

Aziz, R.K., Bartels, D., Best, A.A., DeJongh, M., Disz, T., Edwards, R.A., Formsma, K., Gerdes, S., Glass, E.M., Kubal, M. 2008. The RAST Server: Rapid Annotations using Subsystems Technology. BMC Genomics 9, 75.

Azizian MF, Behrens S, Sabalowsky A, Dolan ME, Spormann AM, Semprini L. 2008. Continuous-flow column study of reductive dehalogenation of PCE upon bioaugmentation with the Evanite enrichment culture. *J Contam Hydrol* 100 (1-2): 11-21.

Azizian MF, Marshall IPG, Behrens S, Spormann AM, Semprini L. 2010. Comparison of lactate, formate, and propionate as hydrogen donors for the reductive dehalogenation of trichloroethene in a continuous-flow column. *J Contam Hydrol* 113: 77-92

Bælum J, Chambon JC, Scheutz C, Binning PJ, Laier T, Bjerg PL, Jacobsen CS. 2013. A conceptual model linking functional gene expression and reductive dechlorination rates of chlorinated ethenes in clay rich groundwater sediment. *Water Research* 47 (7): 2467-2478

Bagley DM. 1998. Systematic approach for modeling tetrachloroethene biodegradation. Journal of Environmental Engineering 124 (11): 1076-1086.

Banerjee R, SW Ragsdale. 2003. The many faces of vitamin B_{12}: Catalysis by cobalamin-dependent enzymes. *Annual Review of Biochemistry* 72: 209-247.

Beaty PS, McInerney MJ. 1987. Growth of *Syntrophomonas wolfe*i in pure culture on crotonate. *Archives of Microbiology* 147 (4): 389-393.

Beaty PS, McInerney MJ. 1989. Effects of organic-acid anions on the growth and metabolism of syntrophomonas-wolfei in pure culture and in defined consortia. *Appl Environ Microbiol* 55(4): 977-983.

Becker JG. 2006. A modeling study and implications of competition between *Dehalococcoides ethenogenes* and other tetrachloroethene-respiring bacteria. *Environ. Sci. Technol* 40(14): 4473-4480.

Behrens S, Azizian MF, McMurdie PJ, Sabalowsky A, Dolan ME, Semprini L, Spormann AM. 2008. Monitoring Abundance and Expression of "*Dehalococcoides*" Species Chloroethene-Reductive Dehalogenases in a Tetrachloroethene-Dechlorinating Flow Column. *Appl. Environ. Microbiol*. 74 (18): 5695-5703

Bhatt P, Kumar MS, Mudliar S, Chakrabarti T. Biodegradation of chlorinated compounds - A review. Critical Reviews in *Environ. Sci. Technol*. 2007, 37 (2): 165-198.

Berggren DRV, Marshall IPG, Azizian MF, Spormann AM, Semprini L. 2013. Effects of sulfate reduction on the bacterial community and kinetic parameters of a dechlorinating culture under chemostat growth conditions. *Environ. Sci. Technol* 47 (4): 1879-1886

Boone DR, Johnson RL, Liu Y.1989. Diffusion of the interspecies electron carriers H_2 and formate in methanogenic ecosystems and its implications in the measurement of Km for H_2 or formate updake. *Appl Environ Microbiol* 55: 1735-41

Boone DR, Castenholz RW, Garrity GM. Bergey's manual of systematic bacteriology. ISBN: 0387950427

Bradley PM, Chapelle FH. 2010. Biodegradtion of chlorinated ethenes. *In Situ Remediation Of Chlorinated Solvent Plumes. SERDP/ESTCP Environmental Remediation Technology*, Stroo, H. F.; Ward, C. H., Eds. Springer: Heidelberg, Germany, 2010. pp 39-67

Brisson VL, West KA, Lee PK, Tringe SG, Brodie EL, Alvarez-Cohen L. Metagenomic analysis of a stable trichloroethene-degrading microbial community. *ISME J.* 2012, *6* (9): 1702-14.

Brovelli A, Barry DA, Robinson C, Gerhard JI. 2012. Analysis of acidity production during enhanced reductive dechlorination using a simplified reactive transport model. Adv Water Resour 43, 14-27

Butler E, Hayes K. 1999. Kinetics of the transformaiton of trichloroethylene and tetrachloroethylene by iron sulfide. *Environ Sci Technol* 33: 2021-2027

Caporaso JG, Kuczynski J, Stombaugh J, Bittinger K, Bushman FD, Costello EK. 2010. QIIME allows analysis of high-throughput community sequencing data. *Nature methods* 7: 335-336.

Carr CS, Garg S, Hughes JB. Effect of dechlorinating bacteria on the longevity and composition of PCE-containing nonaqueous phasBe liquids under equilibrium dissolution conditions. *Environ. Sci. Technol*. 2000, 34(6): 1088-1094.

Chambon JC, Bjerg PL, Scheutz C, Bælum J, Jakobsen R, Binning PJ. 2013. Review of Reactive Kinetic Models Describing Reductive Dechlorination of Chlorinated Ethenes in Soil and Groundwater. Biotechnology and Bioengineering 110 (1): 1-23

Cheng D, He J. 2009. Isolation and characterization of *Dehalococcoides* sp. Strain MB, which dechlorinates tetrachloroethene to trans-1,2-dichloroethene. *Appl Environ Microbiol* 75: 5910-5918

Cheng D, Chow WL, He J. 2010. A *Dehalococcoides*-containing co-culture that dechlorinates tetrachloroethene to *trans*-1,2-dichloroethene. ISME Journal 4 (1):88-97.

Chung J, Krajmalnik-Brown R, Rittmann BE. 2008. Bioreduction of trichloroethene using a hydrogen-based membrane biofilm reactor. *Environ. Sci. Technol* 42 (2), 477-483

Christ JA, Abriola LM. 2007. Modeling metabolic reductive dechlorination in dense non-aqueous phase liquid source-zones. *Adv. Water Res 30*, (6–7): 1547-1561

Clapp LW, Semmens MJ, Novak PJ, Hozalski RM. 2004. Model for in situ perchloroethene dechlorination via membrane-delivered hydrogen. *Journal of Environmental Engineering* 130 (11): 1367-1381.

Clement TP, Johnson CD, Sun YW, Klecka GM, Bartlett C. 2000. Natural attenuation of chlorinated ethene compounds: model development and field-scale application at the Dover site. *J Contam Hydrol*. 42: 113-140

Coleman NV, Mattes TE, Gossett JM, Spain JC. 2002. Biodegradation of cis-dichloroethene as the sole carbon source by a *beta-proteobacterium.* Applied and Environmental Microbiology 68(6): 2726-2730.

Conrad R, Wetter B. 1990. Influence of temperature on energetics of hydrogen metabolism in homoacetogenic, methanogenic, and other anaerobic bacteria. *Arch Microbiol* 155: 94-98

Corapcioglu MY, Sung K, Kim J. 2004. Parameter determination of sequential reductive dehalogenation reactions of chlorinated hydrocarbons. *Transp Porous Media* 55: 169-182

Cord-Ruwisch R, Seitz HJ, Conrad R. 1988. The capacity of hydrogenotrophic anaerobic bacteria to compete for traces of hydrogen depends on the redox potential of the terminal electron acceptor. *Archives of Microbiology* 149 (4): 350-357.

Cupples AM, Spormann AM, McCarty PL. 2003. Growth of a *Dehalococcoides*-like microorganism on vinyl chloride and cis-dichloroethene as electron acceptors as determined by competitive PCR. *Appl Environ Microbiol* 69 (2): 953-959.

Cupples AM, Spormann AM, McCarty PL. 2004. Vinyl chloride and cis-dichloroethene dechlorination kinetics and microorganism growth under substrate limiting conditions. *Environ. Sci. Technol* 38 (4): 1102-1107

Cupples AM. 2008. Real-time PCR quantification of *Dehalococcoides* populations: Methods and applications. *J Microbiol Methods* 72: 1-11

Cuzin N, Ouattara AS, Labat M, Garcia JL. 2001. *Methanobacterium congolense* sp. nov., from a methanogenic fermentation of cassava peel. *Int. J. Syst. Evol. Microbiol 51* (2): 489-493

Dinsdale EA, Edwards RA, Hall D, Angly F, Breitbart M, Brulc JM, Furlan M, Desnues C, Haynes M, Li L. 2008. Functional metagenomic profiling of nine biomes. *Nature* 2008, 452: 629-632

Daprato RC, Löffler FE, Hughes JB. 2007. Comparative analysis of three tetrachloroethene to ethene halorespiring consortia suggests functional redundancy. *Environ. Sci. Technol* 41(7): 2261-2269.

Da Silva MLB, Alvarez PJJ. 2008. Exploring the Correlation between Halorespirer Biomarker Concentrations and TCE Dechlorination Rates. Journal of Environmental Engineering 134 (11): 895-901.

Delgado AG, Parameswaran P, Fajardo-Williams D, Halden RU and Krajmalnik-Brown R. 2012. Role of bicarbonate as a pH buffer and electron sink in microbial dechlorination of chloroethenes. *Microbial Cell Factories* 11:128-138

Delgado AG, Fajardo-Williams D, Popat SC, Torres CI, Krajmalnik-Brown R. 2014. Successful operation of continuous reactors at short retention times results in high-density, fast-rate *Dehalococcoides* dechlorinating cultures. *Appl Microbiol Biotechnol* 98, 2729-2737

De Bok FAM, Plugge CM, Stams AJM. 2004. Interspecies electron transfer in methanogenic propionate degrading consortia. Water Research 38: 1368-1375

Desai N, Antonopoulos D, Gilbert JA, Glass EM, Meyer F. 2012. From genomics to metagenomics. *Curr Opin Biotechnol* 23: 72-76.

Dolfing J, Janssen DB. 1994. Estimates of Gibbs free energies of formation of chlorinated aliphatic compounds. *Biodegradation J* 5: 21-28

Dolfing J. 2003. Thermodynamic considerations for dehalogenation. In dehalogenation: Microbial Processes and Environmental Applications, Häggblom, M. M., Bossert, I.D., Eds.; Kluwer Academic Publishers: Boston/Dordrecht/London.

Dolfing J, van Eekert M, Mueller J. 2006. Thermodynamics of Low Eh Reactions. Battell's Fifth International Conference on Remediation of Chlorinated and Recalcitrant Compounds. May 22-26, Monterey California.

Duhamel M, Mo K, Edwards EA. 2004. Characterization of a highly enriched *Dehalococcoides*-containing culture that grows on vinyl chloride and trichloroethene. *Appl Environ Microbiol*. 70: 5538-5545

Duhamel M, Edwards EA. 2007. Growth and yields of dechlorinators, acetogens, and methanogens during reductive dechlorination of chlorinated ethenes and dihaloelimination of 1,2-dichloroethane. *Environ. Sci. Technol* 41 (7): 2303-2310

Drzyzga O, Gerritse J, Dijk JA, Elissen H, Gottschal JC. 2001. Coexistence of a sulphate-reducing Desulfovibrio species and the dehalorespiring *Desulfitobacterium frappieri* TCE1 in defined chemostat cultures grown with various combinations of sulphate and tetrachloroethene. *Environ Microbiol.* 3(2): 92-99.

Dykstra M J, Reuss LE. 1992. Biological Electron Microscopy- Theory, Techniques, and Troubleshooting. ASM Press. Washington DC ISBN: 0-306-44277-9

Duhamel M, Wehr SD, Yu L, Rizvi H, Seepersad D, Dworatzed S, Cox EE, Edwards EA. 2002. Comparison of anaerobic dechlorinating enrichment cultures maintained on tetrachloroethene, trichloroethene, cis-dichloroethene and vinyl chloride. *Water Research* 36 (17): 4193-4202.

Duhamel M, EA Edwards. 2006. Microbial composition of chlorinated ethene-degrading cultures dominated by *Dehalococcoides*. *FEMS Microbiol Ecol* 58: 538-549.

Duhamel M, Edwards EA. 2007. Growth and yields of dechlorinators, acetogens, and methanogens during reductive dechlorination of chlorinated ethenes and dihaloelimination of 1,2-dichloroethane. *Environ. Sci. Technol* 41 (7): 2303-2310

El Mamouni R, Jacquet R, Gerin P, Agathos SN. 2002. Influence of electron donors and acceptors on the bioremediation of soil contaminated with trichloroethene and nickel: laboratory- and pilot-scale study. Water Science and Technology 45 (10): 49-54

Falta RW. 2008. Methodology for comparing source and plume remediation alternatives. *Ground Water* 46:272-285

Felchner-Zwirello M, Winter J, Gallert C. 2012. Interspecies distances between propionic acid degraders and methanogens in syntrophic consortia for optimal hydrogen transfer. *Appl Microbiol Biotechnol* 12:12-25

Fennell DE, Gossett JM. 1998. Modeling the production of and competition for hydrogen in a dechlorinating culture. *Environ. Sci. Technol 32* (16): 2450-2460.

Ferenci T. 2008. Bacterial physiology, regulation and mutational adaptation in an environment. *Adv Microb Physiol*. 53: 169-229

Ferrer M, Golyshina OV, Chernikova TN, Khachane AN, Martins DSVA, Yakimov MM, Timmis KN, Golyshin PN. 2005. Microbial enzymes mined from the Urania deep-sea hypersaline anoxic basin. *Chem. Biol* 12: 895-904

Fletcher KE, Costanza J, Cruz-Garcia C, Ramaswamy NS, Pennell KD, Löffler FE. 2011. Effects of Elevated Temperature on *Dehalococcoides* Dechlorination Performance and DNA and RNA Biomarker Abundance. *Environ Sci Technol* 45 (2): 712-718

Freeborn RA, West KA, Bhupathiraju VK, Chauhan S, Rahm BG, Richardson RE, Alvarez-Cohen L. 2005. Phylogenetic analysis of TCE-dechlorinating consortia enriched on a variety of electron donors. *Environ. Sci. Technol* 39 (21): 8358-8368

Gerritse J, Kloetstra G, Borger A, Dalstra G, Alphenaar A, Gottschal JC. Complete degradation of tetrachloroethene in coupled anoxic and oxic chemostats.Applied Microbiology and Biotechnology. *Appl. Microbiol. Biotechnol* 1997, 48 (4): 553-562

Gillham RW, O'Hannesin SF. 1994. Enhanced degradation of halogenated aliphatics by zero-valent iron. *Ground Water* 32: 958-967

Gorby YA, Yanina S, McLean JS, Rosso KM, Moyles D, Dohnalkova A, Beveridge TJ, Chang IS, Kim BH, Kim KS, Culley DE, Reed SB, Romine MF, Saffarini DA, Hill EA, Shi L, Elias DA, Kennedy DW, Pinchuk G, Watanabe K, Ishii S, Logan B, Nealson KH, Fredrickson JK. 2006. Electrically conductive bacterial nanowires produced by *Shewanella oneidensis* strain MR-1 and other microorganisms. *PNAS*103 (30): 9536-9542.

Gossett JM. 1987. Measurement of Henry's Law Constants for C1 and C2 chlorinated hydrocarbons. *Environ. Sci. Technol* 21 (2): 202-208.

Gu AZ, Hedlund BP, Staley JT, Strand SE, Stensel HD. 2004. Analysis and comparison of the microbial community structures of two enrichment cultures capable of reductively dechlorinating TCE and cis-DCE. *Environ Microbiol* 6: 45-54.

Haest PJ, Springael D, Smolders E. 2010. Dechlorination kinetics of TCE at toxic TCE concentrations: Assessment of different models. *Water Res* 44, 331-339

Hanselmann KW. 1991. Microbial energetics applied to waste repositories. *Experientia* 47: 645-687

Harkness M, Fisher A, Lee MD, Mack EE, Payne JA, Dworatzek S, Roberts J, Acheson C, Herrmann R, Possolo A. 2012. Use of statistical tools to evaluate the reductive dechlorination of high levels of TCE in microcosm studies. *J Contam Hydrol*. 131, 100-118

Haston ZC, McCarty PL. 1999. Chlorinated ethene half-velocity coefficients (K_S) for reductive dehalogenation. *Environ. Sci. Technol* 33 (2): 223-226.

Haynes WM.2014. CRC Handbook of Physics and Chemistry, 95th edition ISBN 9781482208672

Hazen TC, Dubinsky EA, DeSantis TZ, Andersen GL, Piceno YM, Singh N, Jansson JM, Probst A, Borglin SE, Fortney JL, Stringfellow WT, Bill M. 2010. Deep-sea oil plume enriches indigenous oil-degrading bacteria. *Science.* 330: 204-208.

He JZ, Sung Y, Dollhopf ME, Fathepure BZ, Tiedje JM, Löffler, FE. 2002. Acetate versus hydrogen as direct electron donors to stimulate the microbial reductive dechlorination process at chloroethene-contaminated sites. *Environ Sci Technol* 36, 3945-3952

He J, Ritalahti KM, Yang K-L, Koenigsverg SS, Löffler FE. 2003. Detoxification of vinyl chloride to ethene coupled to growth of an anaerobic bacterium. *Nature* 424:62-65

He J, Sung Y, Krajmalnik-Brown R, Rittalahti KM, Löffler FE. 2005. Isolation and characterization of Dehalococcoides sp. strain FL2, a trichloroethene (TCE)-and 1,2-dichlroethene-respiring anaerobe. *Environ. Microbiol* 7 (9):1442-1450.

He J, Holmes VF, Lee PK, Alvarez-Cohen L. 2007. Influence of vitamin B-12 and cocultures on the growth of *Dehalococcoides* isolates in defined medium, *Appl. Environ. Microbiol* 73 (9): 2847-2853

He Z, Gentry TJ, Schadt CW, Wu L, Liebich J, Chong SC, Huang Z, Wu W, Gu B, Jardine P, Criddle C, Zhou JZ. 2007 b. GeoChip: a comprehensive microarray for investigating biogeochemical, ecological and environmental processes. *ISME Journal* 1(1): 67-77.

He ZL, Van Nostrand JD, Zhou JZ. 2012 b. Application of functional gene microarrays for profiling microbial communities. *Curr Opin Biotechnol* 23: 460-466.

Hendrickson ER, Payne JA, Young RM, Starr MG, Perry MP, Fahnestock S, Ellis DE, Ebersole RC. 2002. Molecular analysis of *Dehalococcoides* 16S ribosomal DNA from chloroethene-contaminated sites throughout North America and Europe. *Appl Environ Microbiol* 68: 485-495

Heavner GL, Rowe AR, Mansfeldt CB, Pan JK, Gossett JM, Richardson RE. 2013. Molecular Biomarker-Based Biokinetic Modeling of a PCE-Dechlorinating and Methanogenic Mixed Culture. *Environ. Sci. Technol* 47 (8): 3724-3733.

Heimann AC, Friis AK, JakobsenR. 2005. Effects of sulfate on anaerobic chloroethene degradation by an enriched culture under transient and steady-state hydrogen supply. *Water Research* 39: 3579-3586

Heimann AC, Jakobsen R. 2006. Experimental Evidence for a lack of thermodynamic control on hydrogen concentrations during anaerobic degradation of chlorinated ethenes. *Environ. Sci. Technol* 40, 3501-3507

Heimann A, Blodau C, Postma D, Larsen F, Viet PH, Nhan PQ, Jessen S, Duc MT, Hue NTM, Jakobsen R. 2007. Hydrogen thresholds and steady state concentrations associated with microbial arsenate respiration. *Environ. Sci. Technol* 41: 2311-2317

Heimann A, Jakobsen R, Blodau C. 2010. Energetic constraints on H2-dependent terminal electron accepting processes in anoxic environments: a review of observations and model approaches. *Environ. Sci. Technol* 44 (1): 24-33

Hoelen TP, Reinhard M. 2004. Complete biological dehalogenation of chlorinated ethylenes in sulfate containing groundwater. *Biodegradation* 15: 395-403

Holliger C, Hahn D, Harmsen H, Ludwig W, Schumacher W, Tindall B, Vazquez F, Weiss N, Zehnder AJB. 1988. *Dehalobacter restrictus* gen. nov. and sp. nov., a strictly anaerobic bacterium that reductively dechlorinates tetra- and trichloroethene in an anaerobic respiration. *Archives of Microbiology* 169 (4), 313-321.

Hopkins GD, Semprini L, McCarty PL. 1993. Microcosms and in-situ field studies of enhanced biotransformation of trichloroethylene by phenol-utilizing microorganisms. *Appl Environ Microbiol* 59 (7): 2277-2285.

Hopkins GD, McCarty PL. 1995. Field-evaluation of in-situ aerobic cometabolism of trichloroethylene and 3 dechloroethylene isomersusing using phenol and toluene as the primary substrates. *Environ. Sci. Technol* 29 (6):1628-1637

Horn MA, Matthies C, Küsel K, Schramm A and Drake HL. 2003. Hydrogenotrophic Methanogenesis by Moderately Acid-Tolerant Methanogenes of a Methane-Emitting Acidic Peat. *Appl Environ Microbiol* 69 (1): 74-85

Hoskisson PA, Hobbs G. 2005. Continuous culture - making a comeback? Microbiology-Sgm 151 3153-3159.

Huang DY, Becker JG. 2009. Determination of intrinsic Monod kinetic parameters for two heterotrophic tetrachloroethene (PCE)- Respiring strains and insight into their application. *Biotechnol Bioeng* 104, 301-311

Hug LA, Salehi M, Nuin P, Tillier ER, Edwards EA. 2011. Design and verification of a pangenome microarray oligonucleotide probe set for *Dehalococcoides* spp. *Appl Environ Microbiol* 77: 5361-5369.

Ishii S, Kosaka T, Hori K, Hotta Y, Watanabe K. 2005. Coaggregation Facilitates Interspecies Hydrogen Transfer between *Pelotomaculum thermopropionicum* and *Methanothermobacter thermautotrophicus*, *Appl. and Environ. Microbiol* 71(12): 7828-7845.

Ishii S, Kosaka T, Hotta Y, Watanabe K. 2006. Simulating the contribution of coaggregation to interspecies hydrogen fluxes in syntrophic methanogenic consortia. *Appl. Environ. Microbiol* 72 (7): 5093-5096.

Ishii, S., Suzuki, S., Norden-Krichmar, T.M., Tenney, A., Chain, P.S., Scholz, M.B., Nealson, K.H. and Bretschger, O. 2013. A novel metatranscriptomic approach to identify gene expression dynamics during extracellular electron transfer. *Nat Commun* 4, 1601.

Isken S, de Bont JA. 1998. Bacteria tolerant to organic solvents. *Extremophiles* 2 (3): 229-238

Jackson BE, McInerney MJ. 2002. Anaerobic microbial metabolism can proceed close to therymodynamic limits. *Nature* 415, 454-456

Janssen DB, Dinkla IJT, Poelarends GJ, Terpstra P. 2005. Bacterial degradation of xenobiotic compounds: evolution and distribution of novel enzyme activities. *Environmental Microbiology* 7(12): 1868-1882

Jeon CO, Park W, Padmanabhan P, DeRito C, Snape JR, Madsen EL. 2003. Discovery of a bacterium, with distinctive dioxygenase, that is responsible for in situ biodegradation in contaminated sediment. *Proc Natl Acad Sci U S A* 100: 13591-13596.

Jin Q. 2007. Control of hydrogen partial pressures on the rates of syntrophic microbial metabolisms: a kinetic model for butyrate fermentation. *Geobiology* 5 (1): 35-48

Johnson DR, Lee PKH, Holmes VF, Alvarez-Cohen L. 2005. An internal reference technique for accurately quantifying specific mRNAs by real-time PCR with application to the tceA reductive Dehalogenase gene. *Appl Environ Microbiol* 71, 3866-3871

Johnson DR, Brodie EL, Hubbard AE, Andersen GL, Zinder SH, Alvarez-Cohen L. 2008. Temporal Transcriptomic Microarray Analysis of "*Dehalococcoides ethenogenes*" Strain 195 during the Transition into Stationary Phase. *Appl Environ Microbiol* 74 (9), 2864-2872

Johnson DR, Nemir A, Andersen GL, Zinder SH, Alvarez-Cohen L. 2009. Transcriptomic microarray analysis of corrinoid responsive genes in *Dehalococcoides ethenogenes* strain 195. *Fems Microbiology Letters* 294: 198-206.

Karadagli F, Rittmann BE. 2005. Kinetic characterization of Methanobacterium bryantii M.o.H. Environ. Sci. Technol 39 (13):4900-4905

Kato S, Watanabe K. 2010. Ecological and evolutionary interactions in syntrophic methanogenic consortia. *Microbes Environ* 25 (3): 145-151.

Kleerebezem R, Stams AJM. 2000. Kinetics of syntrophic cultures: A theoretical treatise on butyrate fermentation. Biotechnol. Bioeng 67 (5): 529-543

Krajmalnik-Brown R, Hölscher T, Thomson IN, Saunders FM, Ritalahti KM, Löffler FE. 2004. Genetic identification of a putative vinyl chloride reductase in *Dehalococcoides* sp. Strain BAV1. *Appl Environ Microbiol* 70: 6347-6351

Kouznetsova I, Mao X, Robinson C, Barry DA, Gerhard JI, McCarty PL. 2010. Biological reduction of chlorinated solvents: Batch-scale geochemical modeling. *Adv. Water Res 33* (9): 969-986.

Krumme ML, Timmis KN, Dwyer DF. 1993. Degradation of trichloroethylene by pseudomonas-cepacia G4 and the constitutive mutant strain G4-5233 PR1 in aquifer microcosms. *Appl Environ Microbiol* 59 (8): 2746-2749

Le Mer J, Roger P. 2001. Production, oxidation, emission and consumption of methane by soils: A review. *Eur. J. Soil Biol* 37, 25-50

Lee IS, Bae JH, Yang Y, McCarty PL. 2004. Simulated and experimental evaluation of factors affecting the rate and extent of reductive dehalogenation of chloroethenes with glucose. *J. Contam. Hydrol* 74 (1–4): 313-331

Lee PKH, Johnson DR, Holmes VF, He J, Alvarez-Cohen L. 2006. Reductive dehalogenase gene expression as a biomarker for physiological activity of *Dehalococcoides* spp. *Appl. Environ. Microbiol* 72: 6161-6168.

Lee IS, Bae JH, McCarty PL. 2007. Comparison between acetate and hydrogen as electron donors and implications for the reductive dehalogenation of PCE and TCE. *J Contam Hydrol* 94,76-85

Lee PKH, Cheng D, Hu P, West KA, Dick GJ, Brodie EL, Andersen GL, Zinder SH, He J, Alvarez-Cohen L. 2011. Comparative genomics of two newly isolated *Dehalococcoides* strains and an enrichment using a genus microarray. *ISME J* 5:1014-1024.

Leininger S, Urich T, Schloter M, Schwark L, Qi J, Nicol GW, Prosser JI, Schuster SC, Schleper C. 2006. Archaea predominate among ammonia-oxidizing prokaryotes in soils. *Nature* 442: 806-809

Lendvay JM, Löffler FE, Dollhopf M, Aiello MR, Daniels G, Fathepure BZ, Gebhard M, Heine R, Helton R, Shi J, Krajmalnik-Brown R, Major Jr CL, Barcelona MJ, Petrovskis E, Tiedje JM, Adriaens P. 2003. Bioreactive barriers: bioaugmentation and biostimulation for chlorinated solvent remediation. *Environ Sci Technol* 37: 1422-1431

Li Q and Logan BE. 1999. Enhancing bacterial transport for bioaugmentation of aquifers using low ionic strength solutions and surfactants. *Wat. Res*. 33 (4): 1090-1100

Li W and Drake MA. 2001. Development of a quantitative competitive PCR assay for detection and quantification of *Escherichia coli* O157:H7 cells. *Appl. Environ. Microbiol* 67:3291–3294.

Liu CX, Zachara JM. 2001. Uncertainties of Monod kinetic parameters nonlinearly estimated from batch experiments. *Environ Sci Technol* 35:133-141

Löffler FE, Tiedje JM, Sanford RA. 1999. Fraction of Electrons Consumed in Electron Acceptor Reduction and Hydrogen Thresholds as Indicators of Halorespiratory Physiology. *Appl Environ Microbiol* 65 (9): 4049-4056

Löffler FE, Sun Q, Li JR, Tiedje JM. 2000. 16S rRNA gene-based detection of tetrachloroethene-dechlorinating *Desulfuromonas* and *Dehalococcoides* species. *Appl. Environ. Microbiol* 66 (4): 1369-1374

Löffler FE, Sanford RA. 2005. Analysis of trace hydrogen metabolism. *Methods Enzymol* 397: 222-237

Löffler FE, Ritalahti KM, Zinder SH. 2013. *Dehalococcoides* and reductive dechlorination of chlorinated solvents. In *Bioaugmentation for Groundwater Remediation*, Stroo, H. F.; Leeson, A.; Ward, C. H., Eds. Springer: Heidelberg, Germany, 2013; pp 39-88

Löffler FE, Yan J, Ritalahti KM, Adrian L, Edwards EA, Konstantinidis KT, Müller JA, Fullerton H, Zinder SH, Spormann AM. 2013 a. *Dehalococcoides mccartyi* gen. nov., sp. nov., obligate organohalide-respiring anaerobic bacteria, relevant to halogen cycling and bioremediation, belong to a novel bacterial class, *Dehalococcoidetes* classis nov., within the phylum *Chloroflexi*, *Int J Syst and Evol Micr* 2013, 63: 625-635

Lovley DR, Goodwin S. 1988. Hydrogen concentrations as an indicator of the predominant terminal electron-accepting reactions in aquatic sediments. *Geochimica et Cosmochica Acta* 52 (12): 2993-3003

Lovley DR. 2003. Cleaning up with genomics: Applying molecular biology to bioremediation. *Nat Rev Microbiol* 1 (1): 35-44

Lu XX, Tao S, Bosma T, Gerritse J. 2001. Characteristic hydrogen concentrations for various redox processes in batch study. *J Environ Sci Health A Tox Hazard Subst Environ Eng* 36 (9): 1725-1734.

Lu X, Wilson JT, Kampbell DH. 2006. Relationship between *Dehalococcoides* DNA in ground water and rates of reductive dechlorination at field scale. *Water Research* 40 (16): 3131-3140.

Lu ZM, Deng Y, Van Nostrand JD, He ZL, Voordeckers J, Zhou AF, Lee YJ, Mason OU, Dubinsky EA, Chavarria KL, Tom LM, Fortney JL. 2012. Microbial gene functions enriched in the Deepwater Horizon deep-sea oil plume. *ISME J* 6: 451-460.

Luijten ML, Roelofsen W, Langenhoff AA, Schraa G, Stams AJ. 2004. Hydrogen threshold concentrations in pure cultures of halorespiring bacteria and at a site polluted with chlorinated ethenes. *Environ. Microbiol* 6 (6): 646-650.

Ma X, Novak PJ, Clapp LW, Semmens MJ, Hozalski RM. 2003. Evaluation of polyethylene hollow-fiber membranes for hydrogen delivery to support reductive dechlorination in a soil column. *Water Research* 37 (12): 2905-2918.

Mackay DM, Cherry JA. 1989. Groundwater contamination: pump-and-treat remediation. *Environ. Sci. Technol* 23: 630-636

Madigan MT, Martinko JM. 2006. Brock Biology of Microorganisms, 11th edition. Chapter 17 Metabolic Diversity. ISBN: 0-13-144329-1

Magli A, Wendt M, Leisinger T. 1996. Isolation and characterization of *Dehalobacterium formicoaceticum* gen nov sp nov, a strictly anaerobic bacterium utilizing dichloromethane as source of carbon and energy. *Archives of Microbiology* 166 (2): 101-108.

Magoc T, Salzberg SL 2011. FLASH: fast length adjustment of short reads to improve 39 genome assemblies. *Bioinformatics* 27: 2957-2963

Malaguerra F, Chambon JC, Bjerg PL, Scheutz C, Binning PJ. 2011. Development and sensitivity analysis of a fully kinetic model of sequential reductive dechlorination in groundwater. *Environ. Sci. Technol 45* (19): 8395-8402

Manefield M, Whiteley AS, Griffiths RI, Bailey MJ. 2002. RNA stable isotope probing, a novel means of linking microbial community function to Phylogeny. *Appl Environ Microbiol* 68: 5367-5373.

Manoli G, Chambon JC, Bjerg PL, Scheutz C, Binning PJ, Broholm MM. 2012. A remediation performance model for enhanced metabolic reductive dechlorination of chloroethenes in fractured clay till. *J. Contam. Hydrol 131* (1–4): 64-78.

Maphosa F, Smidt H, De Vos WM, Röling WFM. 2010. Microbial Community- And Metabolite Dynamics of an Anoxic Dechlorinating Bioreactor. *Environ. Sci. Technol* 44 (13): 4884-4890.

Marshall IPG, Berggren DRV, Azizian MF, Burrow LC, Semprini L, Spormann AM. 2012. The hydrogenase chip: A tiling oligonucleotide DNA microarray technique for characterizing hydrogen-producing and –consuming microbes in microbial communities. *ISME J* 6 (4): 814-826

Martens JH, Barg H, Warren MJ, Jahn D. 2002. Microbial production of vitamin B_{12}. *Appl Microbiol Biotechnol* 58: 275-285.

Mattes TE, Coleman NV, Spain JC, Gossett JM. 2005. Physiological and molecular genetic analyses of vinyl chloride and ethene biodegradation in *Nocardioides* sp strain JS614. *Archives of Microbiology* 183 (2): 95-106.

Mayer HP, Conrad R. 1990. Factors influencing the population of methanogenic bacteria and the initiation of methane production upon flooding of paddy soil. *FEMS Microbiology Ecology* 73, 103-112

Maymó-Gatell X, Chien YT, Gossett JM, Zinder SH. 1997. Isolation of a bacterium that reductively dechlorinates tetrachloroethene to ethene. *Science* 276 (5318): 1568-1571

Maymó-Gatell X, Anguish T, Zinder SH. 1999. Reductive dechlorination of chlorinated ethenes and 1,2-dichloroethane by "*Dehalococcoides ethenogenes*" 195. *Appl. Environ. Microbiol* 65 (7): 3108-3113.

McCarty PL. 2010. Groundwater contamination by chlorinated solvents: History, Remediation Technologies and Strategies. *In Situ Remediation Of Chlorinated Solvent Plumes. SERDP/ESTCP Environmental Remediation Technology*, Stroo, H. F.; Ward, C. H., Eds. Springer: Heidelberg, Germany, pp 1-24

McInerney MJ, Bryant MP, Hespell RB, Costerton JW. 1981. *Syntrophomonas wolfei* gen. nov. sp. nov., an Anaerobic, Syntrophic, Fatty Acid-Oxidizing Bacterium. *Appl. Environ. Microbiol* 41(4): 1029-1039

McInerny, M. J., and M. P. Bryant. 1981. Basic principles of bioconversions in anaerobic digestion and methanogenesis, p. 277–296. *In* S. S. Sofer and O. R. Zaborsky (ed.), Biomass conversion processes for energy and fuels. Plenum, New York, N.Y.

Men YJ, Feil H, Verberkmoes NC, Shah MB, Johnson DR, Lee PK, West KA, Zinder SH, Andersen GL, Alvarez-Cohen L. 2011. Sustainable syntrophic growth of *Dehalococcoides ethenogenes* strain 195 with *Desulfovibrio vulgaris* Hidenborough and *Methanobacterium congoense*: global transcriptomic and proteomic analyses. *ISME J* 6 (2): 410-421

Men YJ, Lee PKH, Harding KC, Alvarez-Cohen L. 2013. Characterization of four TCE-dechlorinating microbial enrichments grown with different cobalamin stress and methanogenic conditions. *Appl. Microbial. Biotechnol* 97 (14): 6439-4350

Men YJ, Seth EC, Yi S, Crofts, TS, Allen RH, Taga ME, Alvarez-Cohen, L. 2014a. Identification of specific corrinoids reveals corrinoid modification in dechlorinating microbial communities. *Environ. Microbiol*

Men YJ, Seth EC, Yi S, Allen RH, Taga, ME, Alvarez-Cohen L. 2014b. Sustainable growth of *Dehalococcoides mccartyi* 195 by corrinoid salvaging and remodeling in defined lactate-fermenting consortia. *Appl. Environ. Microbiol* 80 (7): 2133-2141

Miller SM, Tourlousse DM, Stedtfeld RD, Baushke SW, Herzog AB, Wick LM, Rouillard JM, Gulari E, Tiedje JM, Hashsham SA. 2008. In situ-synthesized virulence and marker gene biochip for detection of bacterial pathogens in water. *Appl Environ Microbiol* 74: 2200-2209.

Moran MJ, Zogorski JS, Squillace PJ. 2007. Chlorinated solvents in groundwater of the United States. *Environ. Sci. Technol* 41 (1): 74-81.

Morris SA, Radajewski S, Willison TW, Murrell JC. 2002. Identification of the functionally active methanotroph population in a peat soil microcosm by stable-isotope probing. *Appl Environ Microbiol* 68: 1446-1453.

Morris RM, Sowell S, Barofsky D, Zinder S, Richardson R. 2006. Transcription and mass-spectroscopic proteomic studies of electron transport oxidoreductases in *Dehalococcoides ethenogenes. Appl. Environ. Microbiol* 8 (9):1499-1509

Morris RM, Fung JM, Rahm BG, Zhang S, Freedman DL, Zinder SH, Richardson RE. 2007. Comparative proteomics of *Dehalococcoides* spp. reveals strain-specific peptides associated with activity, *Appl. Environ. Microbiol* 73 (1): 320-326

Neufeld JD, Vohra J, Dumont MG, Lueders T, Manefield M, Friedrich MW, Murrell J C. 2007. DNA stable-isotope probing. *Nat. Protocols* 2, (4): 860-866.

Oelgeschläger E, Rother M. 2008. Carbon monoxide-dependent energy metabolism in anaerobic bacteria and archaea. *Arch Microbiol* 190 (3): 257-269

Panagiotakis I, Mamais D, Pantazidou M, Rossetti S, Aulenta F, Tandor V. 2014. Predominance of Dehalococcoides in the presence of different sulfate concentrations. *Water Air Soil Pollut* 225: 1785-1799

Pandey J, Chauhan A, Jain RK. 2009. Integrative approaches for assessing the ecological sustainability of in situ bioremediation. *FEMS Microbiol Rev* 33: 324-375

Pantazidou M, Panagiotakis I, Mamais D, Zikidi V. 2011. Chloroethene biotransformation in the presence of different sulfate concentrations. *Ground Water Monit Remediation* 32, 106-119

Pöritz M, Goris T, Wubet T, Tarkka MT, Buscot F, Nijenhuis l, Lechner U, Arian L. 2013. Genome sequences of two dehalogenation specialists-*Dehalococcoides mccartyi* strains BTF08 and DCMB5 enriched from the highly polluted Bitterfeld region. *FEMS Microbiol Lett* 343 (2): 101-104

Popat SC, Deshusses MA. 2011. Kinetics and inhibition of reductive dechlorination of trichloroethene, *cis*-1,2-dichloroethene and vinyl chloride in a continuously fed anaerobic biofilm reactor. *Environ Sci Technol* 45, 1569-1578

Prosser J, Jansson JK, Liu W. 2010. Nucleic-acid-based Characterization of Community Structure and Function, Environmental Molecular Microbiology. Caister Academic Press.

Punta, M., Coggill, P.C., Eberhardt, R.Y., Mistry, J., Tate, J., Boursnell, C., Pang, N., Forslund, K., Ceric, G., Clements, J., Heger, A., Holm, L., Sonnhammer, E.L., Eddy, S.R., Bateman, A. and Finn, R.D. .2012. The Pfam protein families database. Nucleic Acids Res 40(Database issue), D290-301.

Ram RJ, VerBerkmoes NC, Thelen MP, Tyson GW, Baker BJ, Blake II RC, Shah M, Hettich RL, Banfield JF. 2005. Community proteomic of a natural microbial biofilm. *Science* 308 (5730): 1915-1920

Rittmann BE, McCarty PL. 2001. Environmental Biotechnology: Principles and Application. Chapter 2. McGraw Hill Publisher, New York, NY.

Radajewski S, P Ineson, NR Parekh, JC Murrell. 2000. Stable-isotope probing as a tool in microbial ecology. *Nature* 403: 646-649.

Richardson RE, Bhupathiraju VK, Song DL, Goulet TA, Alvarez-Cohen L. 2002. Phylogenetic characterization of microbial communities that reductively dechlorinate TCE based upon a combination of molecular techniques. *Environ. Sci. Technol* 36 (12): 2652-2662.

Rifai HS, Borden RC, Newell CJ, Bedient PB. 2010. Modeling remediation of chlorinated solvent plumes. In *In Situ Remediation Of Chlorinated Solvent Plumes. SERDP/ESTCP Environmental Remediation Technology*, Stroo, H. F.; Ward, C. H., Eds. Springer: Heidelberg, Germany, pp 145-184.

Ritalahti KM, Löffler FE. 2004. Populations implicated in the anaerobic reductive dechlorinaiton of 1,2-dichloropropane in highly enriched bacterial communities. *Appl Environ Microbiol* 70: 4088-4095

Ritalahti KM, Amos BK, Sung Y, Wu Q, Koenigsberg SS, Löffler FE. 2006. Quantitative PCR targeting 16S rRNA and reductive dehalogenase genes simultaneously monitors multiple *Dehalococcoides* strains. *Appl Environ Microbiol* 72: 2765-2774

Robinson C, Barry DA, McCarty PL, Gerhard JI, Kouznetsova I. 2009. pH control for enhanced reductive bioremediation of chlorinated solvent source zones. *Sci. Tot. Environ* 407 (16): 4560-4573

Roden EE, Jin Q. 2011. Thermodynamics of Microbial Growth Coupled to Metabolism of Glucose, Ethanol, Short-Chain Organic Acids, and Hydrogen. *Appl. Environ. Microbiol* 77 (5): 1907-1909

Rodríguez J, Lema JM, Kleerebezem R. 2008. Energy-based models for environmental biotechnology. *Trends Biotechnol* 26 (7): 366-374.

Rodríguez J, Premier GC, Guwy AJ, Dinsdale R, Kleerebezem R. 2009. Metabolic models to investigate energy limited anaerobic ecosystems. *Water Sci. Technol* 60, 1669–1675.

Rowe AR, Lazar BJ, Morris RM, Richardson RE. 2008. Characterization of the Community Structure of a Dechlorinating Mixed Culture and Comparisons of Gene Expression in Planktonic and Biofloc-Associated "*Dehalococcoides*" and *Methanospirillum* Species. *Appl. Environ. Microbiol* 74 (21): 6709 -6719

Rowe AR, Heavner GL, Mansfeldt CB, Werner JJ, Richardson RE. 2012. Relating chloroethene respiration rates in *Dehalococcoides* to Protein and mRNA biomarkers. *Environ. Sci. Technol* 46 (17): 9388-9397

Ryzhkova EP. 2003. Multiple functions of corrinoids in prokaryote biology. *Applied Biochemistry and Microbiology* 39: 115-139.

Sabalowsky AR, Semprini L. 2010. Trichloroethene and cis-1,2-Dichloroethene Concentration-Dependent Toxicity Model Simulates Anaerobic Dechlorination at High Concentrations. II: Continuous Flow and Attached Growth Reactors. *Biotechnol and Bioeng* 107 (3): 540-549.

Sale T, Petersen M, Gilbert D. 2005. Electrically induced redox barriers for treatment of groundwater. ESTCP Final Report.

Saleh N, Kim HJ, Phenrat T, Matyjaszewski K, Tilton R D, Lowery GV. 2008. Ionic strength and Composition Affect the Mobility of Surface-Modified Fe0 Nanoparticles in Water-Saturated Sand Colums. *Environ. Sci. Technol* 42, 3349-3355

Schaefer CE, Condee CW, Vainberg S, Steffan RJ. 2009. Bioaugmentation for chlorinated ethenes using Dehalococcoides sp. : Comparison between batch and column experiments. *Chemosphere* 75: 141-148

Schink B, Thauer RK. 1988. Energetics of syntrophic methane formation and the influence of aggregation, p. 5-17. *In:* G. Lettinga, A. J. B. Zehnder, J. T. C. Grotenhuis, and L. W. Hulshoff (ed) Granular Anaerobic Sludge: Microbiology and Technology. Pudoc. Wageningen, The Netherlands.

Schink. 1997. Energetics of syntrophic cooperation in methanogenic degradation. *Microbiol. Mol. Biol. Rev* 61 (2) 262-280

Schipp CJ, Marco-Urrea E, Kublik A, Seifert J, Adrian L. 2013. Organic cofactors in the metabolism of *Dehalococcoides mccartyi* strains. *Philos. Trans. R. Soc. Lond., B, Biol. Sci* 19 (1616):1-12

Scholz MB, Lo CC, Chain PSG. 2012. Next generation sequencing and bioinformatic bottlenecks: the current state of metagenomic data analysis. *Curr Opin Biotechnol* 23: 9-15.

Schwarzenbach RP, Gschwend PM, Imboden DM. Environmental Organic Chemistry, 2nd Edition. Chapter 3. Partioning: Molecular Interactions and Thermodynamics.

Seshadri R, Adrian L, Fouts DE, Eisen JA, Phillipy AM, Methe BA, Ward NL, Nelson WC, Deboy RT, Khouri HM, Kolonay JF, Dodson RJ, Daugherty SC, Brinkac LM, Sullivan SA, Madupu R, Nelson KE, Kang, KH, Impraim M, Tran K, Robinson JM, Forberger HA, Frasewr CM, Zinder SH, Heidelberg JF. 2005. Genome Sequence of the PCE-dechlorinating Bacterium *Dehalococcoides ethenogenes*. *Science* 307 (5706): 105-108.

Shi Y, Tyson GW, Delong EF. 2009. Metatranscriptomics reveals unique microbial small RNAs in the ocean's water column. *Nature*, 459: 266-269

Shrestha PM, Rotaru AE, Aklujkar M, Liu F, Shrestha M, Summers ZM, Malvankar N, Flores DC, Lovley DR. 2013. Syntrophic growth with direct interspecies electron transfer as the primary mechanism for energy exchange. *Environ. Microb. Rep* 5 (6): 904-910.

Shokralla S, JL Spall, JF Gibson, M Hajibabaei. 2012. Next-generation sequencing technologies for environmental DNA research. *Mol Ecol* 21: 1794-1805.

Sieber JR, Sims DR, Han C, Kim E, Lykidis A, Lapidus AL, McDonnald E, Rohlin L, Culley DE, Gunsalus R, McInerney MJ. 2010. The genome of *Syntrophomonas wolfei*: new insights into syntrophic metabolism and biohydrogen production. *Environ. Microbiol* 12 (8): 2289-2301.

Sieber JR, Le HM, McInerney MJ. 2014. The importance of hydrogen and formate transfer for syntrophic fatty, aromatic and alicyclic metabolism. *Environ Microbial* 16(1): 177-188

Simon C, Herath J, Rockstroh S, Daniel R. 2009. Rapid identification of genes encoding DNA polymerases by function-based screening of metagenomic libraries derived from glacial ice. *Appl. Environ. Microbiol* 75: 2964-2968

Simon C, Daniel R. 2011. Metagenomic Analysis: Past and Future Trends. *Appl. Environ. Microbiol* 77 (4): 1153-1161

Sleep BE, Brown AJ, Lollar BS. 2005. Long-term tetrachloroethene degradation sustained by endogenous cell decay. *J Environ Eng Sci* 4 (1): 11-17

Smatlak CR, Gossett JM, Zinder SH. 1996. Comparative kinetics of hydrogen utilization for reductive dechlorination of tetrachloroethene and methanogenesis in an anaerobic enrichment culture. *Environ Sci Technol* 30: 2850-2858

Smith H, Waltman P. 2005. The theory of the chemostat: dynamics of microbial competition, Cambridge University Press. ISBN 0521470277

Sogin ML, Morrison HG, Huber JA, Welch DM, Huse SM, Neal PR, Arrieta JM, Herndl GJ. 2006. Microbial diversity in the deep sea and the underexplored 'rare biosphere'. *PNAS* 103: 12115-12120

Stams AJM, Plugge CM. 2009. Electron transfer in syntrophic communities of anaerobic bacteria and archaea. *Nature Reviews Microbiology* 7(8): 568-577.

Stams AJM, Worm P, Sousa DZ, Alves MM, Plugge CM. 2012. Syntrophic Degradation of Fatty Acids by Methanogenic Communities, p.127-142. Hallenbeck (ed). Microbial Technologies in Advanced Biofuels Production. Wageningen, The Netherlands.

Stenuit B, Eyers L, Schuler L, Agathos SN, George I. 2008. Emerging high-throughput approaches to analyze bioremediation of sites contaminated with hazardous and/or recalcitrant wastes. *Biotechnology Advances* 26 (6): 561-575

Stroo H.F. 2010. Remedial technology selection for chlorinated solvent plumes. In *In Situ Remediation of Chlorinated Solvent Plumes. SERDP/ESTCP Environmental Remediation Technology*, Stroo, H. F.; Ward, C. H., Eds. Springer: Heidelberg, Germany, pp 281-307.

Stroo HF, Ward CH. 2010. Future directions and research needs for chlorinated solvent plumes. In *In Situ Remediation of Chlorinated Solvent Plumes. SERDP/ESTCP Environmental Remediation Technology*, Stroo, H. F.; Ward, C. H., Eds. Springer: Heidelberg, Germany, pp 699-725.

Summers ZM, Fogarty HE, Leang C, Franks AE, Malvankar NS, Lovley DR. 2010. Direct exchange of electrons within aggregates of an evolved syntrophic coculture of anaerobic bacteria. *Science* 330 (6009): 1413-1415

Su C, Lei LP, Duan YQ, Zhang KQ, Yang JK. 2012. Culture-independent methods for studying environmental microorganisms: methods, application, and perspective. *Appl Microbiol Biotechnol* 93: 993-1003.

Sung Y, Fletcher KF, Ritalaliti KM, Apkarian RP, Ramos-Hernandez N, Sanford RA, Mesbah NM, Löffler FE. 2006. *Geobacter lovleyi* sp nov strain SZ, a novel metal-reducing and tetrachloroethene-dechlorinating bacterium. *Appl. Environ. Microbiol* 72 (4): 2775-2782.

Suyama A, Iwakiri R, Kai K, Tokunaga T, Sera N, Furukawa K. 2001. Isolation and characterization of *Desulfitobacterium* sp strain Y51 capable of efficient dehalogenation of tetrachloroethene and polychloroethanes. *Biosci Biotechnol and Bioch* 65 (7), 1474-1481.

Tang YJ, Yi S, Zhuang W, Zinder SH, Keasling JD, Alvarez-Cohen L. 2009. Investigation of Carbon Metabolism in "*Dehalococcoides ethenogenes*" Strain 195 by Use of Isotopomer and Transcriptomic Analyses, *Journal of Bacteriology* 191 (16): 5224-5231

Taroncher-Oldenburg G, Griner EM, Francis CA, Ward BB. 2003. Oligonucleotide microarray for the study of functional gene diversity in the nitrogen cycle in the environment. *Appl Environ Microbiol* 69: 1159-1171.

Tu QC, Yu H, He Z, Deng Y, Wu LY, Nostrand JDV, Zhou AF, Voordeckers J, Lee YJ, Qin YJ, Hemme CL, Shi Z, Xue K, Yuan T, Wang AJ, Zhou JZ. 2014. Geochip 4: a functional gene-array-based high-throughput environmental technology for microbial community analysis. *Molecular Ecology Resoureces*

U.S.EPA. Trichloroethylene (TCE) TEACH Chemical Summary. 2006 http://www.epa.gov/teach/chem_summ/TCE_summary.pdf

U.S.EPA (2007) Treatment Technologies for site cleanup: Annual Status report. 12th ed. EPA-542-R-07-012.

U.S.EPA. 2011a, Toxicolgical Review of Trichloroethylene. http://www.epa.gov/IRIS/toxreviews/0199tr.pdf.

U.S.EPA 2011b. National Priorities List. http://cumulis.epa.gov/supercpad/cursites/srchsites.cfm,

U.S. EPA 2011c. Common Chemicals found at Superfund Sites. http://www.epa.gov/superfund/health/contaminants/radiation/chemicals.htm

Ueda K, Yamashita A, Ishikawa J, Shimada M, Watsuji TO, Morimura K, Ikeda H, Hattori M, Beppu T. 2004. Genome sequence of *Symbiobacterium thermophilum*, an uncultivable bacterium that depends on microbial commensalism. *Nucl. Acids Res* 32 (16): 4937-4944

Vainberg S, Condee CW, Steffan RJ. 2009. Large-scale production of bacterial consortia for remediation of chlorinated solvent-contaminated groundwater. *J Ind Microbiol Biotechnol* 36 (9): 1189-1197

Wallrabenstein C, Schink B. 1994. Evidence of reversed electron transport in syntrophic butyrate and benzoate oxidation by *Syntrophomonas wolfei* and *Syntrophus buswellii*. *Arch. Microbiol* 162: 136-142.

Walker CB, Redding-Johanson AM, Baidoo EE, Rajeev L, He Z, Hendrickson EL, Joachimiak MP, Stolyar S, Arkin AP, Leigh JA, Zhou J, Keasling JD, Mukhopadhyay A, Stah DA. 2012. Functional responses of methanogenic archaea to syntrophic growth. *ISME Journal* 6, 2045-2055

Wang Z, Gerstein M, Snyder M. 2009. RNA-Seq: a revolutionary tool for transcriptomics. *Nature Reviews Genetics* 10 (1): 57-63

Watts RJ, Tell AL. 2006. Treatment of contaminated soils and groundwater using ISCO. *Pract Period Haz Toxic Rad Waste Mgmt* 10:2-9

Wei N, Finneran KT. 2011. Influence of Ferric Iron on Complete Dechlorination of Trichloroethylene (TCE) to Ethene: Fe(III) Reduction Does Not Always Inhibit Complete Dechlorination. *Environ. Sci. Technol* 45 (17): 7422-7430

WHO. 2000, Air Quality Guidance for Europe 2nd edition, Chapter 5 Organic pollutants. ISBN 92 890 1358 3

West KA, Johnson DR, Hu P, DeSantis TZ, Brodie EL, Lee PKH, Feil H, Andersen GL, Zinder SH, Alvarez-Cohen L. 2008. Comparative genomics of *Dehalococcoides ethenogenes* 195 and an enrichment culture containing unsequenced *Dehalococcoides* strains. *Appl Environ Microbiol* 74, 3533-3540

West KA, Lee PKH, Johnson DR, Zinder SH, Alvarez-Cohen L. 2013. Global gene expression of *Dehalococcoides* within a robust dynamic TCE-dechlorinating community under conditions of periodic substrate supply. *Biotechnol and Bioeng* 110 (5): 1333-1341

Widdowson MA. 2004. Modeling natural attenuation of chlorinated ethenes under spatially varying redox conditions. *Biodegradation* 15, 435-451

Wilkin RT, Digiulio DC. 2010. Geochmical impacts to groundwater from geologic carbon sequestration: controls on pH and inorganic carbon concentrations from reaction path a kinetic modeling. *Environ Sci Technol* 44: 4821-4827

Williams RT and Crawford RL. 1984. Methane production in Minnesota Peatlands. *Appl Environ Microbiol* 47(6), 1266-1273

Wolin EA, Wolin MJ, Wolfe RS. 1963. Formation of methane by bacterial extracts. *J. Biol. Chem* 238: 2882-2886

Yan T, LaPara TM, Novak PJ. 2006. The effect of varying levels of sodium bicarbonate on polychlorinated biphenyl dechlorination in Hudson River sediment cultures. *Environ Microbiol* 8:1288-1298

Yan J, Ritalahti KM, Wagner DD, Löffler FE. 2012. Unexpected specificity of interspecies cobamide transfer from geobacter spp. to organohalide-respiring *Dehalococcoides mccartyi* strains. *Appl. Environ. Microbiol* 78 (18): 6630-6636

Yan J, Im J, Yang Y, Löffler FE. 2013. Guided cobalamin biosynthesis supports *Dehalococcoides mccartyi* reductive dechlorination activity, *Philos Trans R Soc Lond B Biol Sci* 68 (1616): 2012-2020

Yang YR, McCarty PL. 1998. Competition for hydrogen within a chlorinated solvent dehalogenating anaerobic mixed culture. *Environ. Sci. Technol* 32 (22): 3591-3597

Yang YR, McCarty PL. 2000. Biomass, oleate, and other possible substrates for chloroethene reductive dehalogenation. *Biorem J* 4(2): 125-133

Yaws CL. 1999. Chemical Properties Handbook. McGraw-Hill, New York, Ny, USA. pp. 784

Yi S, Seth EC, Men YJ, Stabler SP, Allen RH, Alvarez-Cohen L, Taga ME. 2012. Versatility in Corrinoid Salvaging and Remodeling pathways supports corrinoid-dependent metabolism in *Dehalococcoides mccartyi*. *Appl. Environ. Microbiol* 78 (21): 7745-7752

Yu SH, Semprini L. 2002. Comparison of trichloroethylene reductive dehalogenation by microbial communities stimulated on silicon-based organic compounds as slow-release anaerobic substrates. *Water Research* 36(20): 4985-4996.

Yu S, Semprini, L.2004. Kinetics and modeling of reductive dechlorination at high PCE and TCE concentrations. *Biotechnol. Bioeng* 88 (4): 451-464

Yu SH, Dolan ME, Semprini L. 2005. Kinetics and inhibition of reductive dechlorination of chlorinated ethylenes by two different mixed cultures. *Environ. Sci. Technol* 39 (1), 195-205

Zehnder AJB, Stumm W. 1988. Geochemistry and biogeochemistry of anaerobic habitats. In: Zehnder AJB (Ed), Biology of anaerobic microorganisms.pp 1-38. John Wiley and Sons, New York.

Zheng D, Carr CS, Hughes JB. 2001. Influence of Hydraulic Retention time on extent of PCE dechlorination and preliminary characterization of the enrichment culture. *Bioremediation Journal* 5 (2): 159-168.

Zhuang WQ, Yi S, Feng X, Zinder SH, Tang YJ, Alvarez-Cohen L. 2011. Selective utilization of exogenous amino acids by *Dehalococcoides ethenogenes* strain 195 and its effects on growth and dechlorination activity. *Appl. Environ. Microbiol 77*, (21): 7797-7803.

Zhuang WQ, Yi S, Bill M, Brisson VL, Feng X, Men Y, Conrad ME, Tang YJ, Alvarez-Cohen L. 2014. Incomplete Wood-Ljungdahl pathway facilitates one carbon metabolism in organohalide-respiring *Dehalococcoides mccartyi*. *PNAS* 111 (17): 6419-6424

Ziv-El M, Delgado AG, Yao Y, Kang DW, Nelson KG, Halden RU, Krajmalnik-Brown R. 2011. Development and characterization of DehaloR^2, a novel anaerobic microbial consortium performing rapid dechlorination of TCE to ethene. *Appl Microbiol Biotechnol* 92 (5): 1062-1071

Appendix

Modeling description and calibration

EXE1: thermodynamic control
Input: MH2, Mdonor, Mace,
Output: phi

R=8.314
Document: Gas constant, value=8.314, unit J K^{-1} mol^{-1}
Temp=307
Document: Temperature, unit K. value range: 277K~323K (4°C~50°C)
Vl=0.1
Document: Liquid phase volume, unit: liter
Vg=0.06
Document: Gas phase volume, unit: liter
pH =7.2
Document: pH value in the system is well maintained between 7.0 and 7.3 by using dual buffer system. (10mM TES and 30 mM sodium bicarbonate) unitless
f=0.786
Document: Activity coefficient, value= 0.786. Ionic strength is calculated based on the medium composition (BAV1 medium is used in this study). The activity coefficient f is calculated by using the equation of Debye and Huckel, 1923.
f'=1.02
Document: H_2 activity coefficient, value=1.02. For uncharged species, the activity coefficient is calculated by following a "salting-out" model. unitless
H2O=1
Document: water concentration, value=1. Unitless.
PH2
Document: H_2 partial pressure, unit: bar, value is calculated from MH2.
MH2
Document: mass of H_2 in the system, unit: μmol. MH2=initialH2+deltaMH2
HccH2
Document: Henry's law constant of H_2, unitless, value is affected by temperature. (Gossett, 1987) value=56 at 34°C
Cdonor
Document: electron donor concentration in liquid phase (μmol L^{-1}) Cdonor=Mdonor/Vl
Mace
Document: Acetate mass in the system, unit: μmol. Mace=initialMace+deltaMace
deltaGcrit=-20,000
Document: minimum energy requested for cell maintenance (Schink, 1997). unit: J mol^{-1}, value=-20000
deltaG0=88,700
Document: the number is calculated at standard condition, unit: J mol^{-1} (a suite of fermentation reactions with deltaG0' available in table 6-2)
deltaGpH

Document: Gibb's free energy at a certain pH. deltaGpH=deltaG0-5.708×n×pH. (n: number of protons generated in the reaction)
deltaGrxn
Document: Gibbs energy release from a real reaction, unit: J mol^{-1}.

Equations
PH2=MH2×R×Temp/(Vl/HccH2+Vg)

DeltaGpH=DeltaG0-5.708×n×Ph;
Document: PH2 unit is bar. (equation derived in Chapter 3)

DeltaGrxn=DeltaGpH+R×Temp×log((Mace/Vl×10^{-6}×f)^2×
(PH2/100000×f')^2/H20/(Mdonor/Vl×10^{-6}×f));
Document: this is an example of deltaGrxn calculation when butyrate was used as electron donor.

phi=1-exp((DeltaGrxn-DeltaGcrit)/R/Temp);

EXE2 Fermentation
Input: phi, Mdonor, MH2, Mace, Mferm, Mdhc, Mmeth, Msul, deltat
Output: Mdonor1, MH21, Mace1, Mferm1
Document: there is no output of Mdhc1, Mmeth1, Msul1 in EXE2, the output of Mdhc1, Mmeth1, Msul1 are in each specific sections. Deltat was adjusted to yield the relative tolerance of yield smaller than 10^{-5} gram (Lee *et al*., 2004).

Parameters
Vl=0.1
Document: liquid volume, unit: L
Xinferm=0
Document: Fermenter concentration in influent, unit: cell L^{-1}
Cindonor=0
Document: donor concentration in influent, unit: μmol L^{-1}
Cinace=0
Document: acetate concentration in influent, unit: μmol L^{-1}
Qindonor=0
Document: influent flow rate of electron donor, unit: L day^{-1}
Qe=0
Document: effluent flow rate, unit: L day^{-1}
fedonor=0.9
Document: fraction of electrons goes to energy metabolism during donor fermentation to acetate (fe+fs=1), the value is calculated based on stoichiometry. In modeling approach, 0.9 was used for slow fermenting substrate, 0.85 was used for fast fermenting substrate.
kdonor= 1×10^{-8}
Document: maximum specific electron donor utilization rate (μmol $cell^{-1}$ day^{-1}). In literature range: 3.7×10^{-10} to 2.5×10^{-9} (Fenell, 1998; Kouznetsova, 2010)
Kdonor= 34
Document: Half velocity of electron donor fermentation, unit (μM)

For slow fermenting substrate butyrate, value=34.3 (Fennell, 1998), for faster fermenting substrate lactate, value=2.5. (Fennell, 1998)
CWdhc=4.2×10^{-9}
Document: Cell weight of *Dehalococcoides*, unit μg $cell^{-1}$ (Duhamel, 2004)
CWmeth=1.0×10^{-8}
Document: Cell weight of methanogens, unit μg $cell^{-1}$. (assumption)
CWferm=1.0×10^{-8}
Document: Cell weight of fermenters, unit μg $cell^{-1}$. (assumption)
CWsul=1.0×10^{-8}
Document: Cell weight of sulfate reducer, unit μg $cell^{-1}$. (assumption)
bdhc=0.024
Document: Indigenous decay rate of *Dehalococcoides*, unit day^{-1}, value= 0.024
bferm=0.024
Document: Indigenous decay rate of fermenters, unit day^{-1}, value=0.024
bmeth=0.0085
Document: Indigenous decay rate of methanogens, unit day^{-1}, value=0.085 (Rittmann, 2005)
bsul=0.048
Document: endogenous decay rate of sulfate reducers, unit day^{-1}, value=0.048
μferm=0.62
Document: maximum growth rate of fermenter, unit (day^{-1})
For slow fermenting bacteria, value=0.62. For fast fermenting bacteria, value=2.13 (Malaguerra, 2011) **we could also use Y×kdonor for μferm calculation.
As mentioned in chapter 5, Y_{ferm} for butyrate fermenter was 0.399 g cell/e^--eq accepter at environmental relevant conditions. We assumed CWferm=1.0×10^{-8} μg $cell^{-1}$, then the calculated μferm =1.3 day^{-1}
Massconvert=0.0088
Document: biomass is converted to "slow" fermenting substrate, which is assumed to be butyrate during endogenous decay. 1mol biomass ($C_5H_7O_2N$) goes to 1 mol butyrate. unit: μmol μg $biomass^{-1}$ (assume MWcell=113g mol^{-1})
kdecay=0.02
Document: H_2 releasing rate from endogenous decay, unit day^{-1}, assumed value.

Equation
Mdonor1=Cindonor×Qindonor×deltat-Mdonor/Vl×Qe×deltat - kdonor×fedonor×Mferm×Mdonor/Vl×phi/(Kdonor+Mdonor/Vl) ×deltat
Document: deltaMdonor is denoted as Mdonor1(μmol)
Mdonor1 = influent donor –effluent donor -fermentation

Mdecay=Massconverter×(bferm×Mferm×CWferm+bdhc×Mdhc×CWdhc+bmeth×Mmeth×CWmeth+bsul×Msul×CWsul)×deltat
Document: Endogenous decay is denoted as Mdecay (μmol).
It is not an output of the model. But it is used to calculate H_2 production in EXE2.
Endogenous decay contributes to slow fermenting substrate. In a short period of experiment, decay may not be an important factor.

MH21=-MH2/(Vl+Vg×HccH2)×Qe×deltat+
2×kdonor×fedonor×Mferm×Mdonor/Vl×phi/(Kdonor+Mdonor/Vl)×deltat+
kdecay×Mdecay×deltat
Document: the change of MH2 during fermentation is denoted as MH21
MH21=influent H_2-effluent H_2+ H_2 generation from fermentation+H_2 generation from cell decay contribution

Mace1=-Mace/Vl×Qe×deltat+
2×kdonor×fedonor×Mferm×Mdonor/Vl×phi/(Kdonor+Mdonor/Vl)×deltat
Document: Mace1=influent Ace-effluent Ace+ Acetate generation from fermentation

Mferm1=Xinferm×Vl×deltat-Mferm/Vl×Qe×deltat + μferm
×Mferm×Mdonor/Vl×phi/(Kdonor+Mdonor/Vl)×deltat-bferm×Mferm×deltat
Document: the change of Mferm 1(cells) is denoted as deltaMferm
Mferm1= influent fermenter-effluent fermenter +cell production during deltat-cell decay during deltat

Output
Mdonor=Mdonor+Mdonor1
MH2=MH2+MH21
Mace=Mace+Mace1
Mferm=Mferm+Mferm1
If phi=0, Mdonor1=0

EXE3: Acetoclastic methanogenesis

Input: Mdonor, Mace, Mameth
Output: Mace2, Mameth1
Document: we used Mace2 to differentiate the delta Mace in acetoclastic methanogenesis process (Acetate consumption) from delta Mace in fermentation process (Acetate production, Mace1).

Parameters
Qindonor=0
Document: Flow rate of electron donor in influent, unit: L day^{-1}
Qe=0
Document: effluent flow rate in the system, unit: L day^{-1}
kamth=1.0×10^{-9}
Document: maximum specific methane production rate by acetoclastic methanogens (μmol $cell^{-1}$ day^{-1}). Range: 6.7×10^{-10} to 1.6×10^{-9} (Maillacheruvu and Parkin, 1996; Fenell, 1998).
Kamth=500
Document: Half velocity of acetoclastic methanogenesis, unit (μM)
Acetic concentration was in the range of 450~1000 μM in literature (Maillacheruvu and Parkin, 1996; Fenell, 1998).
μameth=0.20
Document: maximum growth rate of acetoclastic methanogens, unit (day^{-1})

Range: 0.13~0.34 (Clapp 2004; Malaguerra, 2011)

Equations

Mace2=-kamth×Mameth×Mace/Vl/(Kamth+Mace/Vl) ×deltat
Document: the change of Mace is denoted as Mace2, in order to differentiate from Mace1 in fermentation.
Mace2=-acetate converted to methane production (acetoclastic methanogenesis). The part of acetate went to biomass production is relatively small, and is not considered in this step. When biomass production becomes an issue, it should be considered)

Mameth1=-Mameth/Vl×Qe×deltat-μameth×Mameth×Mace/Vl/(Kamth+Mace/Vl) ×deltat-bameth× Mameth×deltat
Document: Mameth1=influent cell number-effluent cell number+ cell yield from acetoclastic methanogenesis-cell decay

Output
Mace=Mace+Mace2
Document: If Mace/Vl> certain level (~20 mM), the kinetic parameters for reductive dechlorination would be affected and an effect factor should be added to k_{donor} to demonstrate inhibition effect of acetate on fermentation.
Mameth=Mameth+Mameth1

EXE4 Hydrogenotrophic Methanogenesis
Input: MH2, Mhmeth, Mhmth, deltat
Document: hydrogenotrophic methanogenesis is the process of H_2+CO_2—CH_4. CO_2 is not a limiting factor in the system. Thus, CH_4 production is a function of H_2 and methanogens cell number.
Output: Mhmth1, Mhmeth1, MH21
Docoment: H_2 could be efficiently used while at high level. When low level of hydrogen is present, dechlorination may outcompete with hydrogenotrophic methanogenesis. K_S could represent this based on mathematical formula.

Parameters
alpha
Document: TCE has inhibitory effect on hydrogenotrophic methane production. The inhibition factor is denoted as alpha.
If Mtce/(Hcctce×Vg+Vl)>400, alpha=0 (unit: μmol//L), if Mtce/(Hcctce×Vg+Vl)<400, alpha=1
H2toCH4=0.25
Document: factor of H_2 to CH_4 ratio, unitless, value=0.25
feH2toCH4=0.89~1
Document: fraction of electrons goes to energy metabolism during methanogenesis, value=0.89
HccCH4= 34
Document: Henry's law constant of CH4, unitless, value is affected by temperature. Value selected here: at 34 °C (Gossett, 1987)
khmeth=1.2×10^{-8}

Document: maximum specific H_2 utilization rate by hydrogenotrophic methanogens, unit: unit: μmol cell-1 day^{-1}. Value range: 2×10^{-9} to 3.3×10^{-7} (Maillacheruvu and Parkin, 1996; Fennell, 1998; Clapp 2004). Value selected here is based on Fennell, 1998
Khmeth=0.5
Document: half velocity of H_2 consumption by hydrogenotrophic methanogens, unit: μmol L^{-1}. value range: 0.5~18 (Fkaradagli and Rittman,2005; Christ, 2007)
Hthmth=0.01
Document: H_2 threshold for hydrogenotrophic methanogenesis. Unit: μM, value 0.008. Value range: 0.011~0.318. Value selected from Yang, 1998
μhmeth= 0.8
Document: maximum hydrogenotrophic methanogen growth rate, unit: day^{-1}. Value range: 0.13~0.34. (Clapp, 2004) Value was chosen from simulation.
bhmeth=0.025
Document: indigenous decay rate of methanogens, unit day^{-1}, value=0.024, assumed value.
Vl=0.1
Document: liquid volume, unit: L.
Vg=0.06
Document: gas volume, unit:L.
Qe=0
Document: effluent flow rate, unit: L/day

Equations

Mhmth1=-Qe×Mhmth/(HccCH4×Vg+Vl) ×deltat +alpha×H2toCH4×kmeth× feH2toCH4× Mmeth× (H-Htmth)/(Kmeth+(H-Htmth))×deltat
Document: the change of hydrogenotrophic methane production is denoted as Mmth1.
Mmth1=influent CH_4-effluent CH_4+CH_4 production by hydrogenotrophic methanogens.

Mhmeth1=-Qe×Mmeth/Vl+H2toCH4×μmeth×Mmeth× (H-Htmth)/(Kmeth+(H-Htmth)) ×deltat-bmeth×Mmeth×deltat
Document: the change of hydrogenotrophic methanogen cells is denoted as Mmeth1.
Mmeth1= Mmth influent (0) -Mmth effluent +Mmth production-Mmth decay

H=MH2/(Vl+HccH2×Vg)
MH21= -khmth×Mhmeth×feH2toCH4× (H-Htmth)/(Khmth+H-Htmth) ×deltat;

Output
Mmth=Mmth+Mmth1
Mmeth=Mmeth+Mmeth1
If H<Htmth, Mmth1=-Qe×Mmth/(HccCH4×Vg+Vl) ×deltat
MH2=MH2+MH21

EXE5 Reductive dechlorination

Input: Mtce, Mdce, Mvc, MH2, Mdhc, deltat
Output: Mtce1, Mdce1, Mvc1, Meth1, Mdhc1, MH23

Assumption: equilibrium between gas and liquid at each small deltat, Mdhc are the reductive respiring bacteria that can metabolic respire TCE to DCE to VC to ETH. Here we do not distinguish the species between different reduction groups.

Parameters

Htdhc=0.0006

Document: H_2 threshold for reductive dechlorination. Unit: μM, value 0.0006 was determined in this study. Value range: 0.0003~0.002 (Loffler 1999, Yang, 1998)

ktce=6×10^{-9}

Document: maximum specific TCE consumption rate, unit: μmol $cell^{-1}$ day^{-1}.

In literature: 2.1×10^{-13} to 1.4×10^{-9}. Value is determined in this study.

kdce=9×10^{-9}

Document: maximum specific DCE consumption rate, unit: μmol $cell^{-1}$ day^{-1}.

In literature: 3×10^{-13} to 2×10^{-9}. Value is determined in this study.

kvc=3×10^{-9}

Document: maximum specific VC consumption rate, unit: μmol $cell^{-1}$ day^{-1}.

In literature: 6×10^{-13} to 2×10^{-9}. Value is determined in this study.

Ktce= 6.0

Document: half velocity of TCE reduction to *cis*-DCE, unit: μmol L^{-1}. Value range: 0.08~23.4. Value is derived from experiments (Chapter 5).

Kdce=6.0

Document: half velocity of cisDCE reduction to VC, unit: μmol L^{-1}. Value range: 0.54~10. Value is derived from experiments (Chapter 5).

Kvc= 290

Document: half velocity of VC reduction to ETH, unit: μmol L^{-1}. Value range: 2.6~290

Value selected here (Fennell, 1998). It is hard to distinguish between energetic respiration or co-metabolism.

Khdhc= 0.007

Document: half velocity of H_2 consumption during reductive dechlorination, unit: μmol L^{-1}. value range: 0.007~0.1. Value selected here (Cupples, 2003)

Kitce= 6.0

Document: Inhibition coefficient of TCE, unit: μmol L^{-1}. Value range: 1.5~10.5. Value selected here is the same as Ktce.

Kidce=6.0

Document: Inhibition coefficient of cisDCE, unit: μmol L^{-1}. Value range: 2.1~3.6. Value selected here is the same as Kdce.

μdhc=0.4

Document: maximum growth rate of TCE/DCE/VC dechlorinators, unit: day^{-1}. In literature: 0.25~0.54 (Cupples, 2004). Value is determined in this study.

feH2toTCE=0.89

Document: fraction of electrons go to dechlorination. Unitless.

HccTCE

Document: Henry's law constant of TCE, unitless, value is affected by temperature.

HccTCE=12200/Temp×exp(11.37-4780/Temp) (Gossett, 1987)

HccDCE

Document: Henry's law constant of DCE, unitless, value is affected by temperature. (Gossett, 1987)(assume cis-DCE was the exclusive reductive product of TCE)
HccDCE=12200/Temp×exp(8.479-4192/Temp)
HccVC
Document:Henry's law constant of VC, unitless, value is affected by temperature. (Gossett, 1987)
HccVC=12200/Temp×exp(7.385-3286/Temp)
HccETH=8.24
Document: Henry's law constant of ETH at 34 °C, unitless. (Gossett, 1987)
Qindonor=0
Document: Flow rate of electron donor in influent, unit: L day^{-1}
Qe=0
Document: effluent flow rate in the system, unit: L day^{-1}
Qinaccep=0
Document: influent flow rate of electron acceptor in the system, unit: L/day
Cintce=0
Document: influent TCE concentration, unit: μmol L^{-1}
Cindce=0
Document: influent DCE concentration, unit: μmol L^{-1}
Cinvc=0
Document: influent VC concentration, unit: μmol L^{-1}
Cineth=0
Document: influent ETH concentration, unit: μmol L^{-1}
Xindhc=0
Document: influent Dehalococcoides cell concentration, unit cell L^{-1}

Equations
Ctce=Mtce/(Hcctce×Vg+Vl)
Document: Ctce is liquid phase TCE concentration, unit: μmol L^{-1}
Cdce=Mdce/(Hccdce×Vg+Vl)
Document: Cdce is liquid phase DCE concentration, unit: μmol L^{-1}
Cvc=Mvc/(Hccvc×Vg+Vl)
Document: Cvc isliquid phase VC concentration, unit: μmol L^{-1}
Ceth=Meth/(Hcceth×Vg+Vl)
Document: Ceth is liquid phase ETH concentration, unit: μmol L^{-1}

H=MH2/(Vl+HccH2×Vg)

Mtce1=Qinaccep×CinTCE-Qe×Ctce×deltat-ktce×Mdhc×feTCE×Ctce/(Ktce+Ctce) × (H-Htdhc)/(H-Htdhc+Khdhc) ×deltat;
Document: Mtce1=influent TCE-effluent TCE -TCE reduction to DCE in liquid

Mdce1=-Qe×Cdce×deltat+ktce×Mdhc×feTCE×Ctce/(Ktce+Ctce)×(H-Htdhc)/(H-Htdhc+Khdhc) ×deltat-kdce×feTCE×Mdhc×Cdce/(Kdce× (1+Cdce/Kitce)+Cdce) × (H-Htdhc)/(H-Htdhc+Khdhc) ×deltat;
Document: Mdce1=influentDCE-effluent DCE+DCE formation from TCE-DCE reduction to VC

Mvc1=-Qe×Cvc×deltat-kvc×Mdhc×feTCE×Cvc/(Kvc× (1+Ctce/Kitce+Cdce/Kidce)+Cvc) × (H-Htdhc)/(H-Htdhc+Khdhc) ×deltat+kdce×Mdhc×feTCE×Cdce/(Kdce× (1+Cdce/Kitce)+Cdce) × (H-Htdhc)/(H-Htdhc+Khdhc) ×deltat;
Document: Mvc1=influentVC-effluent VC -VC reduction to ETH+VC formation from DCE

Meth1=-Qe×Ceth×deltat+kvc×feTCE×Mdhc×Cvc/(Kvc× (1+Ctce/Kitce+Cdce/Kidce)+Cvc) × (H-Htdhc)/(H-Htdhc+Khdhc) ×deltat;
Document: Meth1=influent ETH -effluent ETH+ETH formation fromVC

Mdhc1=μdhc1×(Mdhc×feTCE×Ctce/(Ktce+Ctce)+Mdhc×feTCE×Cdce/(Kdce× (1+Ctce/Kitce)+Cdce)) × (H-Htdhc)/(H-Htdhc+Khdhc) ×deltat-bdhc×Mdhc×deltat-Qe×Mdhc/Vl×deltat;
Document: Mdhc1=influent dhc-effluent dhc + production from TCE-DCE+ production from DCE-VC- decay of dhc

Output
Mtce=Mtce+Mtce1
Mdce=Mdce+Mdce1
Mvc=Mvc+Mvc1
Meth=Meth+Meth1
Mdhc=Mdhc+Mdhc1
MH2=MH2+MH21

Exe6 Sulfate reduction
Hard to track HS^- or H_2S, we model sulfate disappearance instead.
Input: MH2, Msulfate, Msul,deltat (concentrations, time)
Output: Msulfate1, Msul1, MH24

Parameters
Vl=0.1
Document: liquid volume, unit: L.
Vg=0.06
Document: gas volume, unit:L.
Qe=0
Document: effluent flow rate, unit: L day^{-1}
H2toH2S=0.25
Document: factor of H_2 to H_2S ratio, unitless, value=0.25
feH2toH2S=0.89~1
Document: fraction of electrons goes to energy metabolism during sulfate reduction, value=0.89
ksul=3×10^{-9}
Document: maximum specific sulfate consumption rate, unit: μmol $cell^{-1}$ day^{-1}. Assumed value. Value range
Ksul= 10
Document:half velocity of sulfate reduction, unit: μmol/L. assumed value. Value range
Htsul=0.002
Document: Hydrogen threshold for sulfate reduction. Unit μM. Value 0.002.

μsul= 0.4
Document: maximum sulfate reducer growth rate, unit: day^{-1}. Assumed value.
bsul=0.048
Document: indigenous decay rate of sulfate reducers, unit day^{-1}, value=0.048

Equations
H=MH2/(Vl+HccH2×Vg);

Msulfate1=-H2toH2S×feH2toH2S×ksul×Msul×Msulfate/Vl/(Ksul+Msulfate/Vl) × (H-Htsul)/(Khsul+H-Htsul) ×deltat-Msulfate/Vl×Qe×deltat;
Document: Msulfate1=influent sulfate–effluent sulfate- sulfate reduction

Msul1=H2toH2S×μsul×Msul×Msulfate/Vl/(Ksul+Msulfate/Vl) × (H-Htsul)/(Khsul+H-Htsul) ×deltat-bsul×Msul×deltat-Msul/Vl×Qe×deltat;
Document: Msul1=influent Msul- effluent Msul +Msul production-Msul decay

MH21=feH2toH2S×ksul×Msul×Msulfate/Vl/(Ksul+Msulfate/Vl) × (H-Htsul)/(Khsul+H-Htsul) ×deltat;

Output
Msulfate=Msulfate+Msulfate1
Msul=initialMsul+deltaMsul
MH2=MH2+MH21
If H<Htsul, deltaMsulfate=-Qe×Csul